MIRL REPORT NO. 70

EVALUATION OF THE FOUR INCH COMPOUND WATER CYCLONE AS A FINE GOLD CONCENTRATOR USING RADIOTRACER TECHNIQUES

By

DANIEL E. WALSH
MINERAL INDUSTRY RESEARCH LABORATORY

School of Mineral Engineering
University of Alaska Fairbanks
Fairbanks, Alaska 99775-1180

September, 1985

MIRL REPORT NO. 70
EVALUATION OF THE FOUR INCH COMPOUND WATER CYCLONE AS A FINE GOLD CONCENTRATOR USING RADIOTRACER TECHNIQUES

By
DANIEL E. WALSH
MINERAL INDUSTRY RESEARCH LABORATORY
School of Mineral Engineering , University of Alaska Fairbanks
Fairbanks, Alaska 99775-1180

September, 1985

ABSTRACT

A 4 inch compound water cyclone, CWC, was tested to evaluate its gold recovery characteristics when processing minus 3/16 inch, run-of-pit, placer material. Neutron activated placer gold particles (841 to 37 microns) were used as radiotracers concentrator recovery; a procedure believed unique to this study. The effect on gold recovery of gold size and shape, feed pulp density, feed pressure, vortex finder clearance (VFC), CWC cone type, top-size of the feed solids, presence or absence of heavy minerals in the feed, and the quantity of -400 mesh slimes in the feed was investigated in over 300 tests.

CWC concentration ratio and the top-size of the underflow solids were both affected by cone type, VFC, and feed pressure. Gold recovery was significantly affected by gold size, gold shape, and concentration ratio. These effects are complex, since significant size-concentration ratio and size-shape interactions exist. Radiotracer techniques showed gold particles had a residence time within the CWC of approximately one second, thus challenging the three stage, segregated bed theory of CWC concentration. This work suggests CWC gold recovery is a function of particle size and shape, and the water flow rate through the CWC. "Bed density" is considered important only as a thin, protective layer, which shields coarser gold particles from the entraining currents and facilitates their movement through the CWC.

TABLE OF CONTENTS

TABLE OF CONTENTS

LIST OF FIGURES

LIST OF FIGURES

LIST OF FIGURES

LIST OF FIGURES

LIST OF FIGURES

Figure **Page**

LIST OF TABLES

LIST OF TABLES

LIST OF TABLES

LIST OF TABLES

ACKNOWLEDGMENTS

The initiation and completion of this project would not have been possible without the support and advice of those persons listed below. I have chosen to state the nature of each person's contribution after their name and position so that their help can be more fully appreciated by the readers. The order of the alphabetized list implies no ranking as to the value of these persons' help, and I wish to express my deepest and most sincere appreciation to all.

I also wish to thank the Office of Surface Mining for their early funding of MIRL's hydrocyclone research, Northwest Exploration Company and GHD Inc., for their specific funding of continued CWC research, the University of Alaska's School of Mineral Engineering for providing funds for the procurement of some equipment used in this study, and the Fairbanks North Star Borough for financial support of this thesis research.

Finally, my sincerest apology to any person who may have assisted this project whom I have neglected to acknowledge.

Dr. Donald Cook, Director, MIRL; Acting Dean, School of Mineral Engineering, University of Alaska Fairbanks (UAF), who gave his advice and financial support to this project.

Edward T. Fusco, Systems Marketing Specialist and Tracie Ingersoll, Sales Engineer: Both of Canberra Industries Inc. whose help in the initial system design, equipment selection, and activation reactor selection, was invaluable.

Dr. Robin Gardner, Professor, Department of Chemical and Nuclear Engineering, N. Carolina State University, whose very early advice helped this study move forward.

Will Godbey, Graduate Student, UAF, who made readily accessible the products of his literature search of fine gold deposition and recovery.

Dr. Dan Hawkins, Professor of Geology, UAF, who provided advice on the statistical nature of this study.

Dr. Dan Holleman, Radiobiologist, Institute of Arctic Biology, UAF, who gave so freely, his time and advice, to a project which without his assistance and guidance would not have progressed as it did. His loan of radioisotope detection equipment greatly helped the feasibility study of this project.

Susan Husted, Clerk Specialist III, MIRL Staff, UAF, who helped edit and process this thesis.

Dr. Ron Johnson, Professor of Environmental Quality Engineering, UAF, whose advice as a member of my graduate committee and instruction through his course are very much appreciated.

Dr. David R. Maneval, Professor of Mineral Preparation Engineering, UAF, whose early advice as chairman of my graduate committee concerning both academic matters and radioisotope technology helped greatly.

William P. Miller, Associate Director, Nuclear Engineering Laboratories, University of Washington, Seattle, whose advice concerning the activation of samples and their shipment was extremely helpful. His continued assistance throughout this study and his rapid processing of our samples is acknowledged.

Gil Mimken, Support Engineer, Institute of Marine Science, UAF, who offered advice and aided in the initial installation and repair of the detection electronics.

Dr. P. D. Rao, Professor of Coal Technology, UAF, who initially involved me in this project and whose advice and support as a graduate committee member throughout this project is gratefully acknowledged as is his instruction in the many courses he taught during both my undergraduate and graduate years at UAF.

Jane Smith, Coal Petrologist, MIRL Staff, UAF, whose assistance with the graphics of this thesis is greatfully acknowledged.

Dr. Dana Thomas, Professor of Mathematical Statistics, UAF, whose advice as to the statistics and experimental design of this project was invaluable, as was the instruction I received through his statistical analysis course.

Carol Wells, Word Processing Specialist, MIRL Staff, UAF, who did the majority of the word processing of this thesis.

Wu, Ming-Chee, Graduate Student, UAF, who assisted this project by optically sorting gold particles and by redrawing several plots.

A final thanks to the remaining MIRL faculty and staff who assisted this project in many small ways.

INTRODUCTION

Beginning in 1981, the Mineral Industry Research Laboratory, MIRL, began a research project in order to investigate the applicability of concentrating hydrocyclones as fine gold recovery units. The project, in its early stages, was funded by the Office of Surface Mining and the research initiated by Dr. P. D. Rao, whose familiarity with coal processing and coal washery design led him to believe that the compound water cyclone (CWC) could prove to be a reliable, inexpensive, fine gold concentrator.

In particular, the subsequent studies focused on the effectiveness of the CWC to recover fine gold lost by conventional sluice box systems and also gold from such deposits as the Cape Yakataga, Alaska, beach sands, whose size distribution and flatness greatly reduces its recovery by large scale gravity concentration methods. Fine gold here is defined to mean not only that gold finer than 40 mesh (420 microns), but also gold whose low shape factor decreases sluice box recovery of even the coarse size fractions.

Preliminary investigations were conducted using a 2.75-inch concentrating cyclone constructed of pyrex glass to test free gold recovery from placer gravels sampled at three mines located in interior Alaska. Free gold recoveries ranged from 84% to 99% using two stages of concentration to attain overall concentration ratios of approximately 25:1. Testing also revealed the concentrating cyclone performed well for concentrating heavy minerals of density greater than 3.3 and coarser than 270 mesh.

Encouraged by these initial findings it was decided to assemble a pilot scale, concentrating cyclone system with which to conduct both laboratory and field studies. After consulting with Cyclone Engineering Sales Ltd. of Edmonton, Alberta, Canada, two 4-inch compound water cyclones, one 4-inch classifying cyclone, a 2-inch slurry pump, and associated hardware were purchased and the assembly of the two stage, pilot plant was completed in July, 1982 (Figure I-1). The test system was designed for easy disassembly and transport.

Laboratory testing of the CWC pilot plant included single stage concentration of various feed materials. These included a gold bearing beach sand and synthetic feed composed of a barren beach sand with added gold of known size. The primary purpose of these laboratory tests was to determine operating parameters for the CWC, which would be acceptable for field testing. Laboratory recoveries of fine free placer gold ranged from 27% to 61% and seemed to indicate a large influence of the gold's shape on its recovery, also the necessity for low concentration ratios (≤10:1) in order to achieve higher recoveries.

In June, 1983, the pilot plant was transported to and operated at a placer gold mine in the Circle mining district, Alaska. In this one case, a free gold recovery of 92% was realized with a concentration ratio of 13:1 in single stage operation, while processing minus 20 mesh (840 micron) sluice box tailings at the rate of 0.8 tons dry solids per hour.

A similar field test conducted in 1984, processed minus 1/8 inch (3 mm) tailings from the sluice box of a mine in the Fairbanks mining district, Alaska. Here a field recovery of only 53% of the gold lost by the operation's sluice box was realized. Reprocessing the field, CWC concentrate in the laboratory with a subsequent stage of CWC concentration yielded a 55% recovery, or an overall recovery of 29% with a two stage concentration ratio of 33:1.

The wide spread in results of both field and laboratory work indicated the need for additional research. Throughout MIRL's research program, a literature search was carried out in order to locate information published by other CWC researchers which could help them to narrow the search for optimum CWC settings to maximize gold recovery. Though numerous references were found, most of the work, like MIRL's, consisted of single field or laboratory tests giving a general idea of what concentration ratios could be expected and exhibiting a range of recoveries similar to those found by MIRL. In none of the literature could be found a systematic study of the effects of varying cyclone parameters on gold recovery, let alone the recovery of gold of variable size and flatness.

After the completion of the 1984 field test, this author and Dr. P. D. Rao decided it was of no further benefit to proceed with additional field tests until a systematic laboratory study had been completed to evaluate critical operating variables of the CWC and their influence on gold recovery. From their previous sample reduction-analysis they realized that the large factorial experiments they envisioned would be unreasonable, perhaps even unmeaningful, given standard sampling techniques and the experimental error introduced by subsequent stages of concentration, analysis, and the particulate nature of the gold. Therefore, it became the object of this author's research not only to evaluate the CWC systematically, but to research and if possible develop a system to simplify the process of particulate gold recovery analysis for gravity concentration processes.

After conducting a literature search and obtaining advice from others, it was concluded that the use of a radioisotope, as a tracer in the cyclone system, could provide the answer. Radioisotopes are used widely throughout the disciplines of engineering, including mineral preparation engineering, in a variety of research as well as industrial applications. Using a borrowed 3" x 3" NaI(Tl) gamma detector and a scaler, the pulp streams of the closed circuit, 4 inch CWC, test loop were monitored for background

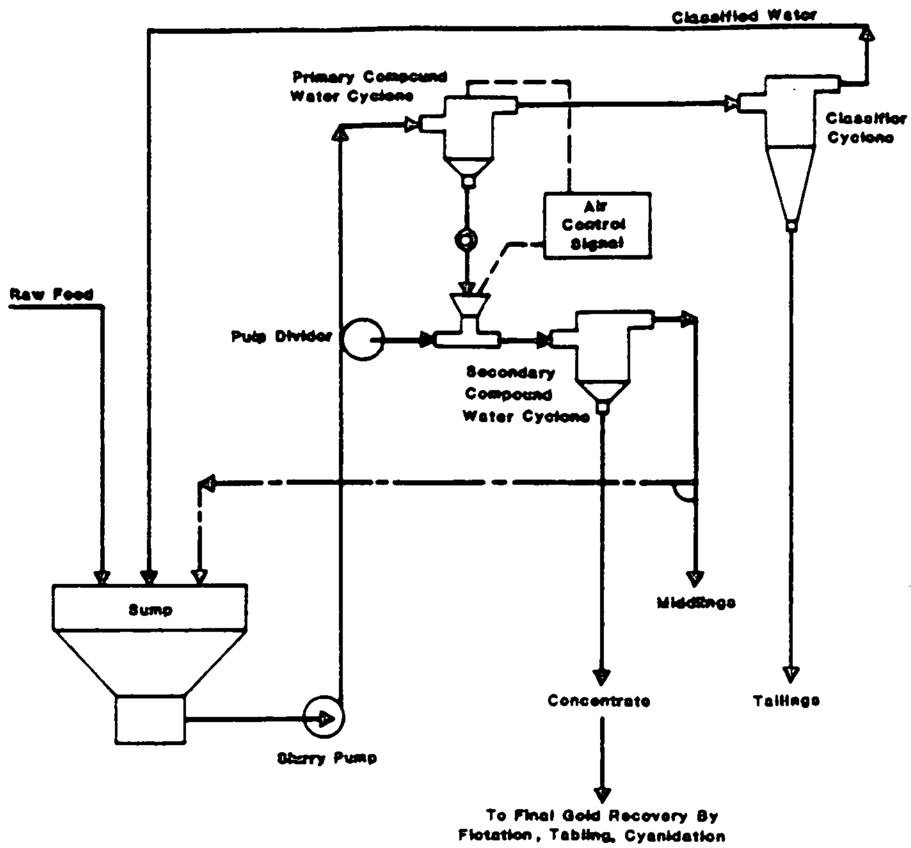

Figure I-1. Schematic of MIRL's two-stage CWC pilot plant.
(Cyclone Engineering Sales Ltd., 1978)

radiation noise. Calculations were made to estimate the radioisotope yields at various activation times for given gold masses in the range of interest. CWC pulp flow rates and various detection chamber dimensions were examined with respect to particle residence time and detectability. Counting statistics were also investigated. All of the preliminary work indicated that not only could activated placer gold serve as a tracer in the cyclone system, but that this system could greatly increase the number of tests which could be completed in a given time period. It also showed promise of reducing the experimental error within factorial treatments of the experiment.

Based on this information, MIRL, in the summer of 1984, ordered the required detection electronics and scintillation detectors from Canberra Industries of Meriden, Connecticut. The following chapters of this report examine not only the data generated by this analytical system and discuss its implications; they also describe the system's development, including design and statistical considerations. Additionally, the early chapters of this thesis review contemporary views of gravity recovery of particles of various size, shape and density, and the research and development to date concerning the compound water cyclone.

CHAPTER 1

PROPERTIES OF PLACER GOLD INFLUENCING ITS DEPOSITION AND RECOVERY

Introduction

In all cases, the size distribution and shape of placer gold particles found in an alluvial placer are a function of the deposit's geologic and hydrologic history. This is also true of the bulk of the detrital material and other valuable minerals which are associated with the deposit. In general, however, mineral particles exposed to erosional forces are continuously reduced in size by natural comminution processes, while gold particles in the same environment become more rounded and progressively flattened because of the element's inherent ductility.

Drs. Cook and Rao (1973) investigated the gold from four types of alluvial deposits as characterized by their water carrying capacity and the associated detrital matrix. They used a variety of laboratory recovery processes to concentrate the gold including elutriation, heavy liquids, electrostatic and magnetic separation, froth flotation, amalgamation and superpanning. The four deposit types they analyzed and their observations are listed below:

(1) Creek Deposits: The valuable component generally constitutes only a minor portion of the mass; the quartz sand with "black sands" make up another portion; the material larger than sand size is the major portion; and all of this material can have various shapes, weights and specific gravities.

Native gold is economically the most important element in these deposits, but other valuable components include platinum, cassiterite, cinnabar, monazite, columbite, ilmenite, zircon, and gems such as diamond, sapphire and ruby. Five placer creeks in Alaska contained from 1% to 33% of their total gold as minus 60 mesh (0.25 mm) gold.

(2) River Bar Deposits: These deposits differ from creek deposits primarily due to the carrying capacity of the water. The shallower gradient of river systems limits their carrying capacity as to particle size so that a more uniform size distribution is present.

The bars are usually formed during periods of highwater in zones of lower stream velocity where the settling velocity of the transported particle is greater than the horizontal velocity of the stream. Gold particles are usually finely divided and difficult to recover, but are similar to the sand particles in that they are of a more uniform dissemination.

(3) Beach Deposits: Like other alluvial deposits, the mineral composition of present and submerged beaches is dependent upon the nature of the source rock from which the detrital material was derived. The source may be from the adjacent sea floor, outcrops along the coast line or more normally from material transported by rivers and streams to the coast line.

These deposits are similar to river bar deposits in regard to uniformity of particle sizes, but differ in percentage of heavy mineral constituents present due to the reconcentration action of the water. Gold in these deposits is generally in the size range of 28 to 150 mesh, but is characterized by an extremely thin, flaky shape that limits recovery by conventional gravity methods.

(4) Off-Shore Deposits: These deposits may take the form of drowned placers of other origin, reconcentration of drowned placers by bottom currents and wave action or extremely fine particles carried some distance off-shore by streams transporting to the coastline. Depending upon the type of deposit, the size distribution of the detrital material including heavy minerals and precious metals, could be similar to or a combination of the other deposits previously discussed.

While placer operators may keep records of the size distribution of the gold they recover, no information is generally available concerning the fine gold content of the placer gravel they process due to the extreme difficulty of analyzing a sufficiently large head sample by means capable of recovering fine gold. Most often properties are evaluated by small scale production practices in order to determine the economics of the ground; the rationale being, "if it can't be recovered by a viable production process, it doesn't matter if it's there or not". The fact that most placer gold properties are evaluated by conventional panning, short sluices, or rocker boxes, all inefficient at recovering gold below 100 mesh, leads in most cases to an underestimation of the fine gold in placer deposits.

In a survey of Alaska's placer gold production records, from selected areas, Cook and Rao (1973), concluded that -100 mesh (150 microns) gold represents from 0% to 5% of the total gold recovery for the state. Cook also estimated sluice gold losses at between 10% and 40% depending on the deposit under production and the expertise and experience of the operator. Wang and Poling (1983) note that gold finer than 200 mesh (74 microns) can vary from a trace to 80% or more. They also cite that tests at several Chinese placer deposits have indicated that the -200 mesh gold varied from 2% to 50% and that placer gold finer than 60 mesh (250 microns) varied from 3% to 95% among 21 placer mining areas in the Soviet Union.

Settling Velocity Theory

A useful concept in understanding the characteristics of gold particles and of associated minerals found in the various alluvial placer deposits throughout the world is that of hydraulic equivalence. According to Tourtelot (1968), hydraulic equivalence is the concept that describes the relationship between different mineral grains of varying size and specific gravity which are deposited in the same hydrodynamic environment. Mineral grains are said to be hydraulically equivalent if they have the same settling velocity under the same conditions. In some Soviet literature the term "hydraulic size" is used as a synonym for settling velocity. Though settling velocity is a basic component of the theory of the dynamic process of alluvial deposit formation, it cannot in itself explain the whole of their depositional history. It can, however, serve as a useful guide to the expected sizes of minerals of different specific gravity that will tend to be simultaneously deposited in a given alluvial environment.

Sedimentation theory, and hence the concept of hydraulic equivalence, is based on the laws of fluid mechanics. These laws are derived for spherical particles and consider a balance of the buoyant, gravitational, and viscous drag forces acting on them.

Stokes' Law states that settling velocity increases as the square of the diameter of the particle. With decreasing particle size the settling velocity drops off very rapidly. Settling velocity also varies with density. This law is applicable for particles with Reynold's numbers (Re) less than one; for particles so small that the liquid flows around them in a laminar fashion (this corresponds to ≤120 mesh for quartz and ≤270 mesh for gold).

$$Re = \frac{Wd}{\mu}\rho$$

W = settling velocity

d = diameter of particle

ρ = density of fluid

μ = absolute viscosity of fluid

Stokes' Law is then stated as:

$$\text{Terminal settling velocity} = \frac{g(\rho_s - \rho)\, d^2}{18\mu}$$

g = acceleration of gravity, 981 cm/sec^2

ρ_s = density of solid, gm/cm^3

ρ = density of liquid, gm/cm^3

d = particle diameter, cm

μ= absolute viscosity of liquid, centipoise

Using Stokes' law, the terminal velocities are:

For quartz: 8990(d^2) cm/sec

For gold: 92,650(d^2) cm/sec

Newton's law applies to coarser spherical particles that settle in the turbulent flow regime. Newton's Law states that terminal velocity varies as the square root of the diameter of a particle. Consequently increase in settling velocity is not as rapid with size as it is with Stokes' Law. This Law applies to particles with Reynold's numbers greater than 1,000 (this corresponds to ≥6 mesh for quartz and ≥14 mesh for gold). For Newton's law:

$$\text{Terminal settling velocity} = \left[\frac{g3.33\,(\rho_s - \rho)d}{\rho}\right]^{1/2}$$

g = acceleration of gravity, 981 cm/sec^2

ρ_s = density of solid, gm/cm^3

ρ = density of liquid, gm/cm^3

d = particle diameter, cm

According to Newton's law, the terminal velocities are:

For quartz: [5390(d)]$^{1/2}$ cm/sec

For gold: [55,500(d)]$^{1/2}$ cm/sec

Between the ranges of Stokes' Law and Newton's Law, there is no single equation that can be applied to calculate settling velocity. Such settling velocities can be determined indirectly, by iteration, using the equation (derived from Cook, 1979):

$$\text{Terminal settling velocity} = \left[\frac{4g(\rho_s - \rho)d}{3\rho\, C_D}\right]^{1/2}$$

g = acceleration of gravity, 981 cm/sec^2

ρ_s = density of solid, gm/cm^3

ρ = density of liquid, gm/cm^3

d = particle diameter, cm

C_D = drag coefficient

The drag coefficient, C_D, is a function of particle shape and the flow characteristics about the particle. Values of C_D are generally available in graphical form as plots of C_D vs. the Reynold's number for given shapes. Such a graph is shown in Figure 1-1.

Another concept that is useful for the understanding of gravity concentration and placer formation is the free settling ratio; the ratio of diameters of particles with equal settling velocities. The general expression for the free settling ratio can be derived from Stokes' and Newton's Laws and can be stated (Wills, 1979):

$$\text{Free Settling Ratio} = \frac{d_l}{d_h} = \left[\frac{\rho_h - \rho_f}{\rho_l - \rho_f}\right]^n$$

d_h = diameter of higher density particle

d_l = diameter of lower density particle

ρ_h = density of higher density particle

ρ_l = density of lower density particle

ρ_f = density of surrounding fluid

n = 0.5 for particles obeying Stokes' Law
1.0 for particles obeying Newton's Law

As an illustration, for particles of gold and quartz, calculations show that the free settling ratio is 3.2 for particles in the Stokes' Law range and 10.3 in the Newton's Law range. Thus, in the Newton's Law range, a 2 mm sphere of gold will settle in water as fast as a 20.6 mm (3/4") sphere of quartz. The greater the free settling ratio, the easier is concentration. Particles which obey Newton's Law are more easily concentrated then those obeying Stokes' Law.

Measures of Gold Particle Shape

Not only does the size and specific gravity of a mineral grain affect its settling velocity, but shape too has a pronounced influence. For particles which obey Stokes' law, the effect of particle shape is proportional to the degree that the grain shape departs from that of a sphere (Tourtelot, 1968). Several ways exist for describing the non-sphericity of particles and the more common ones are listed below. In describing these, the following convention of particle dimensions is adopted; $A \geq B \geq C$, so that for nonequidimensional grains, C corresponds to the grain thickness and A and B dimension the grain's surface of largest projected area.

(1) The Flatness Factor (F.F.) is defined as: F.F. = (A+B)/2C and can be thought of as the arithmetic average of the two largest dimensions divided by the particle thickness. The flatness factor equals 1 for a sphere or cube and gets progressively larger as particles become flattened (Shilo and Shumilov, 1970).

(2) Heywood's (1939) shape constant,

$$K = \frac{\text{Particle volume}}{(\text{projected diameter})^3}$$

where the projected diameter is defined as $(4(AB)/\pi)^{0.5}$. K equals 0.524 for a sphere and becomes smaller as the flatness of the particle increases.

(3) Coefficient of flattening, K_f, is defined by Saks (1975) as: $K_f = \frac{\sqrt{AB}}{C}$

(4) Corey's Shape Factor (C.S.F.) is defined as: C.S.F. = $C/\sqrt{AB}$ and can be thought of as the particle thickness divided by the geometric average of the particle's other two dimensions. Corey's shape factor equals 1 for a cube or sphere and decreases as the flatness of a grain increases (Corey, 1949).

Effects of Gold Particle Shape on Settling Velocity

Throughout this paper, Corey's shape factor is used as the descriptive measure of the sphericity of a grain. Figure 1-2 shows the effect of increased flakiness of particles on their settling velocity. It can be seen that a particle having a 1 mm sieve diameter and a 0.3 shape factor (C.S.F.) will settle at the same velocity as a 0.55 mm sphere. Lower shape factors of gold particles erode the advantage of having a large difference in densities between quartz and gold. Obviously, the farther the gold's shape factor is from unity the more difficult will be its concentration.

S. Ye. Saks (1975) suggests that once gold particles have settled to the bottom of a flowing stream their thickness is the determining factor in their sorting due to remobilization hydrodynamics. Saks goes on to state: "Thus in identical conditions the hydraulic equivalence of different gold particles is determined mainly by their thicknesses, and hydrodynamic sorting will ultimately be governed both by the hydraulic size and by the smallest dimension C. Consequently, in placers with well-sorted fine gold in genetically homogeneous regions, the dimension C should alter only over a narrow range ($C \approx$ constant)". His statistical data lends support to his argument. He argues that if C is constant, or nearly so, then the coefficient of flattening ($K_f = \sqrt{AB}/C$) must be proportional to AB, the mean sieve dimension. Therefore, any increase in K_f is compensated by an increase in A or B or both in order to preserve the hydraulic equivalence of the gold particles of various sieve sizes. Thus, for a well sorted, homogeneous deposit, one would expect to find a broad range of flatnesses of gold grains with the larger screen fractions showing the lower Corey shape factors.

Table 1-1 and Figure 1-3 show the work of Shilo and Shumilov (1970). These Soviet scientists measured the settling velocity of gold spheres of mass ranging from ~600 mg to 2 mg. They then progressively flattened these spheres to obtain particles with lower Corey shape factors and larger sieve sizes, measuring the settling velocity at each stage of flatness. It is quite clear that although each particle remained

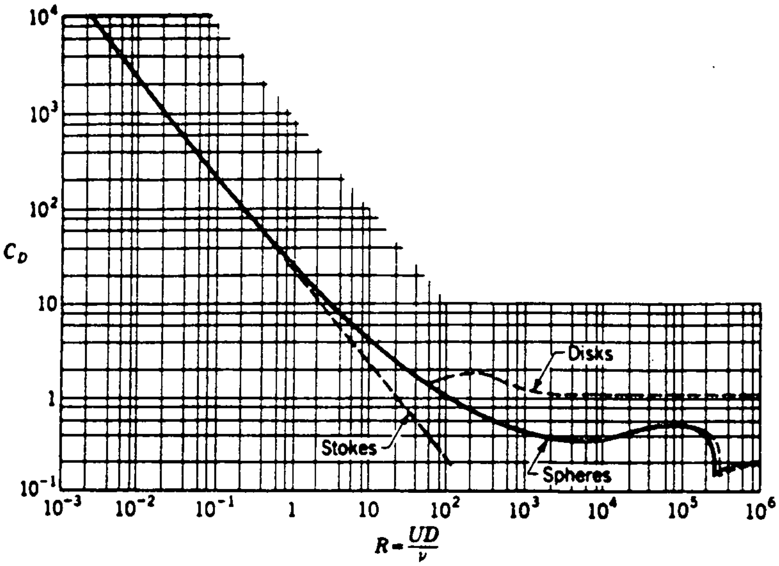

Figure 1-1. Drag coefficient (C_D) for spheres and circular discs as a function of the Reynolds Number. (Streeter and Wylie, 1975)

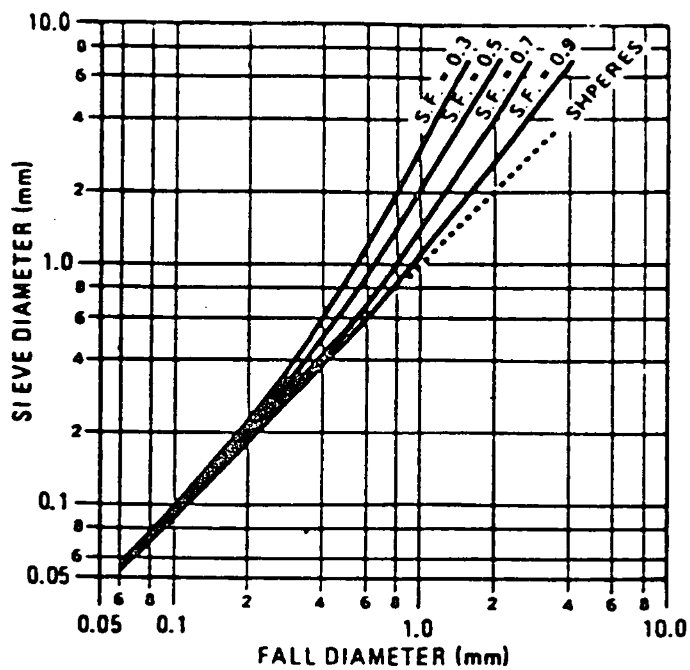

Figure 1-2. Relationship between particle nominal (sieve) diameter and fall diameter. (Wasp, 1977)

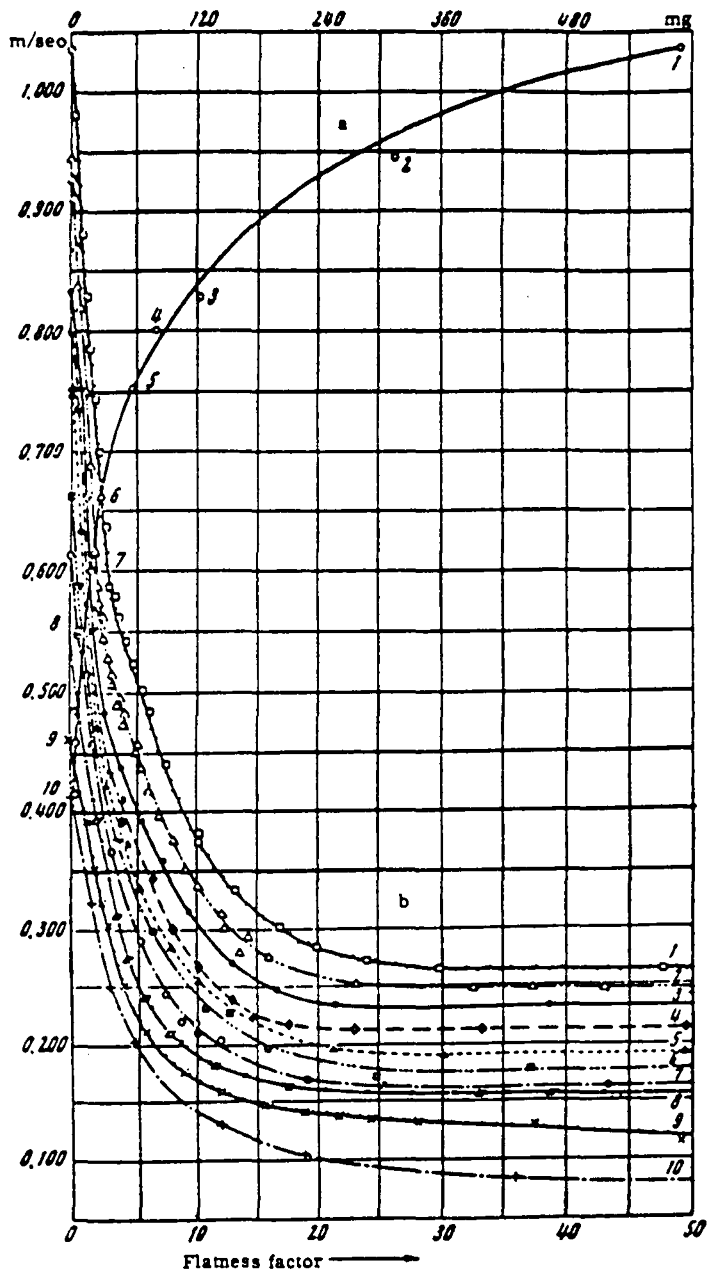

Figure 1-3. Mass of gold particles (a) and their settling velocity (b) versus their flatness factor. (Shilo and Shumilov, 1970)

Table 1-1

Main characteristics of gold particles used in laboratory settling velocity experiments. (from Shilo and Shumilov, 1970)

Particle No.	Particle Wt. (mg)	Particle Flatness Factor (FF) Beginning of Test	End of Test
1	586	1	47.5
2	316	1	42.6
3	122	1	38.3
4	79	1	47.9
5	57	1	47.9
6	28	1	59.0
7	20	1	54.7
8	9	1	51.4
9	5	1	48.6
10	2	1	35.3

FF = (A+B)/2C A,B, and C are length, width, and thickness respectively.

constant in mass, their settling velocity was significantly decreased by even a slight increase in their flatness. The authors note that the settling velocity of large flat particles may be the same as that of small, but more spherical ones. They foreshadow Sak's 1975 conclusions by stating that this is evidently the reason for the range of gold particle sizes found in the "enriched pockets" of many placers, though not the only reason. They continued their work by looking at the gold from 12 placer deposits in the northeastern part of the Kolyma region and found that native placer gold particles of various sizes and shapes followed the same pattern as shown for their laboratory results (Figure 1-4).

Shilo and Shumilov state:

> "According to various investigators, the vertical velocity component of streams may be as much as 5% to 10% of the horizontal component. In view of these values and the fact that the flood velocities of placer forming streams reach 2 to 3 m/sec, we can take a value of 0.14 to 0.3 m/sec for the vertical component. This value is in complete agreement with experimental data since few particles have settling velocities greater than 0.3 m/sec. Thus, they remain suspended at high values of the vertical velocity component. Thus, particle shape is of genetic significance in placer formation. Our example again shows the profound inaccuracy of the idea that gold is divided into active and passive size fractions. All gold fractions, regardless of their size, are relatively active if they have [a very low Corey's shape factor of not more than 0.2]."

Additional work on the hydraulic equivalence of a variety of placer minerals has been conducted by Shumilov and Shumovskiy (1975). They concluded the following:

1) In addition to specific gravity, the settling velocity of mineral grains is strongly influenced by size, shape, and surface roughness.

2) In the case of gold and quartz, their settling velocity depends largely on shape and surface roughness.

3) The fact that the settling velocity of grains of placer minerals less than 0.2 mm in size is almost independent of specific gravity suggests that such particles may accumulate at a considerable distance from their source area.

Despite the unifying concept of hydraulic equivalence, other complex forces acting during alluvial placer formation make each placer deposit unique. This in turn demands that the recovery plant be custom designed for each deposit. This is especially true for placer gold deposits because of the broad range of gold sizes and shapes commonly found.

Gold Recovery Considerations

In the past 25 years, several new methods for processing various placer ores have been developed. Most of these, though not all, have been developed outside the United States, where placer deposits are mined and processed for economic minerals other than gold such as cassiterite, zircon, diamonds, and rutile. Improved recoveries of fine mineral fractions have been achieved by employing stage gravity recovery as well as froth flotation and magnetic and electrostatic separation. Many of these newer methods could be applied to placer gold recovery as well. But despite the known and proven technologies which have been developed, processing technology of the U.S. placer gold mining industry has changed very little since the heyday of the gold dredges. Gravity technology in those days consisted primarily of riffled sluices and amalgamation, though jigging was used to a limited degree. Because of this, fine gold recovery by operations today has improved very little over those achieved several decades ago. As an example, an extremely well regulated Alaskan sluicing operation may recover gold down to 100 mesh (150 micron), but overall, the cutoff point

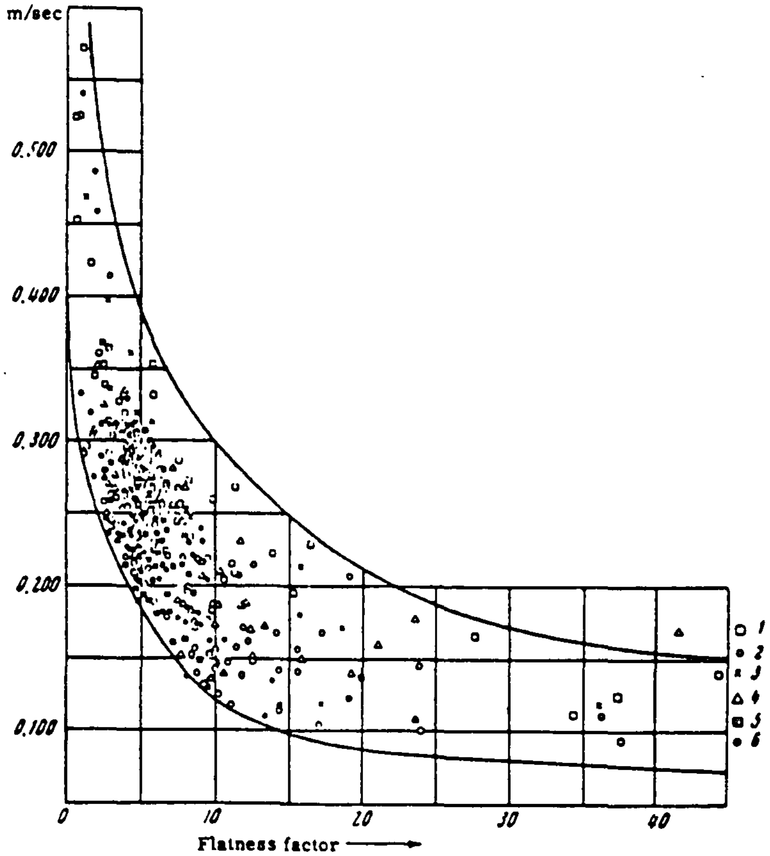

Figure 1-4. Settling velocity of natural gold particles versus their flatness factor. Gold from six placers in the northeastern Kolyma region. (Shilo and Shumilov, 1970)

would be closer to 40 or 60 mesh. Though sluicing operations may be all that is required for deposits where only coarse gold exists, their application as the sole recovery unit in areas rich in fine placer gold is extremely inefficient.

There are several characteristics of placer gold that makes it more difficult to recover despite the very large differences in specific gravity between gold and the associated placer minerals. The first of these characteristics is shape. All that was said earlier regarding gold's shape and its hydraulic equivalence with respect to placer formation applies as well to its concentration by gravity methods. Though it has long been known that flaky gold particles are much more difficult to recover than more spherical ones, little quantitative data describing this phenomena for individual recovery units exist in the literature. It is felt that the analytical technique used by this author and described in detail later in this thesis can be applied to study such effects accurately.

Secondly, the porous nature of placer gold is detrimental to its recovery. While other placer minerals such as ilmenite, rutile, cassiterite, etc., are compact and non-porous, placer gold can be honeycombed with cavities and pores, which may be filled with lower density minerals or clays or even air, significantly lowering the grain's effective specific gravity. Figure 1-5 shows the reduced recovery observed on a concentrating table due to grain shape and surface porosity.

Thirdly, the natural hydrophobicity of placer gold causes floatability which is in direct conflict with gravity concentration. According to Poling and Wang (1983):

> "There has been much controversy in the scientific literature as to whether pure, clean gold surfaces are naturally hydrophobic or barely wetted by water. Native gold surfaces are normally hydrophobic or floatable due to contamination by organics or due to leaching of impurities to make the surface consist of more nearly pure gold. Because placer gold normally has significant silver impurity, the lower the fineness, the less likely the gold will be hydrophobic ... Leaching of Ag from the surface regions also causes porosity of the placer

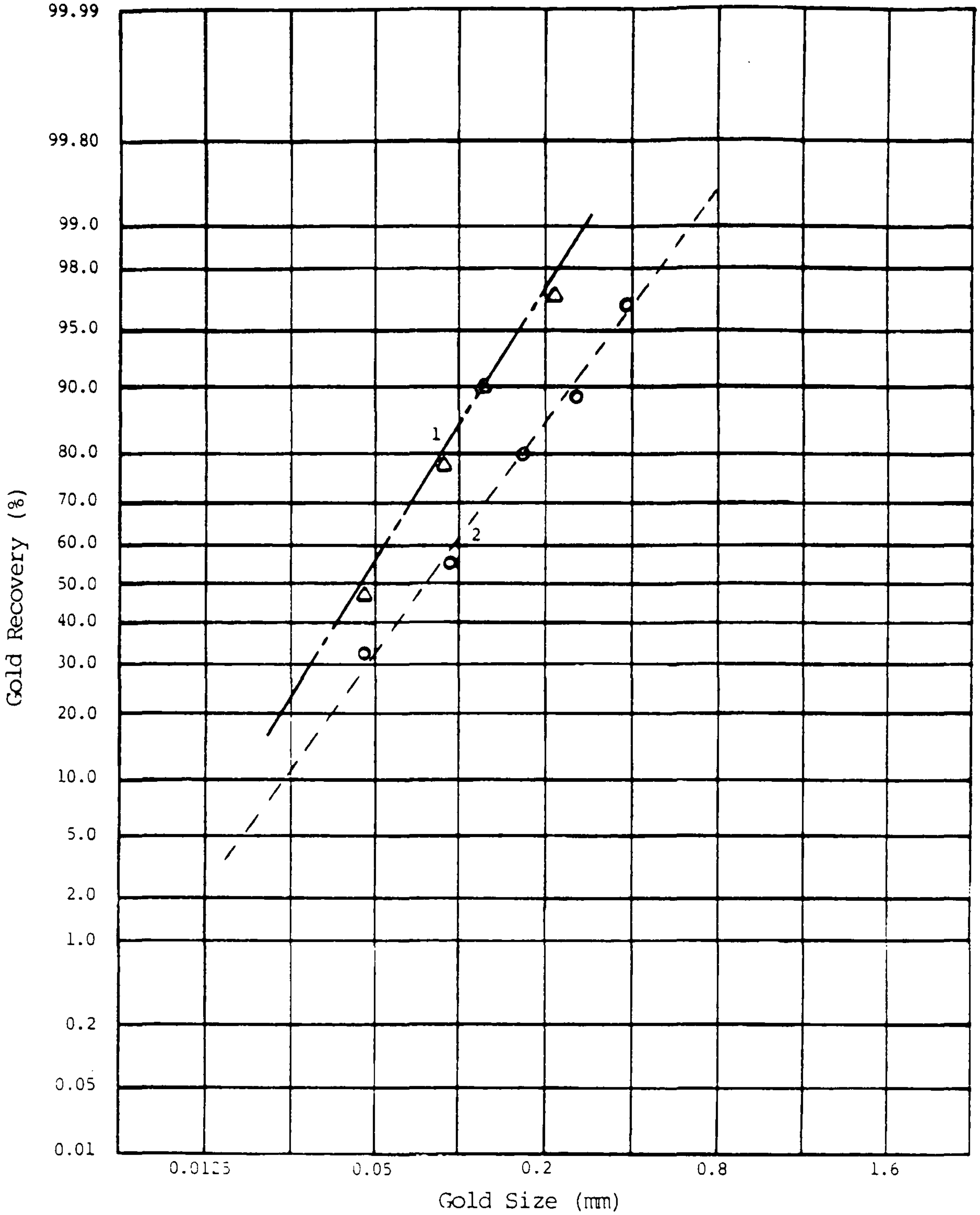

Figure 1-5. Gold recovery on a concentrating table by size for (1) laminar, lumpy grains and (2) porous, needle-shaped grains. (Zamayatin, 1970)

gold, which further deteriorates gravity concentration."

This property of placer gold is particularly apparent once the gold surface is allowed to dry, and is a point to keep in mind if stage processing is practiced.

Bearing in mind those points discussed above, a variety of gravity concentrators have been proposed for the recovery of placer gold. Figure 1-6 shows the recovery characteristics of four such concentrators with respect to gold size. The effect of shape was not addressed. The reader is referred to Mildren (no date) and Guest (1980). Both give an excellent survey of gravity concentrators. Though it is not deemed relevant to this thesis to describe each device as is done by Mildren and Guest, the devices are listed below by Mildren's classification into high, medium and low capacity units.

A. High Capacity Units
   1. Jigs
   2. Pinched Sluices
      a. Reichert Cone
      b. Wright Impact Tray
   3. Spirals
   4. Sluice Boxes

B. Medium Capacity Units
   1. Centrifugal Concentrating Bowls
      a. Knudsen Bowl
      b. Ainlay Bowl
      c. Knelson Bowl
   2. Bartles-Mozley Table
   3. Johnson Type Cylinder Concentration
   4. Plane Table
   5. Riffled Belt (Strake) Concentrator
   6. Heavy Media Separation
   7. Concentrating Cyclone

C. Low Capacity Units
   1. Concentrating Tables
      a. Deister Table
      b. Wilfley Table
      c. Gemeni Table
   2. Elutriators
   3. Spiraled Wheels
   4. Shaken Bed Type Concentrators
   5. Vanners
   6. Chance Cone Separators
   7. Diamond Pans

This author has taken the liberty of inserting two devices into Mildren's scheme. These are the Knelson Bowl and the Gemeni Table; both devices have come into prominent use in Alaska over the past 2-3 years. One other point concerning Mildren's classification, the author feels that concentrating cyclones should be classified as high capacity units due to their processing volume : mass flow rate ratio.

The importance of gravity concentration processes are often overlooked, but as recently as 1973 in the United States, the value of ore treated by gravity methods was more than double that treated by froth flotation. It is especially important in the treatment of gold placer ores, whose grade may be as low as 0.005 oz/yd^3, and which may require concentration ratios on the order of 10^5 to 10^6. Though the capital and operating costs of gravity concentration depend on which process is used, it is always less expensive than other methods of concentration (magnetic, flotation, leaching, ...) and is often a prerequisite for bulk reduction, prior to these other beneficiation processes.

With these points in mind, it became MIRL's intention to evaluate the compound water cyclone as a gravity concentrator for fine gold. It was felt that the CWC would be readily adaptable to the current technology of Alaska's placer mining industry; that they could be used for direct processing of screened run of pit placer material or for retreatment of sluice box tailings. The capital and operating costs of CWCs are low, an important point to Alaska, where many mines are family owned and operated. Additional factors favoring the investigation of compound water cyclones were:

1) The high shear forces active within the CWC might help liberate clay locked fine gold.

2) The enhanced gravity field within the CWC could significantly increase fine gold recovery by

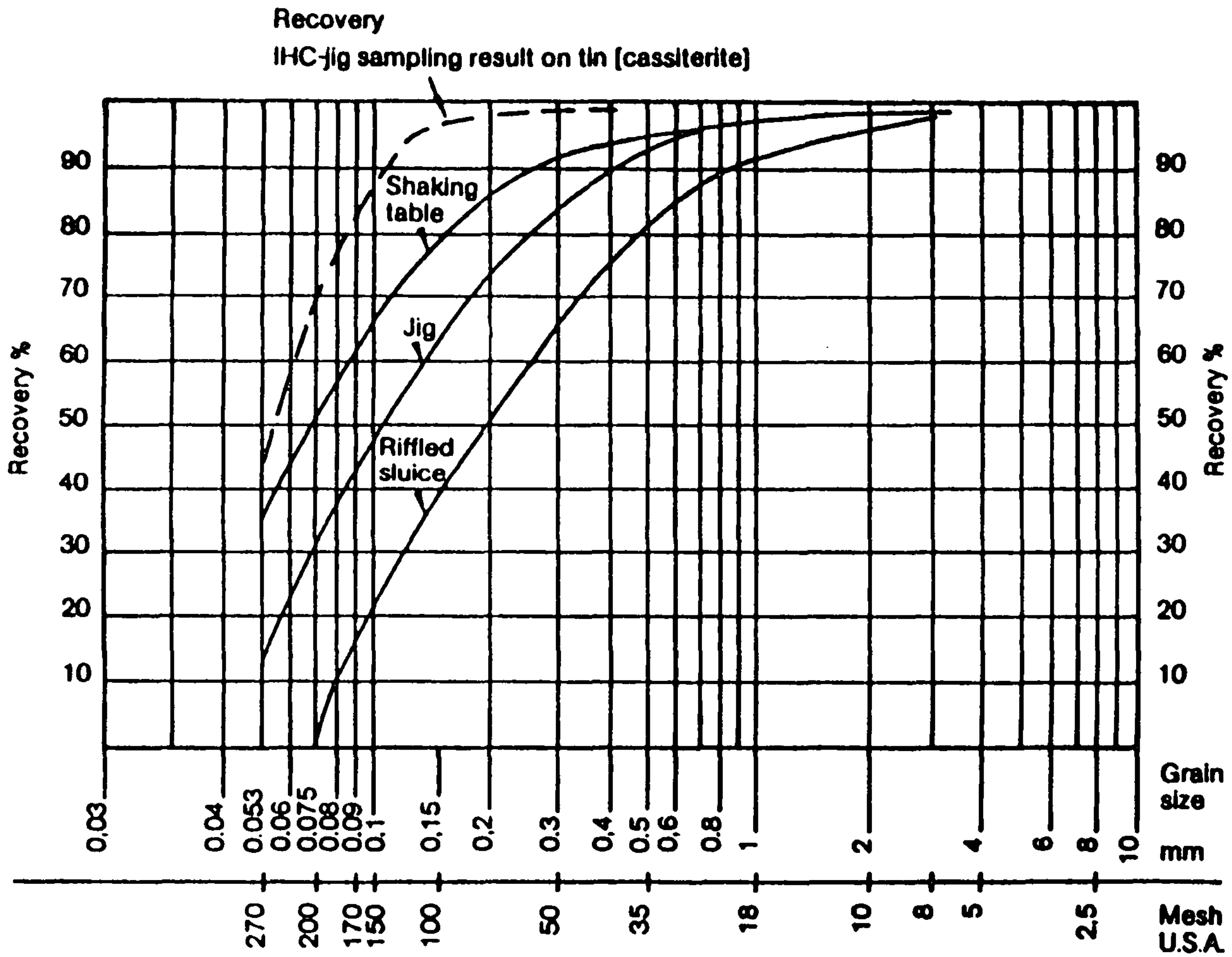

Figure 1-6. Gold (or tin) recovery versus particle size for four gravity concentrators. (Nio, 1984)

overcoming the detrimental effects of gold's shape, porosity, and hydrophobicity.

3) The high shear and gravity forces within the CWC could cause the effect of slimes on gold recovery to become less important, thus allowing for the CWC's application in high percentage recycle operations.

4) The CWC takes a large top size of feed.

5) The CWC operates in a continuous concentration mode, requiring no "clean-up" down time.

The author saw another important reason for a detailed study of a fine gold concentrator. This was the issue of placer evaluation for fine gold. He felt that if a device capable of recovering significant amounts of fine gold and of processing sufficiently large samples could be evaluated in depth as to gold recovery versus grain size and shape, then these results could be used as a first step in accurately assessing the fine gold distribution in placer deposits.

CHAPTER 2

THE COMPOUND WATER CYCLONE

Introduction

The cyclone is a simple yet versatile device used in the treatment of fluid-solid and fluid-fluid suspensions for the purpose of separating one phase from another. Cyclones are used in both processing and pollution control, including food processing, dust collection, sludge removal from petroleum crude, and the mineral processing industry, where cyclones are extensively used in mineral and coal preparation. Historically the main use of hydrocyclones in mineral processing has been as classifiers and they have proven extremely efficient at fine size separation. They are used increasingly in closed circuit grinding operations but have many other uses, such as desliming and thickening. In 1881, the first hydrocyclone patent was granted to Bretney of the United States. The earliest published reference of the use of the hydrocyclones for thickening and classification of liquid-solid slurries, was by M.G. Dreissen in May, 1939. Dutch State Mines cyclones were introduced to the U.S.A. in 1948 and became well known for their simplicity of operation.

Hydrocyclone Structure and Application

Their basic structure is that of a top cylindrical section with a tapering hollow cone as the bottom section (Figure 2-1). The fluid stream is introduced tangentially through a peripheral inlet and is transformed into a spiral flow moving

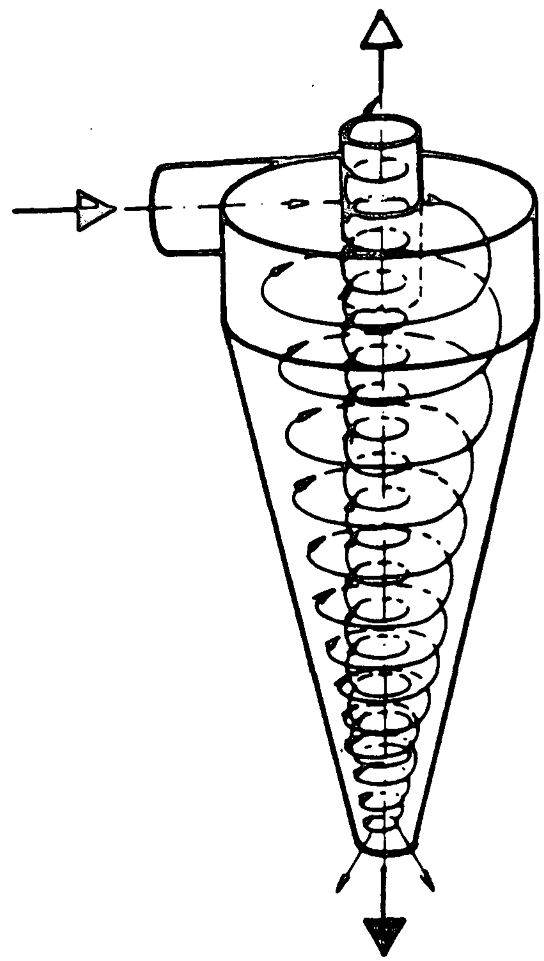

Figure 2-1. Simplified perspective view of the hydrocyclone showing the "spiral within a spiral" flow pattern. (Svarovsky, 1984)

from the inlet to the apex. The taper induces a back flow along a central core which spirals toward the inlet section, while the high centrifugal accelerations of the vortex cause the particles to separate and move in the direction of the apex (Medley, 1972). Strong centrifugal accelerations are induced, from as few as 10 G's for the average cyclone to as high as 4000 G's (Jull, 1972), the number of G's produced being inversely proportional to cyclone diameter.

The centrifugal force developed accelerates the settling rate of the particles. There is evidence to show that Stokes' law applies with reasonable accuracy to separations in cyclones of conventional design, thereby separating particles according to size and specific gravity (Wills, 1979). The tangential velocity which reaches its maximum a short distance from the center decays towards the wall. The faster settling particles move to the wall and are discharged through the apex with a small percentage of the feed water. The remainder of the feed slurry is carried out the vortex finder to the overflow discharge.

After a certain residence time, a solid grain is discharged to either the overflow or underflow product. The particle's size and specific gravity exert a major influence on this separation. The cyclone's "cut point" or separation size (generally given in ASTM mesh units, millimeters, or microns) refers to that size of a specific mineral (generally quartz) at which 50% of the grains report to each of the cyclone products. This size is often termed the d_{50} size.

Other factors which affect the cyclone's cut point, are listed by Dreissen and Fontein (1963).

(1) Shape of particles

(2) Solids concentration

(3) Feed pressure

(4) Back pressure

(5) Cyclone diameter

(6) Diameter of the feed opening

(7) Diameter of overflow opening

(8) Diameter of apex opening

(9) Length of vortex finder

(10) Cone angle

(11) Specific gravity of liquid

(12) Average grain size of particles

(13) Viscosity of the feed suspension and the liquid.

Cyclone operations can be classified according to the main characteristics of the products. The five basic operations cited are (Weyhar, 1969):

(1) Clarification - characterized by a vortex product with a minimum of particles, e.g., dust collecting cyclones.

(2) Thickening - characterized by a maximum solid/liquid ratio in the apex - product, as in the preparation of feed slurry for filters.

(3) Classification - characterized by the separation of particles into size ranges by utilizing the strong influence of the size of a particle on its terminal settling velocity. An example is its use in closed circuit grinding operations.

(4) Gravity separation in a dense medium - characterized by separating particles according to specific gravity, utilizing the opposing buoyant force acting on particles of different densities suspended in a liquid of intermediate density.

(5) Gravity separation without use of a dense liquid or a dense media - characterized by conditions emphasizing particle density.

The most important application of cyclones in the mineral beneficiation industry has been for classifying. Classifying cyclones being distinguished by a short vortex finder and small included angle 10-30°, as compared to the concentrating cyclone, which has a large included angle of 60°-180°, and a long vortex finder. Figure 2-2 shows the design differences between the two.

A cyclone cannot both classify and concentrate a feed efficiently. An increase in classification efficiency automatically results in a decrease in concentration efficiency. This correlation between concentration inefficiency and classification efficiency is understandable when one considers that, for high concentration efficiency, the cyclone is expected to make a separation in which coarse, light particles report to the overflow, and fine, heavy particles report to the underflow. This is contrary to the normal classification action of the cyclone (Bath, 1973).

Recent years have seen the development of various cyclones specifically for concentrating purposes. Their physical design is such that classification effects are suppressed and the influence of particle specific gravity is maximized. These are not heavy-medium cyclones, which have been in use in the mineral processing industry for some years, but true hydrocyclones. They were developed largely as a result of work in the coal industry, where cyclones operating with a water medium are now in wide use for upgrading fine coal.

The basic requirement for classification is the achievement of balance between the centrifugal forces accelerating the particles radially outward and the centripetal drag forces. For this purpose, relatively large vortex finder clearances are common in classification cyclones, which provide the time for particles in the central flow region to reach their terminal free settling velocity relative to the entraining water (Bath, 1973).

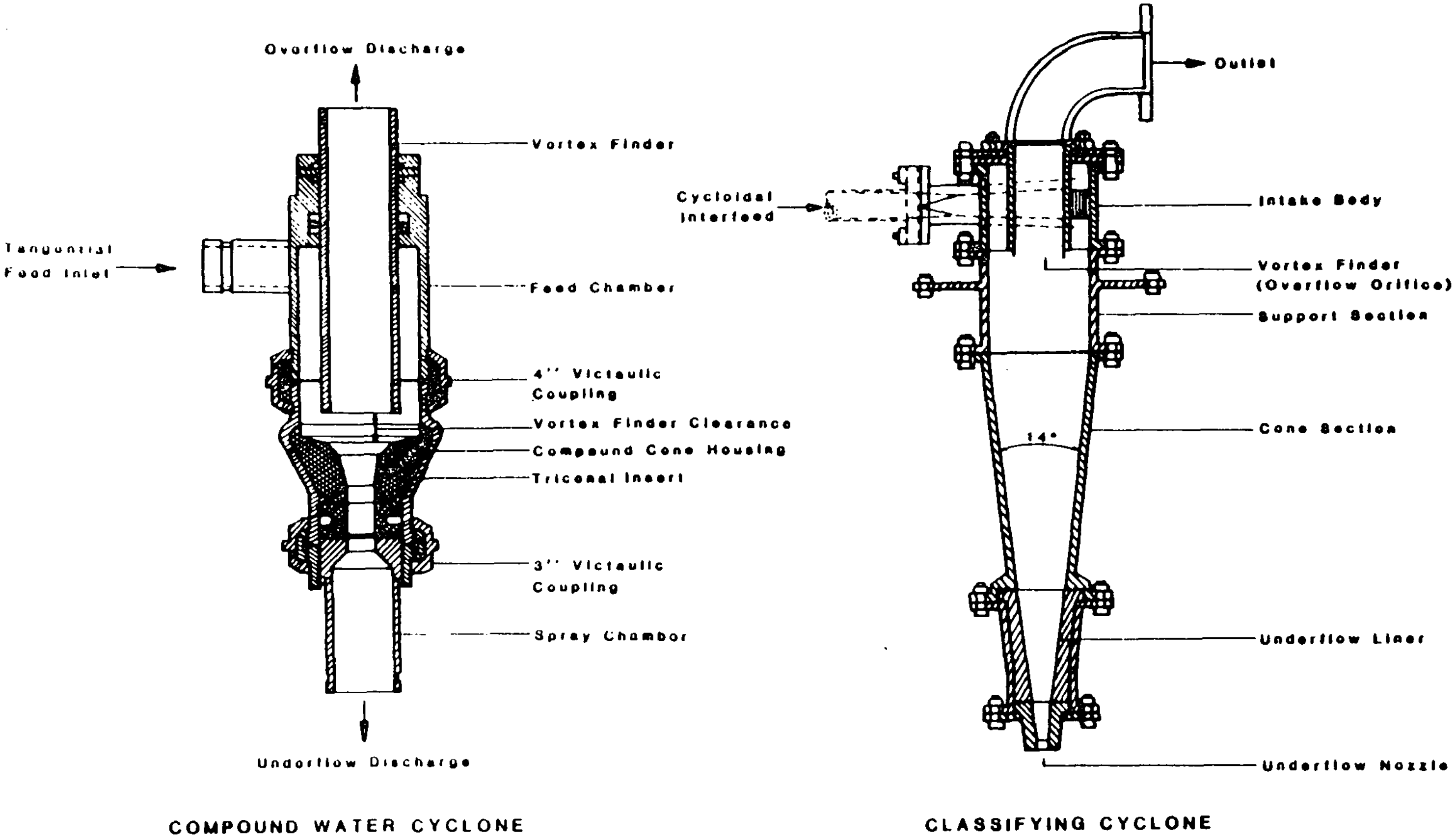

Figure 2-2. Comparison of design features between the compound water cyclone and the classifying cyclone. (Rao, 1982)

In contrast, concentrating hydrocyclones are of squat design, with wide cone angles and long, large diameter vortex finders. They are called compound water cyclones because of the compound slopes of their basal cones (Figure 2-3). They are operated to suppress classification phenomena in favor of gravity concentration effects. Briefly, their design is based on two hypotheses (Visman, 1962): (a) a particle bed stratifies according to density along the conical wall of the lower cyclone section, and (b) particles entering the central spiral flow separate during the initial phase of their acceleration in a radial direction. The former hypothesis has led to the selection of wide cone angles for concentrators, because particles stratify more reliably along the shallower wall of a wide cone than would be possible along the steep wall of a slender cone. The latter hypothesis has led to the preference for relatively short vortex finder clearances in concentrators, because this design assists in separating particles that swirl toward the vortex finder before the centrifugal mass and the centripetal drag forces acting on these particles attain equilibrium. Since it is the drag force that increases the relative influence of particle size on separation, this force must be suppressed in the operation of cyclones as concentrators (Bath, 1973).

Cyclone Hydrodynamics

It is not the intention of this thesis to give a detailed description of the hydrodynamic processes operating within the classifying cyclone. However, since research to date concerning the fluid dynamics within cyclones has emphasized that of classifying cyclones, this author will briefly discuss this past research before moving on to the discussion of the compound water cyclone. The reader is cautioned that, though flow patterns and separation mechanisms between the two types of cyclones may be similar in their upper cylindrical sections, the processes operating in their conical sections differ radically.

The most significant flow pattern in a hydrocyclone is illustrated in Figure 2-1 showing the "spiral within a spiral" (Kelly, 1982). In addition a short circuit flow occurs against the roof, due to an obstruction of the tangential velocity, and the main purpose of the vortex finder is to minimize this flow. In a compound water cyclone, with its long vortex finder, it is unlikely that short circuiting is significant and may be entirely suppressed. Because the overflow opening cannot handle the natural upflowing vortex, an eddy flow also exists in the upper section of the hydrocyclone. Figure 2-4 illustrates the above two phenomenon. In addition, two other flow features are the locus of zero vertical velocity and the second, rising from the apex and passing out through the vortex finder, is the air core, the presence of which indicates vortex stability (Figure 2-5).

The liquid velocity at any point within a simple cyclone may be resolved into three components (Kelsall, 1952), the vertical or axial component (V_a), the radial component (V_r) and the tangential component (V_t). Kelsall measured the vertical and tangential components using a dilute suspension of aluminum particles in a transparent cyclone, using an optical method. Radial velocities were calculated from continuity considerations. The results are shown in Figure 2-6.

Below the bottom of the vortex finder, envelopes of constant tangential velocity are cylinders co-axial with the cyclone (Figure 2-6c). At any horizontal level, V_t increases with a decrease in radius (r) according to the relationship:

$$V_t\,(r^n) = \text{constant (where } 0 < n < l). \qquad \text{Eq. 2-1}$$

This holds for regions near the center of the cyclone where V_t reaches a maximum value at a radius, slightly smaller than the inside wall of the vortex finder. Here the centrifugal acceleration, (V_t^2/r), also reaches a maximum value. Tangential velocity decreases as the radius further decreases and V_t is proportional to r. Above the bottom of the vortex finder there is a tendency for Equation 2-1 to persist from near the outside wall of the vortex finder to the point where V_t reaches a maximum. V_t then decreases rapidly as the wall is approached.

A conical envelope defines regions of zero vertical velocity. All liquid flows downwards towards the apex between the conical wall and the envelope of zero vertical velocity (Figure 2-5). All liquid between the envelope and the axis flows upwards, towards the vortex finder.

Compound Water Cyclone Development and Operational Theory

The compound water cyclone is not a new wet concentrator. It was developed in the late 1950's by Dr. Jan Visman through research sponsored by Canada's Department of Energy, Mines, and Resources. Since its development, Dr. Visman has written numerous research articles describing its application in coal washery design (Visman, 1962, 1963, 1967, 1971), as well as others to be discussed later in this chapter, which describe the CWC's use in extracting heavy minerals. In the early 1960s Cyclone Engineering Sales Ltd. (CES) of Edmonton, Alberta, Canada, was granted the licensee privileges to the Visman Compound Water Cyclone and subsequently sold the device's U.S. patent rights to McNally Pittsburgh Manufacturing Corporation (M-P), a large coal washery design firm. The following description of the operating principles of the CWC is a synthesis of the views developed from the research and development efforts of Dr. Jan Visman, CES, and M-P. Views other than these are noted in the text.

The compound water cyclone has a short cylindrical section fitted with one of the three compound cones (Figures

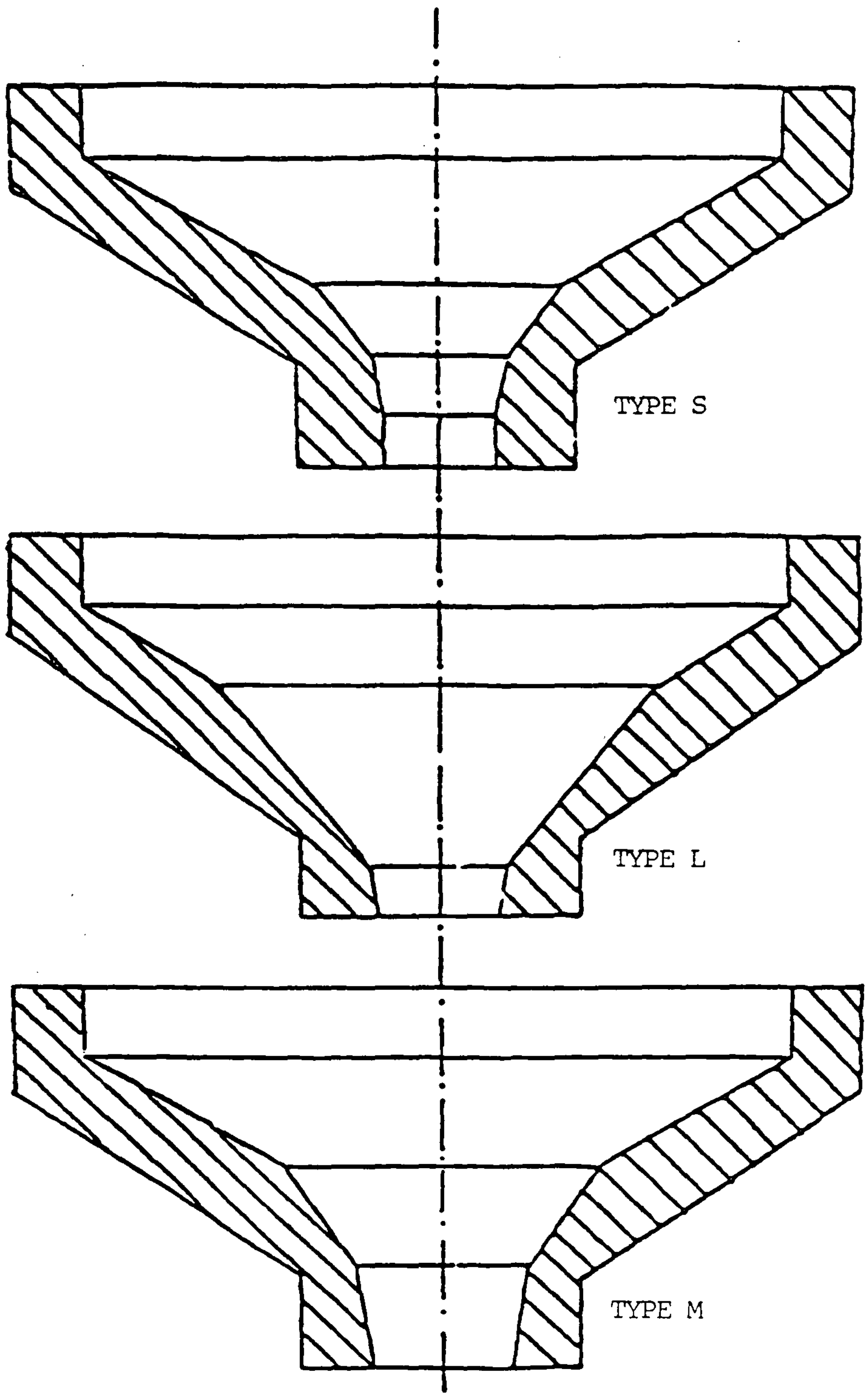

Figure 2-3. Types of compound cones used in the compound water cyclone. (Bath, 1973).

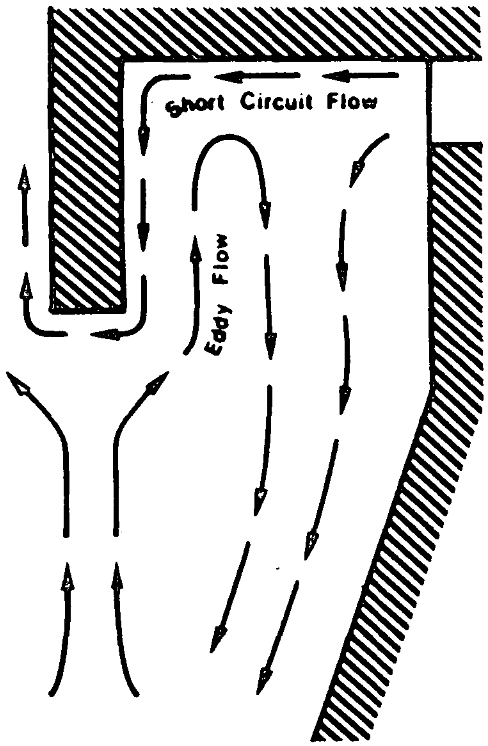

Figure 2-4. Flow patterns in the upper regions of the hydrocyclone. (Bradley, 1959)

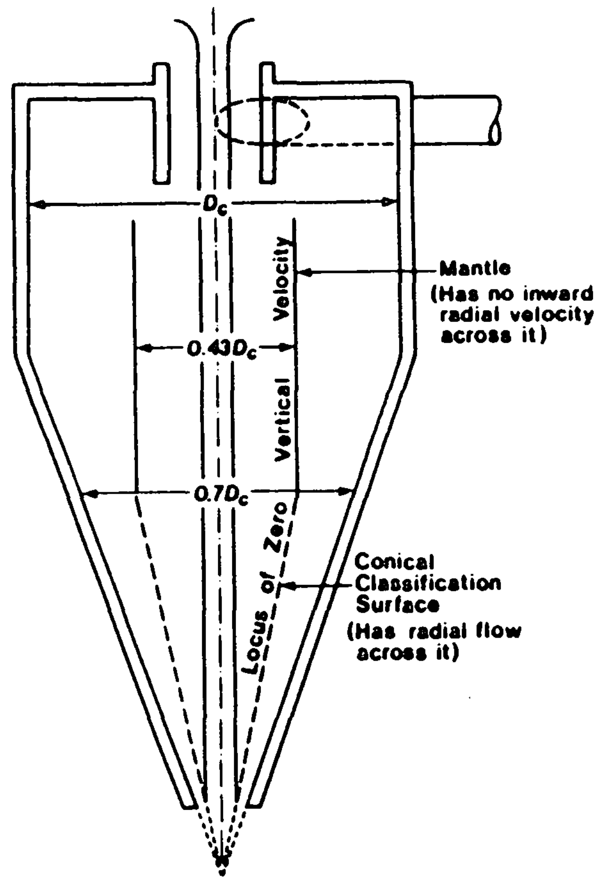

Figure 2-5. The locus of zero vertical velocity in a hydrocyclone. (Bradley, 1959)

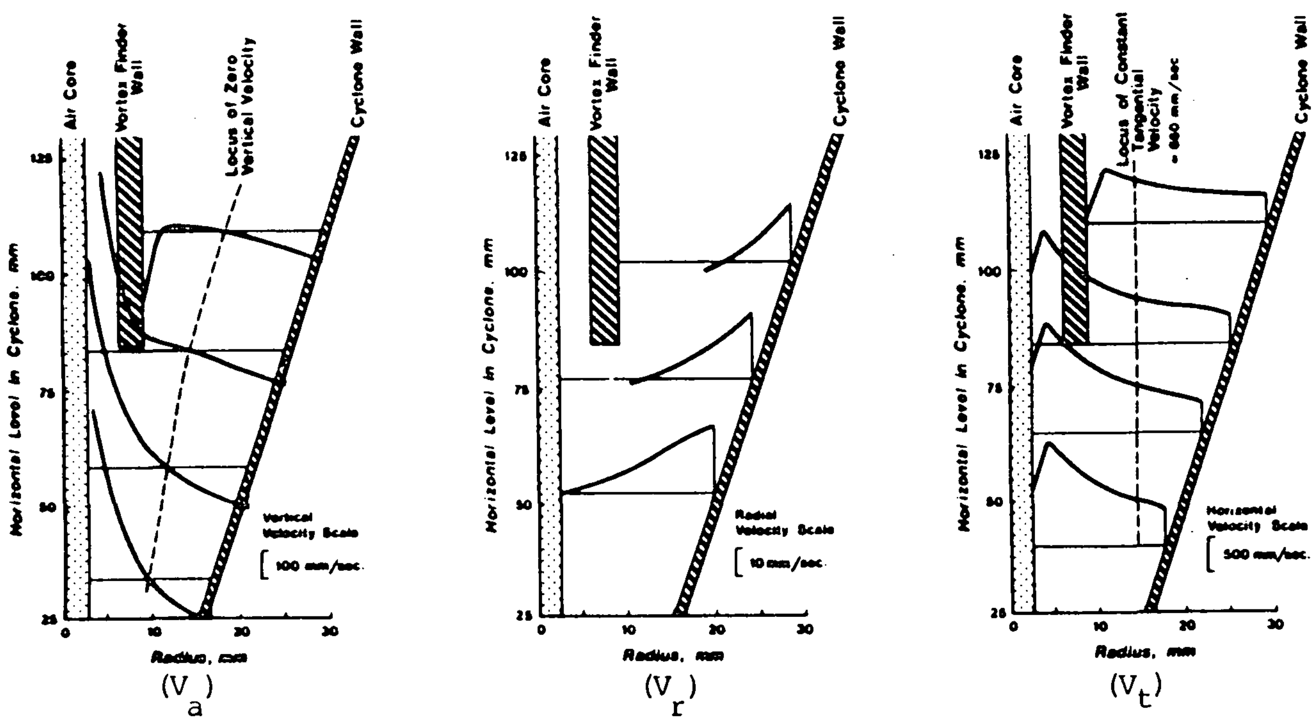

Figure 2-6. The three velocity components in a hydrocyclone. (Kelsall, 1952)

2-3 and 2-7). Each of the compound cones has three sections, with included angles of 120°, 75° and 20°. The three cones differ with respect to the relative area of their inner cone surfaces. Type "L" is used for lightweight materials such as coals, where a low specific gravity cut-point is required. The upper conical section, Section I, is short, whereas Section II is long. Type "S" is used for high density materials (e.g., iron ore), where a high specific gravity cut-point is required. Its relative cone lengths are opposite those of the "L" cone, with Section I length predominating. Type "M" is used for a variety of materials and covers the medium range or cut-points. Its three sections are of approximately equal length.

Particles of different size and specific gravity form a hindered settling bed in Section I of the compound cone. Light, coarse particles are prevented from penetrating the lower strata of this bed by the coarse, heavy fractions and by the fine particles filling the interstices of the bed. Consequently, the water passing from the periphery of the cyclone chamber towards its main outlet (the vortex finder) erodes the top of the stratified bed, removing the light, coarse particles via the "central current" around the air core.

During this phase of the separation, this author believes that the theory proposed by Mayer (1964), for the jigging process, may be applicable. The shallow depth of the bed in Section I and its violent agitation, allow the bed to rapidly and continuously maintain its most stable potential energy profile. Indeed, if this separation scheme is valid for heavy mineral concentration, especially for gold, this segregation must occur very rapidly. Results from this study show that a gold particle's residence time within the 4 inch CWC is of a very short duration, on the order of one second or less, for gold finer than 40 mesh.

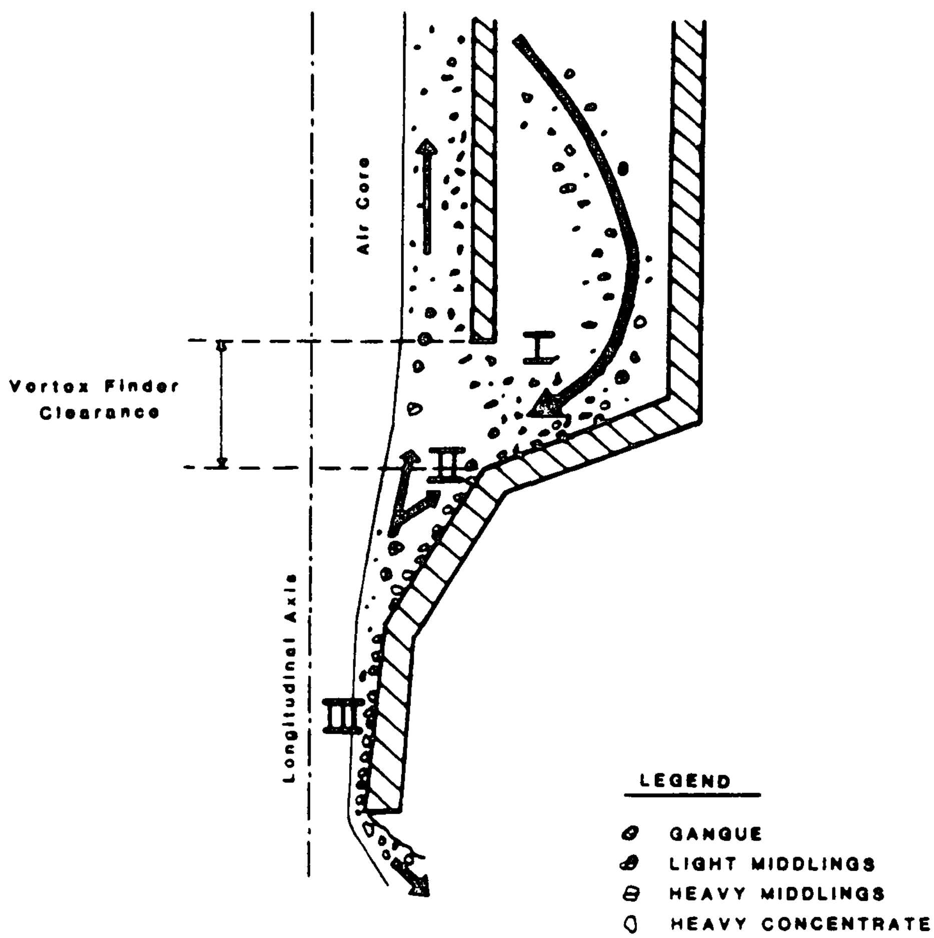

Figure 2-7. Separating process in the compound water cyclone. (Visman, 1963)

The remainder of the bed is forced into conical Section II, by new feed entering the cyclone, without losing its stratified character. Here, the central current is much stronger, further eroding the top of the bed, where the middlings are now exposed. Light middlings are swept up and discharged through the vortex finder.

The heavy middlings that spiral upward in the central current may bypass the orifice of the lower vortex finder owing to their higher specific gravity and the high centrifugal forces in this region. Consequently, the coarse heavy middlings fraction tends to recirculate to the stratified bed. Finally in Section III, the bed is destroyed as coarse particles fan out along the cyclone wall in a single layer, exposing the fine particles which had been shielded. The central current in Section III is relatively weak. The upward current that remains separates the small particles from the remainder of the material, with preference for those of low specific gravity. Thus the fine, light particles are finally discharged through the vortex finder by a process of elutriation. The heavy particles, fine as well as coarse, are discharged through the apex. The entire separation process then, is postulated to take place in three steps, one for each of the sections of the compound cone. Table 2-1 gives the design data for CWCs available from CES.

Compound Water Cyclone Research by Other Agencies

Like the development of the CWC and research of its application to the coal preparation industry, the early research of its ability to concentrate heavy minerals (including gold) was performed in Canada; though some Russian articles also refer to the use of "wide cone" cyclones for heavy mineral recovery in the early 1960's. In 1964, the Liten Company, at a lode gold mine near Yellowknife, NWT, Canada, used a 2-stage, 4 inch compound water cyclone system (Figure 2-8) to process -65 mesh ore pulp from a 3' x 3' ball mill, the CWC middlings product being recirculated to the mill for regrinding. Though no production records are available, it appears that the operation continued successfully for two seasons until the death of one of the two partners (Urlich, November, 1983). In the same report, Mr. Urlich refers to work performed by Canada's Department of Energy, Mines and Resources (EMR) in 1968, to evaluate the CWC's ability to concentrate the very fine gold of the Clinton, B.C., Canada, placer sands. Here a 2 stage, 8 inch CWC pilot plant was used. An overall concentration ratio of 45:1 was achieved. The CWC underflow (concentrate) contained 0.1 oz/ton gold while the tailings assayed at a "trace" only.

In 1974, Mr. W. E. Andersen and Dr. Jan Visman, both of EMR at that time, were asked by Ponderay Exploration Company to investigate the application of CWCs for the recovery of free and intergrown gold, silver, and platinum from their claims on Burwash Creek, Y.T., Canada. According to their report (Visman and Andersen, 1974):

> "At the Burwash Creek it is obvious from direct observation and from analysis of the top gravel that a considerable and variable amount of clay occurs, and that losses of especially the finer gold from the operation's sluice box could very well be explained by the presence of this clay, the more so if the periods between clean-up are relatively long.
>
> In the Compound Water Cyclone, gold and black sand are separated from the sand in a continuous process which operates at 30 to 50 times gravity. One beneficial effect of the high g-ratio is that clay does not pose the serious problems encountered with the recovery of fine gold in conventional equipment, e.g., tables. (Current results support this view).
>
> Problems attending the operation of a sluice box are avoided or can be substantially reduced. The cyclone bed, which is essential for good separation is formed instantly and is automatically maintained in the top of the triconical section. No clogging occurs unless oversize material gets into the feed. Then plugging is noticed immediately and corrective action can be taken without delay. The acceleration attained within the cyclone gives it considerable tolerance in dealing with high and variable clay content, as witnessed by its efficiency of separation for very fine gold. Float-gold problems do not exist inside a cyclone and losses of this kind are thus eliminated."

A screen analysis of the head gravel at Burwash Creek showed a high content of silts and clay, 25% by weight of the -6" gravel was -325 mesh (44 micron). From a 426 pound sample, 0.21 grams of free gold were extracted. This gold was relatively coarse (1% by weight <100 mesh) and the 6" x 0 gravel grade was calculated at 0.032 oz/ton. A sample of the sluice tailings was processed for free gold and a grade for the 6" x 0 sluice tails of 0.02 oz/ton was determined, which based on these small samples, indicated a sluice recovery of 51%. This result showed that a considerable amount of +100 mesh gold was being lost by the sluicing operation.

Three test runs using Burwash Creek gravel, -6 mesh and enriched with free gold, were carried out using a 2 stage 4 inch CWC pilot plant. These test runs A, B, and C attained overall, two stage concentration ratios of 8.3:1, 13.4:1, and 15.9:1 respectively, and gold recoveries of 95%, 95% and

DESIGN DATA OF COMPOUND WATER CYCLONES AND CLASSIFIER CYCLONES

Approximate Flow Characteristics of Single C.W.C. or CL. C.		Top size of feed		Dry feed, tph			Average Flowrate of Water			Inlet Pressure (minimum)			Maximum % Solids		Average Spec. Gravity	
		mm	mesh/in.	metric*	long* (gross)	short* (net)	cu m./h*	usgpm*	igpm*	Kg./Sq. cm. (atmos.)	psi	ft. Head	Wt. %	Vol. %	Solids	Pulp
Multiple 2" C.W.C.-2M CL.C.-2M	coal			3 - 6**	3 - 6**	3 - 7**	31 - 62**	174 - 348**	145 - 290**	0.4 - 1.6	6 - 25	14 - 58	7	5	1.5	1.03
	sand	1.5	10 m	6 - 12	6 - 12	7 - 14	36 - 71	200 - 400	167 - 334	0.6 - 1.6	8 - 25	18 - 58	12	5	2.5	1.08
	ore			8 - 16	8 - 16	9 - 18	36 - 71	200 - 400	167 - 334	0.6 - 1.6	8 - 25	18 - 58	16	5	3.5	1.13
4 in. C.W.C.-4 CL.C.-4	coal			0.5	0.5	0.5	6	27	23	0.2	3	8	7	5	1.5	1.03
	sand	5	3/16	0.8	0.8	0.9	6	27	23	0.3	4	8	12	5	2.5	1.08
	ore			1.1	1.1	1.3	6	27	23	0.3	4	9	16	5	3.5	1.13
6 in. C.W.C.-6 CL.C.-6	coal	8		1.3 - 2.7	1.3 - 2.7	1.5 - 3.0	17 - 16	67 - 64	56 - 53	0.4	5	12	7 - 14	5 - 10	1.5	1.02-1.05
	sand	8		2.2 - 4.5	2.2 - 4.4	2.5 - 4.9	17 - 16	67 - 64	56 - 53	0.4	5 - 6	13 - 14	12 - 22	5 - 10	2.5	1.08-1.15
	ore	8		3.1 - 6.2	3.1 - 6.9	3.4 - 6.9	18 - 16	72 - 64	60 - 53	0.4	6	13 - 15	16 - 28	5 - 10	3.5	1.12-1.24
8 in. C.W.C.-8 CL.C.-8	coal			3 - 6	3 - 5	3 - 6	35	154	128	0.5	7	16	7 - 14	5 - 10	1.5	1.03 - 1.05
	sand	10	3/8	9	9	10	33	146	122	0.6	8	18	22	10	2.5	1.15
	ore			13	13	14	33	146	122	0.6	9	20	18	10	3.5	1.25
12 in. C.W.C.-12 CL.C.-12	coal			15	15	17	92	403	335	0.8	11	25	14	10	1.5	1.05
	sand	19	¾	25	25	28	92	403	336	0.8	12	27	22	10	2.5	1.15
	ore			36	35	39	92	403	335	0.9	13	29	28	10	3.5	1.25
24 in. C.W.C.-24 CL.C.-24	coal			86 - 129	85 - 127	95 - 142	518 - 489	2279-2153	1898-1792	1.5	21 - 22	50 - 51	14 - 21	10 - 15	1.5	1.05 - 1.08
	sand	38	1½	143 - 216	141 - 212	158 - 238	518 - 489	2280-2153	1898-1792	1.6	24 - 25	54 - 58	22 - 31	10 - 15	2.5	1.15 - 1.23
	ore			201 - 301	198 - 296	222 - 332	518 - 489	2279-2154	1898-1793	1.8 - 2.0	26 - 28	59 - 65	28 - 38	10 - 15	3.5	1.25 - 1.38

* Figures apply to C.W. Cyclones and CL. Cyclones with wide vortex finder. When using narrow votex finder, estimates of dry feed rates and flow rates are to be reduced by 1/3.

** The lower feed and flow rates correspond to minimum pressures given in this table. The higher feed rates correspond with inlet pressure of 25 psi (1.76 Kg./sq. cm.; 58 ft. head).

Table 2-1. Design data of compound water cyclones and classifier cyclones. (Cyclone Engineering Sales Ltd., 1978)

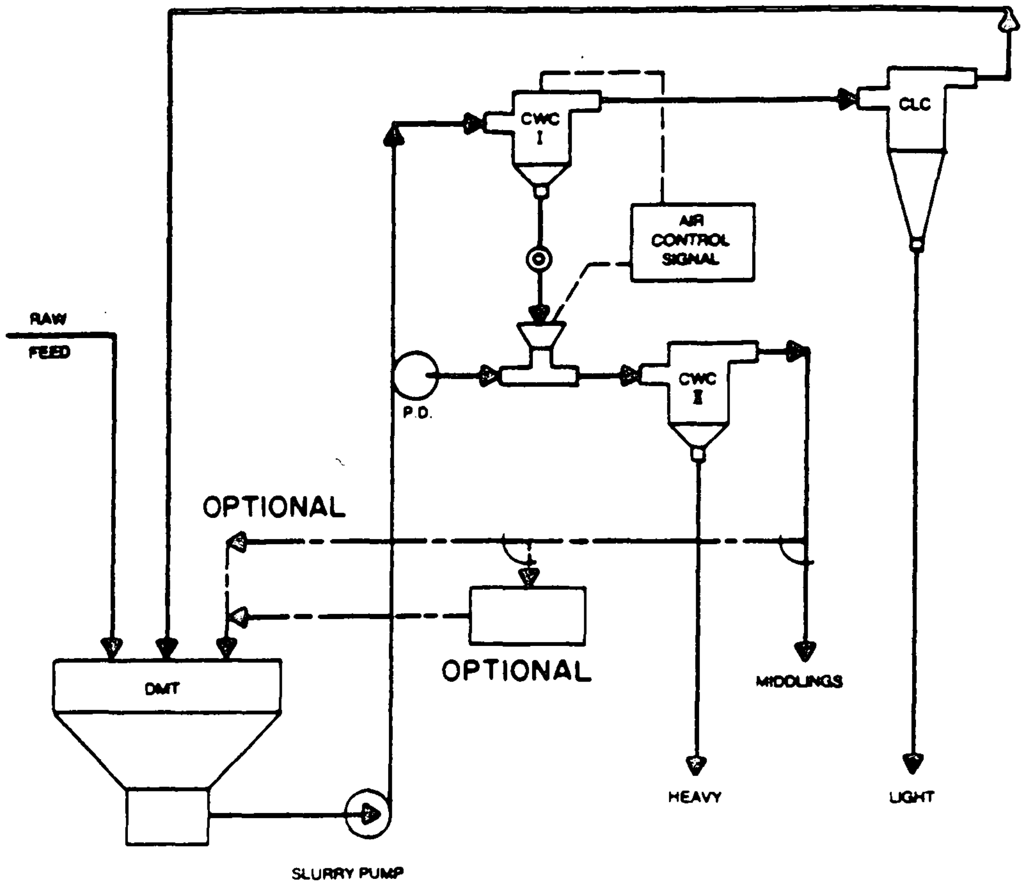

LEGEND

1 — D.M.T.	Dual Mix Tank
2 — P.D.	Pulp Divider.
3 — C.W.C. I	Primary Compound Water Cyclone.
4 — C.W.C. II	Secondary Compound Water Cyclone.
5 — CL.C.	Classifier Cyclone.

Figure 2-8. Two-stage CWC concentration with automatic control. (Cyclone Engineering Sales Ltd., 1978)

99%. Visman and Andersen concluded that the CWC could efficiently recover free gold from the deposit and recommended that Ponderay Exploration Company install a two stage, 12 inch, CWC plant for processing the gravels. Unfortunately, Ponderay's president died soon after and the project folded (Urlich, November, 1983).

Earlier, in 1963, while working with EMR, Dr. Visman had done research work with the CWC on gold recovery from both placer and hard rock sources. In his report (Visman, 1963), he describes the processing of placer sands from the McLeod River, near Peers, Alberta, Canada. These sands contain small amounts of very fine gold (-60 micron) in flake form, and were mined in the 1930's by sluicing operations. Visman used a 2 stage, 3 inch CWC system in closed circuit operation to process samples of the material. In his initial tests he found the sands contained neither enough gold for accurate recovery calculations nor sufficient heavy minerals, a prerequisite, Dr. Visman claims, for the formation of the separation bed in the compound cone. Therefore, fine gold from another placer area was added in order to raise the sample's grade to approximately 1 troy oz/ton, as were sufficient heavy minerals to form a bed in the 3" unit (~60 grams). Table 2-2 shows the results of two test runs described by Visman:

> "In the first test, fine gold only was added to the sand; the concentration was very poor. In the second test, 56 grams of 6 x 48 mesh magnetite (spec. gravity, 5.1) were added, all other conditions being the same. The recovery of gold rose to 95.33%. It is noted that in a continuous process, a bed would quickly build up to the desired level due to heavy minerals passing through the system. In a commercial operation, therefore, no bed material has to be added; the raw feed provides it continuously and the surplus is discharged with the concentrate. A constant amount of bed material is thus present in the cyclone at all times and this bed is constantly removed."

This caution concerning testing of relatively small samples in closed circuit systems is heard many times throughout the literature. Cyclone Engineering Sales (1979) notes:

> "When the overflow and underflow products are recirculated to the feed tank, as is common in laboratory batch investigations, the results depend in part on the amount of the solids used, for the following reason. The bed required for affecting the separation consists of the relatively coarse, heavy particles present in the raw feed. The weight of particles required for forming the bed in the 4 inch CWC is approximately 50 grams. In a continuous process, this does not pose a problem. In a small batch operation, however, a circulating load may not contain sufficient bed material and if this is the case, the results are adversely affected. The remedy is to withdraw overflow and underflow simultaneously from the circuit until it is empty, without stopping the circulation; and to add a fresh batch of material to replace it. The bed material already present from the first batch will be held captive in the cyclone chamber. When the second batch is added, some more heavy material will join the bed. This procedure is repeated until the bed is saturated and the combined cyclone products are representative of the original raw material."

Recent findings by this author tend in part, to contradict these views. This point will be discussed in a later chapter, but is brought to the reader's attention at this point, being in the same context as this earlier research. Likewise, other exceptions to the findings of this thesis will be noted throughout this chapter, and discussed later.

In a later part of Visman's 1963 study, a lode gold ore concentrate from which free gold had been recovered by amalgamation, but which still contained a large fraction of locked gold, was concentrated after regrinding to minus 60 mesh (250 micron). For this study, a 2 stage, 4 inch CWC system was employed, identical to that shown in Figure 2-8, with the middlings stream being recirculated to the feed sump. Samples were taken from the system's four products. These were first amalgamated to recover free gold, then the ferromagnetic minerals were removed with a magnet, leaving a quartz (with some locked gold) fraction. These 3 fractions from each product were then analyzed for gold.

Analysis showed that 96.6% of the free gold, 49% of the gold locked in the black sands, and 14% of the quartz-locked gold was recovered in the CWC system concentrate. To Visman, this indicated the need for additional regrinding of the black sand and quartz fractions.

Canadian research with the CWC continued in 1983 when Reimchen Urlich Geological Engineering of Vancouver, B.C. was commissioned by Triangle Ventures Ltd. of Victoria, B.C., to conduct mineral processing studies for the recovery of fine gold, mercury and other precious minerals from a placer property at Sombrio Point, which is located on the southwest coast of Vancouver Island, B.C. This work was performed by Mr. Cecil Urlich, and Dr. Visman, who acted as a consultant.

In the early stages of their work, 4 field samples ranging in weight from 62 to 143 pounds were collected and processed through a two stage, 4 inch CWC pilot plant at

Material	Test No. 1: Percent of Total Solids	Test No. 1: Pulp Density (%, w/w)	Test No. 1: Gold Grade (oz/ton)	Test No. 1: Percent of gold in new feed	Test No. 2 (magnetite added): Percent of Total solids	Test No. 2 (magnetite added): Pulp Density (%, w/w)	Test No. 2 (magnetite added): Gold Grade (oz/ton)	Test No. 2 (magnetite added): Percent of gold in new feed
New Feed	100	46.9	1.69	100	100	50.6	1.03	100
CWC 1								
Feed	116	7.1	1.42	100.8	119.8	6.4	1.03	118.9
OF	99.3	5.4	1.57	93.2	97.8	5.9	0.05	4.7
UF	16.7	15.5	0.75	7.6	22.0	10.6	5.38	114.2
CWC II								
Feed	18.5	1.2	0.68	7.6	24.2	1.4	4.88	114.2
OF	16.0	0.9	0.09	0.8	19.8	1.2	0.99	18.9
UF	2.5	20.4	4.51	6.8	4.4	37.7	22.48	95.3
Classifier Cyclone								
Feed	99.3	5.4	1.57	93.2	97.8	5.9	0.05	4.7
OF	1.8	0.1	0.00	0.0	2.2	0.2	0.00	0.0
UF	97.5	48.6	1.59	93.2	95.6	51.4	0.05	4.7

Cyclone Settings:

Cyclone	Vortex finder diameter (mm)	Vortex finder clearance (mm)	Apex diameter (mm)	Inlet Pressure (psig)	Cone Type
CWC I	41	20	12.5	26	M
CWC II	41	20	12.5	13	S
Classifier	25	–	12.5	14	–

Table 2-2. Gold recovery from minus 28 mesh placer sand using a two stage, 3 inch compound water cyclone unit. (Visman, 1963)

Cyclone Engineering Sales Ltd.'s laboratory in Edmonton, Alberta. As a precaution and based upon the advice of Dr. Visman, the system was primed with 300 grams of fine magnetite to assure bed formation in the cyclone's compound cones. The operators experienced operational difficulties with the system, especially with respect to plugging of the sump and achieving a uniform feed rate, which may have affected test results. During each test, samples of the system's four products were simultaneously collected. At the end of the fourth sample run the resident bed material, essentially a composite from the four samples and the originally added magnetite, was collected separately. It was the researchers' belief that this bed material should contain a disproportionately high percentage of the sample's gold due to the operational theory of CWC operation held by Dr. Visman.

Of interest are the low concentration ratios they achieved in this two stage operation; these ranged from 3.1:1 to 6.9:1 over the 4 runs. The concentrate's pulp density varied between 10% and 24% (w/w). The large statistical error they cite with reference to their sampling and assaying does not allow for confident interpretation of gold recovery by the CWC system, but assay values they present suggest that in no test did this gold recovery exceed 50%.

In an appendix to this report (Urlich, November, 1983), Dr. Jan Visman describes some optical analysis of gold retained in the composite bed material, which may be of interest to the reader. The technique employs the use of the Quantimet 900 electronic particle analyzer manufactured by Cambridge Instruments. This unit utilizes the particles' reflectances to class them either as gold or non-gold, then measures the length and width of the particles falling into the correct reflectance range. Computer software is used to manipulate this data after certain assumptions are made with respect to grain thickness.

From this scan of gold grains, Dr. Visman concluded that the combined mass of only the 6 largest gold grains of the 245 particles measured equaled 50% of the total gold mass. According to Dr. Visman:

> "This result becomes even more interesting when comparing it with the related particle lengths shown where the dividing line between the same six (6) largest particles and the rest lies at 37 microns (-400 mesh). In other words, the sample as a whole represents the mass of twelve (12) particles of 300 to 400 mesh (50 by 37 microns) in length.
>
> This information now permits the economic ranking of concentrators in terms of gold recovery. For the Auto Medium Cyclone, it is now possible to evaluate the recovery, not only in terms of size cutpoint - the particle size at which 50% of the particles is recovered and 50% is lost to reject - but also in terms of fine gold lost for any given feed composition.
>
> For the four cyclone sizes of interest the recoveries in terms of large particles saved per dozen are as follows:

Concentrator	Gold Grain Size cutpoint (μm)	Gold recovery (300/400 mesh)
AMC - 2M	2	12 out of 12
AMC - 4	3	12 out of 12
AMC - 12	7	12 out of 12
AMC - 24	15	9 out of 12

> These figures refer to the 1 to 50 micron interval. If coarser gold occurs in the sand it will be recovered, thereby improving the gold recovery of the AMC - 24 beyond 9 out of 12 particles."

In an earlier article (Visman, 1963), Dr. Visman quoted similar gold size cutpoints: "Particles of gold (sp. gravity, 15.6 - 19.3, depending on silver content) are concentrated down to 4 microns when processed in a CW Cyclone with a chamber diameter of 4 ins. This separating particle size rises to 10 microns when using a 12-in. CW Cyclone and to 15 microns for a 24-in. CW Cyclone."

The results of experiments conducted during the course of this author's thesis research suggest that these values are overly optimistic; that even for 270 x 400 mesh gold of high CSF (0.6 x 0.8) gold recoveries with a 4 inch CWC range from 50% to 65% for concentration ratios of 93:1 and 10:1 respectively. Poor gold recoveries for coarse gold with low CSF's were also observed. It is also the view of this author that to suggest optical methods are applicable for "ranking concentrators in terms of gold recovery" is invalid. To be applicable a representative sample of gold from both concentrate and tailings products would need to be examined, a formidable task, if at all possible, requiring steps of reconcentration by processes of known efficiency and microscopic hand sorting.

Returning to Dr. Visman's appendix report (Urlich, November, 1983) he writes the following:

> "In tests like this where relatively small samples are used, the bed material holds a considerable portion of the gold contained in the field sample. More gold may be held in the beds than in the concentrate. Example: with a relatively small field sample of say 50 lb. of raw feed, containing perhaps 40 milligrams of gold, most of

it will be held in the beds, there being enough room in the lower interstices. The transfer of this gold to the concentrate depends on the relative abundance of bed material such as magnetite, ilmenite and pyrrhotite which will entrain some gold as these black minerals are being expelled by other incoming material of the same kind, and discharged as concentrate through the apex of AMC-II.

It is of interest to note that in continuous operation it would take the 4 inch CWC system hours to reach a state of equilibrium in the bed, to the point where the amount of gold removed per unit of time would equal the amount of gold entering the system with the raw feed. In a larger plant this point would be reached in a time span inversely proportional to the throughput capacity."

Exception is again taken with these statements. MIRL's work using activated gold as a radiotracer has indicated that for the gold sizes studied (20 x 28 mesh through 270 x 400 mesh), all particles have a very short residence time within the cyclone body. Therefore, to believe that the bed material may contain a disproportionate amount of fine gold could lead to an underestimation of the actual grade of samples processed. The reader is cautioned in this regard.

In November and December of 1983, another series of CWC tests were run on 10 bulk samples from the Sombrio Point property. During the period between the two test series, the sample feeding arrangement was modified, as were the feed sump and the pulp stream sampling device. Other than these modifications, the same cyclone engineering 2 stage, CWC pilot plant was used. In their report (Urlich, December, 1983) they do not mention using additional magnetite with these samples. This is probably due to the size of the samples, which ranged from 500 to 1400 pounds. The -4 mesh samples were fed to the mixing feed sump by a vibrating feeder at rates between 0.52 and 1.29 tons per hour. Once in equilibrium, the systems 4 pulp products were sampled for a 2-3 second interval, dried and weighed. At the end of each sample run the bed material from the CWC's comes was drawn off and saved separately. Concentration ratios for this primary concentration series ranged from 1.7:1 to 3.6:1, similar to those achieved in their earlier test work, but still low.

The concentrates from this series of 10 samples were combined on the basis of geologic origin to yield 4 new samples which were again processed through the CWC system in a secondary stage of concentration, achieving concentration ratios from 3.5:1 to 5.3:1. Finally, a tertiary concentration was run on the largest concentrate resulting from the secondary upgrading and a concentration ratio of 3.6:1 was achieved.

After running all of these tests, the CWC's were dismantled for cleaning, 4.7 lb. of material including 12 particles of gold were found accumulated in the piping and coupling. It was also discovered that the vortex finder clearances (VFC) were larger than intended by approximately 0.25" for CWC I and 0.5" for CWC II. This fact alone, from MIRL's experience, could explain the low concentration ratios they achieved. During the test work, the researchers again had problems maintaining even feed rates and they also experienced some apex plugging due to long, narrow, -4 mesh particles.

After the VFC discrepancy was discovered, these were reset and another of the secondary concentrates was processed in a third concentration stage through the CWC system by Dr. Visman and Mr. Ted Reimchen. This time, a concentration ratio of 12.8:1 was observed. Reimchen performed a qualitative mineralogical study on the products and observed that heavier minerals occurred in significantly greater amounts in the underflow.

Once again, their assay values have a large variance and no gold recovery conclusions can be drawn, only inferred. In their conclusions they state: "For the present it is sufficient to state that gold down to 2 microns in size and other heavy minerals were recovered in both the cyclone beds and misplaced material even though the test plant was limited in its capacity to process bulk placer samples. A test run in closed circuit with the correct settings produced a concentration ratio of 12.85. This concentrate contained a high particle content of specific gravity greater than 3.3." Again the reader is alerted to the claim of 2 micron gold recovery. Many devices will recover micron gold; even a sluice box. What is important and relevant, is what percentage of the total processed gold of any size fraction, including micron sizes, is recovered and at what concentration ratio.

Based on the results of these two 1983 studies, the research group recommended that Triangle Ventures continue their Sombrio Point property investigations, and construct a larger two-stage CWC pilot plant for bulk field testing. Figure 2-9 shows the system which consists of a 12-inch primary CWC and 8-inch secondary CWC. Subsequently the system was installed in a building on-site and plumbing tests run in 1984. Factorial tests are presently being run in an effort to calibrate the system. In communications with Mr. Urlich, this author was informed of the following regarding the plant:

1) During the plumbing tests, the CWC plant processed 1/4" x 0 feed which caused a large recirculating load of 1/8" x 1/4" gravel to build up in the

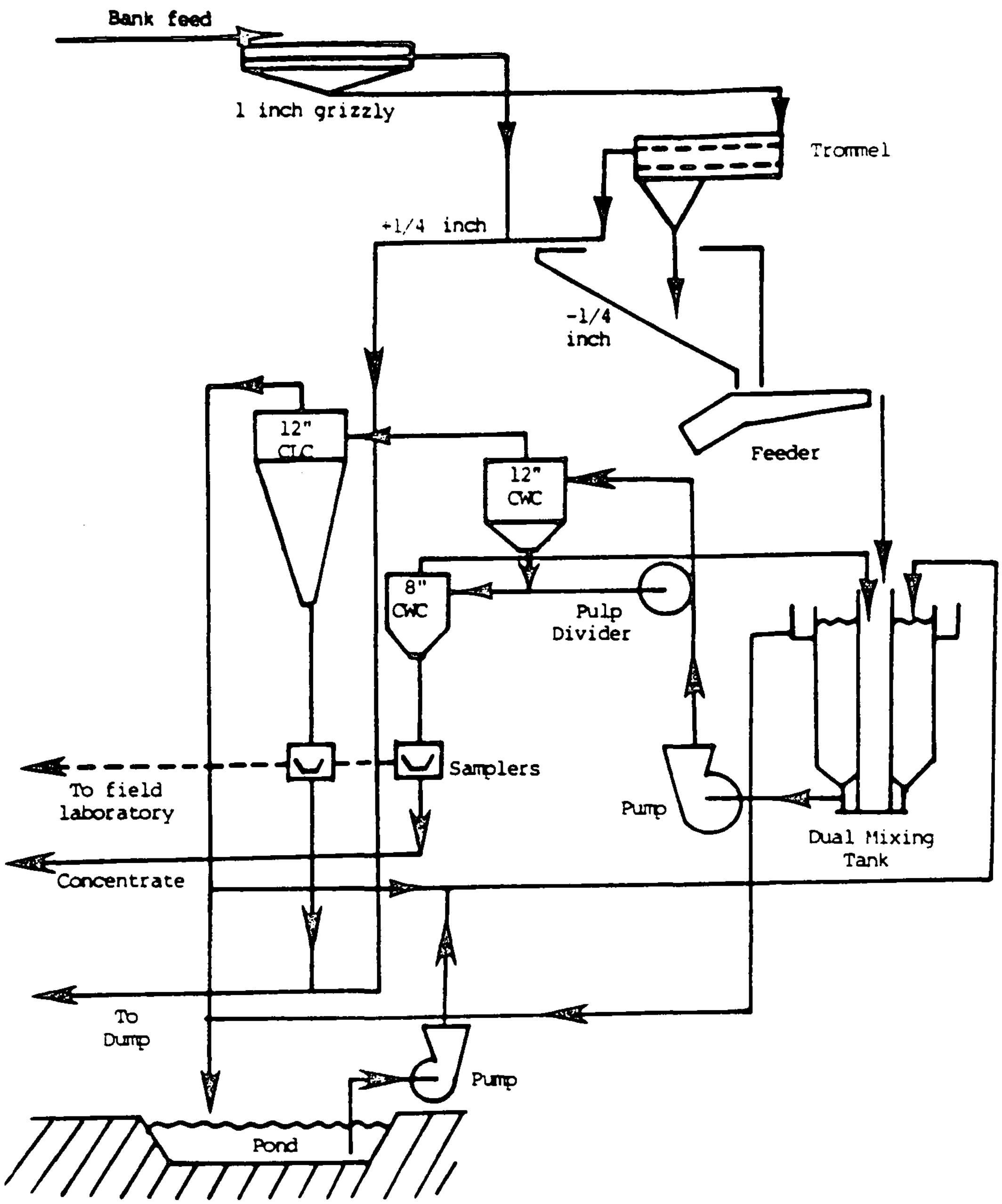

Figure 2-9. 20 ton/hour, two-stage CWC pilot plant. (Urlich, December 1983)

system which led to apex plugging. By altering the CWC feed to 1/8" x 0 this problem was eliminated.

2) Visual inspection of panned products revealed that more than 99% of the mercury reported to underflow. Similar amounts of heavy minerals appeared to report to underflow and overflow.

3) In addition to the primary 12" CWC and secondary 8" CWC units, a tertiary two stage 4" CWC system has been added to the system. The 12" x 8" two stage plant regularly achieved concentration ratios in the 60:1 to 100:1 range, or approximately 7.7:1 to 10:1 per stage. The plant has been operated at a concentration ratio as high as 400:1 (20:1/stage).

4) Factorial testing has been completed in closed circuit independently on each CWC unit. Testing is now underway on the plant in an effort to calibrate it and optimize gold recovery and concentration ratio.

Short cone water only cyclones with 60° and 90° taper angles have been used in the U.S.S.R. at the Eniseizoloto plant (since 1973) and the Baleizoloto plant (since 1975) for the recovery of gold from dilute and finely ground hard rock ore pulps. An article by Lopatin and four others (1977), discusses the performance and wear characteristics of the 14" and 20" cyclones used. According to the paper, the incorporation of these concentrating cyclones into the processing flowsheets made it possible to eliminate an amalgamation step prior to cyanidation and also increase the extraction of free gold. Table 2-3 shows the operating results from cyclones processing the overflow from a mechanical classifier. The pulp density of the feed was 25% solids, with 70% of the solid -325 mesh. From their research and operational experience they concluded that the gold recovery efficiency of the cyclones is a function of the concentration ratio (The Soviet article refers to concentration ratio as "sand yield"). In the study, the Soviets examined the various effects of varying certain cyclone operational parameters on sand yield and gold recovery. These included:

1) Sand ratio, Δ defined by them as d_s/d_o, where d_s is the diameter of the apex, and d_o the inside diameter of the vortex finder,

Table 2-3

Average results of concentration in short-cone wet cyclones. (Lopatin et al., 1977)

Cyclone Product	Product Weight Percent	Gold Grade (g/ton)	Gold Recovery (%)	Feed Content (%) Solids	Feed Content (%) -200 mesh	Cyclone Parameters
UF	11.2	12.5	41.8	---	---	d_s = 45 mm (1.75 in.) d_o = 130 mm (5 in.)
OF	88.8	2.2		---	---	P = 0.9 atm. (13 psi) h = 0 mm
Feed	100.0	3.3	100.0	---	---	Q = 120m^3/hr (530gpm) α = 90° Cyclone Diameter = 600 mm (24 in.)
UF	11.8	12.9	39.6	68.7	13.1	d_s = 32 mm (1.25 in.) d_o = 90 mm (3.5 in.)
OF	88.2	2.4		17.8	70.7	P = 1 atm. (15 psi) h = 0 mm
Feed	100.0	3.6	100.0	23.0	64.2	Q = 50 m^3/hr (220gpm) α = 90° Cyclone Diameter = 350 mm (14 in.)

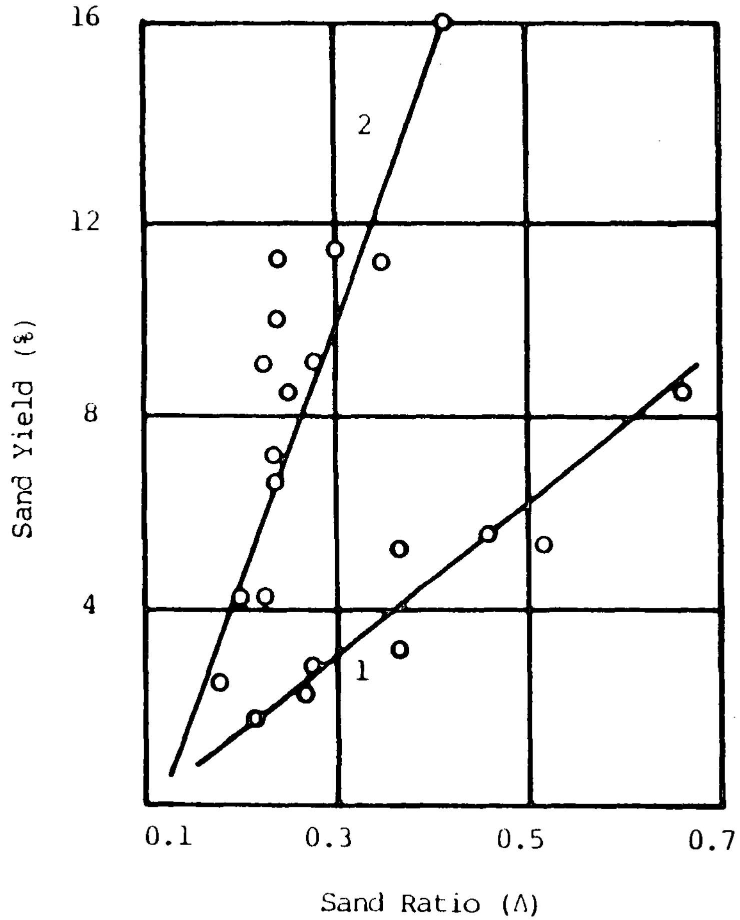

For (1): $\alpha = 90^{\circ}$, 350 mm diameter.
For (2): $\alpha = 90^{\circ}$, 500 mm diameter.

Figure 2-10a. Sand yield vs. sand ratio. (Lopatin, 1977)

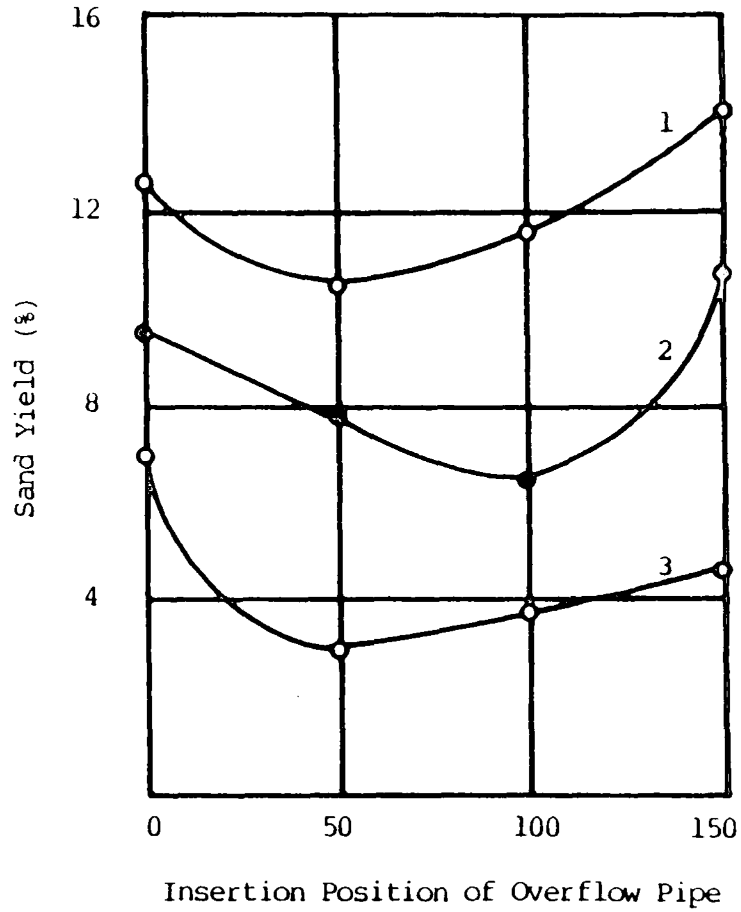

For (1): Δ = 32/90
For (2): Δ = 24/90
For (3): Δ = 25/110

Figure 2-10b. Sand yield vs. overflow pipe insertion position. (Lopatin, 1977)

2) Taper angle, α, which is the included angle of the lower cone body of the cyclone.

3) Vortex finder clearance, which they refer to as "the position of the overflow section". Their position "0" is taken at the point of transition from the cylindrical section to the conic section. Values given are then references from "0" upward, further from the apex opening, in millimeters.

4) They did not investigate the effect of the feed's pulp density due to the stringent requirements set upon the density of the feed fed to the cyclones.

Many of the Soviets' conclusions and much of their data is in agreement with the present finding's of MIRL's investigations despite the difference in the size of the cyclones studied and the large difference in cone types studied. The Soviet's principle conclusions are given below:

1) The sand yield of the cyclone can be varied by altering (1) d_f/d_o, (2) VFC, and (3) α. See Figures 2-10 and 2-11.

2) The efficiency of gold (-200 mesh) recovery depends not only on the sand yield, but also on which parameters are varied to achieve a given sand yield. See Figure 2-12. Note that altering the VFC to achieve desired sand yield consistently gives superior gold recoveries to achieving like sand yields by varying $\Delta = d_f/d_o$.

3) Altering the VFC has an ambiguous effect upon sand yield (Figure 2-11). Note that the sand yield minimum for cyclones of different diameter does not coincide for a given VFC, but that for cyclones

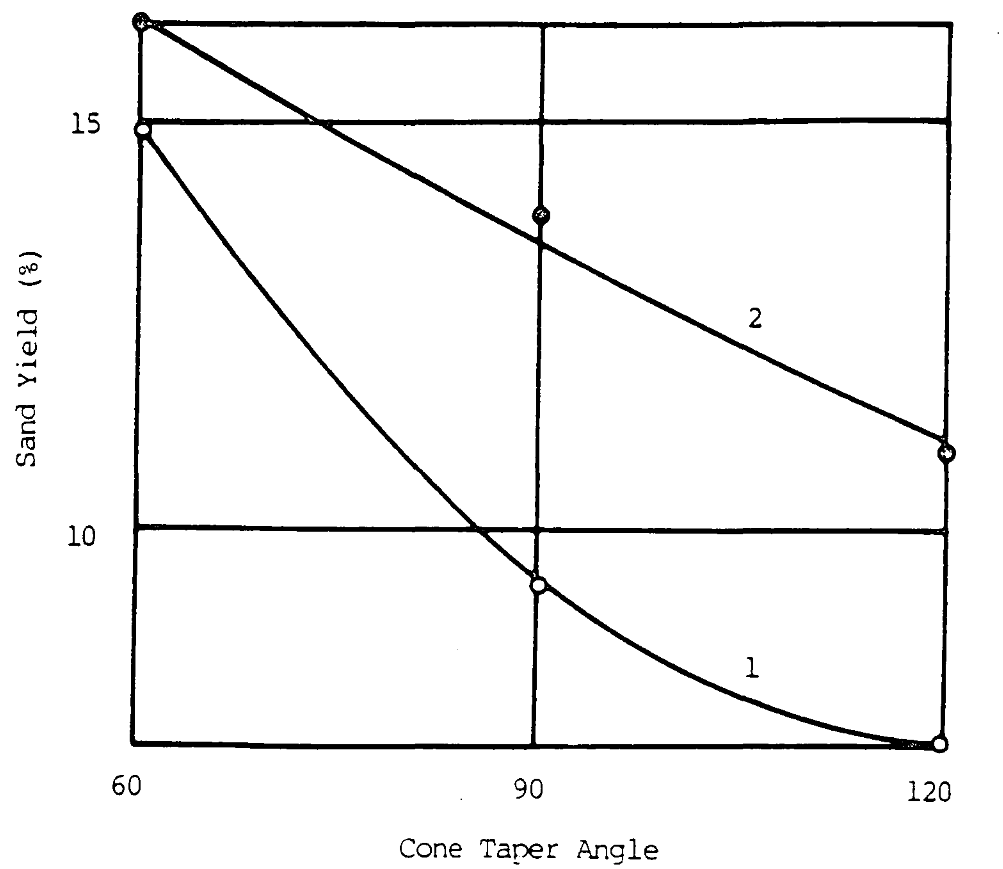

For (1): Δ = 24/90
For (2): Δ = 32/90

Figure 2-11. Sand yield vs. cone taper angle for a 350 mm diameter cyclone. (Lopatin, 1977)

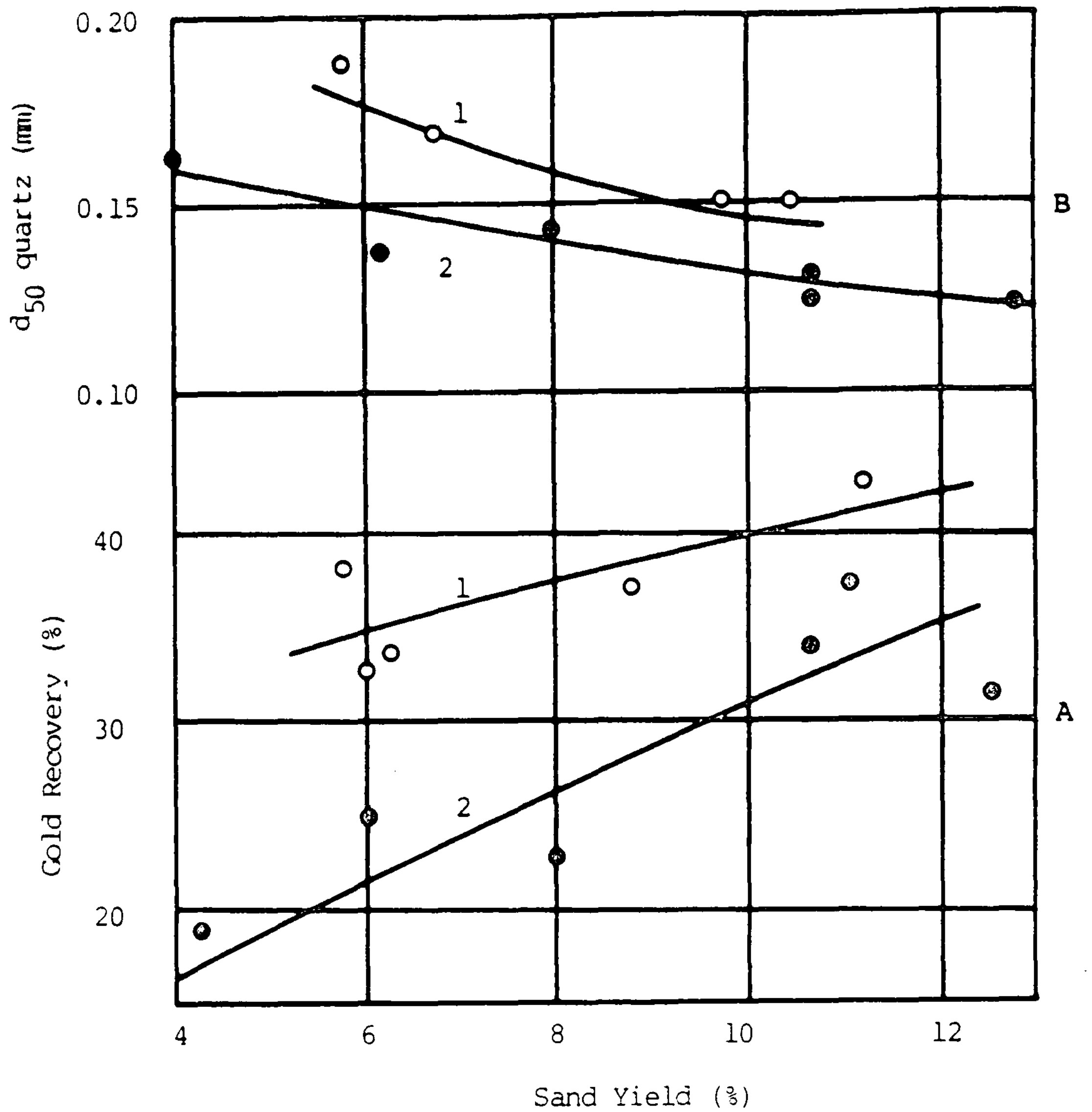

For (1): Sand yield was regulated by varying the insertion position of the overflow pipe.
For (2): Sand yield was regulated by varying the apex opening diameter.

Figure 2-12. Effect of sand yield on -200 mesh gold recovery (A) and cut point, d_{50} quartz, (B). (Lopatin, 1977) of the same diameter the minimum sand yield lies along the same VFC line and is affected by d_s/d_o.

4) There is a common pattern of change in gold recovery for various VFC given various vortex finder diameters. See Table 2-4. According to the researchers: "Unit operation with overflow sections of smaller cross section is more stable; a reduction in the section with respect to height (for example, due to wear) will therefore have little effect upon efficiency in concentration; however, in these circumstances, maximum concentration effectiveness is not achieved. Operation with large cross section overflow sections offer greater concentration effectiveness when the section cutoff is in the zero position; however, in these circumstances wear in the section or slight accidental changes in its position in terms of height, relative to the zero position, leads to a sharp drop in concentration effectiveness. This characteristic of short-cone wet cyclones should be kept in mind when choosing optimum sand ratios."

5) Gold extraction effectiveness is superior for cone tapers of 90° compared to cone tapers of 60°. See Table 2-5 and Figure 2-13.

Table 2-5. Effect of cone angle (α) on gold recovery. (Lopatin, 1977)

Sand Yield (%)	Gold Recovery (%) Total	Free	Cyclone Parameters
8.0	21.6	38.2	α=60°, h=0mm, Δ=25/117
9.3	26.4	68.0	α=90°, h=0mm, Δ=35/117

6) High pressures are not required for the efficient operation of concentrating cyclones of the large diameters studied, 12-15 p.s.i.g. is adequate.

Several other Soviet articles discussing concentrating cyclones were found in abstract form during the literature search. Unfortunately only two of these were obtainable by this author and one of those has yet to be translated (Lopatin, 1971). The other, however, (Man'kov, 1976) was obtained as an English translation. This study concluded that gold recovery from -100 mesh placer sands was 38-40%, using a 2.5" cyclone with a d_s/d_o ratio of 4:10 to process a slurry of approximately 17% pulp density at a flow rate of 3.7 gallons per minute. They claim to have established that gold grains of size 100 x 150 mesh are recovered more efficiently than finer sizes. This, of course, would seem reasonable.

Table 2-4

Effect of overflow pipe insertion position on gold recovery. (Lopatin, et al., 1977)

Apex Diameter d (mm)	Overflow Pipe Diameter (mm)	Overflow pipe insertion position (mm upwards from cyclone's conebody interface) 0	60	120	150	Cyclone Parameters
25	110	26.7	28.0	29.1	—	Cyclone Diameter = 500 m, = (20 in.)
35	117	26.4	17.7	14.9	20.2	Feed Inlet Diameter = 100 mm (4 in.)
35	130	34.0	25.3	19.7	—	α = 90°
18	70	27.7	22.4	23.1	23.9	Cyclone Diameter = 350 mm = (14 in.)
18	74	23.7	19.2	23.9	27.0	Feed Inlet Diameter = 60 mm (2.5 in.)
18	78	20.8	8.2	12.8	21.4	α = 90°
18	80	30.1	5.6	11.9	21.0	

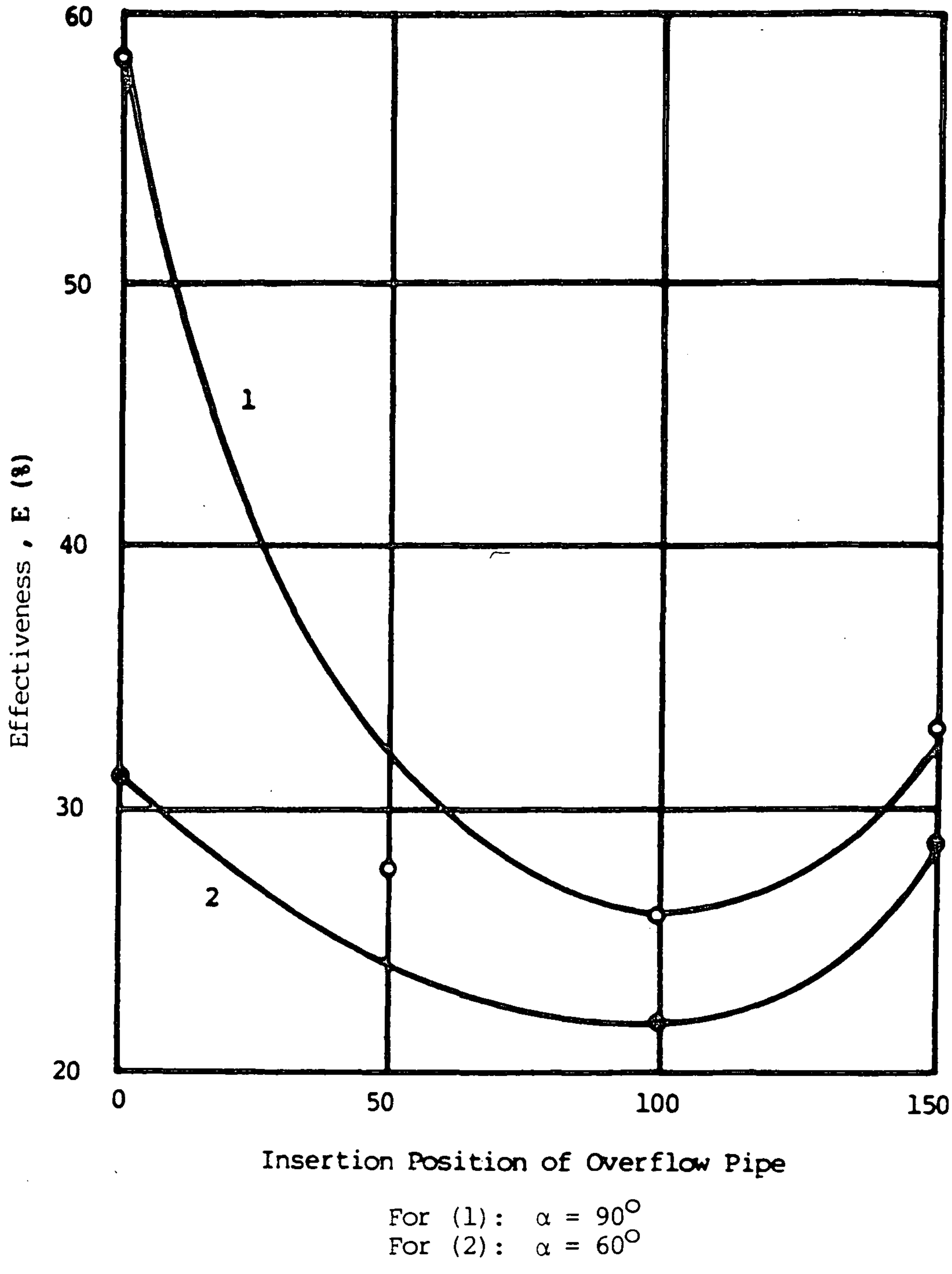

Figure 2-13. Change in the effectiveness (E) of free gold recovery versus the insertion position of the overflow pipe in a 500 mm diameter concentrating cyclone. (Lopatin, 1977)

This study then focused its attention on increasing the gold recovery of the cyclone by experimenting with the following:

1) Externally induced vibration of the cyclone. The wet cyclone was vibrated through an amplitude of 2-4 mm at a frequency of 1460 cycles/minute. The researchers claim a 10-15% increase in gold recovery by this modification (Table 2-6).

2) Addition of 60 x 100 mesh magnetite to the feed. Magnetite was added to the initial samples at 5-8% of their weight in order to create an artificial bed. This modification was also claimed to yield an additional 10-15% gold recovery (Table 2-6).

3) The paper describes the third modification as follows:

"The main subject of attention was the possibility of increasing the centrifugal forces in the wet cyclone, keeping them constant over the height of the cylindrical part, and altering the nature of pulp flow circulation in the wet cyclone. An additional element in the form of a rotatable overflow delivery pipe with radial blades mounted on it was introduced into the cyclone for this purpose; the blade height corresponded to the height of the cylindrical part of the cyclone and a gap of no more than 2-5 mm (depending upon the size of the material being concentrated) was left between the inside wall of the apparatus and the blade edges.

The blade overflow delivery pipe is rotated by the hydrodynamic current of pulp entering the cyclone; additional angular accelerations occur, centrifugal forces acting upon the particles are imposed, and the nature of fluid-flow circulation in the wet cyclone and the patterns of tangential and radial velocity altered."

Table 2-7 shows their data with respect to the effect of adding the additional element, suggesting an increase in gold recovery of 15-20% with a corresponding 10 fold reduction in sand yield, when compared with the original, unmodified cyclone performance shown in the upper third of Table 2-6. The authors conclude by stating these modifications are now being incorporated into a pilot plant to process the classifier overflow in a jigging circuit.

In their paper of 1973, Bath, Duncan, and Rudolph (Bath, 1973) discuss the application of compound water cyclones to South African gold milling circuits. At the time of their writing, a blunt cone cyclone, with an included cone angle of 120°, was operating successfully at Western Hold-

Table 2-6. Average concentration results of the wet cyclone under various operating conditions. (Man'kov, 1976)

Cyclone Products	Yield (%)	Gold Recovery (%)	Gold Grade (g/ton)	Conditions
UF	23	40	0.75	Normal
OF	77	60	0.34	
UF	26	54	0.68	Vibration used
OF	74	46	0.20	
UF	21	56	0.61	Artificial bed used
OF	79	44	0.12	

Note: Tests were conducted using a wet cyclone 62 mm in diameter with the cylindrical part 65 mm long and a taper angle of 120°.

Table 2-7. Gold recovery of the wet cyclone fitted with an additional element. (Man'kov, 1976)

Cyclone Products	Yield (%)	Gold Recovery (%)	Gold Grade (g/ton)
UF	2	62	6.1
OF	98	38	0.07
UF	2	57	5.5
OF	98	43	0.09
UF	14	83	0.64
OF	86	17	0.02

Note: Tests were conducted using a wet cyclone 75 mm in diameter with the cylindrical part 110 mm long and the a taper angle of 90°.

ings Limited mill, replacing a Johnson drum concentrator. A concentration ratio of ~3.1 with a 70% gold recovery are cited. Tertiary cyclones serve the same purpose in Anglo American circuits.

The South African team also conducted test work with 2 inch and 4 inch CWCs. The test cyclones were run in single stage, closed circuit operation, and the overflow and underflow pulp streams were simultaneously sampled, generally for a 5 second period. The feed material for these tests was secondary grinding mill discharge from the Western Deep Levels mill. The effect of varying feed pulp density, vortex finder clearance, cone type, and feed pressure were investigated. The results of their test series are shown in Table 2-8. The reader should note two points with reference to Table 2-8. First, the concentration ratio used by this group differs from the definition of concentration ratio used in this thesis, which is C.R. = (wt. of feed/wt. of concentrate). Secondly, the group has included the use of Gaudin's selectivity index as a measure of cyclone performance. Though the index is used as a convenient means of comparing concentrator performance it must be noted, as the South Africans do, that it is not a complete descriptive measure. A large selectivity index value may result from a high concentration ratio and low recovery, or from a low concentration ratio and high recovery. Neither of these cases is desirable from the viewpoint of the CWC as a fine gold recovery device, the most desirable case being the highest possible recovery at a reasonable concentration ratio. Table 2-9 gives some very interesting data on gold recovery by size fraction of the CWC products. It is obvious that gold recovery falls off with decreasing size fraction. What is not known is how much of this gold loss could be accounted for by locked gold values in the finer sizes. Since the major portion of the feed's gold is in the minus 44 micron fraction, it is this fraction's gold recovery which most influences the overall gold recovery.

Conclusions from the South African research can be stated:

1) Results show that 80% of the gold can be recovered by either 2 inch or 4 inch CWC, at concentration ratios of 2-3:1.

2) The recoveries appear better than those of the tertiary cyclones operating in the Anglo American circuits, though data on the latter is rather limited. Also, the test cyclone's diameters are much smaller which could be a significant factor, plus, test conditions were ideal.

3) Small diameter cyclones would not be applicable in plant conditions due to the level of operator attention they would require. For this reason research using 8" and 12" CWCs was suggested.

Preliminary Compound Water Cyclone Research by MIRL

Beginning in 1981, the Mineral Industry Research Laboratory, MIRL, began an aggressive research project in order to investigate the applicability of concentrating hydrocyclones as fine gold recovery units. The project, in its early stages, was funded by the Office of Surface Mining and the research initiated by Dr. P. D. Rao (1982) whose familiarity with coal processing and coal washery design led him to believe that the compound water cyclone could prove to be a reliable, inexpensive, fine gold concentrator. In particular, the subsequent studies focused on the effectiveness of the CWC to recover fine gold lost by conventional sluice box systems and also gold from such deposits as the Cape Yakataga, Alaska, beach sands, whose size distribution and flatness greatly reduces its recovery by large scale gravity concentration methods.

Preliminary experiments were conducted using a 2.75 inch pyrex cyclone (Figure 2-14) with 3/4 inch feed inlet, 1 inch diameter vortex finder, and a 75° included cone angle. The apex orifice was adjusted by inserting tygon tubing of required inside diameter. A 1/4 inch apex orifice was found satisfactory. The cyclone was fed from a head tank which supplied 55 inches of head to the cyclone feed inlet. This resulted in 8 gallons per minute of cyclone overflow and 0.16 gallons per minute of underflow. Gold bearing placer materials from three Alaskan deposits were tested with the

Table 2-8. Selected results from concentration test work using compound water cyclones. (Bath, 1973)

				CWC Feed			CWC Underflow				
Test no.	Cyclone Diameter (mm)	Cone Type	Vortex Finder Clearance (mm)	Pressure (kg/cm^2)	Solids %	Gold Grade (g/t)	Solids %	Mass %	Concentration Ratio	Recovery %	Gaudin's S.I.
1	50	M	13	0.60	25	108.1	62.0	17.4	3.39	59.0	2.6
2	50	M	13	0.35	25	108.6	60.4	23.4	2.68	62.8	2.3
3	50	M	38	0.15	25	81.3	44.6	54.8	1.63	83.1	2.0
4	50	S	13	0.40	20	99.2	54.5	3.6	10.20	36.7	4.0
5	50	S	13	0.20	20	98.1	44.7	17.4	2.95	51.3	2.2
6	50	S	38	0.25	30	133.5	63.1	25.5	2.53	64.6	2.3
7	50	L	13	0.05	20	71.1	26.9	57.1	1.37	78.4	1.6
8	50	L	13	0.60	30	90.9	62.1	36.6	2.26	82.6	2.9
9	50	L	38	0.20	30	133.0	45.8	57.0	1.51	86.3	2.2
10	100	M	35	1.30	12	90.5	43.5	26.2	1.95	51.1	1.7
11	100	M	55	1.30	12	87.3	61.9	37.5	2.05	76.4	2.4
12	100	M	90	1.30	12	98.8	64.9	45.7	1.85	85.3	2.6
13	100	L	35	1.05	12	91.1	61.7	27.4	2.31	63.3	2.1
14	100	L	55	1.05	12	105.6	61.7	33.5	2.33	78.0	2.6

Concentration Ratio = (underflow grade/feed grade)

Gaudin's Selectivity Index (S.I.) = $(R_a(J_b)/R_b(J_a)$

1 kg/cm^2 = 14.2 psi

R_a = Recovery of gold to underflow
R_b = Recovery of gangue to underflow
J_a = Rejection of gold to overflow
J_b = Rejection of gangue to overflow

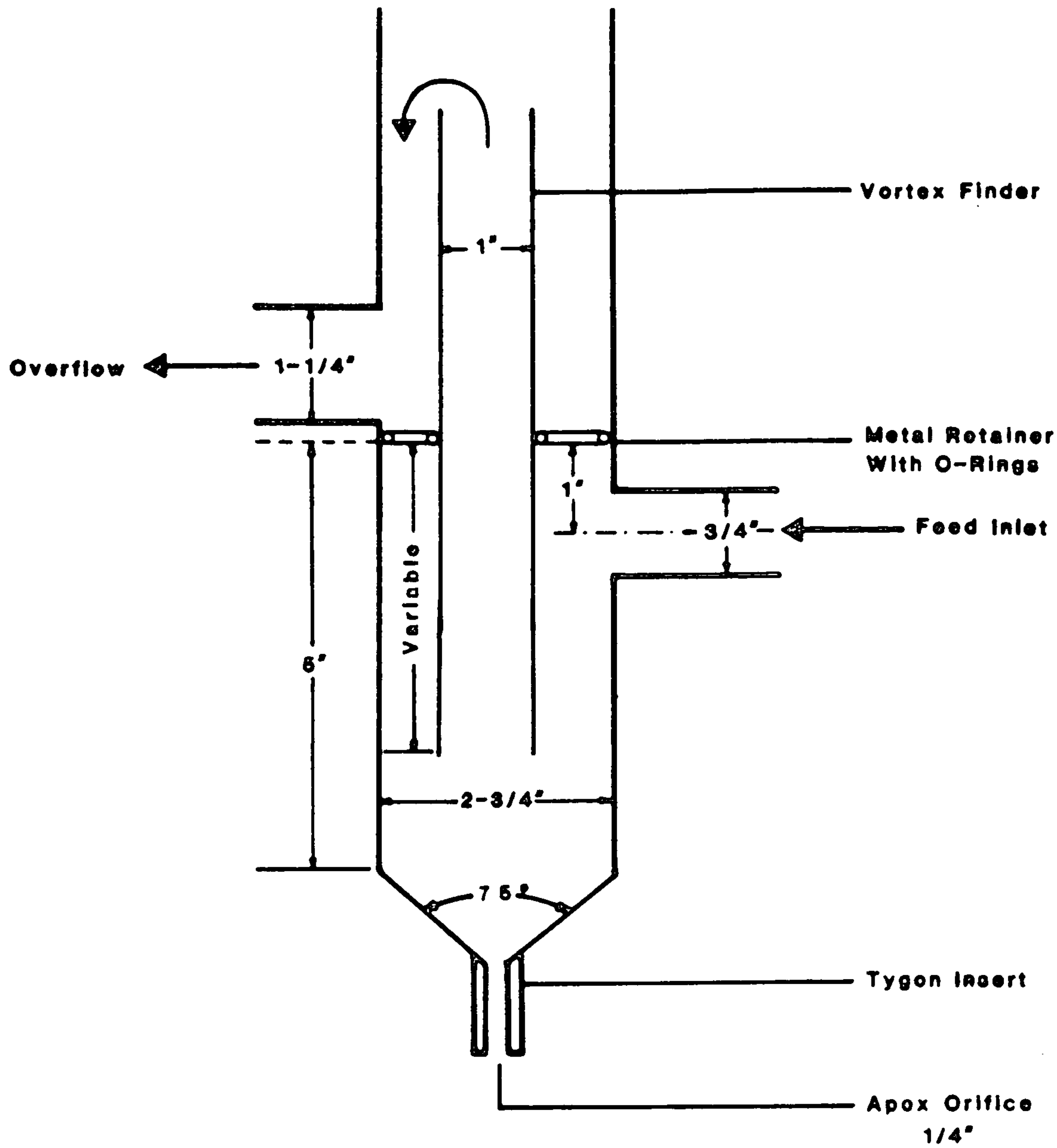

Figure 2-14. Design of pyrex concentrating cyclone used by Rao. (1982)

Table 2-9
Screen analysis and gold distribution of products from selected tests.
(Bath, 1973)

Test no.	Size fraction (μm)	Overflow Mass (%)	Overflow Gold (g/t)	Overflow Gold Distribution (%)	Underflow Mass (%)	Underflow Gold (g/t)	Underflow Gold Distribution (%)	% Gold Recovery to CWC UF
	297	–	–	–	3.7	120.6	3.5	92
	210	2.9	22.6	0.5	4.1	67.6	2.1	92
	149	10.4	7.8	0.6	6.5	52.6	2.7	82
	105	15.6	9.5	1.2	4.4	98.9	3.4	74
6	74	12.0	11.9	1.1	2.9	178.2	4.0	78
	53	12.0	18.1	1.7	1.9	325.6	4.8	74
	44	5.6	41.5	1.8	0.9	834.8	5.8	76
	-44	16.0	254.9	31.6	1.1	4138.6	35.2	53
	Feed	74.5	67.0	38.5	25.5	316.4	61.5	
	105	3.5	14.0	0.6	8.6	29.3	2.9	83
	74	9.8	5.8	0.7	8.3	32.3	3.0	81
	53	14.4	6.3	1.1	5.8	64.8	4.4	80
13	44	8.3	11.3	1.1	2.6	186.1	5.7	84
	-44	36.6	78.3	33.5	2.1	1914.5	47.0	58
	Feed	72.6	42.5	37.0	27.4	197.6	63.0	

system. Samples were first wet screened on a 65 mesh (147 micron) screen. The -65 mesh material was fed as a slurry to the head tank. Additional water was added to the head tank, in order to maintain a constant level and to dilute the feed slurry. Typical results obtained with a 132 pound sample using three stages of concentration are given in Table 2-10.

Encouraged by these initial findings, a pilot scale, compound water cyclone system was assembled for both laboratory and field studies. The system consisted of two 4 inch CWCs, one 4 inch classifying cyclone, and a 2 inch slurry pump. The test system was designed for easy disassembly and transport for field tests.

Laboratory testing of the pilot plant included single stage concentration of various feed materials. Figure 2-15 shows the laboratory flow sheet used for CWC processing of a gold bearing beach sand from Cape Yakataga, Alaska. The entire concentrate was collected. CWC tailings were sampled for 5 seconds every 30 seconds. Gold from both the concentrate and tailings was further concentrated by froth flotation. The froth products were assayed for gold. Portions of the froth products were used to isolate gold particles for determination of their Corey shape factors. The concentrate assayed 0.94 g Au/t while the tailings assayed 0.17 g Au/t, giving a recovery of 27%. The concentration ratio was 16:1.

Examination of the gold's shape factors from the tailings and concentrate showed gold from both products to have an average shape factor of 0.1. Low recoveries point to the need to operate the cyclone so as to achieve lower concentration ratios. Recovery of gold with such a low shape factor requires concentration ratios much lower than 8:1; normally considered a good practice in mineral beneficiation systems. The fact that the CWC did recover gold with Corey's shape factors ranging from 0.05 to 0.15 was very encouraging.

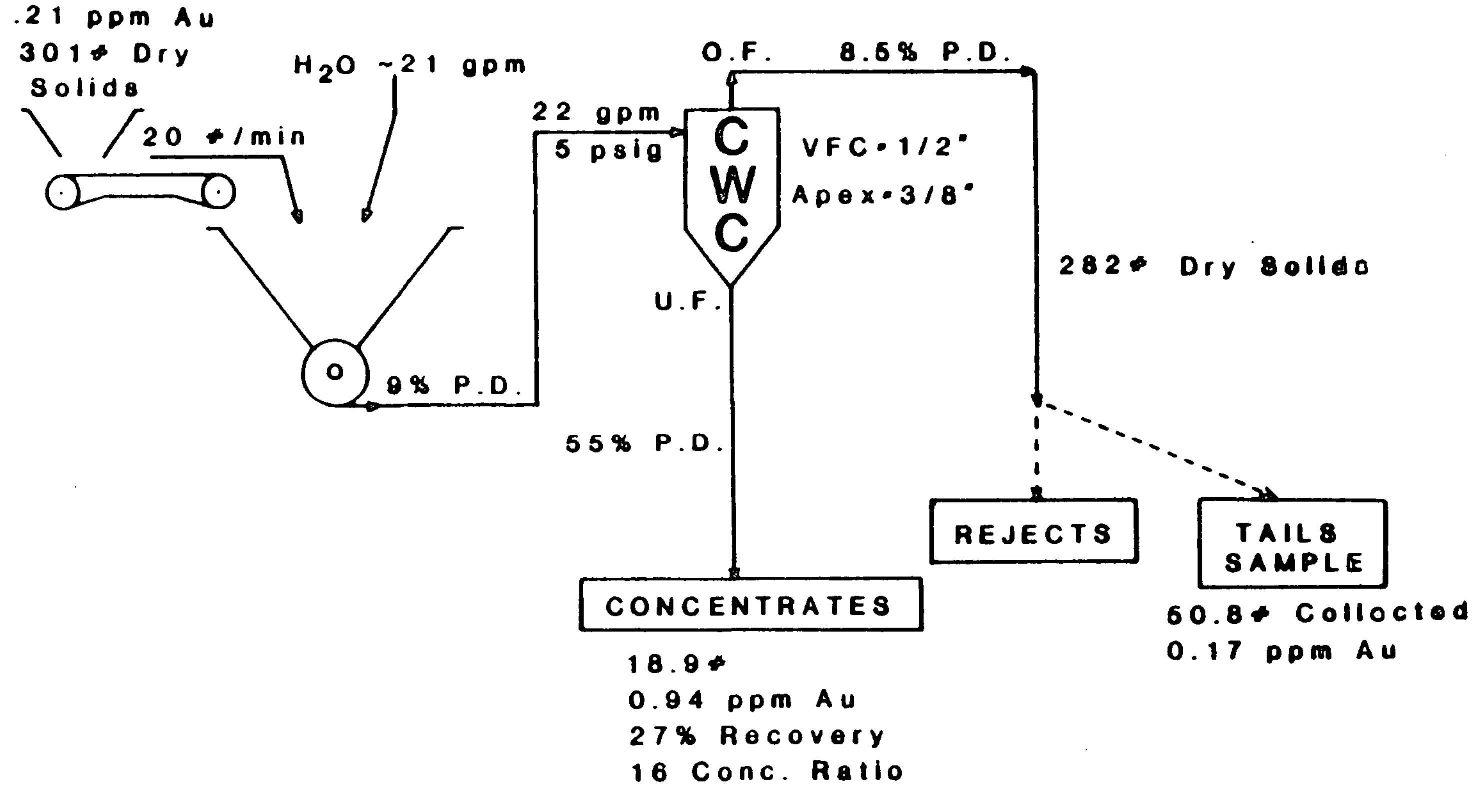

O.F. = Overflow

U.F. = Underflow

P.D. = Pulp Density

VFC = Vortex Finder Clearance

Figure 2-15. Flowsheet for CWC single-stage test of -16 mesh Yakataga beach sands. (Rao, 1983)

Table 2-10

Typical concentration results of 2 3/4 inch glass cyclone. (Rao, 1982)

	Concentration Ratio	Gold Distribution (%) Cyclone Concentrate	Gold Distribution (%) Cyclone Tailings
Primary Concentration	5.4	95.6	4.4
Secondary Concentration	7.4	85.9	9.7
Tertiary Concentration	5.7	84.0	1.9
Total	227.8	84.0	16.0

A synthetic sample was prepared by mixing 0.08 grams of 100 x 200 mesh (150 x 74 microns) placer gold with 50 pounds of the tailings from the Cape Yakataga CWC laboratory test. Shape factors for the added gold ranged from 0.25 to 0.89. Figure 2-16 shows the flow sheet used in processing the sample. Concentrate and tailings were assayed for gold. The concentration ratio for the single stage system was 31:1. Concentrates assayed 28 g. Au/t while the tailings assayed 0.6 g. Au/t. Again use of lower concentration ratio should improve recovery.

The Cape Yakataga beach sand test, with a concentration ratio of 16:1, yielded a gold recovery of 27%. The synthetic sample gave a higher gold recovery (61%) at a concentration ratio of 31:1. This is attributable to the more favorable shape factors of the gold used in preparing the synthetic feed. The level of tolerable recoveries and the shape factor of the gold will dictate practicable concentration ratios per stage.

In June, 1983, the pilot plant was transported to and operated at a placer gold mine (GHD Inc.) located in the Circle mining district, Alaska. The feed to the CWC pilot plant was a split from the operations sluice box tailings. A split from the main middle channel of the three channel sluice box was processed in a single stage concentration circuit at a rate of 0.8 tons dry solids per hour.

Figure 2-17 shows the procedure used for testing and evaluating the field work. A wedge wire screen with 1/8 inch openings was mounted at the sluice box's middle channel discharge. Sampling was restricted to 10 inches of the 30 inch wide middle channel, and only the under current from the 9/16 inch punch plate was sampled. The minus 1/8 inch material was collected in a 50 gallon sump and pumped to two 4 inch compound water cyclones operated in parallel. Total underflow was collected and the overflow was sampled for one minute every fifteen minutes of operation. The CWC concentrate and tailings samples were further concentrated in the laboratory using a Reichert Mark VII spiral. Both the spiral concentrate and tailings were assayed to obtain an estimate of the grade of the CWC products.

The Reichert spiral concentrate was upgraded by froth flotation to facilitate hand picking of gold particles for microscopic measurement of their shape factors. The average shape factor for 20 x 40 mesh particles was 0.11, which explains their loss by the sluice box. As particle size becomes finer, even particles of higher shape factors (0.2-0.5) report to the sluice box tailings. The compound water cyclones achieved a concentration ratio of 13:1, upgrading a feed containing 0.004 oz. Au/ton to 0.03 oz. Au/ton. The froth flotation concentrate had a grade of 44.2 oz. Au/ton. There was 92% gold recovery by the cyclone system. The spirals operated at a 19:1 concentration ratio with 91% gold recovery.

In December, 1983, Mr. Ravi Aluru, a mineral preparation graduate student of the University of Alaska, Fairbanks, completed a study of the effectiveness of the CWC for concentrating scheelite from a calcareous host rock (Aluru, 1983). A tungsten ore was ground to -14 mesh (1.19 mm) in a rod mill to achieve complete liberation of the coarse scheelite. A small quantity of the scheelite was finely disseminated and locked. The ore contained 0.76% tungsten. 4 inch CWC parameters investigated were apex opening; 3/4 inch, 9/16 inch, and 3/8 inch, vortex finder clearance; 1 inch, 3/4 inch, 1/2 inch, and 3/8 inch and pulp

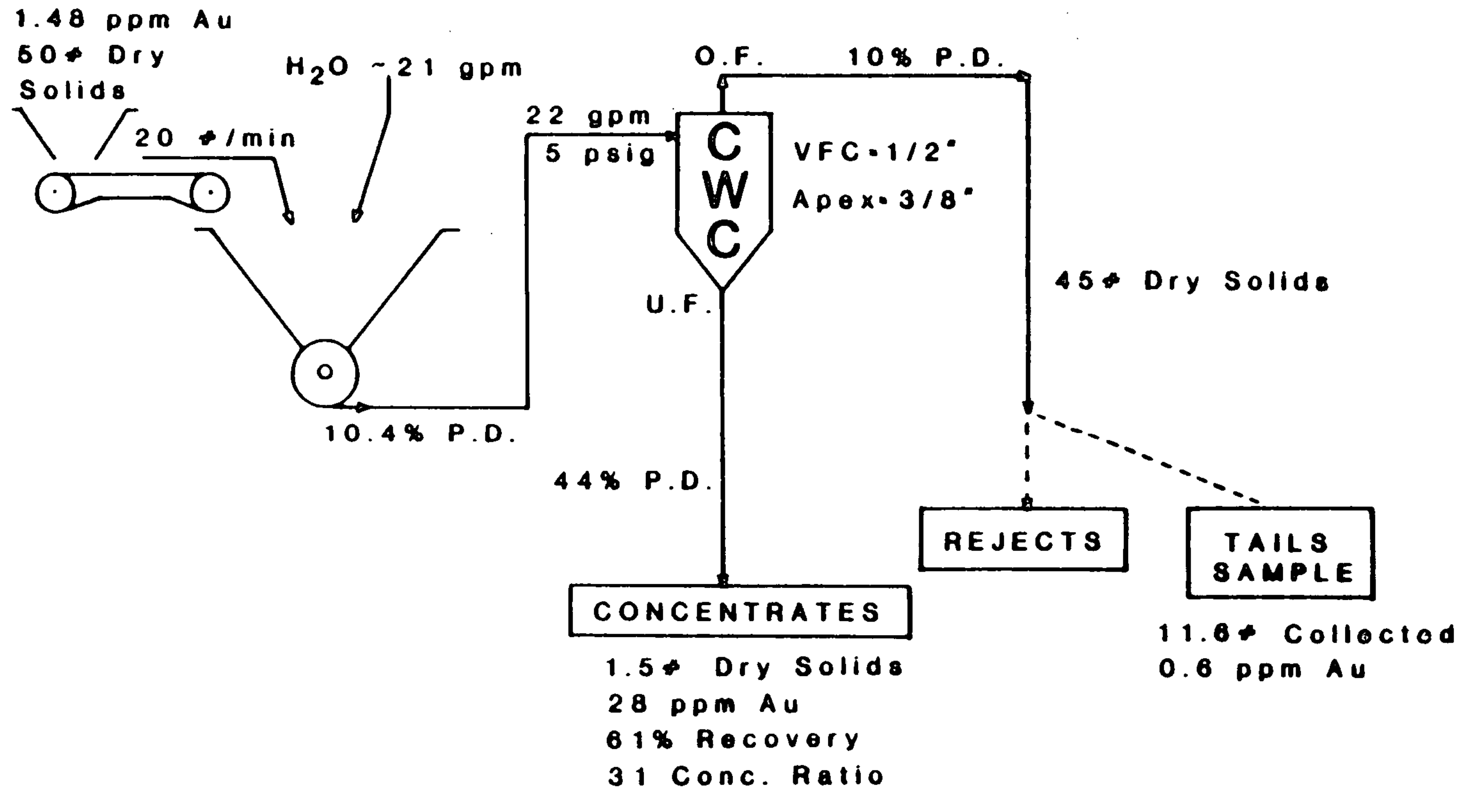

O.F.=Overflow

U.F.=Underflow

P.D.=Pulp Density

VFC=Vortex Finder Clearance

Figure 2-16. Flowsheet for CWC single-stage test of -16 mesh synthesized feed. (Rao, 1983)

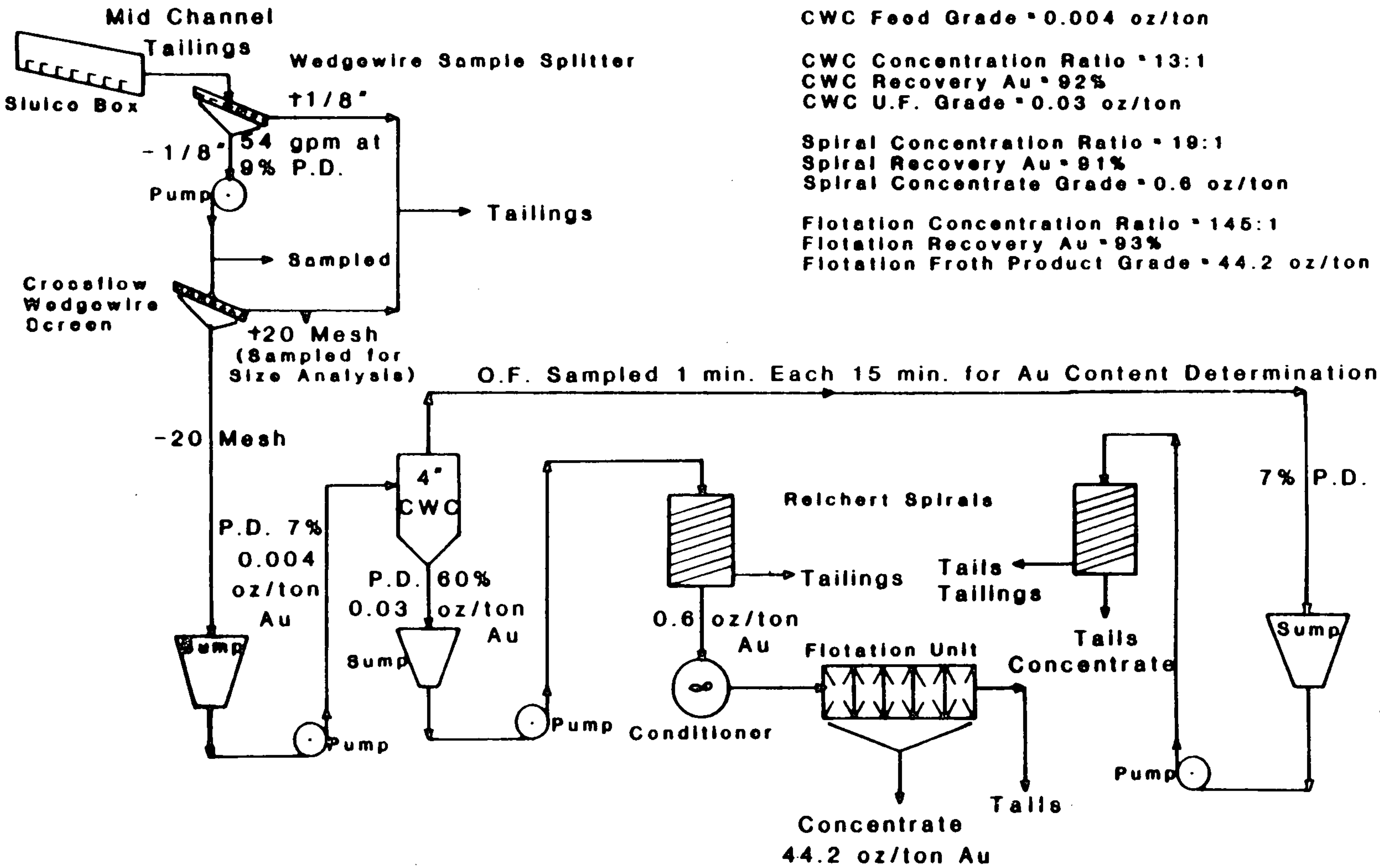

Figure 2-17. Flowsheet for CWC field test at GHD, Inc., Circle mining district, Alaska. (Rao, 1983)

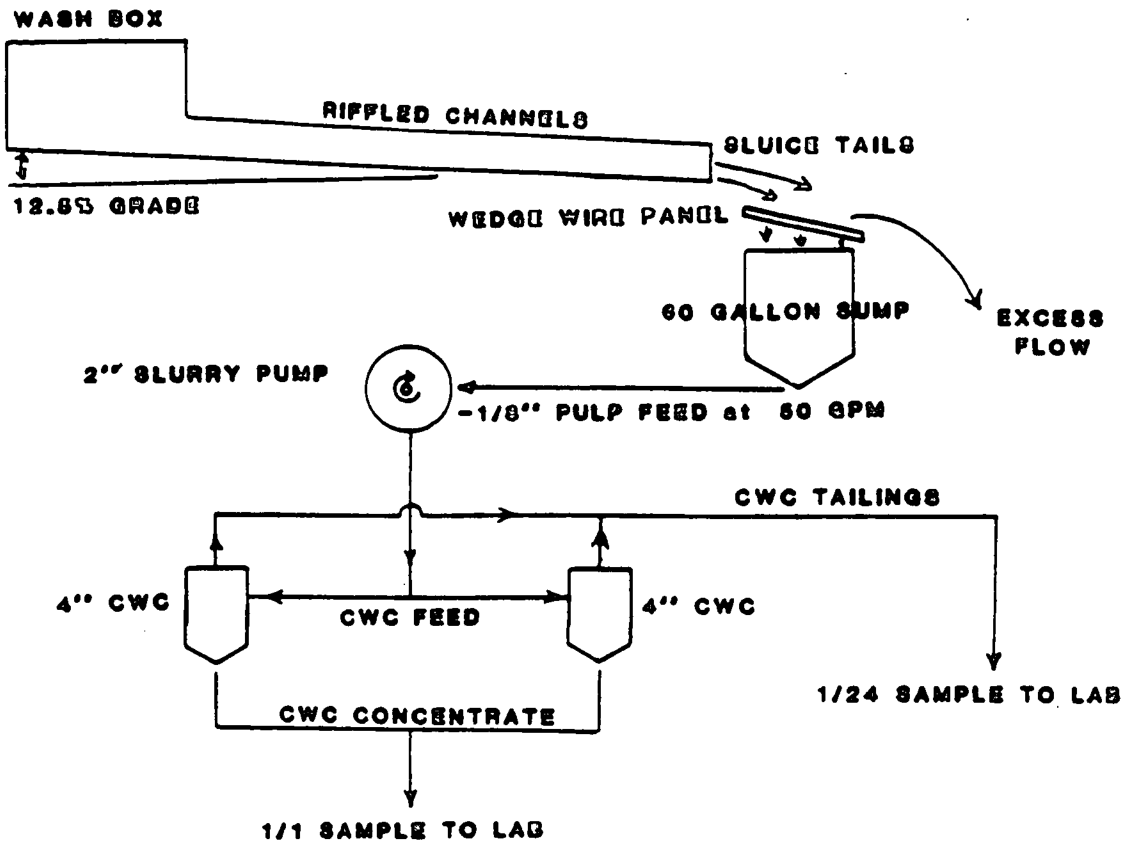

Figure 2-18. Flowsheet for CWC field test at Northwest Exploration Company's Fish Creek placer mine, Fairbanks mining district, Alaska. (Walsh, 1984)

density (nominal); 5, 10, 15, 20, 25, and 30% solids by weight.

The tests showed that:

1. Lower pulp densities gave higher concentrating efficiency.

2. A vortex finder clearance of 3/4 inch and apex opening of 3/4 inch gave the optimal concentrating efficiency.

3. In a typical test, 34% of the tungsten was recovered in the +100 mesh (150 microns) fraction of cyclone concentrates which assayed 1.65% W. This can be further concentrated by eliminating garnet, the major impurity, by high intensity wet magnetic separation.

4. Minus 270 mesh (53 microns) sheelite reporting to the CWC overflow accounted for 47% of the total tungsten. These tailings would need to be classified and concentrated by flotation. Much of the remaining tungsten is distributed as finely disseminated scheelite.

5. The author concluded that compound water cyclones can be applied for preliminary concentration of heavy minerals.

In May 1984, a project was conducted for Northwest Exploration Company to investigate the free gold being lost from their sluicing operation (Walsh, 1984). The placer mine is located on Fish Creek in the Fairbanks mining district, Alaska.

A portion of the sluice tailings was passed over a 1/8 inch opening wedge wire panel located above a 50 gallon sump. The -1/8 inch slurry was then pumped under 7 psig pressure at 50 gallons/min to two 4 inch CWCs operated in parallel (Figure 2-18). The concentrate (CWC underflow) was collected continuously throughout these tests while the tailings (CWC overflow) were sampled for 5 seconds every two minutes. These products, CWC underflow and overflow, were processed in the laboratory (Figure 2-19).

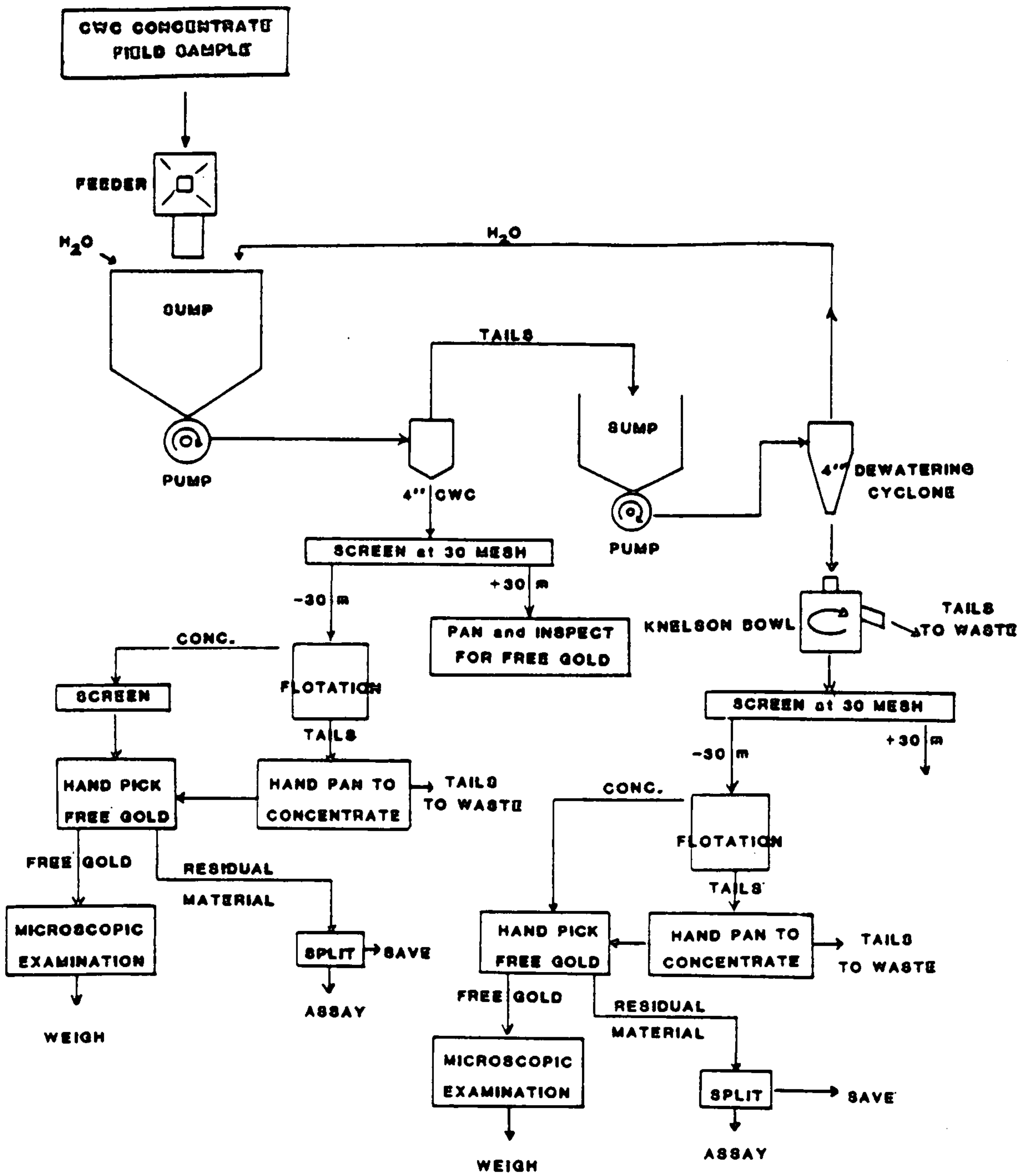

Figure 2-19. Flowsheet for in lab processing of CWC field test products from Fish Creek, Fairbanks mining district, Alaska. (Walsh, 1984)

The cyclone concentrate from the field test was processed in an additional stage of compound water cyclone to reduce the sample bulk prior to froth flotation. The laboratory CWC tails were passed through a dewatering cyclone, then to a 6 inch Knelson centrifugal concentrator to act as a check on CWC gold losses. Both the cyclone concentrate and the Knelson bowl concentrate were wet screened at 30 mesh (595 micron) and gold in the -30 mesh fractions was recovered by froth flotation. Aeroxanthate 350, aerofloat 208 and aerofloat 15, were the reagents used.

The field test's CWC tailings sample was wet screened at 30 mesh. Again, -30 mesh gold was recovered by froth flotation. Both the flotation concentrates were assayed for gold. Total gold recovered by the flotation concentrates was 16.2 mg. Considering 47% of the sluice box feed was 1/8 inch and that the cyclone system processed 484 kg (calculated) of dry solids, gold lost in the sluicing operation was 28.0 mg per cubic yard of sluice box feed. Here a field recovery of only 53% of the gold lost by the operations sluice box was realized. Reprocessing the field's CWC concentrate in the laboratory with a subsequent stage of CWC concentration yielded a 55% recovery, or an overall recovery of 29% with a two stage concentration ratio of 33:1.

From all of their previous test work with the CWC, MIRL concluded the following:

1. Concentrating cyclones can be used for recovering free gold lost by sluicing operations and for evaluating sluicing gold losses. CWCs showed promise in the preconcentration of heavy minerals such as scheelite.

2. CWC gold recovery is related to shape factor and concentration ratio. Low concentration ratios are recommended for gold particles with low shape factors (less than 0.1).

3. A final high grade gold concentrate can be achieved by froth flotation of the cyclone concentrates.

After the completion of the 1984 field test, this author and Dr. P. D. Rao decided it was of no further benefit to proceed with additional field tests until a systematic laboratory study had been completed to evaluate critical operating variables of the CWC and their influence on gold recovery. From their previous sample reduction-analysis they realized that the large factorial experiments they envisioned would be unreasonable, perhaps even unmeaningful, given standard sampling techniques and the experimental error introduced by subsequent stages of concentration, analysis and the particulate nature of the gold.

Therefore, it became the object of this author's research not only to evaluate the CWC systematically, but to research and if possible develop a system to simplify the process of gold recovery analysis for gravity concentration processes. The following two chapters describe the development of such a method and its application in the experimental design for investigating the 4" CWC as a fine gold recovery unit.

CHAPTER 3

RADIOTRACER APPLICATION

Introduction

After conducting a literature search and obtaining advice from others, it was concluded that the use of a radiotracer could provide the answer to the question of how one might efficiently and accurately evaluate the compound water cyclone as a fine gold recovery device. Radiotracers are used widely throughout the disciplines of engineering, including mineral preparation engineering, in a variety of research as well as industrial applications. It is not the intention of this chapter to go into great depth discussing the chemistry, physics, mathematics or engineering applications of radioisotopes. Entire texts are devoted to these disciplines. Rather, this author intends to discuss only that information concerning radiotracers required to understand their application in the experimental design and systems operation as they pertain to this thesis. The basic nuclear physics information which follows was gathered primarily from Gardner (1967) and Kohl (1961).

Atomic Structure

An atom can be visualized as a small positively charged core (nucleus) surrounded by a cloud of electrons which move about the nucleus at a very high speed. The nucleus contains over 99% of the atom's mass but occupies only a fraction of its volume. This model for the atom, proposed by Bohr in 1913, is the most useful for the elementary discussion which follows.

The nucleus is composed of relatively heavy, densely packed large subnuclear particles called nucleons. Approximately one half of the nucleons are particles with a +1 positive charge, and a relative atomic mass of 1; these are called protons. The remainder of the nucleons have no charge but the same atomic mass as the proton; these are neutrons. The total charge of all of the nucleons is known as the atomic number, labeled Z. The total mass of the nucleons is called the mass number, A. Any atomic species may then be uniquely designated by the notation:

$^{A}_{Z}M$

where M is the chemical symbol for the element. This shorthand notation is often reduced to ^{A}M since both Z and M uniquely describe the element. In an electrically neutral atom, there is one electron orbiting the nucleus for each proton therein. These electrons inhabit orbitals which have unique energy levels, and which may contain only a limited number of electrons.

By using these atomic components, the elements are built up from hydrogen, ^{1}H, to Lawrencium, ^{257}Lw. Although all the atoms of an element essentially show the same chemical characteristics, their nuclei may have different masses. The nuclei of any elemental species have the same number of protons but their neutron composition may vary from one atom to another. These species of a given element whose number of protons and electrons are equal but whose mass of neutrons varies are called "isotopes". Two principle types of atomic nuclei exist, stable and radioactive. Radioactive nuclei undergo spontaneous disintegration with the emission of particulate or electromagnetic radiation and in the process decay to a more stable nuclear composition. Stable nuclei do not undergo spontaneous change. For example, seven isotopes of the element neon, Ne, exist, three stable isotopes (^{26}N, ^{22}N, ^{21}N) and 4 radioactive isotopes (^{18}Ne, ^{19}Ne, ^{23}Ne, ^{24}Ne).

When an isotope is radioactive, it is called a "radioisotope" and when it is not, it is referred to as a "stable isotope". Radioisotopes may occur naturally or they may be artificially produced. There are about 1,175 known isotopes of the presently known elements. 275 of these are stable, 50 are naturally occurring radioisotopes, and 850 are artificially produced radioisotopes. When a radioisotope is used in tagging or tracer studies, it is known as a "radiotracer".

Radioactive Decay

A number of mechanisms account for the decay of radioactive isotopes. The majority of these take place within the nucleus and the resulting emission is referred to as nuclear radiation. Some radiation emitting processes, such as x-ray emission, may occur in the atom's electron cloud.

Physicists postulate the presence of about thirty-two fundamental units of matter in the nucleus which may take place in or be produced by nuclear reactions. For the purpose of understanding this thesis, only three of these are important; the electron, the photon, and the neutron. Of these three, only the neutron has a significant relative mass, being approximately 3 orders of magnitude more massive than the electron. The photon is a quantum of electromagnetic radiation and has neither mass nor charge.

In certain radioactive isotopes, the neutron is unstable, having a half-life of about 13 minutes, decaying with the emission of an electron to form a proton. Electrons emitted from a nucleus are called "beta particles". Though the photon is not considered an atomic constituent, it can be emitted during nuclear decay. If a photon is emitted from the nucleus, it is known as a "gamma ray". Alternatively, photons may result from electron energy level changes. In this case they are termed "x-rays". X-rays and gamma rays are indistinguishable electromagnetic radiation and differ only in their source.

Beta particle emission occurs when an unstable nucleus possesses an excess of neutrons. By emission of an electron from the nucleus (beta particle), a neutron is transformed to a proton. This increases the atomic number of the nucleus by 1, but does not materially alter the atomic mass. The properties of the nucleus having undergone beta emission are therefore those of an element of atomic number one greater than the original radioisotope. As an example of this decay process, consider the radiotracer used in this thesis, ^{198}Au.

Of the seventeen isotopes of gold, only one, ^{197}Au, is stable, containing 79 protons and 118 neutrons in its nucleus and 79 electrons distributed in orbitals in its electron cloud. ^{198}Au, an artificial radioisotope, is identical to ^{197}Au except that it contains an additional neutron in its nucleus, resulting in an unstable nuclear configuration. By beta emission, this additional neutron is transformed into a proton causing the atomic number to increase to 80, the atomic number of mercury, Hg. The atomic mass remains 198 and hence the nuclear decay of ^{198}Au forms ^{198}Hg, a stable isotope of mercury. This decay process may be written:

$$^{198}_{79}Au \to ^{198}_{80}Hg + \beta^-$$

where β^- indicates a beta particle.

In the previous discussion, the beta emission process was treated as though all of the energy inherent to the unstable nucleus was carried away by the beta ray. This is not generally the case and the resulting nucleus from the transformation may be left in one of several intermediate unstable states, the beta ray carrying with it only a portion of the available energy. In such cases, the decay process may be characterized by a gamma radiation spectrum as well as the beta emission. Gamma ray emission carries off the destabilizing energy remaining in the nucleus after beta emission. Again, ^{198}Au can serve as an example of such a decay scheme. Figure 3-1 shows the overall radioactive decay scheme of ^{198}Au. Note that three decay routes are available for ^{198}Au. One of these is dominant occurring approximately 98% of the time and is characterized by the emission of a 0.960 MeV beta particle followed by gamma ray emission of photon energy, 0.410 MeV, where MeV is a unit of energy, the Mega electron volt. Nuclear gamma rays are monoenergetic and the gamma spectrum of decaying nuclei show peaks at specific energy levels.

Interactions of Nuclear Radiation with Matter

As previously described, beta particles are high energy electrons ejected from the nucleus, having maximum energies ranging from 50 KeV to 13 MeV. Beta particles lose most of their kinetic energy by the interaction with the orbital energy fields of atomic electrons, giving up approximately 26 eV to 40 eV per interaction. The energy loss is proportional to the duration and proximity of the interaction.

Since the mass of a beta particle and an orbital electron are nearly equal, a low energy beta particle may give up a large percentage of its energy in several such encounters. Conservation of momentum theory dictates that a maximum of one half the beta particle's energy could be transferred during a collision with an orbital electron. Scattering of beta particles is also a consequence of interaction with atomic electrons and large angle deflection may result from beta ray collisions with nuclei.

The distance through a substance, which a product of radioactive decay will penetrate before it loses its ability to produce ionization is termed its range. Range for radioactive emissions is generally quoted in terms of the face density (mg/cm^2) of some common material such as aluminum. The range of beta particles, expressed in mg/cm^2 of aluminum, will not be significantly different from the range in most other elements, since it is electron density, (Z/A), which determines beta particle range and this changes only slightly with increasing atomic number. An exception to this is hydrogen, whose (Z/A) is almost twice that of other elements. This phenomena is used in hydrogen concentration gauges. Beta particles have a very short range compared to that of gamma rays. Betas are relatively easy to stop with glass, water, lucite, or thin metal. Only 0.25 inches of lucite or 0.20 inches of aluminum are needed to serve as safety shields for beta emitters. This restricts their use as tracer radiation in water slurry systems and for all practical purposes, except safety, their emission with respect to this thesis study may be ignored.

By contrast, gamma rays like x-rays have great penetrating ability. Gamma rays, like other electromagnetic radiation, have properties of both waves and discrete particles (quanta). At the high energies of gamma rays the quantum characteristics are predominant. It has been proven experimentally, that the interactions between photons (gamma rays) and orbital electrons are confined to direct collision rather than field interactions. Thus, in considering their interactions with matter, gamma rays may be thought

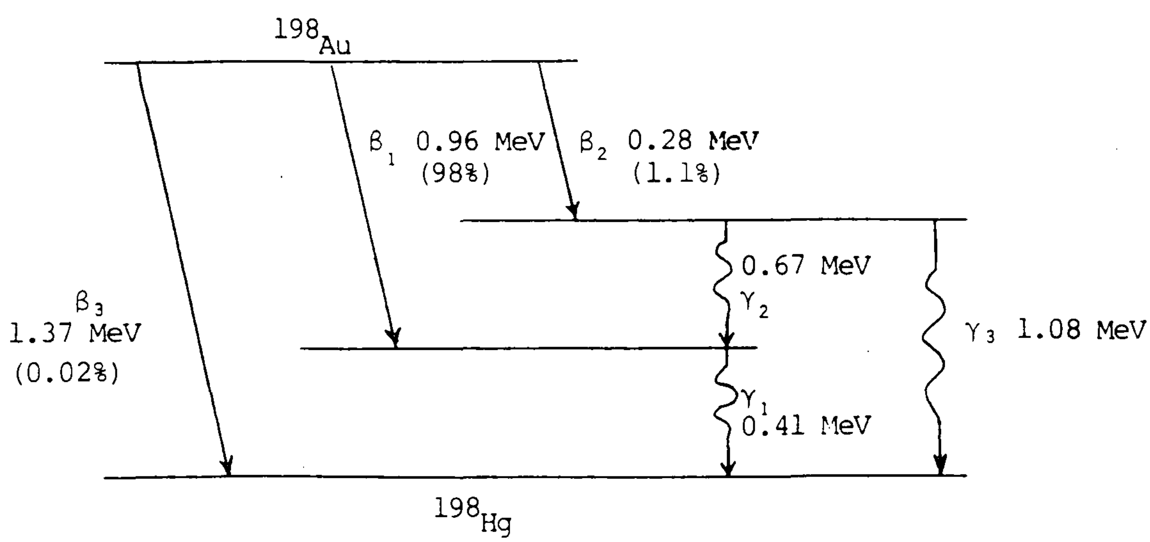

Figure 3-1. Decay scheme of ^{198}Au, showing type, energy and frequency of radiation.

of as massless particles possessing a certain energy.

Gamma rays are the most penetrating form of radiation produced by radioactive decay, having theoretically infinite range. Practically speaking, however, their range is finite. Gamma rays lose their energy by interaction with matter by three main mechanisms involving orbital electrons. These are the (1) photoelectric effects, (2) Compton effect, and (3) pair production. Of these three only the photoelectric effect and Compton effect are important with respect to ^{198}Au gamma ray (0.410 MeV) attenuation, accounting nearly equally for their absorption. Pair production is important for gamma ray energies of 1.02 MeV or greater.

For photons of lower energies, the ionization produced by ejected orbital electrons (photoelectrons) is predominant. In this photoelectric process (Figure 3-2), an incident gamma ray photon, colliding with an orbital electron transfers all of its energy to the electron, ejecting it from the atom, and in the process the photon disappears. In general, the photoelectric effect is unimportant for photons of energy greater than 1 MeV.

In a Compton interaction, instead of giving up all of its energy to the electron, the photon yields only a portion of its energy. The effected orbital electron, which after the interaction may still be bound to the atom or free, is deflected. The photon, having lost a portion of its initial energy, exits the interaction along a deflection angle (Figure 3-3). Compton scattering is the predominant mechanism for gamma attenuation where photon energies range from 0.6 MeV to 2.5 MeV. It is also proportional to the number of electrons in the atoms of the absorbing matter and therefore is greater for elements of high atomic number. In order to satisfy the conditions of energy and momentum conservation, there is a maximum energy that can be transferred to the electron. This energy level, known as the Compton edge, occurs when the photon is scattered from the collision at 180° from its approach. The resultant energy imparted to the orbital electron can take on values from zero to this maximum value. Figure 3-5 shows the gammas spectrum for ^{198}Au. Note the locations (energy levels) of the photoelectric effect's peak and the Compton edge, and their respective count rates (vertical axis).

For each of the absorption mechanisms noted above for gamma radiation, there exists a corresponding absorption coefficient, which is a property of the radiation energy and the absorbing matter. The total gamma ray absorption coefficient is equal to the sum of these individual absorption coefficients and is given by the following equation:

$$U = T + K + S_1 + S_2 \qquad \text{Eq. 3-1}$$

where U = total absorption coefficient

T = photoelectric absorption coefficient

K = pair production absorption coefficient

S_1 = Compton scattering coefficient

S_2 = Compton absorption coefficient

This total absorption coefficient (also called "narrow beam attenuation coefficient") is measured by observing the attenuation of radiation traversing an absorber with an experimental arrangement like that shown in Figure 3-4. The absorption coefficients as determined from this type of experiment are used in the basic exponential attenuation equations:

$$\frac{I}{I_o} = e^{-(u(x))} \qquad \text{Eq. 3-2}$$

$$\frac{I}{I_o} = e^{-((u/p)d)} \qquad \text{Eq. 3-3}$$

$$\frac{I}{I_o} = e^{-u'(d)} \qquad \text{Eq. 3-4}$$

I_o = incident radiation

I = radiation exiting the absorbing material

x = thickness of absorber in cm

u = linear absorption coefficient in cm^{-1}

p = absorber density in gm/cm^3

d = thickness of absorber in terms of gm/cm^2

u' = mass absorption coefficient, cm^2/gm

Since these equations assume that no scattered gamma rays reach the detector, person, etc., which is untrue in actual practice, they are not strictly applicable to all attenuation calculations. A factor to account for incident scattered radiation was proposed by Fano (Fano, 1953) and termed the "build-up" factor. Fano's factor, (B), can be incorporated into Equation 3-2 to yield:

$$I = I_o (B) e^{-(u(x))} \qquad \text{Eq. 3-5}$$

Values of B, like values of u and u' are available in nuclear chemistry and physics texts. Often these same texts include graphs or charts from which attenuated radiation beam strength may be taken directly for known materials and radiation energies.

Figure 3-2. The photoelectric process. The gamma ray is completely absorbed. An electron is ejected with the gamma ray's energy minus the electron's binding energy. (Kohl, 1961)

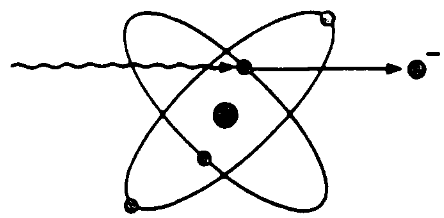

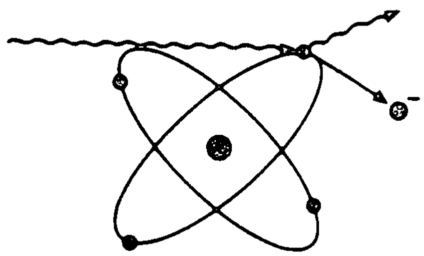

Figure 3-3. The Compton effect. A gamma ray of lower energy proceeds in a new direction. An electron is deflected with the energy difference. (Kohl, 1961)

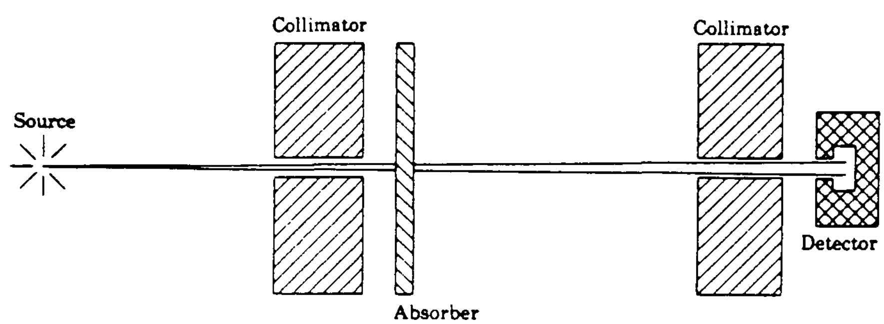

Figure 3-4. Arrangement for measuring narrow beam attenuation coefficient. (Kohl, 1961)

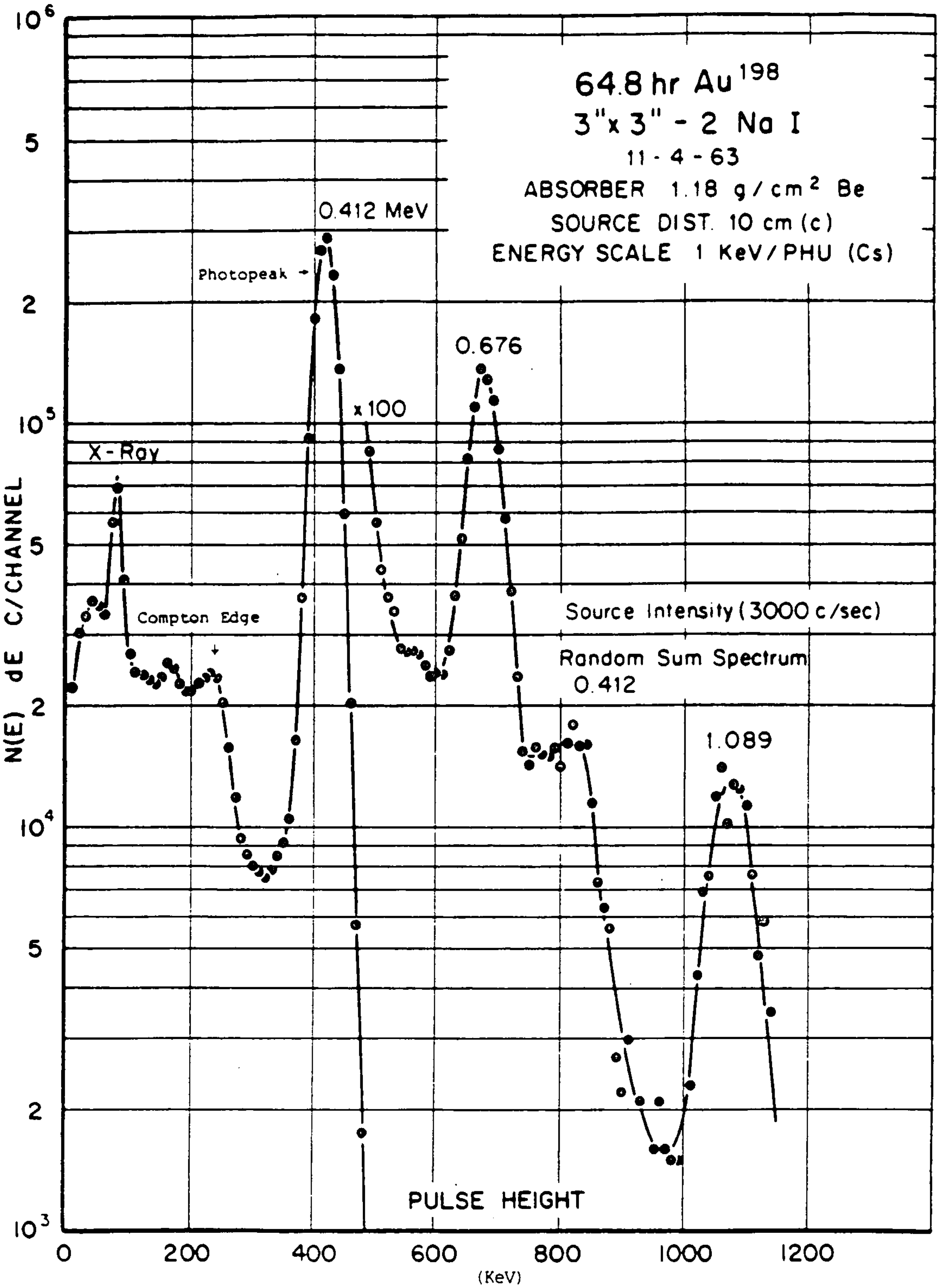

Figure 3-5. Gamma spectrum of ^{198}Au. (Heath, 1964)

Radioactive Half-life

Once a radioisotope is produced (or exists as a natural radioisotope) the rate at which it decays is a function of nuclear structure and is not accelerated or retarded by chemical or physical means. The decay of radioactive nuclei is a statistical process and it depends solely on the number of nuclei of a given isotope present and on the half-life of these nuclei. The probability of an individual nuclei decaying is independent of its age, environment, or history. An equation for the expected number of radioisotope's nuclei, N, remaining at a given time, t, from an original number of radioisotope nuclei, N_o, can be developed from the equation:

$$\frac{\Delta N}{\Delta t} = -\lambda (N) \qquad \text{Eq. 3-6}$$

which simply states that the decrease in number of radioactive nuclei over any given time period is equal to a constant times the number of nuclei present. Lambda (λ) is known as the decay constant. Each radioisotope has a characteristic λ. In cases where the number of radioisotope nuclei is large and the interval of time, t, is small, the foregoing equation may be written in differential form; $dN/N = -\lambda dt$, and solved to yield:

$$\ln\left(\frac{N}{N_o}\right) = -\lambda t \qquad \text{Eq. 3-7}$$

or;

$$N = N_o\, e^{-\lambda(t)} \qquad \text{Eq. 3-8}$$

Where e is the base of the natural logarithm and λ has units of reciprocal time.

A more convenient way to express decay rates is the half-life. The half-life is the time required for one half of the nuclei present to decay. Restating this in terms of Equation 3-8, the half life (T) would be that value of t such that N equals 1/2 (N_o).

$$1/2\, N_o = N_o\, e^{-\lambda(T)} \qquad \text{Eq. 3-9}$$

Solving this equation for (T) yields:

$$T = 0.693/\lambda \qquad \text{Eq. 3-10}$$

This equality relates the decay constant, λ, to the half-life. Because half-life is generally a conveniently measured constant, it is more frequently found in the literature than is λ. Equation 3-8, may be rewritten as:

$$N = N_o\, e^{(-0.693(t)/T)} \qquad \text{Eq. 3-11}$$

Radiotracer Production

The process of neutron capture is the mechanism by which many artificial radioisotopes are produced. In the process, the target atoms, those which are desired to be rendered radioactive, are bombarded with neutrons. The probability that a target nucleus will capture a passing neutron is inversely proportional to the speed of the neutrons. Neutrons are emitted from nuclear reactions at rather high energies, on the order of MeV. It is therefore the common practice in activation facilities to reduce the neutron energies by subjecting them to a number of energy absorbing collisions, generally by passing the fast neutrons through suitable thicknesses of paraffin, water or graphite before the target material is reached.

The concept of "reaction cross section", is a useful one here. It has the dimensions of area, commonly cm^2, and refers to a hypothetical area available for reaction with the bombarding particle. It may be greater or less than the actual geometric cross section of the target nucleus and if there is zero probability of a reaction, the reaction cross section will be zero. Therefore, the value of the reaction cross section depends on the target nucleus, the specific nuclear reaction of interest, and the kinetic energy of the bombarding particle.

After capturing a neutron, the target nucleus is raised to an excited configuration, from which it may decay by a radioactive decay scheme compatible to the energy level of the nucleus. For the activation of ^{197}Au to ^{198}Au, the neutron capture reaction may be written:

$$^{197}Au + {}^{1}_{0}n \rightarrow {}^{198}_{79}Au + \gamma$$

^{198}Au then follows the decay scheme of Figure 3-1 discussed previously. A composite equation, describing the nuclear reaction and decay process of relevance to this thesis may be written as:

$${}^{197}_{79}Au + {}^{1}_{0}n \rightarrow {}^{198}_{79}Au \rightarrow {}^{198}_{80}Hg + \beta^- + \gamma$$

This equation simply states that ^{197}Au captures a neutron, resulting in the activation product ^{198}Au, which decays to ^{198}Hg, in the process emitting a gamma ray and a beta particle. Neutron capture is the mechanism by which the material of interest in this study, i.e. gold, was labeled with an easily detectable tracer (^{198}Au).

The neutron capture reactions, also known as neutron activation, are easily implemented in a reactor. The sample to be activated, in a suitable container, is placed in the reactor and withdrawn after a suitable time. Although most neutron activation is due to thermal neutron capture, fast neutrons also present, can produce reactions forming radioactive or stable nuclei nonisotopic with the target material.

The use of various nuclear reactor facilities throughout the United States for the production of radioisotopes is common practice. For the purpose of activating the native placer gold particles used by this author, the University of Washington, (UW), Seattle, Nuclear Engineering Laboratories' reactor was used. Samples of gold particles were sent to UW in sealed 0.4 dram polyethylene vials. After activation, these samples were returned to MIRL by shipment conforming to NRC and DOT regulations.

For those persons submitting samples for activation, and for the reactor technician, the quantitative aspects of nuclear reactions are of concern. Generally, the person who submits the target samples has a definite radiotracer yield in mind. With knowledge of the desired yield, the operating conditions of the reactor, and parameters of the radiotracer, the required activation time can be calculated by rearranging the following equation:

$$A_o = \sigma\varphi NK \left(1-e^{(-0.693(t)/T)}\right) \qquad \text{Eq. 3-12}$$

where,

A_o is the radioisotope yield in disintegrations/second (dps)

σ is the reaction cross section of the radioisotope (cm^2)

φ is the neutron flux (Thermal neutrons/$cm^2 \cdot$ sec)

N is the numbers of atoms in the target material

K is the fraction of atoms in the target material which will yield the desired radioisotope upon nuclear reaction. This term is known as the "fractional abundance".

t is the activation time

T is the radiotracer's half-life

Viewing this equation with respect to the activation of placer gold used in MIRL's work, preliminary study and calculations indicated that each gold particle should possess a delivered activity of 10,000 disintegrations per second. Thus, this figure coupled with an estimate of delivery time was used to calculate A_o using Equation 3-12. The activation cross section, σ, for ^{198}Au is 96 barns (1 barn = 10^{-24} cm^2). At UW's reactor, φ, the neutron flux, is 10^{12} thermal neutrons/$cm^2 \cdot$ sec. K, the fractional abundance, for ^{197}Au -> ^{198}Au is 1.

Determining N, the number of atoms in the target material, necessitated estimating the mass of the gold particle to be activated. With an estimate of the gold particle's mass, Avogadro's number (6.02×10^{23} atoms/mole) can be used to calculate N. In this study, the most massive particle used was 20 x 28 mesh gold with a CSF of 0.6 x 0.8 and the least massive 270 x 400 mesh gold with a CSF of 0.05 x 0.15. Estimates for these particles' masses were 3.66 mg and 0.13 µg respectively. One mole of ^{197}Au has a mass of 196.967 grams, hence, the number of gold atoms contained in these gold grains was approximately 1.1×10^{19} and 4.0×10^{14} respectively, if one assumes a gold fineness of 1000.

The half-life of ^{198}Au is 2.69 days (64.56 hours). This is a convenient length of time for the half-life of a radiotracer to be used as MIRL intended. It is sufficiently long so that its activity will remain above a certain productive threshold for one to two weeks and short enough that after 2 months the activity is reduced to approximately 1/5,000,000 of its original value, posing no long term containment problems.

Using Equation 3-12 it can be calculated that an activation time of less than 1 minute is required for 20 x 28 mesh gold (CSF = 0.6 x 0.8), to yield a delivered activity of 10,000 dps (assuming 48 hr. delivery time). Likewise, for 270 x 400 mesh gold (CSF = 0.05 x 0.15), 54 hours is required. Reactor restrictions affect the times actually available to the researcher. For example, UW's reactor performs no irradiations longer than 4 hours and charges a minimum rate of .5 hour ($50.00/hr plus service charges). None of MIRL's samples were activated for less than 1/2 hour. Increased activity did not interfere with the experimental design.

There was some doubt that the extremely fine gold to be used in this project could be sufficiently activated by UW's facility. However, after initial work with 80 x 100 mesh gold (CSF = 0.3 x 0.4), which was useful as a radiotracer at calculated activity levels of 500 dps, 3 weeks after activation, this ceased to be a concern. After a 4 hour activation time, a 270 x 400 mesh gold particle of CSF range 0.3 x 0.4, would possess an activity of approximately 1500 dps. This allowed for the adequate, though not preferred, activation of even the least massive gold in the maximum 4 hour reactor time.

Several points concerning the application of Equation 3-12, are worth noting. First, the calculated value of A_o is applicable only at the end of the irradiation period, time zero. At times after time zero the activity must be computed from;

$$A_t = A_o e^{(-0.693(t)/T)} \qquad \text{Eq. 3-13}$$

where t is the time passed since the end of activation. Second, when using tabulated values for σ, the activation cross section, the values listed must be compatible with the desired nuclear reaction. This is necessary since σ varies as a function of bombarding particle type and energy. Third, the exponential portion of Equation 3-12 is reduced to asymptotically low values when $(t/T) \geq 6$. Thus for all practical purposes an activation time of 6 half-lives can be considered as yielding the maximum activity.

Radiotracer Detection

The measurement of radiation may include the measurement of type, quantity, and energy of the nuclear radiation. With respect to this study the author was concerned only with measuring the quantity of gamma radiation emitted, though the energy of the gamma radiation was a consideration. The radiotracer detection system as applied to CWC evaluation is shown in Figure 3-6 and is composed of two basic parts, (1) the detectors, with which the radiation interacts and causes physical phenomena which are measured by (2) a measuring device (electronics). The detection system is discussed first.

In this study, a solid scintillation detector was used because of its detection efficiency, cost, and availability. Scintillators belong to a class of detectors, which produce a measurable effect by excitation or molecular disassociation of their constituent material. These devices operate by producing a a pulse of light for each interaction of radiation with the detector. The radiation detected may be alpha, beta, or gamma radiation, or neutrons. However, their most common application is in gamma ray detection and spectroscopy. The liquid, gas, or solid in which the light flash occurs is known as the scintillator.

Present understanding of inorganic scintillators suggests that the light generating process results from the presence of luminescent centers where the transition from an elevated energy state (caused by the interaction of radiation) to the ground state results in the emission of light. These centers of light emission are prepared by the inclusion of impurity atoms into the structure of the scintillator. For example, the sodium iodide (NaI) scintillator used in this study, was doped with thallium (Tl) to enhance its luminescent properties. The discovery, that thallium doped NaI crystals emitted light upon gamma ray interaction has led to the high efficiency of gamma scintillation counters.

NaI crystals, the most popular inorganic scintillation material, can be grown to large sizes in controlled environments. The crystals are highly transparent to the light flashes generated internally, and the material has a high probability of producing a "photoelectric interaction" from incoming gamma rays. In addition, the emitted light covers a spectral range of from 350 to 500 nanometers, a range particularly well matched to the spectral response of conventional photomultiplier tubes, to which they are coupled. The main disadvantage of NaI is that it is hygroscopic (picks up water readily) and must be encapsulated in air tight containers, generally aluminum, with a transparent window facing the photomultiplier tube.

Radiation interacts with the crystal by the processes previously described as the photoelectric effect, Compton effect and pair production, producing light flashes of frequencies characteristic to the interaction. In the photomultiplier tube (Figure 3-7) the light flash falls upon the photocathode, releasing photoelectrons. These photoelectrons are accelerated by an applied voltage grid to a series of dynodes where the number of photoelectrons generated by collision increases and eventually are directed to the collector, or anode. The emission current is proportional to the light frequency striking the photocathode, and hence to the energy of the incoming gamma radiation.

Different photocathode materials show different spectral response. In contemporary photomultipliers, the most often used photocathode material is an antimony-cesium alloy. For the case of a K_2CsSb photocathode and a NaI(Tl) scintillator, the average photoelectron yield is 8 per KeV absorbed by the crystal, or 125 eV per photoelectron.

Secondary emission by the dynode material produces the amplification across the photomultiplier. Secondary emission is defined as the emission of more electrons than are absorbed in the collision process. The process occurs when suitable materials are bombarded by electrons having an energy of approximately 100 volts. Again, antimony-cesium alloy is the common secondary emitter material used. It has a per stage gain of 5 to 8. To obtain the maximum amplification from the dynodes, it is necessary to precisely guide the photocathode photoelectrons and the subsequent secondary emission electrons through the dynode stages. This guiding is done by the design of the dynode structure and the applied dynode voltage. A high voltage supply and voltage divider network are the hardware required for this purpose.

The measuring device following the detector as seen in Figure 3-6, was comprised of (1) a preamplifier, to act as an impedance matching device and provide some signal conditioning, (2) the amplifier, to shape the signal to that acceptable by (3) a single channel analyzer to give the operator control over which part of the gamma energy spectrum he wishes to monitor and allows for background noise reduction, (4) a ratemeter to monitor the detector counting rate and provide output signal to (5) a chart recorder to give a hard copy record of the detector count rate. There can be many modifications to such a system. Often times, total counts might be more desirable in some applications than count rate. In this case a scaler could be substituted for the ratemeter. If many gamma energies were desired to be monitored simultaneously, a multichannel analyzer would replace the single channel analyzer. In the present application it has been suggested to the author that a personal

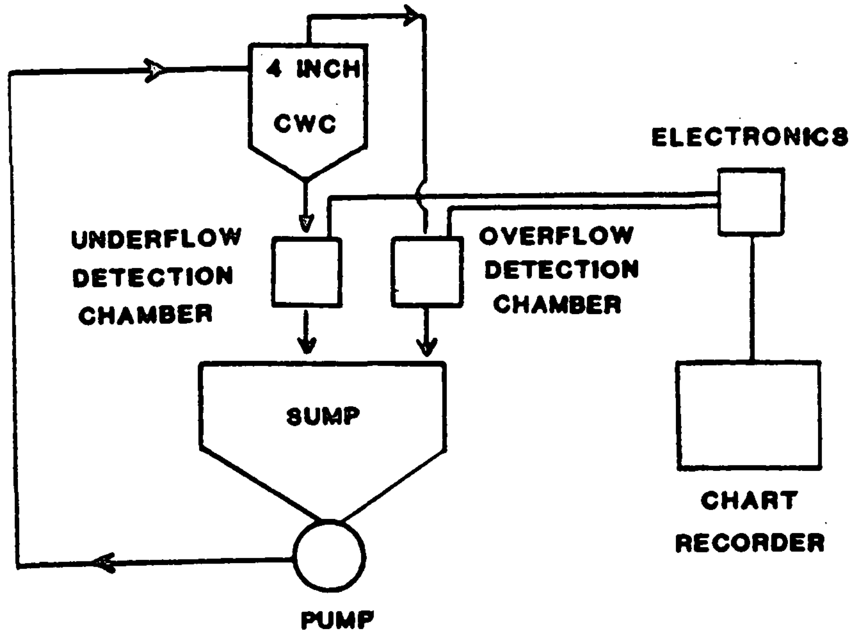

Figure 3-6. MIRL's CWC test loop schematic showing radiotracer detection chambers and measurement electronics.

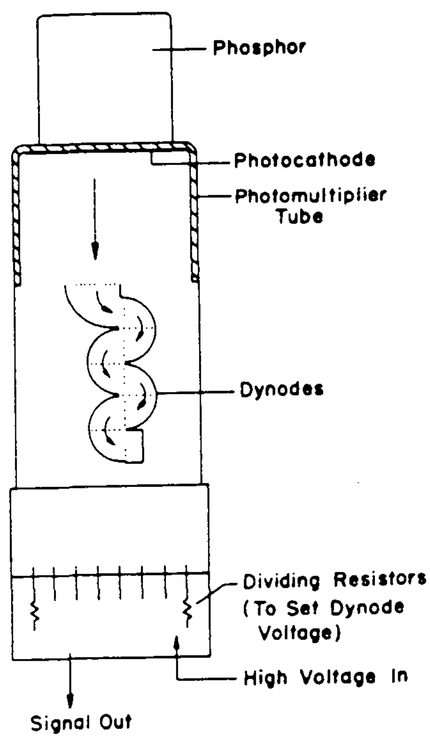

Figure 3-7. Photomultiplier tube coupled to a scintillator. (Kohl, 1961)

computer could be substituted for the chart recorder. The computer would be programed to monitor the two detectors' measuring systems and provide direct, updated, gold recovery values; performing the required statistical calculations and signaling when the test had been completed according to a prescribed statistical accuracy.

A discussion of the electronics of these measuring devices is found in many radioisotope texts. Only two aspects of their electronics are discussed here. In the averaging circuitry section of the ratemeter there exists a combination of resistance (R) and capacitance (C). This determines the rapidity with which the output current to the front panel meter and the chart recorder reflects changes from the input signal (count rate) of the detector. The product of R times C is time in seconds when R is given in ohms and C in farads, and is known as the time constant of the rate meter. The time constant may also be thought of as that period of time over which the input signal is averaged and corrected to give an output reading in the units of the front panel meter. For applications of detecting radiotracer particles moving past the detector at high velocities, a ratemeter must have the flexibility to average counts over short time intervals; in other words have a short time constant. Many manufactured ratemeters provide the option of selecting several time constants by a indicator knob on their front panel. The author found that a time constant of 0.5 seconds was suitable for his application.

The function of the single channel analyzer (SCA) is that of a voltage discriminator, allowing only signals falling within a set voltage band to pass to the ratemeter and be registered as detected radiation. Relating this back to the ^{198}Au gamma spectrum (Figure 3-4), the SCA allows the operator to monitor an energy band (horizontal scale) of the gamma spectrum. If for example, there existed a high background level of radiation in addition to the signal from the gold radioisotope, the ratio of the gold gamma signal to the background signal (^{198}Au: background), could be maximized by choosing to monitor only that portion of the ^{198}Au gamma spectrum centered about the photopeak (0.410 MeV). In general, the functional selection of the discriminator setting is accomplished by adjustment of two control knobs on the front panel of the SCA: (1) the choice of a lower voltage level, E, below which signals will not pass and (2) selection of a voltage window, ΔE. Voltages, V, $E \leq V \leq E + \Delta E$ are allowed to pass to the ratemeter for counting. All other signals are discriminated against.

Radiotracers in Mineral Preparation Research

The use of radioisotopes as tracers has been extensively used in the field of mineral preparation research, particularly in the field of froth flotation research. An article by Gaudin (1949) gives a good summary of work to that date on the subject. Flotation problems are very amenable to study by tracer techniques since they often require the detection of low concentrations of substances. As an example, it is of interest to measure the degree of surface saturation by collectors and modifying agents in froth flotation, and study the rate of this adsorption phenomena. Both of these goals are researchable by labeling the chemicals in question with radiotracer atoms.

Spinks (1955) references a number of flotation studies done using radiotracers. He also notes a number of metallurgical research problems they have helped to solve. Kohl et al. (1961) devoted several pages to metallurgical applications of tracer techniques.

The use of particulate radioactive material is somewhat rarer in mineral preparation studies though Gaudin references grinding studies done by Hukki (1944). Gaudin et al. (1951) used irradiated sodium (^{24}Na) in the mineral albite, to study the size distribution and reduction of size fractions during dry grinding in a ball mill. Gardner (1975) has used particulate radioisotopes of sodium and manganese to study the residence time of mineral grains in a production wet ball milling operation.

Though this author's literature search in this area was by no means exhaustive, no reference was found applying radiotracers to evaluate the efficiency of gravity concentration processes. This is probably due to the fact that recovery of most minerals, which are amenable to gravity concentration, is easily determined by accurate sampling and assaying. With respect to particulate gold, the ease of sampling and assaying is still applicable, but the accuracy and reproducibility of these operations are much discussed and debated points. Also, in gold placers, where grades of 0.01 oz/ton (466 mg/yd^3) are common, primary concentration products collected in the field may require significant upgrading in the laboratory before sampling and assays can take place. Each subsequent concentration introduces its own recovery error into the overall evaluation process and often the researcher wonders how meaningful the back calculated, primary stage recovery values are. Similarly, closed circuit, in lab testing of run of pit placer sands, which generally contain so little gold that only a few small grains of gold distinguish the concentrate from the tails, makes the wisdom of product sampling highly suspect. These problems are not unique for placer gold ores and apply to any low grade ore with particulate values.

The rationale for applying radiotracer techniques to this problem becomes obvious if we take an extreme example. Suppose a placer gold sample is to be processed by a 4 inch compound water cyclone in laboratory, closed circuit operation (Figure 3-8). Past laboratory practice would dictate allowing the system to reach operational stability and sampling the overflow and underflow streams simultane-

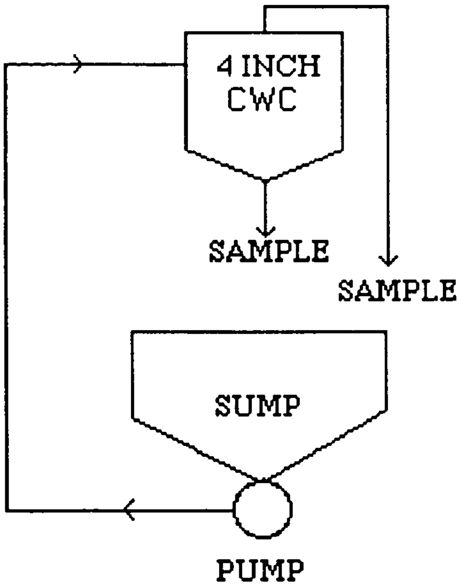

Figure 3-8. Conventional closed circuit CWC test loop used by MIRL.

ously for 2 to 5 seconds. Then, dismantling the cyclone to clean out any trapped gold, not to mention all the possible gold traps existing in the system's plumbing.

Let's assume we want a CWC feed pulp density of 10%. For MIRL's system this requires a -4 mesh solids charge of approximately 3,000 grams. Let's also assume that our -4 mesh material has a relatively high grade of 0.1 oz/ton. Then, on the average one would expect a 3,000 gram sample to contain 10 mg of gold, perhaps as one fairly flaky 10 x 20 mesh gold grain. If the grain is lost in the overflow does this mean the CWC's gold recovery is zero? Should it be recovered, can the investigator claim 100% recovery? The answer to these questions is both yes and no. Based on the results of this one very limited test, yes, but from a common sense and scientific reference the test is meaningless.

What would be preferable? One answer would be to salt the sample with a large number of gold particles of similar size and shape, sample the products, and determine their gold content. This is a reasonable approach until the amount of work of sample reduction and assaying are considered as well as the experimental error they will introduce. Also, the gold recovery of the CWC would be evaluated only for that particular period (X number of seconds) for which its products were sampled.

The advantage of using a radiotracer technique to evaluate CWC gold recovery becomes apparent, considering the facts listed below:

1) The recovery of a particular size and shape of gold is deducible under run of pit grade conditions.

2) The recovery is obtained (calculated) over a long period of time allowing for perturbations of the cyclone's bed, flow patterns, etc.

3) No sampling or assaying of products is required. Recovery is calculated by simple summation and division.

4) The accuracy of the test is predictable from the number of gold transit cycles observed.

5) Depending on the recovery range one is observing and the desired degree of confidence in the gold recovery estimate, test lengths may range from 10 minutes to an hour. Shorter total test times allow the researcher to run a greater number of tests, using time which would otherwise be required for sample reduction, etc.

6) The experimental error is considerably reduced allowing for greater power in statistical conclusions.

Radiotracer Considerations for Compound Water Cyclone Evaluation

Before it was ever decided to proceed with the development of the CWC evaluation system shown in Figure 3-6, much preliminary investigation was devoted to establishing the feasibility of the project. A 3 inch x 3 inch NaI(Tl) scintillator with its associated scaler-discriminator circuit was borrowed from University of Alaska's Institute of Arctic Biology. This was used to check the background radiation level of the CWC, closed circuit system while processing -3/16 inch placer sands of the same origin as would be used for future CWC testing. A background level of 1 to 2 counts per second (cps) was observed for narrow discriminator settings. A level of 10-20 cps was observed over the full range of the discriminator. These results gave the author confidence that background radiation would not interfere with radioisotope detection. Based on the maximum background reading of 10-20 cps it was desirable to use a lower level of radioisotope activity to yield a count rate an order of magnitude above background, or 100-200 cps observed by the detector. The units, counts per second refer to successful radiation interaction with the detection system. This is not to be confused with disintegrations per second (dps), which are units of radiotracer activity.

The next question which arose was that of detection chamber design. This process involved many practical aspects such as available materials for fabrication and compatible piping dimensions but also the consideration of detector counting geometry. A radioactive particle, (considered a point source here) can be thought of as projecting spherical shells of activity, decreasing with distance from the source. A useful equation in this respect can be derived using integral calculus, yielding:

$$A_r \cong \frac{A_o}{2}(1 - \cos\varphi) \qquad \text{Eq. 3-14}$$

where

A_r is the activity seen by a square detector of side length d at distance r from the point source of radiation.

A_o is the total activity of the point source.

$$\varphi = \tan^{-1}\left(\frac{d}{2r}\right)$$

Thus a square 2 inch x 2 inch detector 2 inches from a point source will see only 5.3% of the total point source radiation. At a 3 inch distance the percentage is reduced to 2.6% and at a 1 inch distance this fraction becomes 14.6%.

Cost dictated that the maximum crystal size MIRL could budget was a 2 inch diameter by 2 inch long crystal. Since this crystal was not square the values of Equation 3-14 are only approximate but they serve as useful indicators.

The two inch diameter detectors could be housed in a dry well constructed of 2.5 inch PVC pipe. Flow rate considerations suggested that gold particle transit times past the detector of the CWC underflow would be primarily dependent on gold particle settling velocity. If the detector dry well was centered in a 6 inch steel pipe this would make the maximum radius of detection 2 inches. In the worst case then, the detector would see only 5.3% of the particle's total activity. Returning to the desired detector count rate of 100-200 cps, this would imply a desired particle activity of 1,890 to 3,773 dps. Allowing for 5 days of useful working time indicated the need for a delivered activity per particle of 6,800 to 13,600 dps.

The overflow detection chamber would handle a much higher flow rate than the underflow chamber. It was decided to start the overflow detection chamber in an 8 inch steel pipe and reduce this to 6 inch at the level of the detector. The feed was to be fed into the 8 inch section tangentially. It was thought that gold particles would be thrown outwards to the wall of the chamber where they would pass the detector more slowly. Figures 3-9 and 3-10 show the design the overflow and underflow detection chambers respectively.

When carrying out studies using radiotracers one should recognize that these decay in a "random" manner; the laws of probability describing their behavior. Probability theory can be used to optimize counting time, estimate counting error, and to determine the limits of accuracy of experimental design. In this thesis study, probability and statistics played a very important part in experimental design but their use in evaluating the decay rate of ^{198}Au was rather limited. This is due to the fact that the author was not interested in obtaining total counts of radiation from which to make statements as to the amount of radioactive isotope present. Instead, it was only desired to detect significant pulses above the background radiation level to confirm that a gold particle either exited via the CWC overflow (tails) or underflow (concentrate). Of interest however, was the probability of obtaining an unusually low count rate from a ^{198}Au labeled particle passing the detector. For example, if a ^{198}Au labeled particle has an average activity of 10,000 dps, what is the probability that while in the proximity of the detector, say over a period of 1 second, only 1900 nuclei will disintegrate (5.3% of 1900 would imply a detector count rate of 100 cps). To answer this question a brief explanation of the probability of radioactive decay is required.

The binomial distribution is the basic frequency distribution describing random events such as radioactive decay, failure or success of a task, heads or tails of a coin toss, etc; where an event may produce one of two possible outcomes. In this case, we are concerned with, "does a nucleus decay or not?" The Poisson distribution can be used as an approximation to the binomial distribution when (1) $\frac{0.693}{T}(t) << 1$, (2) $N_o >> 1$, and (3) $n << N_o$. Where t is the time over which n nuclei decay and there are N_o radioactive nuclei. Conditions 1 to 3 are met by this study. The Poisson distribution has the unique property that its standard deviation, s, is equal to the square root of its mean value ($s = \sqrt{n}$). Thus, for a ^{198}Au labeled grain of activity 10,000 dps, we would expect its count rate distribution to be centered about 10,000 dps with standard deviation, s, equal to 100 dps.

These values of n and s allow us to answer our question about the probability of a particle passing the detector without giving a signal significantly above the background level. It is essentially zero since such an occurrence would lie some 81 standard deviations below the mean value. As a comparison, a decay rate of 9,700 dps, lying only 3 standard deviations below the mean, has about one chance in 1000 of occurring. Therefore, the probability of a particle passing the detector without being detected was seen to be of little consequence.

Figure 3-11 shows a reproduction of a section of chart recorder output from one of MIRL tests. Each peak represents the passage of a gold particle through the detection chamber, and hence its recovery or loss. The peak height is proportional to:

(1) the rate meter's front panel, full scale reading

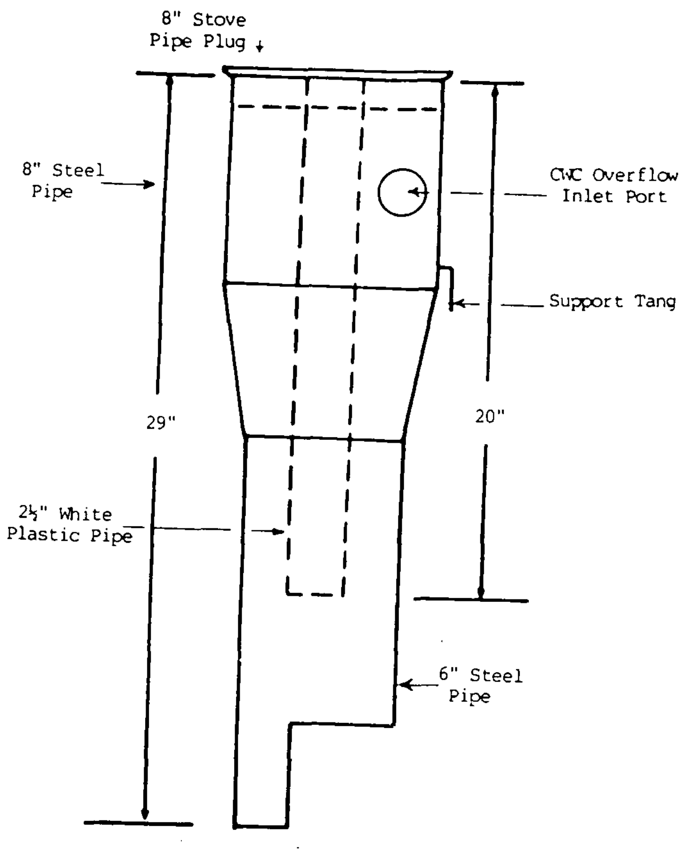

Figure 3-9 CWC overflow detection chamber.

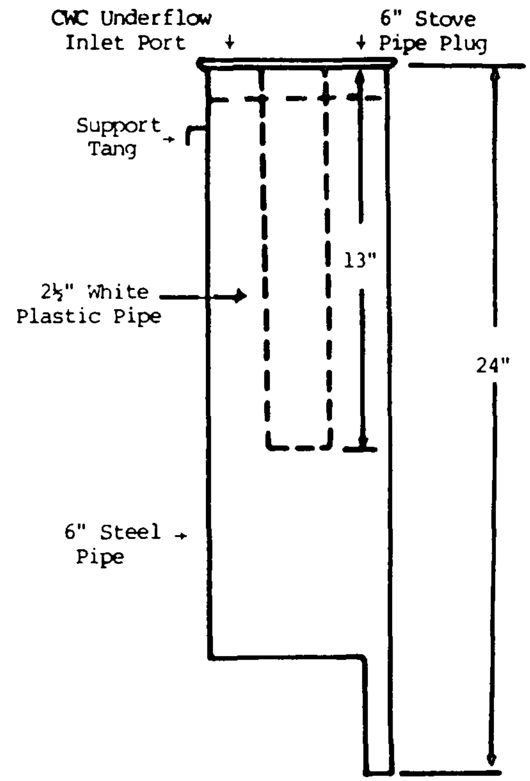

Figure 3-10 CWC underflow detection chamber.

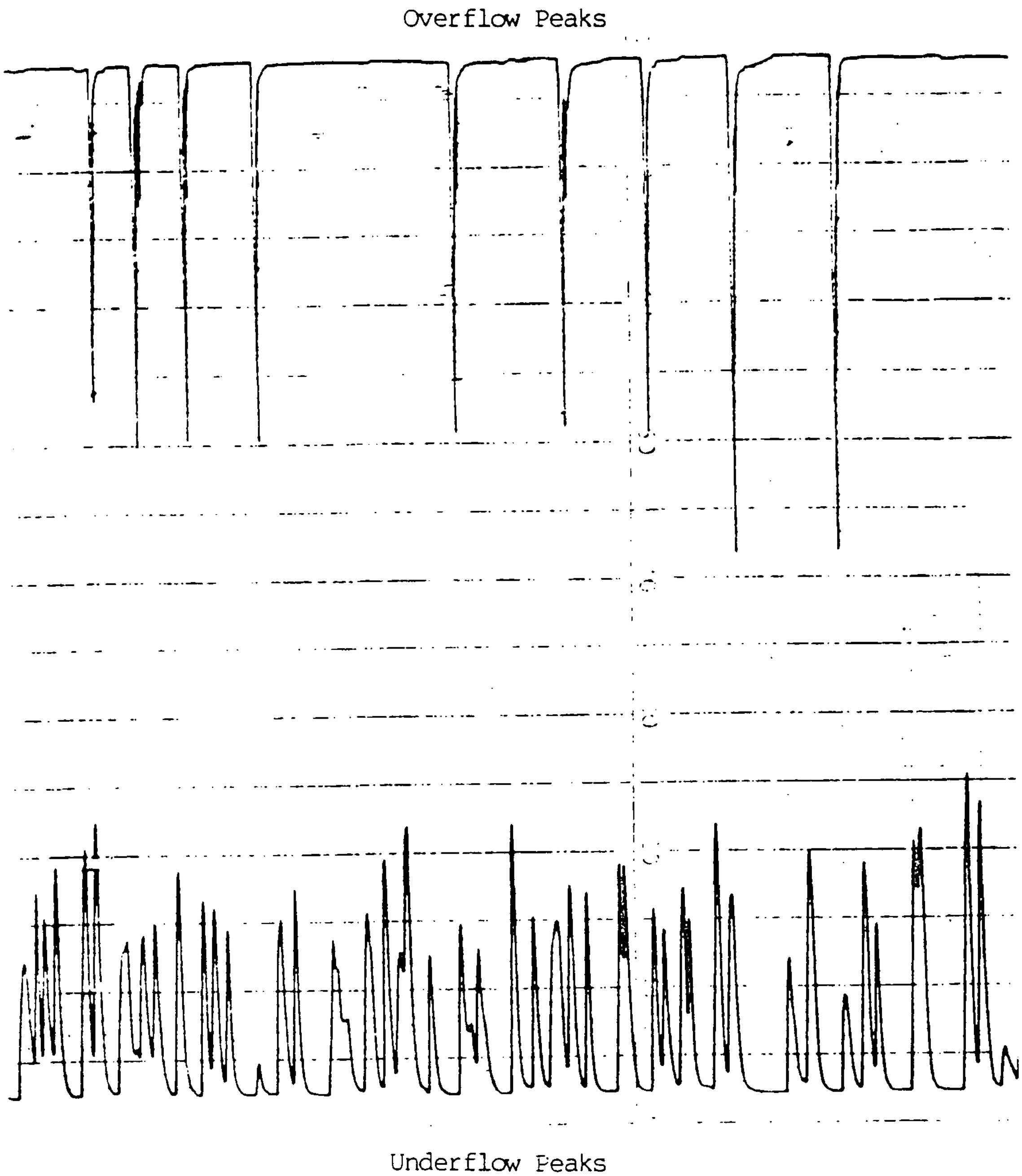

Figure 3-11. MIRL's radiotracer detection system's chart recorder output. Each peak indicates a gold particle's transit through the respective detection chamber.

(2) particle mass (for particles activated for an equal time period)

(3) Particle residence time in the detection chamber i.e. flow rate or settling velocity.

(4) Proximity to the detector of the particle as it transits the detection chamber.

Radiological Safety

One final remark concerning the use of radioactive materials is necessary. This is the matter of radiological safety. It is discussed last in this chapter since much of the preceding information is required for more complete appreciation of the subject. The health and safety considerations discussed below are limited to gamma and beta emitters. The reader should be alerted to the fact however, that other radiation may require different precautions.

As pointed out earlier in this chapter, beta particles and gamma rays interact with matter. This interaction is always harmful in biological systems where it alters cell chemistry. Exposure to radiation should be kept to a minimum, requiring careful experimental planning and adequate radioisotope containment. Hazards from radiation can arise from large doses over a short time period or from long exposure to low level radiation. Both may be equally harmful. Since, like exposure to the ultra violet tanning rays of the sun, nuclear radiation cannot be detected by the senses, dosages received must be monitored by detection devices and a careful record of exposure maintained.

The basic unit of radioactivity is the "curie", which having been redefined in 1950, is equivalent to the quantity of radioisotope in which the number of disintegrations per time is 3.7×10^{10} dps. Many radioactive nuclei emit more than one radiation per disintegration. Therefore to convert curies to actual radiation requires specific knowledge of the radioactive decay scheme of interest. For example, ^{198}Au decays with the emission of one beta particle (0.96 MeV) and one gamma ray (0.4 MeV). Consequently, one curie of ^{198}Au emits 3.7×10^{10} gamma rays and 3.7×10^{10} beta particles per second. Because the curie is a large unit of radioactivity the millicurie (mCi = 3.7×10^7 dps) and microcurie (μCi = 3.7×10^4 dps) are often more convenient units. The new SI unit for activity is the "bequerel" (Bq), 1 Bq = 1 dps.

Both the nature and the intensity of radiation must be considered in assessing radioactive exposure. The consideration of both of these factors leads to the concept of "dose" in biologic systems. Dose is defined as the energy delivered to an area or volume of the biologic unit. "Dose rate" refers to the dose received per unit time.

A unit commonly used to express radiation exposure is the roentgen (r), defined as the amount of radiation (gamma) which produces one electrostatic unit of charge (+ or -) in one cubic centimeter of air at standard conditions. Since the roentgen defines the ionizing effect of gamma or x radiation in air only, other units are necessary to express the absorbed radiation dose to medium such as animal tissue. Common units are the "rad" and "rem". The SI unit for exposure is the "coulomb/kilogram", and for dose, the "gray" and the "sievert".

The rad is the absorbed dose received by a biologic unit exposed to one roentgen of x or gamma radiation. The "rem" is frequently encountered in NRC regulations and is defined as the quantity of radiation, "of any type", which causes the same effect in man as one rad of x or gamma radiation. Both the range and effect of radiation in matter is dependent upon the charge, size, and energy of the radiation. If effectiveness factors are assigned to the various forms of radiation, then their radiation effects can be related to the roentgen. The effectiveness factor is known as the relative biological effectiveness (rbe) factor and the relating equation is:

absorbed equivalent dose (rem) = rbe x absorbed dose (rad)

Beta and gamma rays both have rbe values of 1. Other common forms of radiation, however, have rbes which range from 2 to 20.

Exposure in roentgens per hour (R) at an unshielded distance, d, from a point source of gamma radiation is approximated by the equation:

$$R = \frac{6CE}{2d}$$

where C is the number of curies in the source and E is the energy in MeV of the gamma rays; d is given in feet. As an example, at one yard from a one millicurie point source of ^{198}Au, the exposure rate is approximately 0.23 milliroentgens per hour. A dose of 0.23 millirads per hour would be accumulated. Since the rbe for gamma radiation is 1, the absorbed equivalent dose is 0.23 millirems per hour. Normal background radiation exposure is about 0.025 milliroentgens/hour. The maximum permissible occupational exposure (MPE), is 2.5 milliroentgens per hour, not to exceed 5 roentgens in any year. The maximum allowable permissible dose (MPD) accumulated to a certain age is given by:

$$MPD = 5(N - 18) \text{ rems}$$

where N is the age of the worker. As one might suspect, certain body organs and parts are either more or less susceptible to damage due to radiation. Table 3-1 gives the permitted weekly exposure levels for various body parts.

Table 3-1. Permissible weekly radiation dose to critical body organs. (Gardner, 1967)

Radiation	Skin of whole body	Blood-forming organs	Gonads	Lens of eye
Any type, mrem	600	300	300	300
X and gamma radiation or beta particles, mrad	600	300	300	300
Thermal neutrons, mrad	120	60	60	60
Fast neutrons, mrad	60	30	30	30
Alpha particles, mrad	30	15	15	15

Gamma radiation, because of its uncharged electromagnetic nature, interacts less intensely with the body than other radioactive decay emissions. They penetrate matter more easily and are therefore the greatest hazard from external sources. Gamma rays easily penetrate the skin and reach the inner body organs. Clothing offers little protection, the greatest factors for reducing dose rate being distance from and shielding of the source. As with other forms of radiation, precaution against ingestion of gamma sources is mandatory. Their close association to the body (on clothes, in pores, skin adhesion, etc.) must be avoided.

Before shielding requirements for gamma sources can be considered, it's first necessary to determine the dose rate to the worker from an unshielded source. From this knowledge, the factor by which exposure must be reduced can be calculated and the methods discussed earlier in this chapter used to calculate the shielding material thickness.

Beta particles have a finite range in matter and though they are capable of penetrating thin glass and clothing they are readily absorbed by 3 to 4 mm of glass, plastic or metal (Figure 3-12). Since their range in human tissue is short they produce dosages confined to the body surface (from the skin to a few millimeters in depth). Effects may include the appearance of burns (reddening, blistering). Ingestion of beta emitters is more serious since all of their energy is given up in the tissues.

Soft x-rays are given off when beta particles are absorbed by matter, and are present therefore in addition to beta particles from the source. These soft x-rays have a relatively low penetrating power and may be shielded using a thickness of material only slightly greater than that required for beta absorption.

The measurement of dosages of radiation to which workers are exposed is accomplished by a variety of devices. The simplest and most common type is the film badge. The badge unit is a light tight envelope containing radiation sensitive film. The badge may contain several slips of film, each sensitive to a different level of radiation. Frequently, the film is covered by a film of lead sheet of variable thickness so that the type and energy of the radiation may be identified. Determination of the dose is accomplished by comparison of the film badge darkening to standard comparative film.

Another device and one used by the author is the pocket dosimeter. These are about the size and shape of a felt pen and clip to the pocket with a pen clip. The dosimeter is a rechargeable ionization chamber and may be of either the direct or indirect reading variety. In the direct reading dosimeter a scale (generally in mrems) and indicator hair line are visible when one end of the dosimeter is aimed at a light source. The worker views the scale by sighting through the device, much like a pocket level. Though film badges are sensitive to many forms of radiation, pocket dosimeters are sensitive to only gamma and high energy beta rays.

In addition to the personal monitoring units, it is useful to have available for laboratory use a hand held survey meter. These units are useful for surveying lab floors and furniture for misplaced radioactive material. They may also be used to monitor one's clothing, etc., by passing the detector about the body. The survey meter used in this project, a hand held, battery powered, NaI scintillator, was extremely useful in locating ^{198}Au labeled particles which hung up in the CWC system plumbing. This allowed for remedying trouble spots with bonding agents and for assurance that the system was radioactively clean between runs of various sizes and shapes of gold.

Disposal of ^{198}Au labeled particles was not necessary in this study. No longer useful particles were simply placed in suitably shielded containment and allowed to decay until their radiation level was no longer detectable above background. This gold was saved and will be used in subsequent experiments. The NRC regulates the disposal of radioactive wastes and the reader is referred to these regulations for a full treatment of the subject. The NRC also requires the placement of signs announcing the presence of radioactive

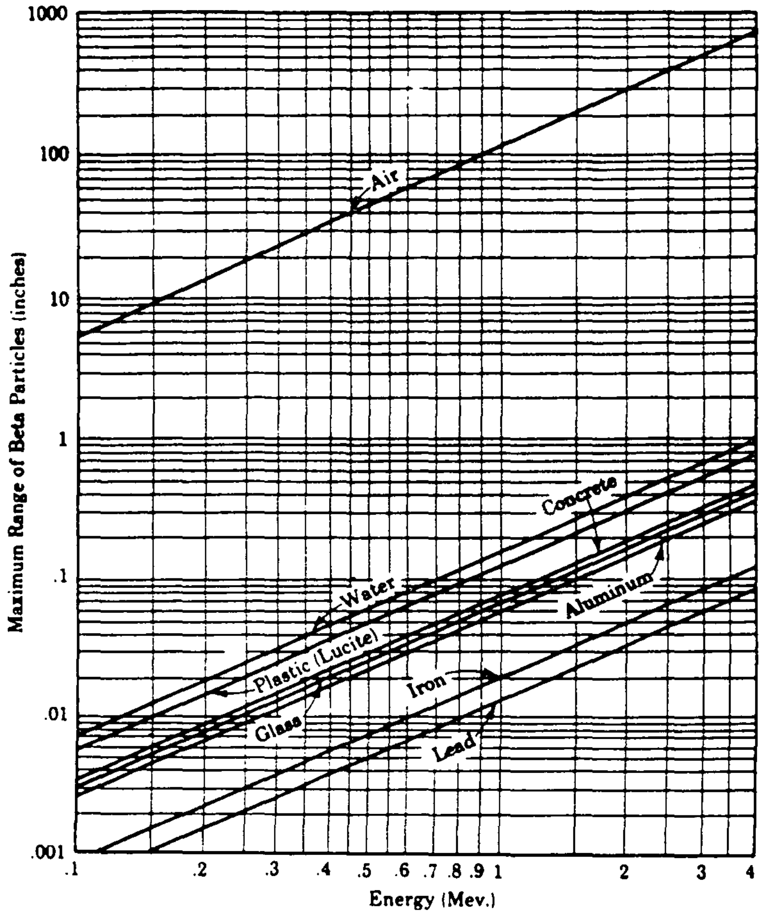

Figure 3-12. Penetration characteristics of beta particles in common materials. (Kohl, 1961)

substances in laboratories using radioisotopes and on containment vessels.

CHAPTER 4

EXPERIMENTAL DESIGN

Introduction

The main reason for performing experiments is to obtain answers to questions. When results (data) from the experiment contain variability which can be explained in part by the influencing factors being studied and in part by experimental error, the use of statistical analysis is crucial to its interpretation. In order for experimental results to be statistically meaningful careful pre-experimental planning is mandatory.

There were, essentially, two major purposes for the initiation and completion of this study. One purpose, of course, was to perform a number of experiments, the data from which would allow the investigator to make specific statements concerning the ability of the CWC to concentrate and recover fine placer gold. The other major objective was to develop and construct a simple, reliable, and efficient analytical system for evaluating gravity concentrators with respect to their recovery of particulate gold.

The data from this study was intended to be of sufficient statistical significance to allow:

1) Estimation of the effect of the investigated factors on gold recovery

2) Comparison of the relative effect of the investigated factors on gold recovery.

3) Confirmation or rejection of hypotheses which MIRL had formed concerning the CWC's ability to recover fine gold.

So that these goals could be attained, the author was aware that conscientious experimental planning would be required in order to provide a systematic and efficient method for conducting the study.

It is not uncommon for experiments to be performed without first identifying the important factors and response variables, setting control levels (seriousness of type I and type II errors), and determining the required sample sizes, a sampling plan, and a method for data analysis. This practice often leads to data which are often of no value at all; the experiment having wasted time, energy, and money.

On the other hand, adequate pre-experimental research and planning can save the same three commodities. Early work to evaluate factors, sample size, measurement accuracy, data analysis, etc., may prove the experiment unfeasible. It may also suggest better ways to approach the problem. Much preliminary research of the statistical and analytical aspects of this study took place before it was ever decided to proceed with the actual experimental work. This chapter discusses the relevant aspects of experimental design which applied to this thesis.

Definition of Terms

Some definition of terms is a prerequisite to the subsequent discussion of this chapter. These are given below:

Factor: A factor is an independent variable to be studied in an experiment, with respect to its effect on the response variable. As used in this study, it refers to those variables of the CWC system or of the gold particles which were suspected of influencing gold recovery (%), the response variable.

Factor Level: A factor level is a particular setting, value, or form of a factor. As an example, there were 3 factor levels of the factor, vortex finder clearance (VFC): 1/2", 3/4", and 1". Similarly, there were 5 levels of the factor, gold size, corresponding to 5 ASTM mesh ranges used: (20 x 30, 40 x 50, 80 x 100, 140 x 200, 270 x 400).

Treatment: Treatment corresponds to a combination of factor levels whose effect on the experimental unit is measured via the response variable. For instance, one treatment level might consist of the CWC settings: VFC = 1", Feed pulp density = 10%, Feed pressure = 6 psig and Cone = Type S. This treatment's effect on gold particles (experimental units) would be measured by the response variable, gold recovery.

Experimental Unit: The piece of experimental material to which one treatment is applied. In this study, a gold particle(s) was the experimental unit.

Replication: Replication refers to the repetition of an experiment. There are three primary purposes for including replication in experimental design: (1) to increase estimate precision; (2) to provide an estimate of the experimental error inherent to the investigation; and (3) to make inferences from the data applicable over a broader base. A replicate observation, or simply replicate, refers to this repetition of a treatment level.

Factorial Experiment: An experiment in which the influence of factors upon the experimental unit are studied. Factorial experiments may be either single factor or multifactor investigations. They may also be either "complete", where all possible combinations of factor levels of the different factors are included or "fractional", if all combinations are not included. In this study only complete, multifactor, factorial experiments were conducted.

Population: In this study, population refers to the infinite (theoretically speaking) number of transits through the CWC by selected gold particles of a particular size and flatness under specific system conditions.

Sample: A subset of the population described above.

In addition, it is assumed that the reader has a basic knowledge of statistics, hypothesis testing, and analysis of variance and linear regression models.

Though the term, experimental design, may include different aspects of preliminary work depending upon who is defining it, in this application it is meant to include the following phases of planning:

I) Response variable identification

II) Factor identification

III) Sample size planning

IV) Sampling plan

V) Data analysis.

These will now be discussed in detail as they applied to this author's study.

Response Variable Identification

This phase was not difficult. MIRL was interested in evaluating the CWC with respect to <u>placer gold recovery</u>.

More difficult was development of an analytical system with which to accurately and precisely measure the response variable.

Factor Identification

The factors to be studied were determined from the results of MIRL's previous field and laboratory work with the CWC and from a literature search for relevant CWC research. Though factors studied varied between experimental phases, there were a total of 9 factors to be evaluated.

a) CWC Vortex Finder Clearance (inches), 3 levels

b) CWC Feed Pressure (psig), 3 levels

c) CWC Feed Pulp Density (%, w/w), 3 levels

d) CWC Cone Type, 2 levels

e) Top size of the solids in the CWC feed, 3 levels

f) Presence or absence of heavy minerals in the CWC feed, 2 levels

g) Presence or absence of a high percentage of -400 mesh slimes in the CWC feed, 2 levels

h) Gold size (mesh x mesh), 5 levels

i) Gold shape (Corey shape factor range), 3 levels

The complete study of these 9 factors was broken down into 5 experimental phases. These are listed in the order of their original planning. In practice, phase 5 was actually performed prior to the completion of phase 4.

1) Prestudy work to determine what sump charges of -4 mesh placer material would yield the desired feed pulp densities.

2) Experimental work to determine CWC overflow and underflow pulp flow rates and pulp densities and CWC concentration ratios at 54 treatment levels (VFC (3) x Feed Pulp Density (3) x Feed Pressure (3) x Cone Type (2)).

3) Using activated gold of 80 x 100 mesh size, with a Corey Shape Factor range of 0.3 x 0.4, its recovery at each of the 54 treatment levels of phase 2 would be determined with 2 replicates per treatment.

4) At various CWC concentration ratios, recovery of gold of size ranges 20 x 30, 40 x 50, 80 x 100, 140 x 200, and 270 x 400 mesh and CSF ranges 0.05 x 0.15, 0.3 x 0.4, 0.6 x 0.8 would be determined.

5) A series of tests would be run to study the influence of (1) the feed's top size, (2) presence or absence of heavy minerals in the feed, and (3) the percentage of slimes in the feed, on gold recovery.

Sample Size Planning

The selection of a sample size is determined by two considerations, (1) the cost in time or money of collecting progressively larger samples and (2) the degree of confidence desired in forming conclusions regarding the sample statistics. Both cost and the level of confidence increase with increasing sample size.

As mentioned earlier, the population, with respect to this study, is considered as all possible transits of selected gold particles of known size and flatness through the CWC. Thus, this population is characterized by a gold particle's passage into the body of the CWC and its subsequent exit after a period of residence through either the vortex finder to the overflow (tails) or the apex with the underflow (concentrate). A gold particle is considered either recovered in the underflow or lost to the overflow. Which ever exiting route the gold grain takes from the cyclone's body, it reenters the feed sump and is pumped back to the CWC where it is again either recovered or lost. In theory then, this is an infinite process, making the population size infinite.

Like the process of radioactive decay, the recovery of these populations of gold particles may be described by the binomial probability distribution, with mean μ = P and variance σ^2 = PQ, where μ and σ^2 have units of percent and percent squared respectively. P, here denotes the probability that a gold particle is recovered, and Q denotes the probability that a gold particle is not recovered, Q = (100%-P). Let us also define N, as the number of transits through the cyclone body which the population of gold particles may make. We have already stated that for our purposes, $N \rightarrow \infty$.

As a general rule of thumb, the binomial distribution may be reasonably approximated by the normal probability distribution whenever the values of N(P) and N(Q) both equal or exceed 5. N in our case approaches a very large value and hence we may safely assume that our populations will be approximated well by a normal distribution. Our populations' recovery distributions may be summarized by the shorthand notation, $P_i \sim N(\mu, \sigma^2)$, which is read; the ith population is normally distributed with mean μ and variance σ^2. This information, in conjunction with the Central Limit Theorem, aided this author in the selection of sample size, n.

The Central Limit Theorem (CLT) may be summarized as follows (Johnson, 1976):

"If all possible random samples, each of size n, are taken from any population with mean μ and [variance σ^2], the sampling distribution of sample means will have:

(1) mean, μ,

(2) variance, σ^2/n, and

(3) will be approximately normally distributed."

With respect to point number 3, the shape of the sampling distribution of sample means will more nearly approach that of the normal distribution as the sample size, n, increases, regardless of the form of the parent population. For non-normal parent populations, sample sizes of $n \geq 30$ will in most instances yield a near normal sampling distribution of sample means. If the parent population is indeed normally distributed, then even very small sample sizes (n=2) yield normal distributions.

Regarding points (1) and (2) of the CLT, if all random samples of size n (n observations) are taken from the recovery distribution of the parent population, then the sampling distribution of these sample means will have mean $\mu = P$ and variance $\sigma^2 = PQ/n$.

Given a desired level of confidence, $1-\alpha$, and estimates of E (the maximum allowable error) and P; n may be calculated as:

$$n = \frac{[z(\alpha/2)]^2 PQ}{(E)^2} \qquad \text{Eq. 4-1}$$

Equation 4-1 solves for the value of n when a single sample is taken, where;

$z(\alpha/2)$ is the standard score of the critical values bounding the confidence interval.

P is the mean recovery percentage of the parent population and will be estimated by p, the samples recovery percentage.

Q is (1-P) estimated by (1-p)

E is the maximum error of estimate, to be allowed by the investigator, about p. As an example, one might state that the true value of the population mean, P, is contained in the interval $p \pm E$, with a level of confidence of $(1 - \alpha)$.

Since in this experimental work, it was known in advance that each treatment was to have two replicate experimental values of p determined for it, Equation 4-1 may be modified, yielding;

$$n = \frac{[z(\alpha/2)]^2 PQ}{2(E)^2} \qquad \text{Eq. 4-2}$$

One will notice that Equation 4-2 is identical to Equation 4-1 excepting the factor 2 in the denominator of Equation 4-2, which reflects the effect of two replications for each treatment on sample size.

Table 4-1 shows the values of sample size, n, required for various values of P, based on the values of $\alpha = 0.1$ and $E = 2.5\%$ (the reason for choosing $E = 2.5\%$ is presented later). Hence, taking into account only the random error inherent to binomial probability and neglecting the possible error introduced by experimental procedures, Table 4-1 gives the required number of gold particle transits through the CWC which must be observed in order to state at a confidence level of 90% that the observed sampling distribution mean, plus or minus the maximum error of estimate, $p \pm 2.5\%$, contains the true value of the population mean. Note that the maximum number of required observations occurs when P = Q = 0.5 (50%). Note also that Equation 4-2 does not address the level of significance (β) of a Type II error.

This author could see no reason to include β in his calculations of n, sample size. The consideration of a Type

Table 4-1

Values of n Required for Estimates of P ($p \pm E$), at level of significance α.

P	Q	PQ	n	β
.99	.01	0.01	31*	0.005
.95	.05	0.048	147	0.003
.90	.10	0.09	276	<.001
.80	.20	0.16	491	<.001
.70	.30	0.21	645	<.001
.60	.40	0.24	737	<.001
.50	.50	0.25	768	<.001

$\alpha = 0.1$ $(Z(\alpha/2)) = 1.96$
$E = 0.025$ (2.5%)

* In actual experimental practice, no fewer than 100 observations ($n \geq= 100$) were ever made. The beta value listed for P = .99 assumes n = 100.

II error most generally applies to sampling, where it is desired to detect a consequential difference from a known population mean and at the same time limit one's chances of erroneously accepting a false hypothesis. In the case of this experimental work, population means were unknown. Samples were taken to estimate this population parameter and to estimate the difference between population means. Nonetheless, the author has included in Table 4-1 a column which lists the level of significance, β, for the Type II error given p, n, E, and α and assuming that it is desired to know the probability (β) of accepting a false hypothesis as true, where the consequential difference is assumed to be P $\pm$ 10%.

As was mentioned earlier, Equation 4-2 also neglects any variability which may be introduced by experimental procedures. For example, the variation in experimental parameters between replicates of a treatment. Several factors that were subject to introduce additional variability into the treatment replicates were:

1) Size of the gold particles. Though the size of gold particles used in replications was restricted to an adjacent sieve range, this still allowed for considerable size variation within a size range. This variation increased with increasing sizes of gold. For instance, 270 mesh and 400 mesh sieves have respective mesh openings of 53 and 37 microns, whereas 20 and 30 mesh sieves have 841 and 595 micron openings respectively.

2) Flatness of gold particles. Flatness of gold particles was controlled only within a range. Since it was possible that different gold particles were used for treatment replication, flatness as well as size of gold grains many have introduced variability.

3) Vortex finder wear. Both the inside diameter of the vortex finder and the vortex finder clearance varied due to abrasive wear of the slurry. The VFC was allowed to increase by no more than 1/16 to 1/8 of an inch before it was readjusted. The increase of the vortex finders inside diameter was slight compared to the change in VFC, however, it is mentioned here as a possible source of variability.

4) CWC cone wear. Rubber inserts in the cone housing of the CWC did wear slightly over the test period.

5) Pressure gauge inaccuracies.

In order to estimate a reasonable value of E for use in Equation 4-2 the author inspected the results of past laboratory tests of the CWC which MIRL had conducted using standard sampling and assaying procedures. These results suggested that for CWC gold recoveries near 60%, the assaying procedure could introduce errors into percent recovery equal to about 3%. These calculations assumed that standard laboratory assaying procedures are followed for gold analysis employing aqua regia digestion and atomic absorption spectroscopy. Such an assay is considered to yield results accurate to within $\pm$10% of the assay value.

The 3% error figure does not consider the sampling error of products containing particulate values. Sampling error as shown by Wells (1969), can be large in such cases. Errors of 30-40% of the true values are not uncommon due to sampling. It was considered desirable by the author to keep his maximum error of estimate, due to measurement, no worse than that imposed by the assaying procedures of standard laboratories. An E of 2.5% was therefore chosen, while realizing that additional variability introduced by experimental error would increase the estimates of standard errors used for subsequent data analysis.

Sampling Plan

Sample size, n, was determined from Equation 4-2, which reduces to;

$$n = PQ\ (3073) \qquad \text{Eq. 4-3}$$

for $\alpha = 0.1$, $E = 0.025$ (2.5%), and $Z(\alpha/2) = 1.96$.

Once the system was functioning, a minimum of 100 observations was made. An observation here refers to a gold particle passing through the CWC and being detected by the gamma ray detection system as exiting via either the underflow (recovered) or overflow (lost to the tailings) product. Based on the initial 100 observations, a percent recovery value, p, was calculated. This value of p was then used in Equation 4-3 and a value for n determined. If $n \leq 100$ the test was considered complete. However, if the calculated n exceeded 100, the test was continued until n observations were completed, and a new value of p, p', calculated. Using p', a new n, n', was computed. This process continued until $n' \leq n$, yielding the desired degree of accuracy to the estimate of P by p.

Randomization is a major concern to the sampling plan. Randomizing the order of treatments and their replicates helps minimize bias introduced to the experiment by factors (possibly unknown) other than those considered by the investigation. It will also insure that observations are independent of one another.

Practical considerations ruled out the possibility of completely randomizing the order of the tests as they were run in the individual experimental phases of this study. The order, however, was randomized to the greatest degree possible, while still maintaining a reasonably time efficient format for testing. Discussion of the exact mechanics of this randomization is saved for Chapter 5, where each of the experimental phases is discussed in detail.

Data Analysis

After acquisition of the data from a particular experimental phase of the study, the data was to be analyzed using analysis of variance techniques. For this purpose, SPSSX software on the University of Alaska's Vax computer would be employed. The complete factorial experiments carried out in this study were analyzed using either 3 or 4 factors, fixed effects models allowing for the examination of factor interactions. The four factor model is given below:

$$P_{ijkmo} = \mu .... + \alpha_i + \beta_j + \gamma_k + \pi_m (\alpha\beta)_{ij} + (\alpha\gamma)_{ik} + (\alpha\pi)_{im} + (\beta\gamma)_{jk} + (\beta\pi)_{jm} + (\gamma\pi)_{km} + (\alpha\beta\gamma)_{ijk} + (\alpha\beta\pi)_{ijm} + (\alpha\gamma\pi)_{ikm} + (\beta\gamma\pi)_{jkm} + (\alpha\beta\gamma\pi)_{ijkl} + \varepsilon_{ijkmo} \qquad \text{Model 4-1.}$$

where i = levels of factor A ($i = 1, ...a$)

j = levels of factor B ($j = 1, ...b$)

k = levels of factor C ($k = 1, ...c$)

m = levels of factor D ($m = 1, ...d$)

o = number of replicates per treatment ($o=1,...n$)

P_{ijkmo} = The population recovery value at factor levels i, j, k, l, for the oth observation.

$\mu ....$ = The overall mean value of recovery over all levels of factors A, B, C, D.

α_i = The main effect of factor A at level i.

β_j = The main effect of factor B at level j.

γ_k = The main effect of factor C at level k.

π_m = The main effect of factor D at level m.

ε_{ijkmo} = independent, normally distributed random error term. $\varepsilon_{ijkmo} \sim N(0,\sigma^2)$

Terms 6-16 of model 4-1 denote the effects of interaction terms between respective factors at respective factor levels.

The three factor fixed effects model is similar to model 4-1 excepting that terms 5, 8, 10, 11, 13, 14, 15, 16 and subscript m are dropped from the model. The three basic assumptions incorporated into these analysis of variance models are:

(1) The probability distribution of each group of treatment replicates is normal.

(2) The variances of each treatment probability distribution are equal.

(3) Observations from treatment probability distributions are random and independent of all other treatment observations.

Given that the data does not radically depart from these assumptions, analysis of variance techniques allow the investigator to answer the two following questions:

(1) Is there a significant difference between factor level means?

(2) If there is a significant difference between factor level means, how do they differ?

Analysis of variance answers question (1) by comparing the mean error sum of squares of observation within treatments (MSE) to the mean error sum of squares between treatments (MSTR). These two estimates of variability are compared using an F statistic, as one would expect when comparing variances. The connection between comparing variances and comparing the equality of means is made through the mathematics of analysis of variance.

As an illustration, consider the following. The expected value of MSE, written E(MSE), is σ^2, the variance of the random error term ε_{ijkmo}. The expected value of the mean error sum of squares between levels of factor A, (MSA), written E(MSA), is given by the expression:

$$E(MSA) = \sigma^2 + \frac{bcdn}{a-1} \sum_{i=1}^{1} (\alpha i)^2 \qquad \text{Eq. 4-4}$$

The F test statistic for comparing these two variances, MSE and MSA, is defined as:

$$F_{TEST} = \frac{MSA}{MSE} \qquad \text{Eq. 4-5}$$

This F_{TEST} is compared to tabulated F values defined by $F(1-\alpha; df_n, df_d) = F^*$

where: α = level of significance of Type I error

df_n = degrees of freedom of the numerator of Equation 4-5.

df_d = degrees of freedom of the denominator of Equation 4-5.

F^* values range typically from 1 to 64 depending on values of df_n and df_d for an α of 0.1, with larger df values yielding lower values of F^*.

The null hypothesis tested is:

H_o: All factor level means are equal.

The alternative hypothesis being:

H_a: At least one factor level mean is significantly different from the others.

The decision rule here is:

If $F_{TEST} \geq F^*$ reject H_o.

If $F_{TEST} < F^*$ fail to reject H_o.

Hence, Equation 4-5 shows that in order for the researcher to conclude H_a; that at least one factor level mean of factor A is significantly different from other factor A level means, $F_{TEST} \geq F^* \geq 1$, and $MSA \geq MSE$. Note that E(MSE) and E(MSA) differ by the term $\frac{bcdn}{a-1}\sum_{i=1}^{a}(\alpha_i)^2$. Recall that α_i is the main effect of Factor A at the ith level. Therefore, in order that $MSA \geq MSE$, $\sum_{i=1}^{a}(\alpha_i)^2$ must be significantly greater than zero. Significance is determined by sample sizes, the number of factor levels, the number of replicates, and the level of confidence desired by the investigator. Similar mathematics can be used to explain tests for the significance of model 4-1's other factor effects as well as interaction effects.

If significant differences between factor level means exist, analysis of variance may then be used to answer the question, "How do the means differ?" Here the analysis of variance model uses MSE as an estimate of within treatment variability. Depending on how many, and what combination of factor levels or treatment means are compared, MSE is modified to reflect the variability of the comparison. The discussion of the mathematics behind the comparison of the difference of factor level means, contrast estimation, and multiple comparison techniques lies beyond the intended scope of this chapter. An excellent treatment of these topics, as well as the analysis of variance models used in this thesis, is given by Neter and Wasserman (1974).

Regarding multiple comparison techniques, prior to the completion of the individual experiments which made up this study, it was not known by the author, which comparison of factor effects would be of interest, excepting of course the initial multiple comparison to determine which factors and interactions were significant. For this reason, the Tukey method was used to maintain an experiment wise error rate for the family of comparisons made after concluding significant factor or interaction effects. The Bonferroni method of multiple comparisons was used to maintain a family significance level for the initial joint statement concerning factor and interaction effects, since this testing process did not involve "data snooping".

In summary, then, the data analysis of this study proceeded according to the format set forth below for experimental phases 3, 4 and 5.

1) The data was tabulated and entered into a computer data file.

2) An analysis of variance (ANOVA) was run on the data using SPSSX software.

3) The data was inspected as to its conformity to the ANOVA model assumptions, by an applicable residual plot to confirm independence of treatment observations and an equal variance test (Bartlett Test). No plot was made to inspect the normality of the sample distributions since their normality is implied by the populations' normality and the Central Limit Theorem.

4) The ANOVA results were used to make statements concerning the significance of factor and interaction effects at a family level of confidence (90%) employing the Bonferroni method of multiple comparisons.

5) The ANOVA results were used to make estimates of the difference between factor level means and other contrasts of interest suggested by the data. These statements were made using a family level of confidence of 90%. The Tukey method of multiple comparisons was used.

6) Graphic plots were produced using SPSSX graphics software to pictorially present significant factor and interaction effects.

CHAPTER 5

EXPERIMENTAL DESCRIPTION AND RESULTS

Introduction

In this chapter, a detailed description of the individual phases of this study is given. In addition to detailing those five phases cited in Chapter 4, Experimental Design, the acquisition and sieve analysis of the run of pit placer material used as the base charge material in all tests is discussed, as is the process used for sorting the gold particles into their respective size-shape classes. Near the end of the project (completion of phase 4), two additional experiments were run. Their inclusion was suggested by previous tests. These two experiments are discussed as phases 6 and 7 at the end of this chapter.

Sample Acquisition and Size Analysis

In July of 1984, the author drove to Northwest Exploration Company's placer mining operation on Fish Creek in the Fairbanks mining district in order to collect a sufficient quantity of run of pit placer material to run the proposed experiments. Three 55 gallon drums were filled from a mound of pit material. This material was located several feet above bedrock and contained no visible clay lumps, which would make screening difficult. Previous field work in the summer of 1984 showed that this material washed and screened easily. The drums were filled using a shovel. Large rocks (+ 3 inches) which were visible were rejected.

This sample was transported to MIRL's laboratory, where it was dry screened at 1/4 inch using a Leahy vibrating screen. The oversize material, which had some fines and surface clay adhering to it was discarded. The undersize material was split down, using a large bar riffle, to a sample of approximately 35 pounds. This split was saved for screen analysis. The remaining undersize material was mixed thoroughly on a concrete pad and shoveled into four 30 gallon garbage cans. A plastic liner was placed between the top of the can and the lid to limit moisture loss.

The 35 pound split was weighed in its moist run of pit condition. Its net weight was 16,554 grams. This value was later compared to the after screening, dry material, weight (14,516 grams) to obtain a value for the "as received" sample moisture content of 12.3% (w/w). After weighing, the sample was soaked overnight in water to facilitate wet screening the following day.

After soaking, the sample was wet screened by hand at 12 mesh. The oversize was placed in an oven to dry. Wash water was decanted from the undersize through a 400 mesh sieve. This wash water was then flocculated and allowed to settle overnight before the clarified water was siphoned off and the solids filtered, dried, and weighed.

The minus 12 mesh, wet screened material was dried and split to a 650 gram sample, which was wet screened at 400 mesh. +400 mesh material was dried, and rotapped for 15 minutes through an ASTM$\sqrt{2}$ series of sieves from 12 mesh to 400 mesh. The minus 400 mesh wash water was again flocculated, filtered, dried and weighed.

The plus 12 mesh material (~5,000g) from the original 35 pound sample was screened over 4, 6, 8, and 12 mesh sieves. Table 5-1 shows the tabulated screen analyses data for the -1/4 inch sample. Since it was desired to feed the 4 inch CWC only -4 mesh solids, each sump charge was screened through 4 mesh as it was added to the CWC system. Table 5-2 shows the screen analysis of the sample adjusted to -4 mesh CWC feed.

Gold Size and Shape Sorting Procedure

Five gold size ranges (20 x 30, 40 x 50, 80 x 100, 140 x 200, 270 x 400) were used during the course of this study, with three Corey shape factor ranges (0.05 x 0.15, 0.3 x 0.4, 0.6 x 0.8) for each size fraction. The gold from a size range was positioned on a gridded microscope slide. Irregularly shaped grains were excluded; only those gold grains approaching disc or rectangular profiles were included. It was hoped that this discrimination against irregular shapes would decrease the spread between gold recovery values within treatment levels.

Once the gold was positioned on the gridded slide, it was measured under a microscope at a suitable magnification using the calibrated ocular scale to determine the dimensions of particle length and width (A and B). Grain thickness, dimension C, was determined from differential focus height using the calibrated fine focus adjustment. The slide surface was taken as height zero, and the average focal surface of the gold grain was taken as height C. A Corey shape factor ($CSF = C/\sqrt{AxB}$) was then calculated for the grain and assigned to the grid location. After all grains on the slide were measured and assigned CSF values, they were sorted into one of the three CSF ranges or to a reject group. When a sufficient number of particles had been separated, the specific size-shape fraction was placed in a 0.4 dram polyethylene vial, the top sealed with a soldering iron, and the vial set aside for later activation.

Phase 1

In phase one, preliminary work was done with the closed circuit CWC test system (Figure 5-1), without its associated gamma detection circuits, to determine the quantity of feed solids necessary in order to achieve the desired feed pulp density levels. The cyclone was set at VFC = 3/4" and fixed with an S type cone. Various charge weights of -1/4 inch feed sample were then added to the running system through a 4 mesh sieve. 60 grams of 12 x 70 mesh magnetite were also added with each charge. The 2 inch variable speed slurry pump was then adjusted to one of three pressure settings (4, 6, 8 psig).

After the system was stabilized at a specific pressure (read from a 0-30 psi gauge) both the overflow and underflow pulp streams of the CWC were cut simultaneously for 5 or 2 seconds (± 0.5 seconds). These products were

Table 5-1

Sieve analysis of -1/4 inch run of pit placer material.

ASTM MESH		SIEVED WT.(g)			CUMULATIVE WT%	
PASSED	RETAINED	ACTUAL	CALCULATED	WT%	PASSED	RETAINED
-	1/4	-	-	-	-	-
1/4	4	1355	1355	9.3	100	9.3
4	6	1179	1179	8.1	90.7	17.4
6	8	1337	1337	9.2	82.6	26.6
8	12	1050	1050	7.2	73.4	33.8
12	16	66.4	894	6.2	66.7	40.0
16	20	61.6	829	5.7	60.0	45.7
20	30	58.5	787	5.4	54.3	51.1
30	40	58.0	780	5.4	48.9	56.5
40	50	52.5	706	4.9	43.5	61.4
50	70	55.1	741	5.1	38.6	66.5
70	100	53.5	720	5.0	33.5	71.5
100	140	50.4	678	4.7	28.5	76.2
140	200	40.6	546	3.8	23.8	80.0
200	270	38.9	523	3.6	20.0	83.6
270	400	34.8	468	3.2	16.4	86.8
-400 dry		26.1				
-400 wet		58.7	1081	13.2	13.2	
-400 wet		840	840			
TOTAL			14,516	100		

Table 5-2

Sieve analysis of -4 mesh CWC feed material

ASTM MESH PASSED	ASTM MESH RETAINED	WT%	CUMULATIVE WT% PASSED	CUMULATIVE WT% RETAINED
4	6	9.0	100	9.0
6	8	10.2	91.0	19.2
8	12	8.0	80.8	27.2
12	16	6.8	72.8	34.0
16	20	6.3	66.0	40.3
20	30	6.0	59.7	46.3
30	40	5.9	53.7	52.2
40	50	5.4	47.8	57.6
50	70	5.6	42.4	63.2
70	100	5.5	36.8	68.7
100	140	5.2	31.3	73.9
140	200	4.1	26.1	78.0
200	270	4.0	22.0	82.0
270	400	3.6	18.0	85.6
-400		14.4	14.4	

weighed, then their solids were filtered, dried and weighed. These weights allowed the calculation of product and feed pulp densities. Table 5-3 shows the results from this series of tests. Using this data, Figure 5-2 was plotted from which the charge weights of 1850 g, 3350 g, and 4975 g were chosen for nominal feed pulp densities (w/w) of 5%, 10%, and 15% respectively.

Phase 2

The purpose of this phase of the study was to provide data on the effect of 4 factors (VFC, Cone Type, Feed Pressure, and Feed Pulp Density) on the concentration ratio of the CWC. In addition, such design data as product pulp densities, product flow rates, and feed flow rates were also calculated. One caution here, these flow rate values were calculated from only 2 second (± 0.5 second) samples. Therefore their calculated values may contain considerable error. They should be viewed as estimates only.

As with the tests in subsequent experimental phases of this project, phase 2 tests were randomized to the maximum degree which allowed for efficient material use and their timely completion. Though phase 2 results were not intended for data analyses it was still considered prudent to randomize.

Because the VFC and the cone type of the CWC are built in but adjustable parameters of the cyclone, their randomization was only partial. The factorial design of phase 2 is shown in Figures 5-3 and 5-4, and its randomization proceeded as follows:

1) VFC was selected first since its adjustment required the most time. A fair die was rolled with a 1 or 2 indicating VFC = 1 inch, a 3 or 4 indicating VFC = 3/4 inch, and a 5 or 6 on the die's upward face indicating VFC = 1/2 inch.

2) Cone type was selected next, again using a fair die, 1, 2, or 3 dictated cone type M; 4, 5, or 6 indicated cone type S.

3) In phase 2, factors feed pressure and feed pulp

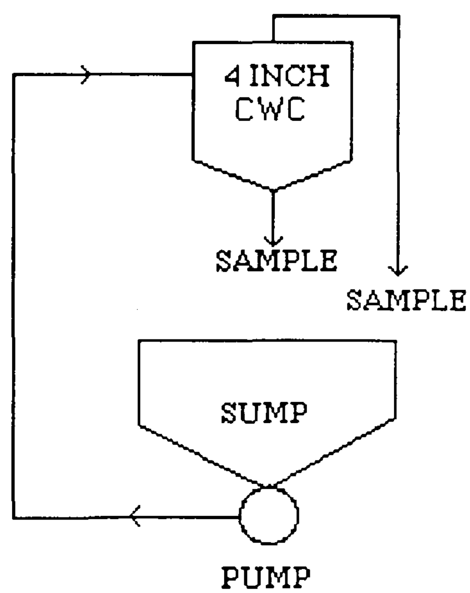

Figure 5-1. Closed circuit test system used in phases one and two.

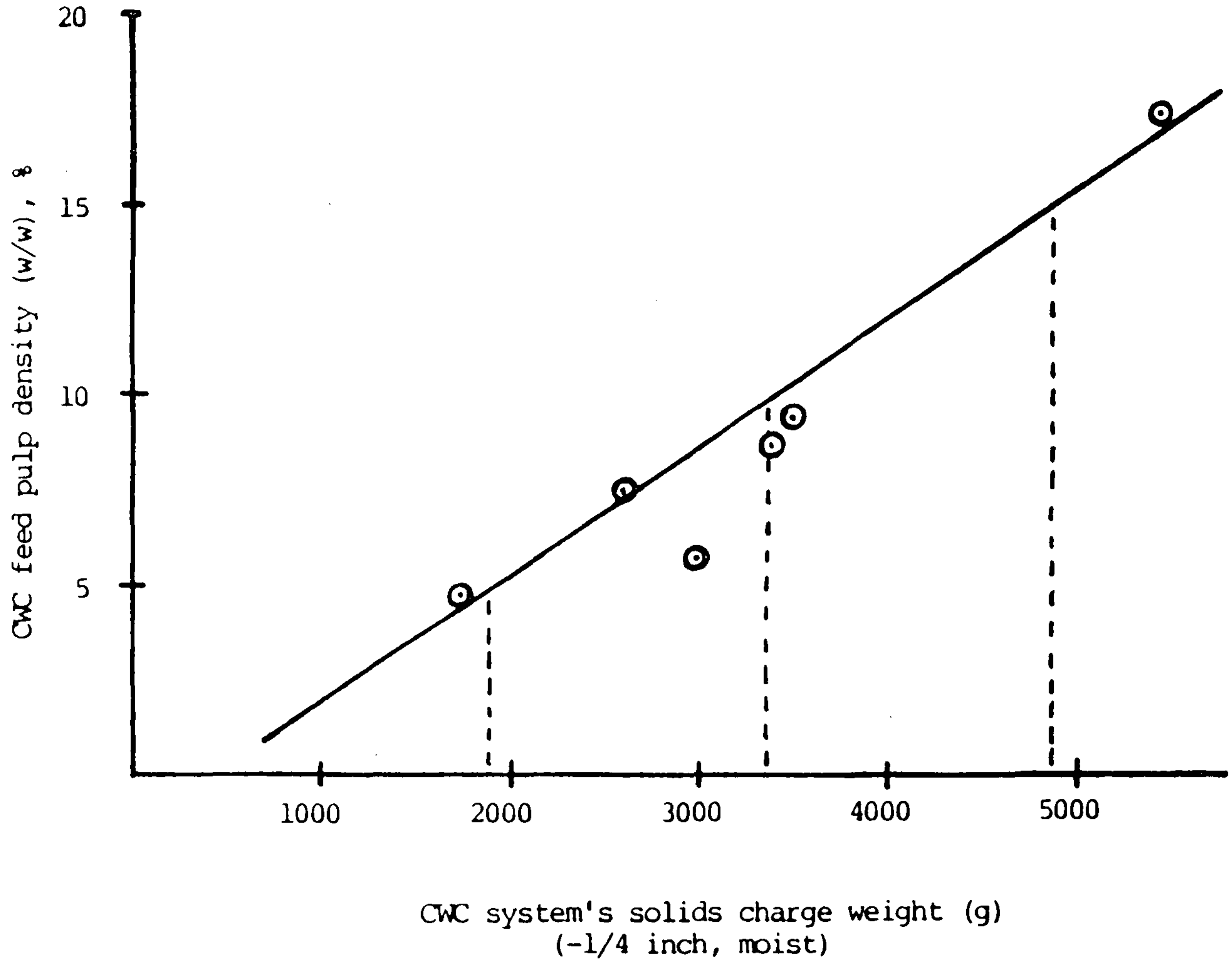

Figure 5-2. Solids charge weight versus feed pulp density.

Table 5-3

Moist, -1/4 inch solids, charge weights and resulting CWC feed pulp density data.

Test No.	Test Length	-1/4 inch Charge Wt (g)	CWC Product	Feed Pressure (psig)	Pulp Wt (g)	Dry Solids Wt (g)	Water Wt (g)	Product Pulp Density	Feed Pulp Density
1	5 sec.	1726	UF	7	329	94	235	28.6%	4.8%
			OF		13,172	561	12,611	4.2%	
2	5 sec.	1071	UF	4	232	49	183	21.1	2.0
			OF		7,529	103	7,426	1.4	
3	5 sec.	3387	UF	7	396	148	248	34.7	8.7
			OF		13,901	1,100	12,801	7.9	
4	5 sec.	2595	UF	10	342	101	241	29.5	7.5
			OF		15,981	1,117	14,864	7.0	
5	2 sec.	5436	UF	4	351	184	267	19.4	17.8
			OF		4,398	764	3,634	17.4	
6	2 sec.	3508	UF	6	169	66	103	39.0	9.4
			OF		5,349	455	4,894	8.5	
7	2 sec.	2987	UF	8	122	40	82	32.2	5.7
			OF		6,514	339	6,175	5.2	

density were completely randomized. After VFC and cone type were selected a random permutation table of 9 was used to randomize feed pressure and pulp density within each VFC x CONE combination.

After the determination of the test sequence the tests were run in a very similar fashion to those of phase 1. The CWC was set with the appropriate VFC and cone, the system filled with water (~30 gallons), and the pump started. A charge of -1/4 inch feed material was then weighed out to yield the appropriate test pulp density. This charge was added to the sump through a 4 mesh sieve along with 60 grams of 12 x 70 mesh magnetite and the system pressure adjusted to test specifications. After approximately one minute, to allow the system to stabilize, a simultaneous 2 second cut was made of the CWC products. These were weighed, dried and reweighed. Tables 5-4a through 5-4f show the data from these tests.

In general, the actual pulp densities of the tests agreed well with the desired nominal pulp densities of 5%, 10%, and 15%; averaging 5.6%, 10.3%, and 14.2% respectively. The CWC's underflow pulp flow ranged from 1 to 3 liters per minute for concentration ratios above 10:1 (S cone) and from 6 to 20 liters per minute for concentration ratios less than 3:1 (M cone). Over this flow rate range, the CWC underflow pulp density varied from 7% to 60%. CWC overflow flow rates averaged 108 1/min at 4 psig feed pressure, 143 1/min at 6 psig, and 166 1/min at 8 psig; carrying from +99% to 83% of total feed water.

Concentration ratios varied from 1.7:1 to 3.4:1 for the M cone and from 5.6:1 to 93.4:1 for the S cone. Figures 5-5 (a-c) and 5-6 (a-c) present the factorial variation in concentration ratio. Both Tables 5-4 (a-c) and Figures 5-5 (a-c) show that the concentration range over the M cone type is narrow and affected only slightly by VFC and feed pressure levels, being proportional to increases in feed pressure and inversely proportional to VFC. Pulp density shows no pattern of influence for cone type M.

For the S cone type (Tables 5-4 (d-f), Figures 5-6 (a-c)) the effect of increasing pulp density appears to lower the CWC's concentration ratio especially at higher feed pressures and narrower VFCs. The effects of VFC and feed

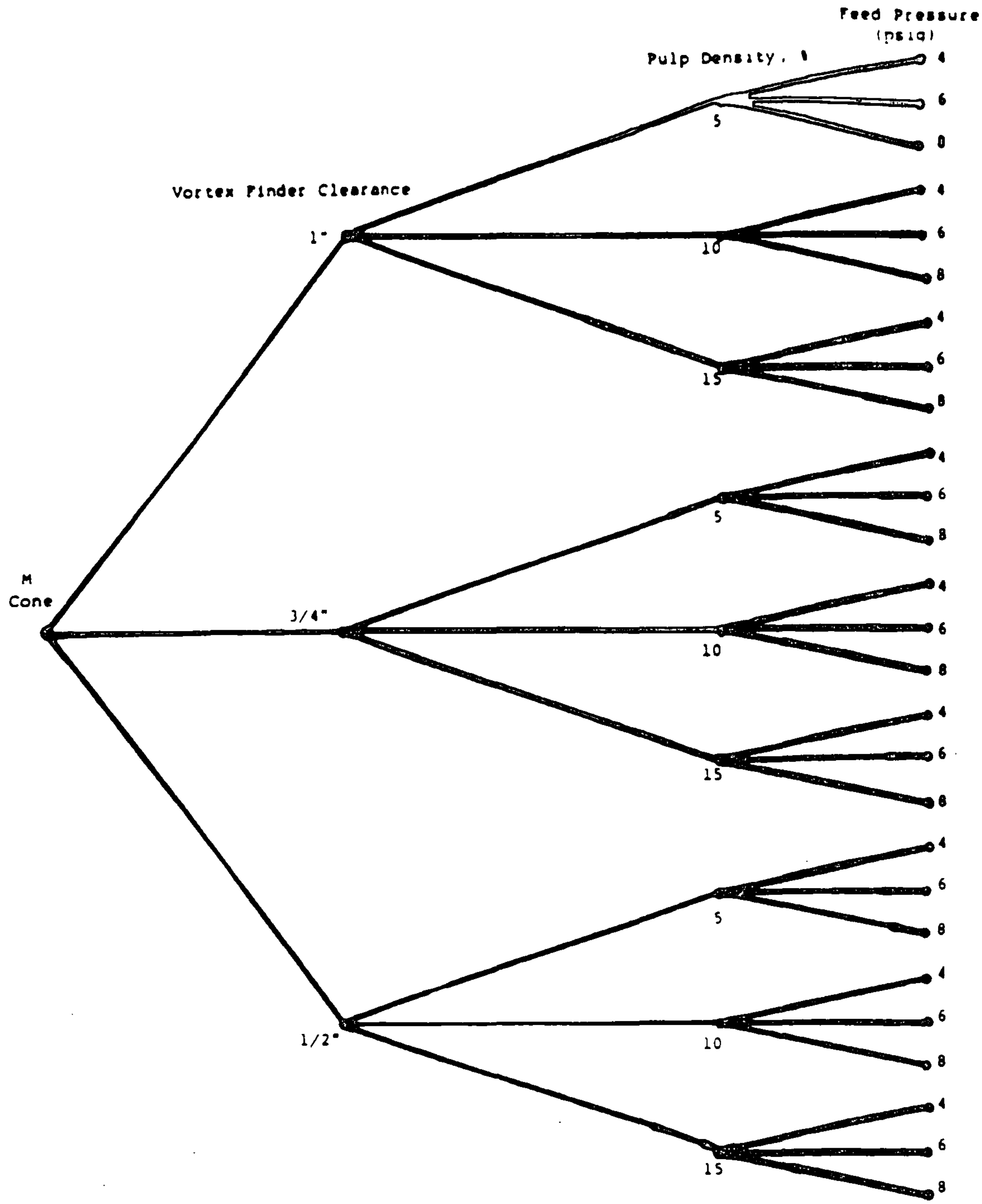

Figure 5-3. Factorial design of phases two and three for cone type M.

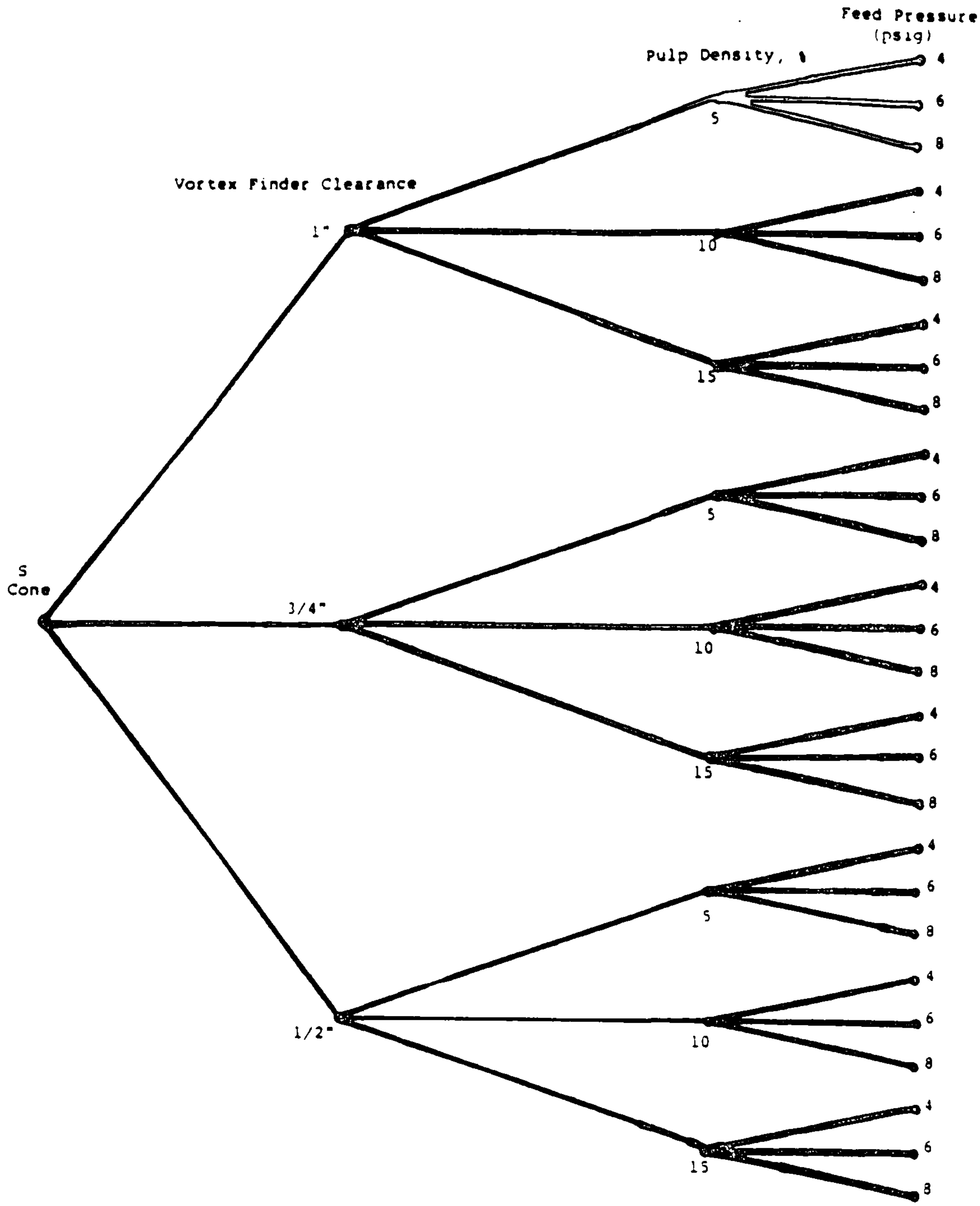

Figure 5-4. Factorial design of phases two and three for cone type S.

Table 5-4a
CWC concentration ratios and products data as affected by CWC feed pulp density and pressure.
VFC = 1 inch, Cone Type = M

Nominal Feed Pulp Density (%)	CWC Feed Pressure (psig)	Test No. (n of 54)	CWC Product	Pulp Wt. (g)	Dry Solids Wt.(g)	Water Wt. (g)	PRODUCTS PD (%)	PRODUCTS Water Flowrate (1/min)	FEED PD (%)	FEED Water Flowrate (1/min)	Concentration Ratio
	4	2	UF	641	168	473	26	14	7	120	1.7
			OF	3,660	115	3,545	3	106			
5	6	7	UF	519	168	351	32	10	6	155	1.9
			OF	4,988	151	4,837	3	145			
	8	4	UF	423	135	288	32	9	4	174	1.9
			OF	5,630	121	5,509	2	165			
	4	9	UF	785	257	528	33	16	11	120	1.8
			OF	3,700	218	3,482	6	104			
10	6	3	UF	660	286	374	43	11	10	157	2.1
			OF	5,170	311	4,859	6	146			
	8	8	UF	588	259	329	44	10	8	189	2.0
			OF	6,231	274	5,957	4	179			
	4	1	UF	1,025	366	659	36	20	15	120	1.9
			OF	3,678	344	3,334	9	100			
15	6	5	UF	819	403	419	49	12	15	147	2.1
			OF	4,963	456	4,507	9	135			
	8	6	UF	707	396	311	56	9	14	175	2.4
			OF	6,062	542	5,520	9	166			

Table 5-4b
CWC concentration ratios and products as affected by CWC feed pulp density and pressure.
VFC = 3/4 inch, Cone Type = M

							PRODUCTS		FEED		
Nominal Feed Pulp Density (%)	CWC Feed Pressure (psig)	Test No. (n of 54)	CWC Product	Pulp Wt. (g)	Dry Solids Wt.(g)	Water Wt. (g)	PD (%)	Water Flowrate (1/min)	PD (%)	Water Flowrate (1/min)	Concentration Ratio
	4	35	UF	624	141	483	23	14	4	110	1.9
			OF	3,320	127	3,193	4	96			
5	6	33	UF	520	157	363	30	11	6	158	2.0
			OF	5,063	152	4,911	3	147			
	8	31	UF	445	137	308	31	9	5	176	2.2
			OF	5,734	161	5,573	3	167			
	4	30	UF	759	238	521	31	16	10	119	1.9
			OF	3,657	216	3,441	6	103			
10	6	32	UF	630	263	367	42	11	10	148	2.0
			OF	4,819	263	4,556	5	137			
	8	29	UF	556	236	320	42	10	9	177	2.5
			OF	5,910	350	5,560	6	167			
	4	36	UF	890	330	560	37	17	15	113	2.0
			OF	3,558	345	3,213	10	96			
15	6	34	UF	759	371	388	49	12	14	148	2.2
			OF	4,995	459	4,536	9	136			
	8	28	UF	700	362	338	52	10	14	168	2.4
			OF	5,808	525	5,283	9	158			

Table 5-4c
CWC concentration ratios and products data as affected by CWC feed pulp density and pressure.
VFC = 1/2 inch, Cone Type = M

Nominal Feed Pulp Density (%)	CWC Feed Pressure (psig)	Test No. (n of 54)	CWC Product	Pulp Wt. (g)	Dry Solids Wt.(g)	Water Wt. (g)	PRODUCTS PD (%)	PRODUCTS Water Flowrate (1/min)	FEED PD (%)	FEED Water Flowrate (1/min)	Concen-tration Ratio
	4	39	UF	436	107	329	24	10	6	120	2.6
			OF	3,835	167	3,668	4	110			
5	6	44	UF	309	107	202	35	6	6	155	3.0
			OF	5,172	210	4,962	4	149			
	8	41	UF	230	85	145	37	4	5	166	3.4
			OF	5,588	200	5,388	4	162			
	4	43	UF	522	178	344	34	10	10	114	2.4
			OF	3,701	243	3,458	7	104			
10	6	42	UF	426	206	220	48	7	10	140	2.5
			OF	4,747	318	4,429	7	133			
	8	37	UF	417	203	214	49	6	10	170	3.0
			OF	5,860	408	5,452	7	164			
	4	40	UF	798	307	491	38	15	16	119	2.5
			OF	3,927	457	3,470	12	104			
15	6	38	UF	550	299	251	54	8	15	137	2.6
			OF	4,792	496	4,296	10	129			
	8	45	UF	487	290	197	60	6	14	159	2.9
			OF	5,644	536	5,108	9	153			

Table 5-4d
CWC concentration ratios and products data as affected by CWC feed pulp density and pressure.
VFC = 1 inch, Cone Type = S

Nominal Feed Pulp Density (%)	CWC Feed Pressure (psig)	Test No. (n of 54)	CWC Product	Pulp Wt. (g)	Dry Solids Wt.(g)	Water Wt. (g)	PRODUCTS PD (%)	PRODUCTS Water Flowrate (l/min)	FEED PD (%)	FEED Water Flowrate (l/min)	Concentration Ratio
			UF	257	54	203	21	6			
	4	10	OF	4,288	247	4,041	6	121	7	127	5.6
5			UF	183	56	127	31	4			
	6	15	OF	6,005	333	5,672	6	170	6	174	6.9
			UF	138	39	99	28	3			
	8	14	OF	6,351	338	6,013	5	180	6	183	9.7
			UF	305	89	216	29	6			
	4	16	OF	4,132	468	3,664	11	110	12	116	6.3
			UF	223	100	123	45	4			
10	6	17	OF	5,743	636	5,107	11	153	12	157	7.4
			UF	172	73	99	42	3			
	8	18	OF	6,495	723	5,772	11	173	12	176	10.9
			UF	475	142	333	30	10			
	4	11	OF	5,106	696	4,410	14	132	15	142	5.9
			UF	222	101	121	45	4			
15	6	12	OF	5,910	691	5,219	12	157	13	161	7.9
			UF	161	73	88	45	3			
	8	13	OF	6,543	761	5,782	12	173	12	176	11.4

Table 5-4e
CWC concentration ratios and products data as affected by CWC feed pulp density and pressure.
VFC = 3/4 inch, Cone Type = S

Nominal Feed Pulp Density (%)	CWC Feed Pressure (psig)	Test No. (n of 54)	CWC Product	Pulp Wt. (g)	Dry Solids Wt.(g)	Water Wt. (g)	PRODUCTS PD (%)	PRODUCTS Water Flowrate (1/min)	FEED PD (%)	FEED Water Flowrate (1/min)	Concentration Ratio
			UF	142	22	120	15	4			
	4	19	OF	4,342	159	4,183	4	125	4	129	8.2
			UF	103	24	79	23	2			
5	6	22	OF	5,359	282	5,077	5	152	6	154	12.8
			UF	64	12	52	19	2			
	8	26	OF	5,855	297	5,558	5	167	5	169	25.8
			UF	229	52	177	23	5			
	4	21	OF	4,080	330	3,750	8	112	9	117	7.3
			UF	135	43	92	32	3			
10	6	23	OF	4,918	485	4,433	10	133	10	136	12.3
			UF	102	29	73	28	2			
	8	24	OF	5,830	505	5,325	9	160	9	162	18.4
			UF	370	96	274	26	8			
	4	27	OF	4,341	605	3,736	14	112	15	120	7.3
			UF	180	73	107	41	3			
15	6	20	OF	5,237	673	4,564	13	137	14	140	10.2
			UF	147	53	94	36	3			
	8	25	OF	6,162	735	5,427	12	163	12	166	14.9

Table 5-4f
CWC concentration ratios and products data as affected by CWC feed pulp density and pressure.
VFC = 1/2 inch, Cone Type = S

							PRODUCTS		FEED		
Nominal Feed Pulp Density (%)	CWC Feed Pressure (psig)	Test No. (n of 54)	CWC Product	Pulp Wt. (g)	Dry Solids Wt.(g)	Water Wt. (g)	PD (%)	Water Flowrate (l/min)	PD (%)	Water Flowrate (l/min)	Concentration Ratio
	4	47	UF	140	30	110	21	3			
			OF	4,022	260	3,762	6	113	7	116	9.7
5	6	52	UF	76	15	61	20	2			
			OF	4,906	287	4,619	6	139	6	141	20.1
	8	49	UF	37	2.5	34.5	7	1			
			OF	5,670	231	5,439	4	163	4	164	93.4
	4	54	UF	254	58	196	23	6			
			OF	4,021	490	3,531	12	106	13	112	9.4
10	6	48	UF	105	36	69	34	2			
			OF	5,655	630	5,025	11	151	12	153	18.5
	8	53	UF	60	13	47	22	1			
			OF	6,190	499	5,691	8	171	8	172	39.4
	4	46	UF	337	77	260	23	8			
			OF	3,907	577	3,330	15	100	15	108	8.5
15	6	50	UF	152	58	94	38	3			
			OF	5,035	705	4,330	14	130	15	133	13.1
	8	51	UF	95	31	64	33	2			
			OF	5,972	777	5,195	13	156	13	158	26.1

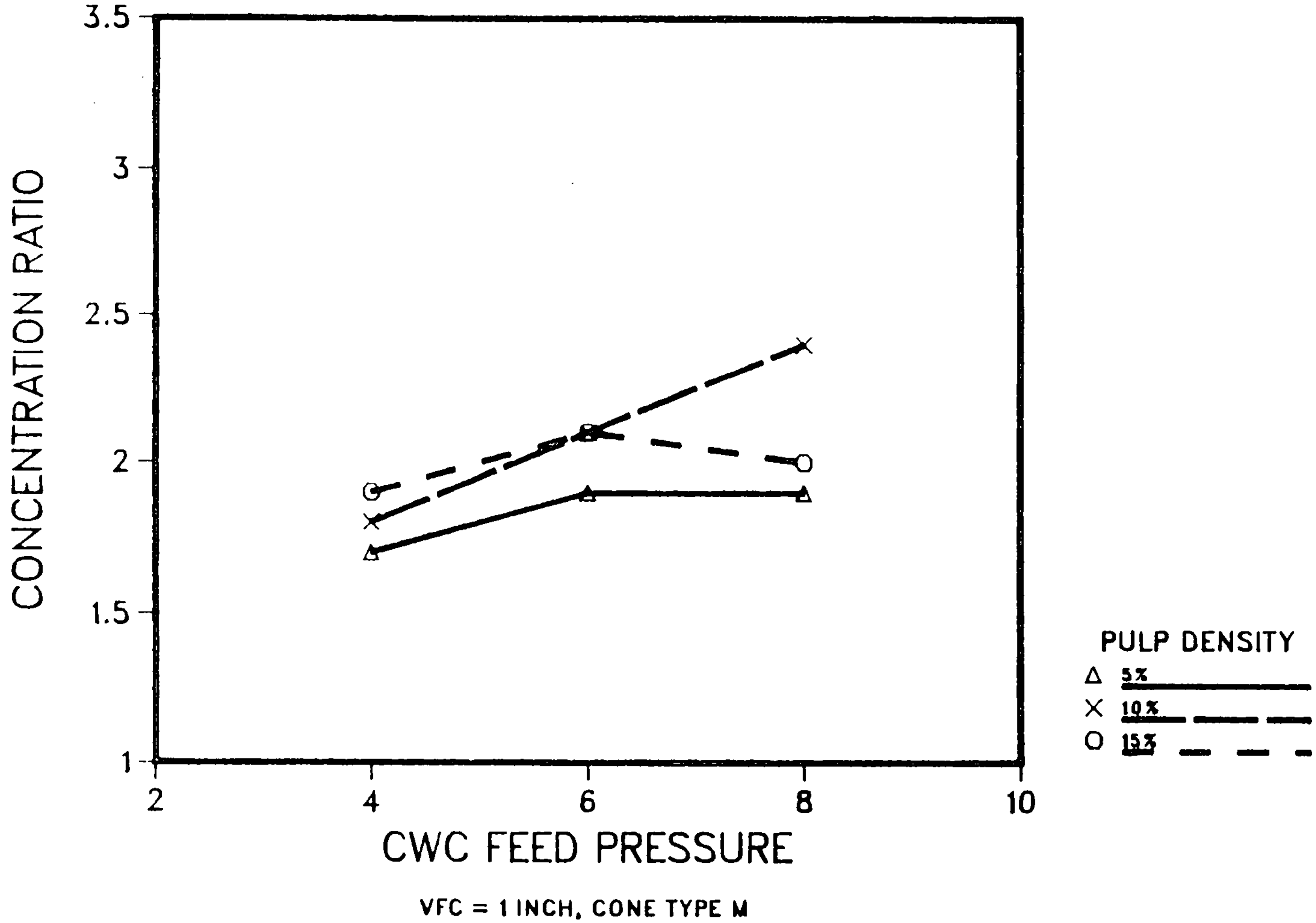

Figure 5-5a. Concentration ratio as a function of CWC feed pulp density and pressure given a VFC of 1 inch, Cone Type = M.

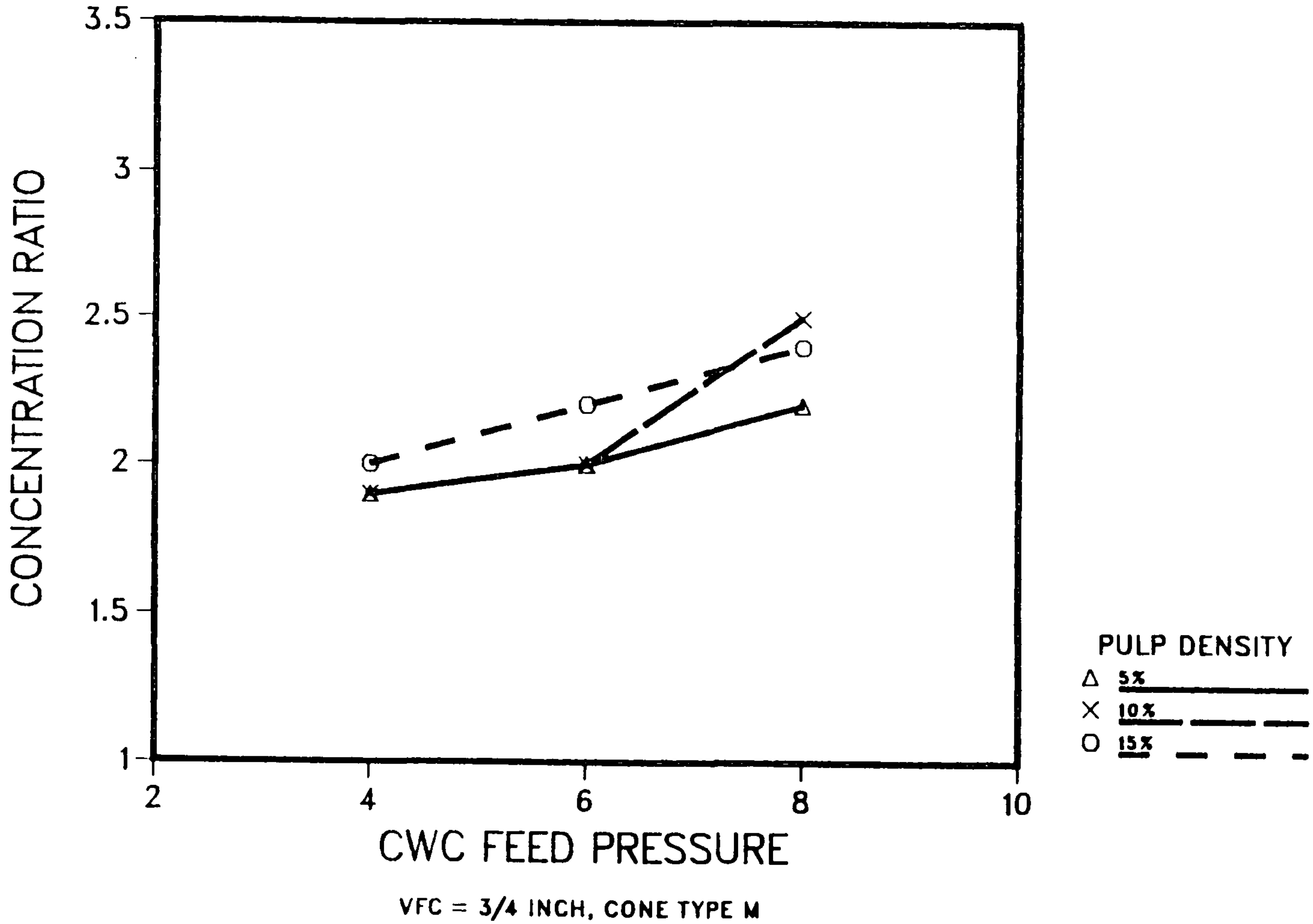

Figure 5-5b. Concentration ratio as a function of CWC feed pulp density and pressure given a VFC of 3/4 inch, Cone Type = M.

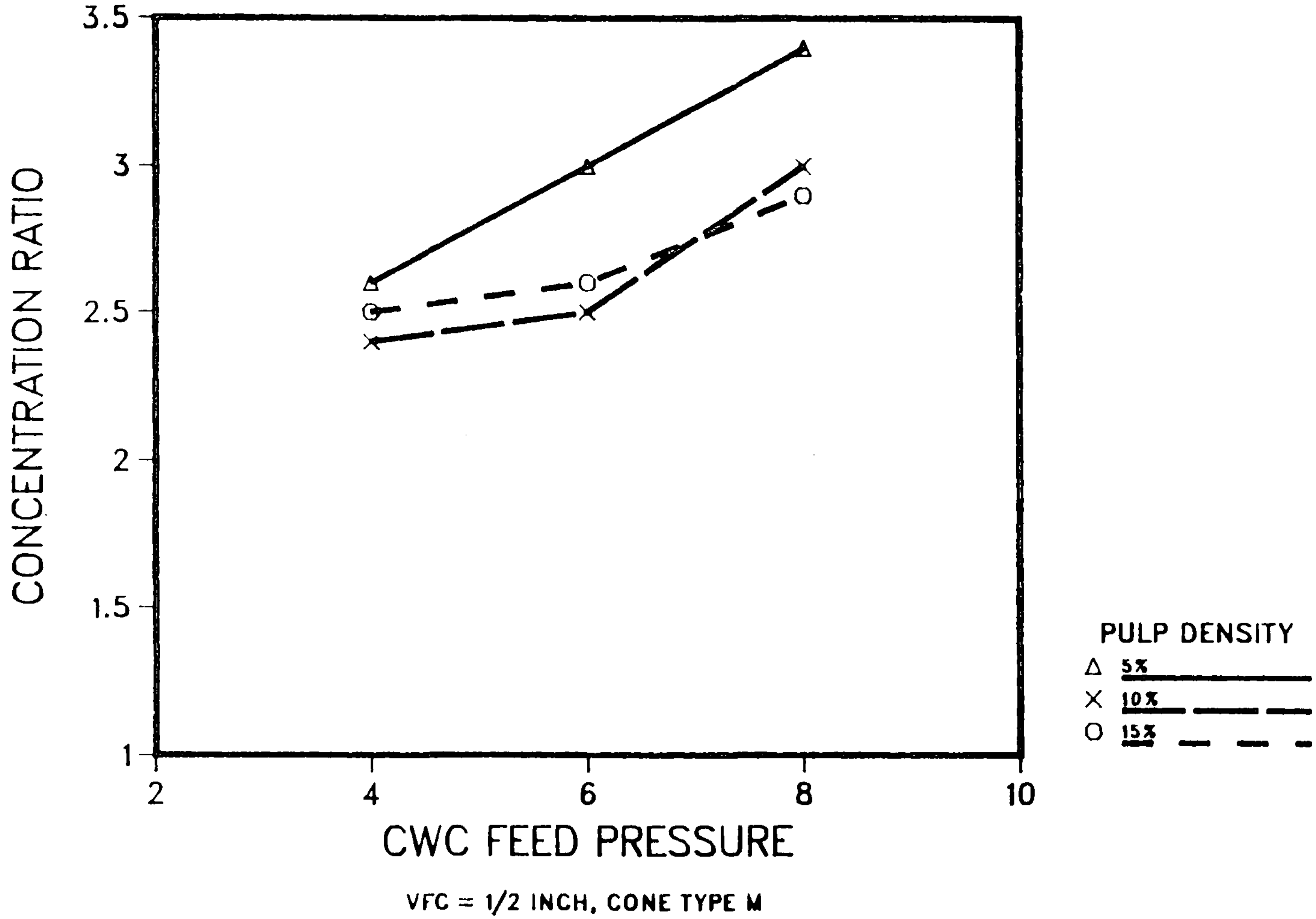

Figure 5-5c. Concentration ratio as a function of CWC feed pulp density and pressure given a VFC of 1/2 inch, Cone Type = M.

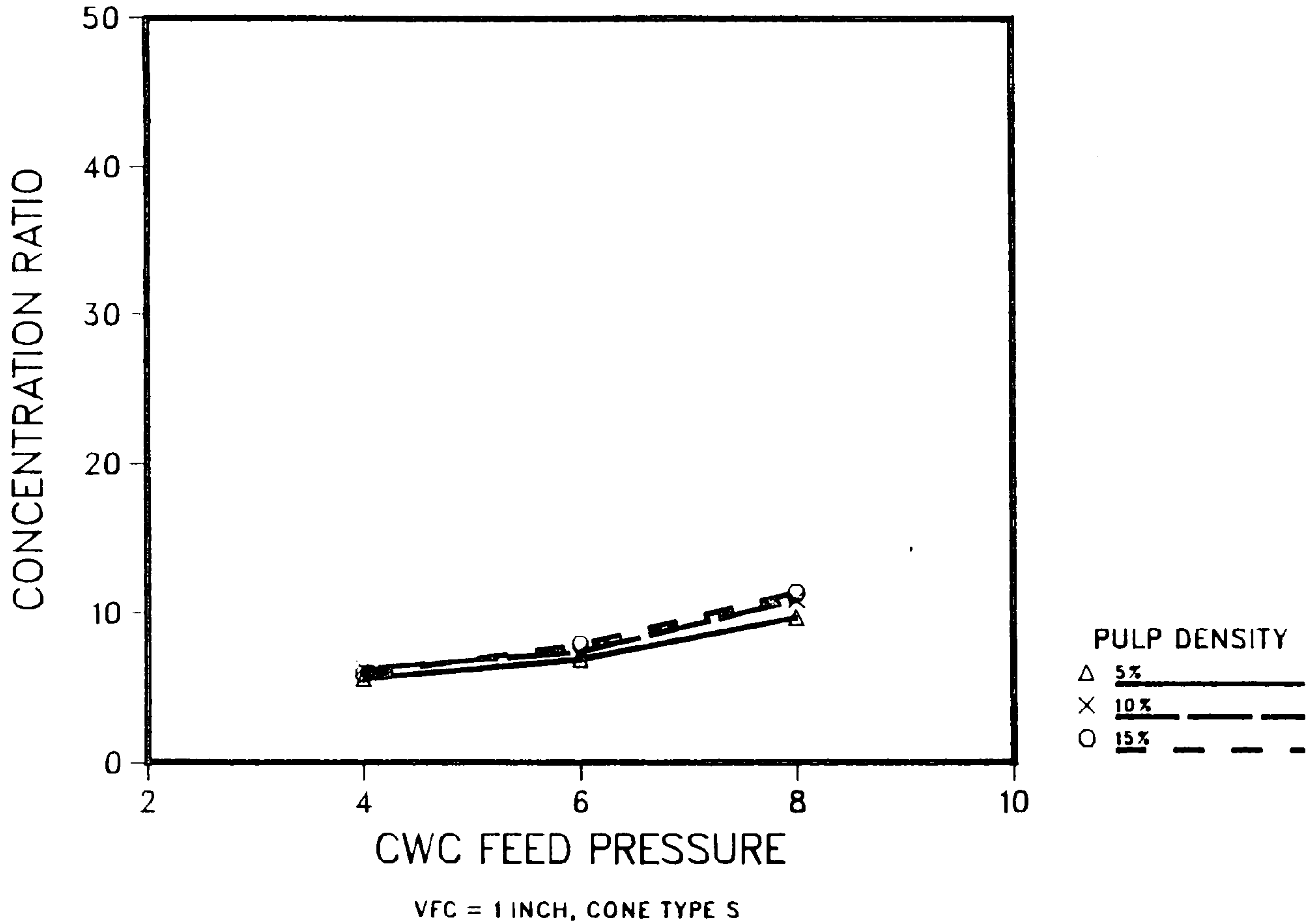

Figure 5-6a. Concentration ratio as a function of CWC feed pulp density and pressure given a VFC of 1 inch, Cone Type = S.

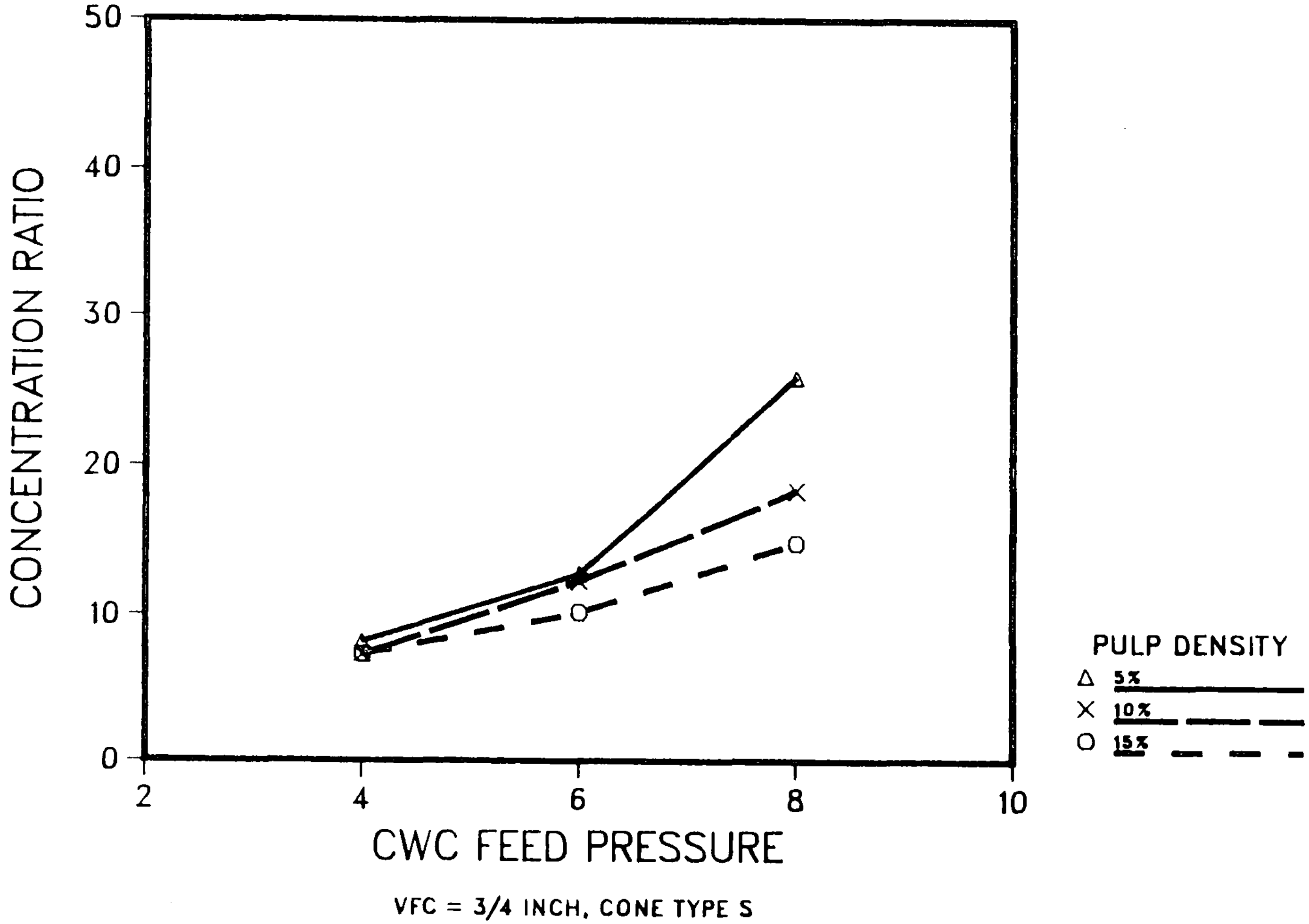

Figure 5-6b. Concentration ratio as a function of CWC feed pulp density and pressure given a VFC of 3/4 inch, Cone Type = S.

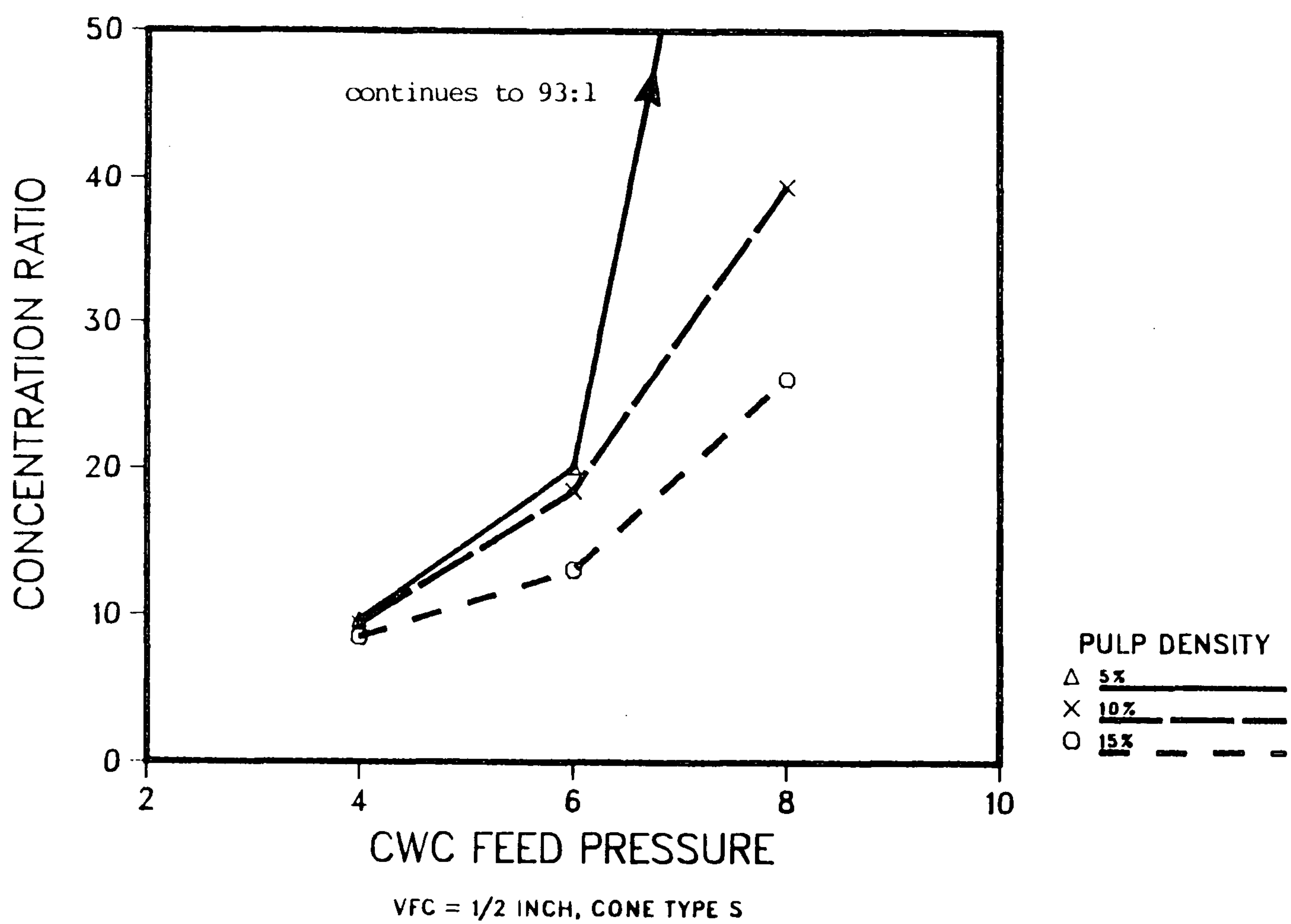

Figure 5-6c. Concentration ratio as a function of CWC feed pulp density and pressure given a VFC of 1/2 inch, Cone Type = S.

pressure on concentration ratio maintain their trend from the M cone but become more pronounced for cone type S. The data suggests that of the varied factors, their effect on the CWC's concentration ratio can be listed in decreasing order; cone type > VFC ≥ Feed Pressure > Pulp density.

During the CWC product sample collection of phase 2 it was noticed that the topsize of underflow product was definitely affected by the varied factors. Screen analyses were run on 10 test products (20 screen analyses) in order to gain some understanding of this underflow topsize variation. Figures 5-7 (a-d) highlight the factor effects. In all 10 cases, it may be noted that although the 4 x 6 mesh fraction comprised approximately 9% of the CWC feed solids there is essentially no +6 mesh material passed to the CWC underflow. Figure 5-7a shows the effect of VFC on underflow topsize over the two cone types. In both cases a decrease in VFC leads to a decrease in the fraction of coarse material in the CWC underflow. The three VFC curves for each cone type have been averaged and plotted in Figure 5-7b to show the influence of CWC cone type on underflow topsize. Cone type appears to have a very significant impact on decreasing the topsize of the underflow product. Note that essentially all of the +12 mesh material reported to the overflow product when the CWC was fitted with an S cone, compared to an underflow product averaging 12% +12 mesh when an M cone was used.

Over the ranges studied, pulp density again seems to show little effect (Figure 5-7c). Likewise, Figure 5-7d indicates a rather ambiguous feed pressure influence. However, it is this author's belief that the pressure effect on underflow top size scalping could become more obvious where it is coupled to the use of an S type cone and lower VFC's. Though these plots are based on only 10 pairs of CWC products, the pattern suggests that the effect of the four factors on underflow topsize is similar to their influence on the concentration ratio of the CWC, being Cone Type > VFC ≥ Feed Pressure > Pulp Density.

To state that decreasing VFC and increasing pressure would tend to both increase the concentration ratio and decrease underflow topsize seems reasonable since either action in itself increases the fluid velocity across Section I of the compound cone, where the water is forced through the narrow gap between the base of the vortex finder and Section I.

Table 5-5 presents these velocities as a function of VFC and feed flow rate. Note the magnitude of the flow velocities necessary to maintain the water mass balance within the cyclone body. According to Cook (1954) a flow velocity of 2 ft/sec will move 1" pebbles through an unriffled sluice and a velocity of 10 ft/sec will move boulders 12" to 18" in diameter. This gives the reader some feel for the material carrying capacity of the water flowing over Section I of the compound cone. If it were not for the high centrifugal forces acting on the solids here, and the diminished velocities near the surface of Section I, all particles would be scoured away. The notion that a bed-like layer of material can form at the VFCs investigated in this study does not seem reasonable. It is this author's belief that under these conditions only a thin layer of particles coexists with the violent currents and that size plays a significant role in concentration as do the solids' specific gravities. Particles above a certain size extend too far into the current where the current's drag and lift forces overcome the particles centrifugal force component, giving the particle a greater probability of rejection to the overflow.

Note also from Table 5-5 that the calculated water residence time is approximately 0.5 to 1.0 seconds. This corresponds well with the measured residence times of gold particles within the CWC. This will be discussed later in this chapter.

The pronounced effect of cone type for both CWC concentration ratio and the topsize of the underflow product is not fully understood. It is suggested that the shortening of Section I in the type M cone allows material to fall away from the high velocity current more quickly than in the S cone. Hence it has a shorter exposure to the scouring current. The fact that both VFC and pressure show greater effects in an S cone than in an M cone gives some evidence for this hypothesis. The work of Lopatin et al (1977) (Figure 2-11) which showed that concentration ratio decreases for smaller included cone angles, also supports this view.

Table 5-5

Calculated water flow velocities between the base of the vortex finder and section I of the compound cone

	FEED WATER FLOW RATES l/min (gpm)		
VFC	119 (31)	150 (40)	171 (45)
1" (25 mm)	48 cm/sec (1.6 ft/sec)	62 (2.0)	70 (2.3)
3/4" (19 mm)	64 (2.1)	82 (2.7)	93 (3.0)
1/2" (13 mm)	97 (3.2)	125 (4.1)	140 (4.6)
Average water residence time in CWC (sec)	.95	.75	.65

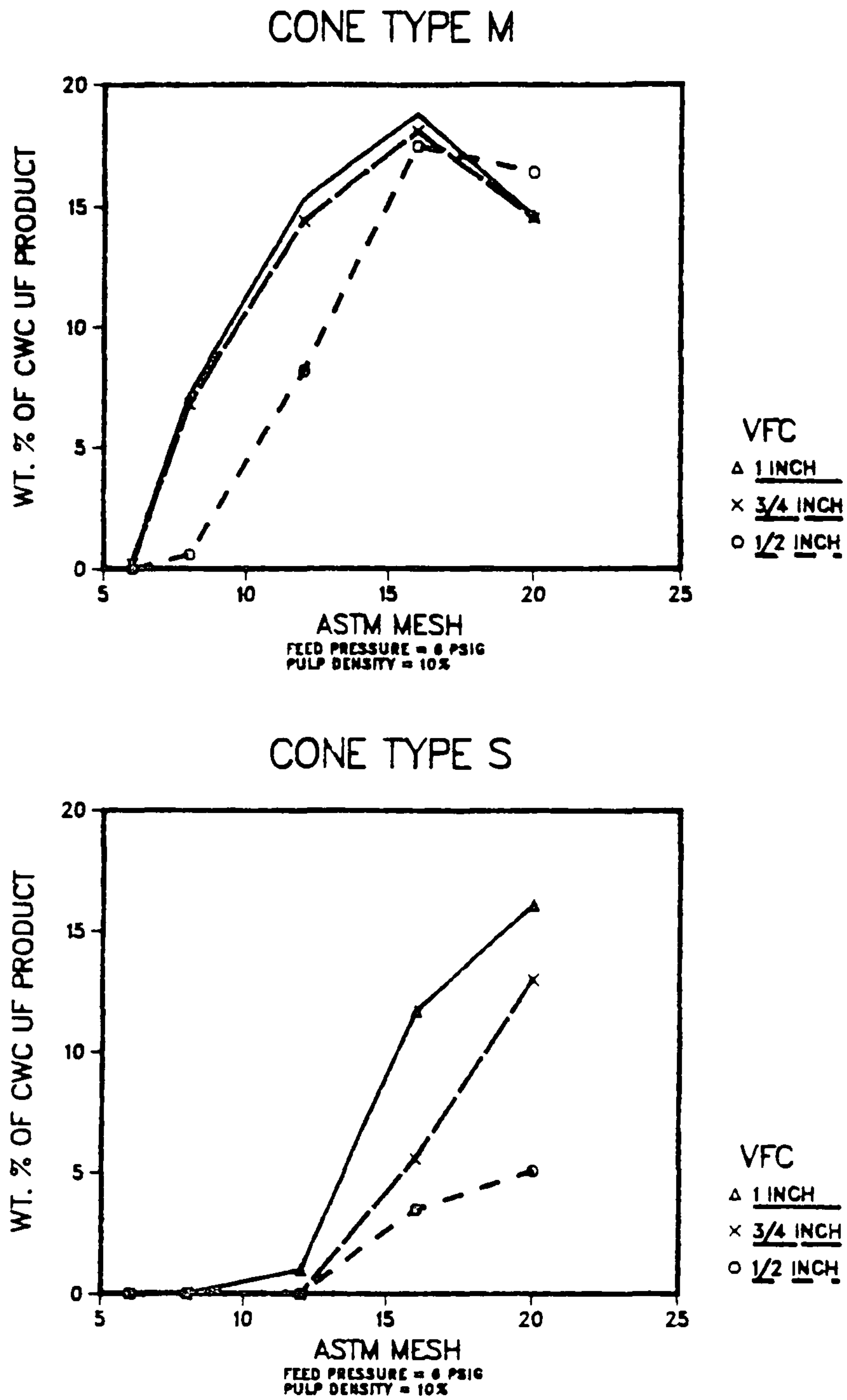

Figure 5-7a. Effect of VFC on CWC underflow top-size for cone types M and S.

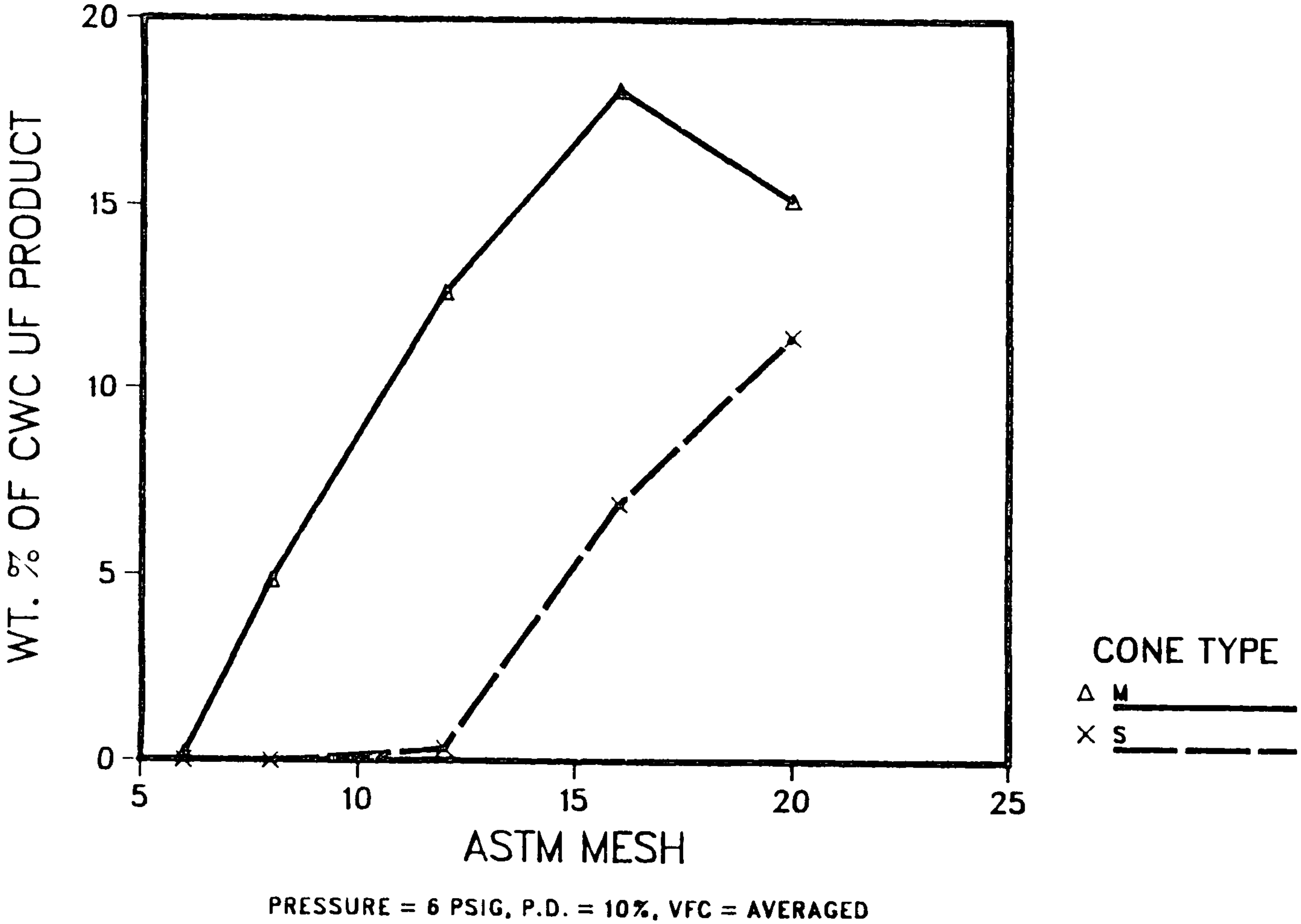

Figure 5-7b. Effect of cone type on CWC underflow top-size.

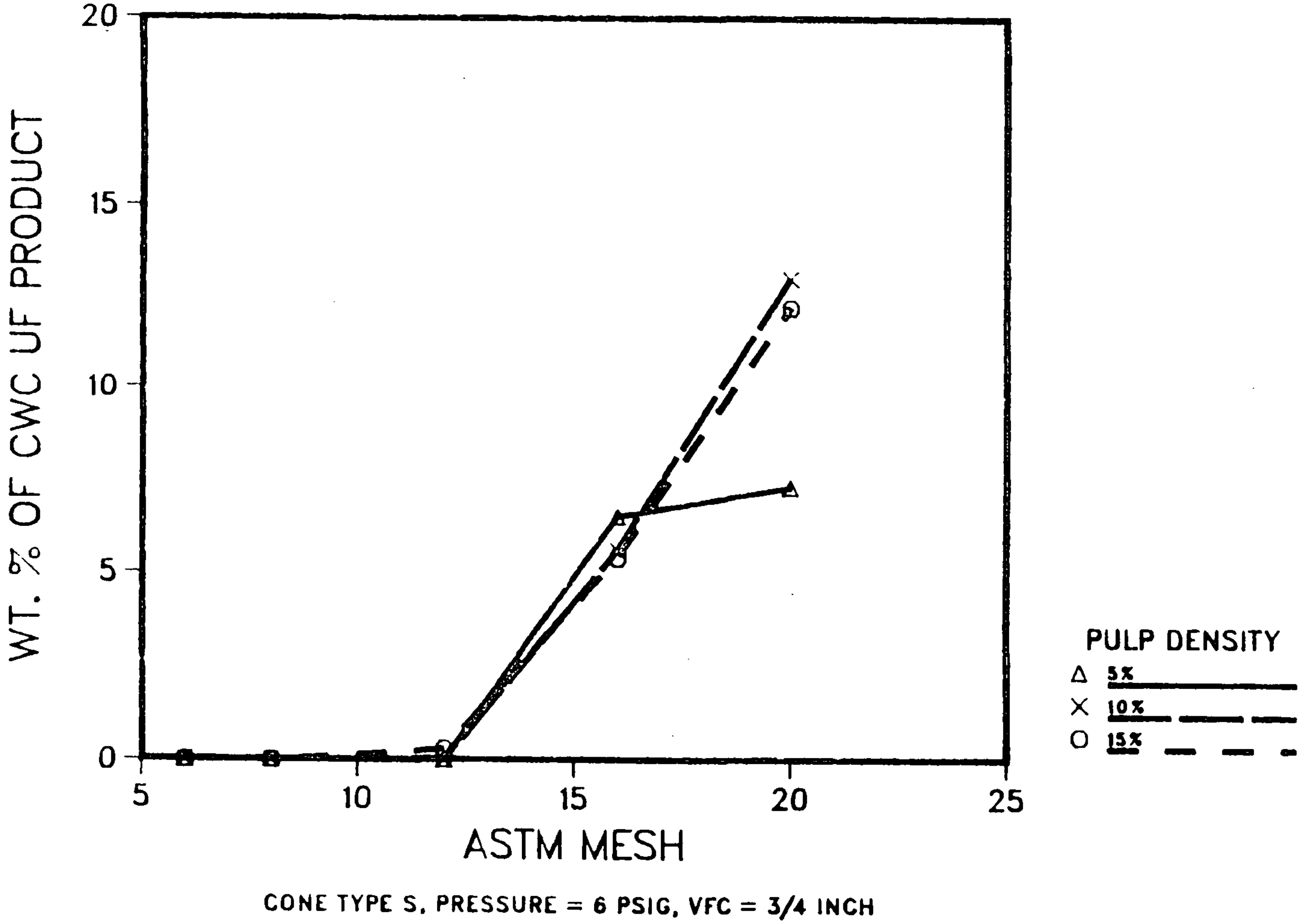

Figure 5-7c. Effect of feed pulp density on CWC underflow top-size.

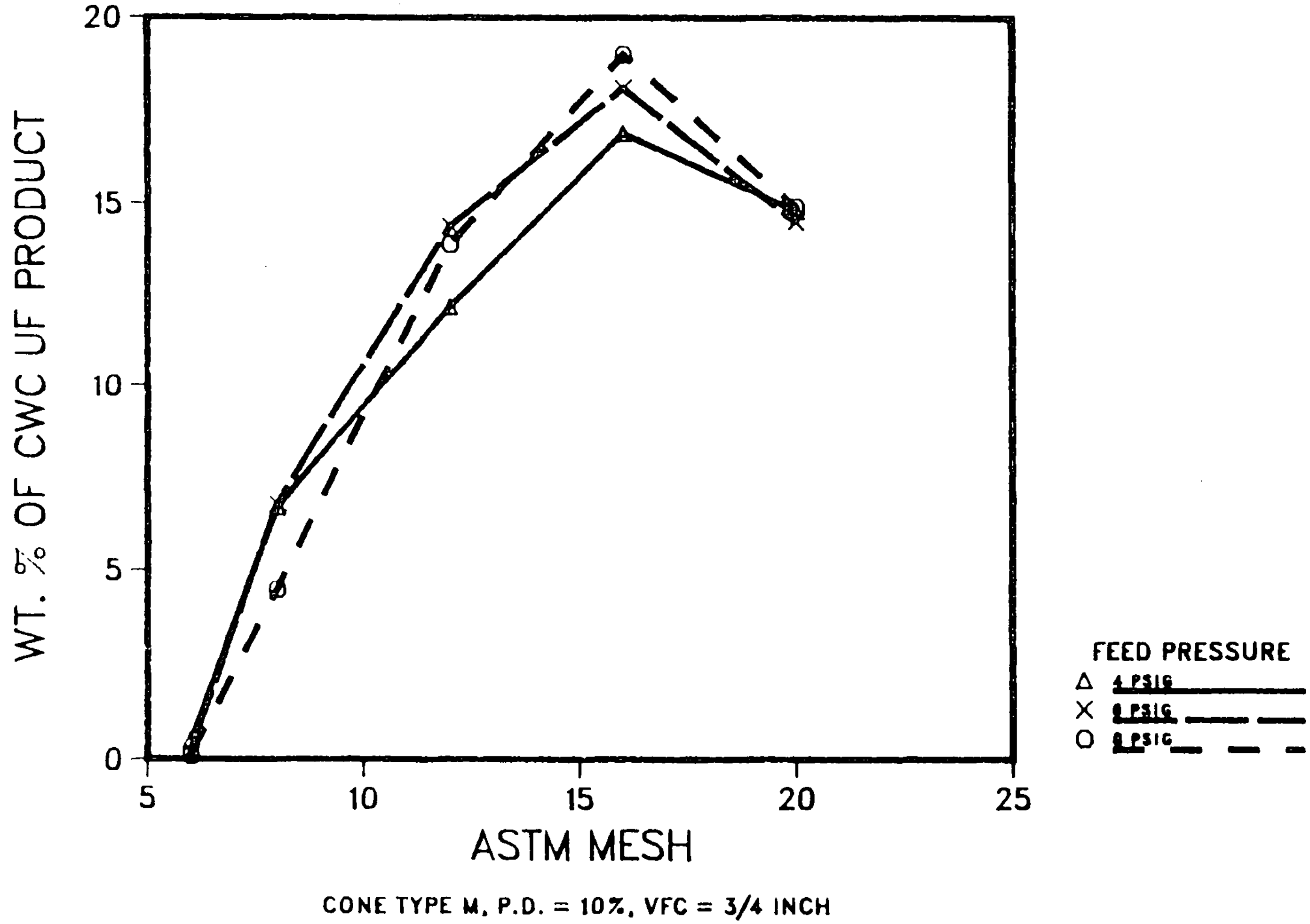

Figure 5-7d. Effect of feed pressure on CWC underflow top-size.

No doubt the larger apex diameter of the M cone, compared to that of the S cone (1 inch vs. 3/4 inch), also plays a role in their differential influence, perhaps by varying the air core diameter and hence affecting the separation processes in Sections II and III. The larger apex obviously allows more pulp flow through it, but whether this increased flow tends to pull particles with it from the upper sections, or whether it is caused by a lower percentage of material rejection in the upper sections, or both, is not clear.

The effect of pulp density on concentration ratio, though rather nondescript under M cone operation, becomes obvious in combination with an S cone, especially at lower VFCs and higher feed pressures. The author proposes two possible explanations for this.

1) The increase in feed pulp density is accompanied by an increase in the Section I particulate density, thereby effectively decreasing interparticle scour.

2) An increase in the solids mass flow rate through the CWC is accompanied by a decrease in their residence time in Section I and therefore a decrease in their rejection frequency.

The fact that pulp density seems to affect the underflow topsize little if at all, would tend to rule out the possibility that an increase in pulp density is overloading the carrying capacity of the scour current in Section I, which could also lead to a decrease in concentration ratio.

Phase 3

In Phase 3 a series of tests were run to evaluate the effect of those same factors studied in Phase 2 on the gold recovery characteristics of the CWC. For this purpose approximately two hundred 80 x 100 mesh gold particles (CSF = 0.3 x 0.4), were shipped for neutron activation. A number of these particles (generally from 4 to 6 particles) were then introduced into the CWC closed circuit system and their transits through the CWC monitored by the radiotracer technique previously described. After the appropriate number of observations had been made to yield the predetermined statistical accuracy to the estimate of recovery, the test was considered complete.

The method of randomizing this series of tests was similar to that described for Phase 2. In Phase 3, however, in order to further expedite the tests and to conserve the placer material being used to charge the system, the order of these tests was yet another step removed from a completely randomized design. The randomization process is described sequentially below:

1) As in Phase 2, the VFC setting was chosen first, followed by the selection of cone type, by rolling a fair die.

2) The procession thru pulp density levels <u>always</u> followed from 5% to 10% to 15%. This allowed the system to operate continuously through a series of 9 tests (3 levels of Pulp Density x 3 levels of Feed Pressure), and required a total feed solids charge weight of only 4,975 grams. 1,845 grams of solids were first added to the system (5% P.D.) along with 60 grams of 12 x 70 mesh magnetite. The three levels of the feed pressure were then randomly assigned. At the completion of this first set of 3 tests, 1,510 grams of additional solids were added to bring the system pulp density up to 10% solids and another three levels of feed pressure randomly run, and so forth.

3) For each pulp density level the levels of feed pressure were randomly assigned by rolling a fair die; an upturned face value of 1 or 2 indicating 4 psig, 3 or 4 indicating 6 psig and values of 5 or 6 indicating 8 psig.

4) The replication of this test series followed the same randomization format. After first assigning test numbers to the first set of 54 treatments, steps 1-3 above were repeated to assign an order to the test sequence of the replicates.

After a series of 9 tests had been completed, the CWC closed circuit system was drained and flushed out. The solids were panned down and the activated gold saved for subsequent tests. The pan tailings were monitored for the presence of radiotracer particles and disposed of. Since only one size and shape of gold was used during this phase of the study, system contamination was not a problem.

Because this was the first phase where radiotracer particles were used, problems were encountered. Initially it was found that many gold traps existed in the closed circuit system despite the fact that the author had mended what he considered problem spots with bonding compound. Eventually, each plumbing transition was removed and smoothed using a die grinding tool. A bonding agent was required to smooth the flange transitions into and out of the slurry pump. The gap between the victaulic connections of the cyclone body and cyclone feed couplings proved particularly troublesome, but this was eventually solved by using rubber washers of the appropriate diameter.

The cyclone's compound cone inserts also offered another gold entrapment area where they interfaced with the casting. A bonding agent was used, but because of the wear in this area, it was necessary to reapply it several times over the course of the investigation.

These were the major obstacles to progress, and after they were remedied, over a two day period, the system functioned extremely well. The gold particles remained in circulation and approximately 4 radiotracer grains were all that were required to expeditiously conduct a test series. As will be seen in the discussion of Phase 4, this was not the case with finer, flakier, gold, which required from 20 to 30 particles for rapid testing.

Tables 5-6 a and b show the data from Phase 3. Table 5-7 shows the analysis of variance (ANOVA) table for this data. Figure 5-8 is a plot of the standardized treatment residuals versus test number. No departure from independence of treatments was observed. Because some treatments contained zero variance, a Bartlett F test could not be run to check homogeneity of variance. Instead Cochran's C test was run, which showed a significant departure ($p = 0.001$) from the constant variance assumption. This is due to the large number of cells (28) containing zero variance, 21 of which existed from M cone treatments. For this reason, when making estimates between factor level means, the following rules were followed:

1) When making factor level comparisons within the M cone, the average within treatment variance for the M cone treatments was used.

2) When making factor level comparisons within the S cone, the average within treatment variance for the S cone treatments was used.

3) When making factor level comparison between cone types, the average within treatment variance for the S cone treatments was used for more conservative estimates.

The ANOVA results indicate significant factor effects for factors; Cone Type, VFC, and Feed pressure. Pulp density does not show a significant effect on gold recovery. Also of statistical significance is a two way interaction between the factors cone type and VFC, which can be seen in Figure 5-9.

A gold recovery of +99% indicates that no gold particles reported to the overflow product in 100 observations. As can be seen from table 5-6a, there exists very little difference between Cone type M treatments level mean gold recoveries. This is also apparent from the near horizontal line in Figure 5-9, which represents the factor level means of VFC for the M cone. Table 5-8 shows the VFC factor level means for each cone type.

Here, and throughout the rest of this paper, the following format is used to present multiple comparisons. The factor level means are set out in array form (Table 5-9) running horizontally from the largest at left to the smallest at right and vertically from smallest at top to largest at bottom. The difference between respective means is listed as an element in common to their row and column, followed by an asterisk (*) indicating significance, or (n.s.) indicating nonsignificance. The variance of the estimates (S^2) and the Tukey T used in constructing the estimates' confidence intervals are listed at the right of the array as is the maximum error of estimate (E) of the confidence intervals.

A summary of significant differences between three or more means is given as shown below.

P_2 P_3 P_1

Again the means are ordered from largest at left to smallest at right. Any pair of factor level means sharing a common underline do not differ significantly. For the example above, only P_2 and P_1 are significantly different.

Due to the cone x VFC interaction, cone factor level means are compared only within a VFC level and VFC factor level means are compared only within a cone type. Because of the lack of variation in the response variable for the type M cone and the VFC x cone interaction effect, the M cone was dropped from the analysis and a 3-way ANOVA was carried out for the S cone data, Table 5-13. Removal of the M cone treatments from the ANOVA also reduced the Cochran C test significance to $p = 0.06$. Heteroscedacity at this level of significance was not considered a problem to ANOVA conclusions or estimates.

ANOVA results again indicate a significant pressure and VFC influence on gold recovery. Feed pulp density is nonsignificant. Figure 5-10 shows the effects of VFC and feed pressure on gold recovery graphically.

A summary of phase 3 conclusions is given below. These conclusions are valid only for 80 x 100 mesh gold (CSF = 0.3 x 0.4).

1) CWC gold recovery is significantly affected by the levels of the factors cone type, VFC, and feed

Table 5-8
VFC factor level means for cone type M and S.

VFC	CONE M	CONE S
1"	+98.97	+98.54
3/4"	+98.88	97.21
1/2"	+98.87	96.31

Table 5-6a
80 x 100 mesh gold recovery (%) and concentration ratios of the CWC as a function of VFC, feed pressure, and pulp density for cone type M

	CONE TYPE M								
	CWC FEED PULP DENSITY (%)								
	5			10			15		
	CWC FEED PRESSURE (PSIG)								
VFC	4	6	8	4	6	8	4	6	8
1"	(12) +99 (102) +99 (1.7)	(10) +99 (101) +99 (1.9)	(11) +99 (100) +99 (1.9)	(13) +99 (105) +99 (1.8)	(14) 99.0 (103) +99 (2.1)	(15) +99 (104) +99 (2.4)	(17) +99 (107) +99 (1.9)	(16) 98.5 (108) 99.0 (2.1)	(18) +99 (106) +99 (2.0)
3/4"	(20) 99.0 (66) +99 (1.9)	(21) 99.0 (65) +99 (2.0)	(19) +99 (64) 99.0 (2.2)	(24) 99.0 (68) +99 (1.9)	(22) 97.8 (69) 98.0 (2.0)	(23) 99.0 (67) +99 (2.5)	(27) 99.0 (72) +99 (2.0)	(26) +99 (71) +99 (2.2)	(25) +99 (70) +99 (2.4)
1/2"	(37) 99.0 (73) +99 (2.6)	(38) +99 (74) +99 (3.0)	(39) +99 (75) +99 (3.4)	(42) +99 (77) 98.8 (2.4)	(40) 99.0 (78) 99.0 (2.5)	(41) 98.0 (76) 99.0 (3.0)	(43) +99 (80) 98.8 (2.5)	(45) 98.1 (81) 99.0 (2.6)	(44) +99 (79) +90 (2.9)

Parenthetic integers indicate test number.
Parenthetic decimals indicate concentration ratio.

Table 5-6b
80 x 100 mesh gold recovery (%) and concentration ratios of the CWC as a function of VFC, feed pressure, and pulp density for cone type S

CONE TYPE S									
	CWC FEED PULP DENSITY (%)								
	5			10			15		
	CWC FEED PRESSURE (PSIG)								
VFC	4	6	8	4	6	8	4	6	8
1"	(1) +99	(3) +99	(2) +99	(4) +99	(6) +99	(5) +99	(9) 97.1	(7) 95.7	(8) 98.3
	(92) +99	(93) 99.0	(91) +99	(94) 99.0	(95) +99	(96) +99	(98) +99	(99) 97.2	(97) 98.4
	(5.6)	(6.9)	(9.7)	(6.3)	(7.4)	(10.9)	(5.9)	(7.9)	(11.4)
3/4"	(29) 97.7	(28) 97.1	(30) 96.5	(31) 98.6	(33) 98.4	(32) 95.8	(35) 95.4	(36) 97.1	(34) 97.7
	(55) 99.0	(57) 97.5	(56) 97.0	(58) +99	(60) 96.0	(61) 95.8	(62) 97.5	(63) 96.0	(64) 97.5
	(8.2)	(12.8)	(25.8)	(7.3)	(12.3)	(18.4)	(7.3)	(10.2)	(14.9)
1/2"	(48) 97.7	(47) 96.5	(46) 94.6	(50) 99.0	(49) 99.0	(51) 96.0	(54) 97.5	(52) 96.0	(53) 97.0
	(84) 97.5	(83) 95.6	(82) 93.5	(86) 97.5	(85) 95.0	(87) 95.8	(88) 95.7	(90) 95.5	(89) 94.3
	(9.7)	(20.1)	(93.4)	(9.4)	(18.5)	(39.4)	(8.5)	(13.1)	(26.1)

Parenthetic integers indicate test number.
Parenthetic decimals indicate concentration ratio.

Table 5-7

4 way ANOVA of phase 3 data for factors cone type, VFC, feed pressure, and pulp density

Response Variable = Gold Recovery (%)

Source of Variation	df	MS	F_{Test}	F*	Comment
MAIN EFFECTS					
A. Cone Type	1	65.3	133.4	8.14	p < .001
B. VFC	2	12.4	25.3	5.63	p < .001
C. Pulp Density	2	1.9	3.9	5.63	n.s.
D. Feed Pressure	2	3.6	7.4	5.63	p < .01
2-WAY INTERACTIONS					
A x B	2	10.3	21.0	5.63	p < .001
A x C	2	2.5	5.1	5.63	n.s
A x D	2	2.7	5.4	5.63	n.s
B x C	4	0.8	1.6	4.07	n.s
B x D	4	1.2	2.6	4.07	n.s
C x D	4	1.3	2.7	4.07	n.s
3-WAY INTERACTIONS					
A x B x C	4	0.6	1.3	4.07	n.s
A x C x D	4	1.0	2.1	4.07	n.s
A x B x D	4	1.1	2.2	4.07	n.s
B x C x D	8	0.5	0.9	3.11	n.s
4-WAY INTERACTIONS					
A x B x C x D	8	0.5	1.0	3.11	n.s
TREATMENTS	53	3.10			
ERROR	54	0.49	(MSE)		
TOTAL	107				

Bonferroni B=15, α= 0.1, $(1 - \frac{\alpha}{B}) = 0.993$

F(.993, 1, 54) = 8.14
F(.993, 2, 54) = 5.63
F(.993, 4, 54) = 4.07
F(.993, 8, 54) = 3.11

pressure used in these tests. It is unaffected by the levels of pulp density.

2) Decreasing the VFC decreases gold recovery when using an S cone type. VFC has no significant effect on gold recovery using a type M cone.

3) Increasing feed pressures above 4 psig decreases gold recovery using an S cone type.

4) An M cone gives superior gold recoveries to an S cone over all levels of VFC.

In viewing these conclusions, the effects of the factors on concentration ratio, discussed previously, should be kept in mind. These would suggest that lower concentration ratios

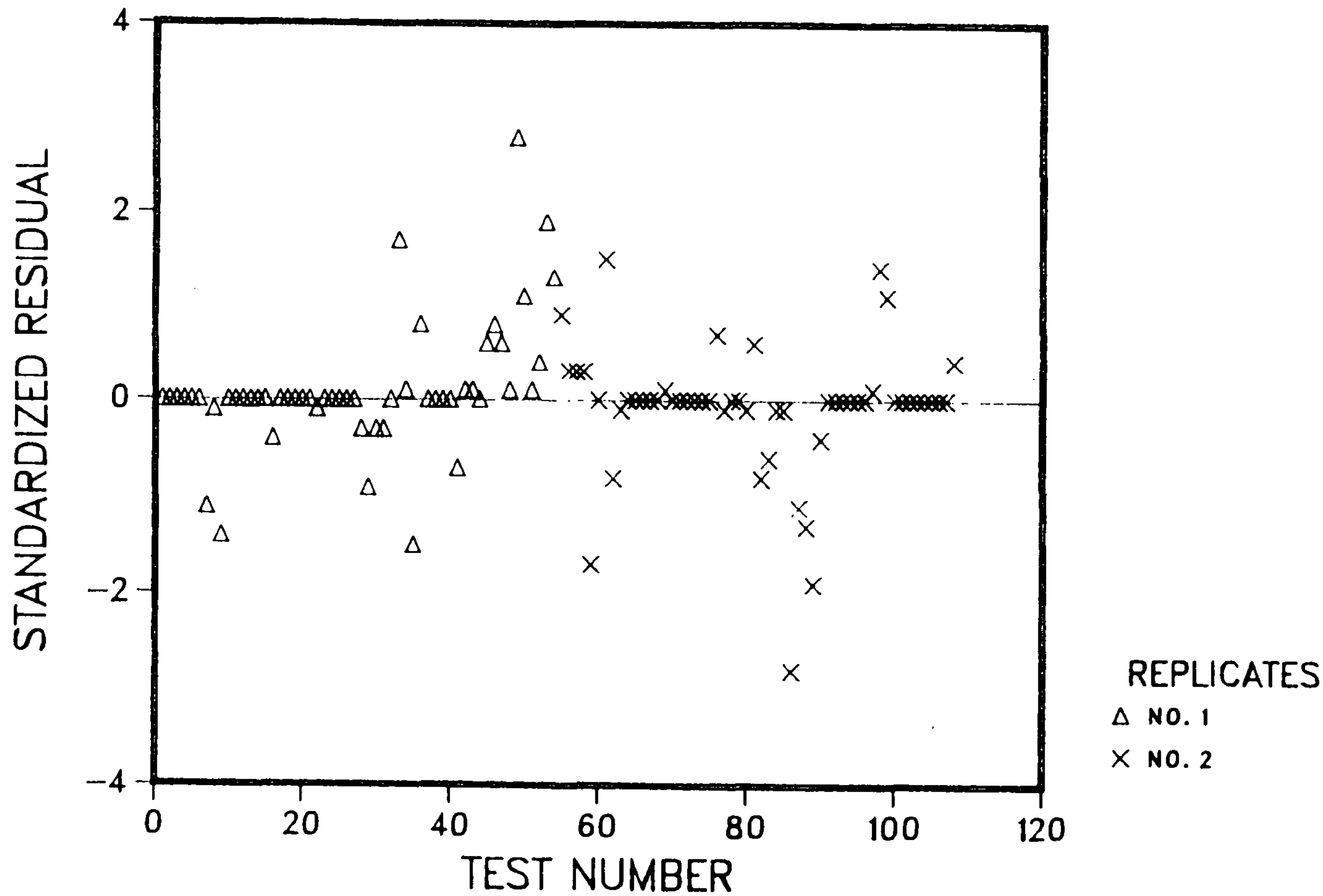

Figure 5-8. Standardized residuals versus test number for phase three data.

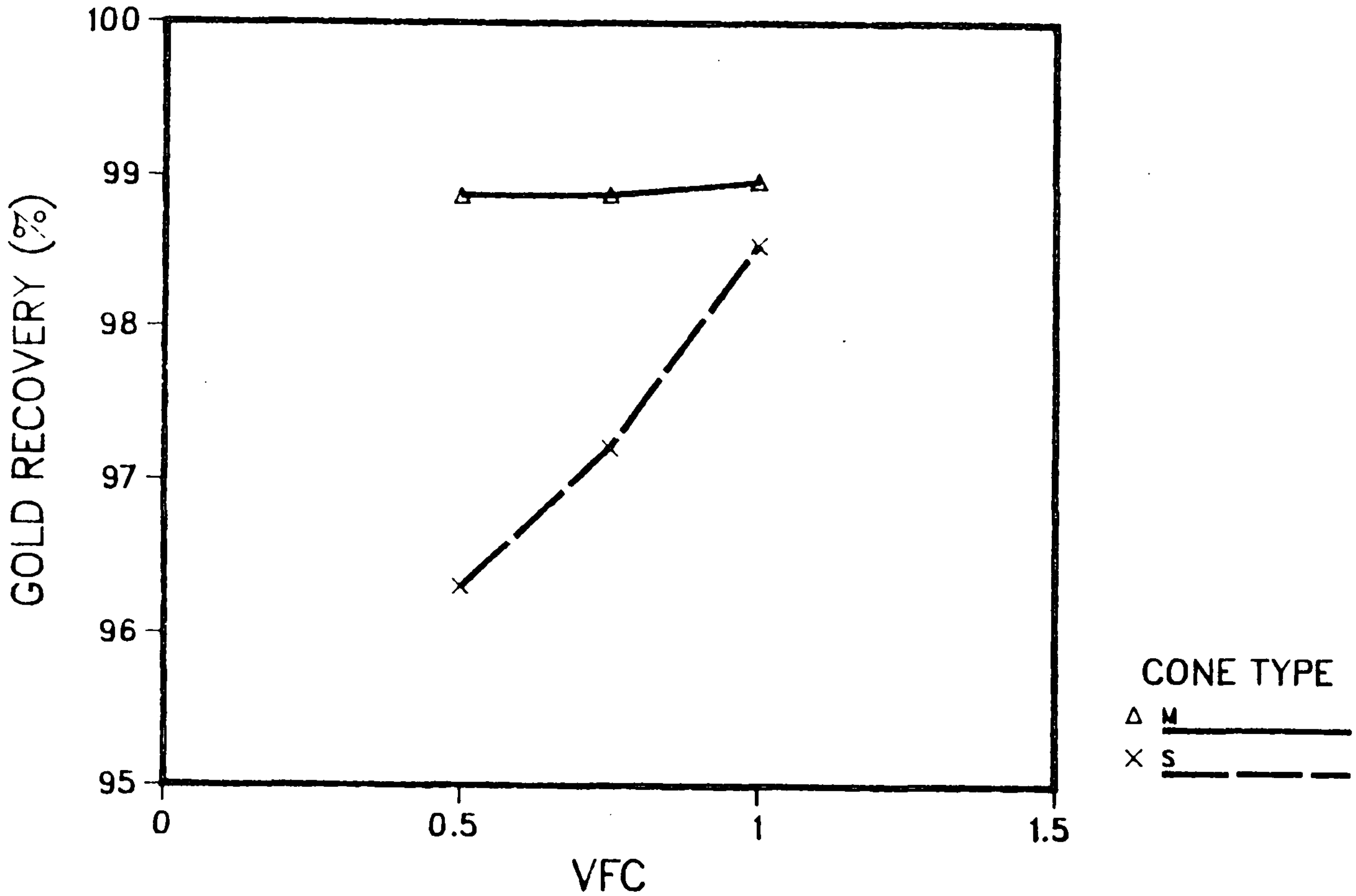

Figure 5-9. 80 x 100 mesh gold (CSF = 0.3 x 0.4) recovery versus CWC cone type and VFC.

Table 5-9
Multiple comparisons format

	P_B	P_D	P_C	P_E	P_A	
P_A						$s^2 =$
P_E						$T =$
P_C						$E =$
P_D						
P_B						

are accompanied by improved gold recoveries.

Phase 4

The experimental design of this project called for Phase 4 to study the effects of gold size and shape on its recovery by the 4 inch CWC, at a restricted number of the 54 treatment levels of phases 2 and 3. The author and Dr. P. D. Rao decided to use 3 treatment levels (Cone type S, VFC = 1/2 inch, P.D. = 5%, Pressure = 4, 6, 8 psig), which yielded concentration ratios of approximately 10:1, 20:1 and 93:1. It was felt that these concentration ratios were of practical importance to the placer mining industry, and at the same time, this selection of factor levels allowed for expeditious testing.

After the extremely high recoveries achieved for the 80 x 100 mesh gold in Phase 3, it was decided to look at only the extremely flaky (CSF = 0.05 x 0.15) gold of the two size fractions coarser than 80 x 100 mesh (20 x 30 and 40 x 50). Also, only 10 particles of gold for each of the seven size-shape ranges less massive than the 80 x 100 x .3 range were sent for activation. Both of these actions were ill-taken. Subsequent recovery estimates for the 20 x 30 and 40 x 50 gold (CSF = 0.05 x 0.15) indicated that it would be of importance to investigate their higher CSF ranges also. Likewise, 10 particles of the extremely fine gold proved too small a number with which to run the tests because the turbulence within the sump kept the gold grains suspended. In addition, these fine, flaky particles tended to come to rest and remain on the conic sides of the sump. Brushing was required to reassociate them with the dynamic system.

Because of these problems, it became obvious that a new batch of gold would need to be prepared for shipment after running those tests which could be conducted. The lower recoveries for the 40 x 50 gold (CSF = 0.05 x 0.15) made it a suitable material with which to conduct phase 5 tests. Thus, in actual practice, Phase 5 was completed prior to Phase 4, but the description of Phase 4 follows in its entirety.

Phase 4 was adaptable to more complete randomization, since the experimental design employed only one pulp density level and procedure required that the system be thoroughly cleaned between test series. The three levels of feed pressure however, were still run in adjacent tests. Also, contrary to true randomization, was the forced alternation of coarse and fine gold sizes. This pattern was followed to purge the system of any fine activated gold, which might remain undetected in the system. During the subsequent test

Table 5-10

CWC cone type factor levels comparisons

	P(M,1') 98.97%	P(M,3/4") 98.88%	P(M,1/2") 98.87%	
P(S,1/2") 96.31%	-	-	2.56%*	$s^2 = 0.06$
P(S,3/4") 97.21%	-	1.67%*	-	T = 1.73 E = 0.40%
P(S,1") 98.54%	0 43%*	-	-	

Summary: <u>P(M,1") P(M,3/4") P(M,1/2")</u> P(S,1") P(S,3/4") P(S,1/2")

Conclusion: At all levels of VFC the M cone gives superior gold recovery to the S cone, though at a reduced concentration ratio.

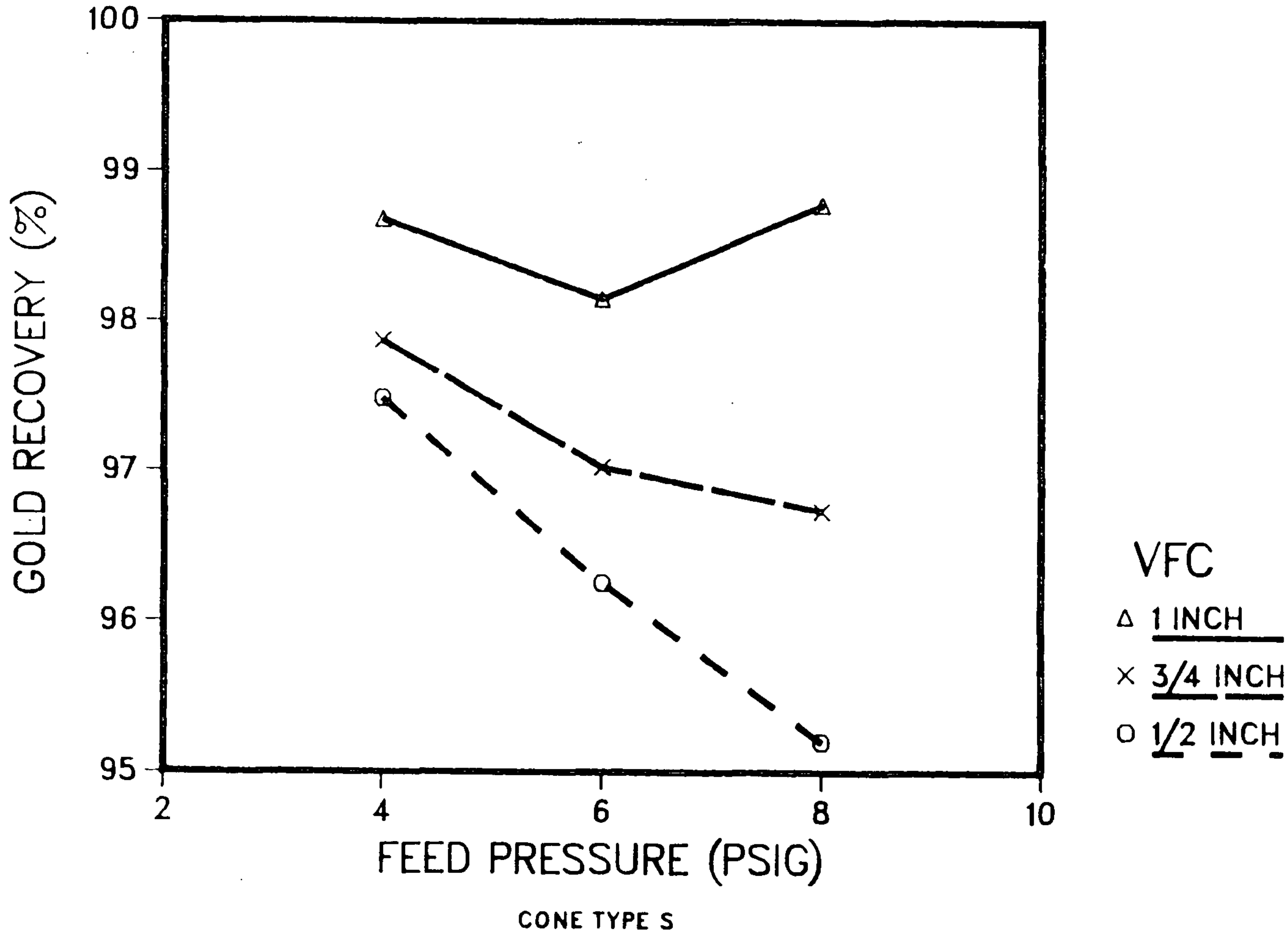

Figure 5-10. 80 x 100 mesh gold (CSF = 0.3 x 0.4) recovery versus CWC feed pressure and VFC.

Table 5-11

Vortex finder clearance factor levels comparisons
(M cone)

	P(1") 98.97%	P(3/4") 98.88%	P(1/2") 98.87%	
P(1/2")	0.1% ns.	0.01% n.s		$s^2 = 0.06$
				T = 2.15
P(3/4")	0.09% n.s.			E = 0.49%
P(1")				

Summary: $\underline{P_{(1,)}\ P_{(3/4")}\ P_{(1/2,)}}$

Conclusion: VFC has no significant effect on gold recovery in conjunction with the M cone.

Table 5-12

Vortex finder clearance factor levels comparisons
(S cone)

	$P_{(1")}$ 98.54%	$P_{(3/4")}$ 97.21%	$P_{(1/2")}$ 96.31%	
$P_{(1/2")}$	2.23%*	0.90%*		$s^2 = 0.06$
				T = 2.15
$P_{(3/4")}$	1.33%*			E = 0.49%
$P_{(1")}$				

Summary: $P_{(1")}$ $P_{(3/4")}$ $P_{(1/2")}$

Conclusion: Narrower VFCs in conjunction with the S cone yield lower gold recovery, through at an increased concentration ratio.

using coarse (more active) gold, any fine gold still in the system would be unnoticeable due to the higher count rate set on the ratemeter. With these limitations in mind, the randomization proceeded as follows:

1) Two columns of size-shape ranges were arranged as shown in Table 5-15. A random permutations of 16 table was employed to assign a test sequence number to each range and its replicate.

2) For each size-shape range, a fair die was employed to determine the pressure level sequence as described in phase 3.

The test procedures were as previously described with the exception of the thorough cleaning between gold size-shape test series. This included a thorough monitoring of the system with a gamma survey meter, and the almost invariable dismantling of the slurry pump to clean out trapped gold particles. This clean out procedure took about 30 minutes.

Data from this series of tests is shown in Table 5-16. Note that the usage of the term concentration ratio has been substituted for feed pressure. This is done to enhance the readability of the data, but it should be noted that it has not been established that gold recovery at given concentration ratios is independent of how the concentration ratios are achieved.

Table 5-13

3 way ANOVA of phase 3 s-cone data for factors; VFC, feed pressure, and pulp density.

Source of Variation	df	MS	F_{Test}	F*	Comment
	Response Variable = Gold Recovery (%)				
MAIN EFFECTS					
B. VFC	2	22.6	24.1	5.14	$p < 0.001$
C. Pulp Density	2	4.2	4.5	5.14	n.s.
D. Feed Pressure	2	6.1	6.5	5.14	$p < 0.01$
2-WAY INTERACTIONS					
B x C	4	1.3	1.4	3.89	n.s
B x D	4	2.2	2.4	3.89	n.s
C x D	4	2.3	2.4	3.89	n.s
3-WAY INTERACTIONS					
B x C x D	8	0.8	0.8	3.11	n.s
TREATMENTS	26	3.68			
ERROR	27	0.94	(MSE)		
TOTAL	53				

Bonferroni B = 7, $\alpha = 0.1$, $(1 - \frac{\alpha}{B}) = 0.986$

$F(0.986, 2, 27) = 5.14$
$F(0.986, 4, 27) = 3.89$
$F(0.986, 8, 27) = 3.11$

An analysis of variance of this data is presented in Table 5-17. A plot of the treatments standardized residuals versus test number (Figure 5-11) shows no deviation from the assumption of independence of treatment observations. A Bartlett F test for homogeneity of variance gave a highly significant value (p = 0.004) indcating heteroscedacity of treatment distributions. An inspection of the residual plot for the data shows one treatment level (20 x 30, 0.6 x 0.8, 20:1) to contain a large amount of variability (std. residual = ± 3.3). This treatment was dropped from the data and another ANOVA run on the remaining data. A Bartlett F test, after deletion of the one treatment, gave a value of p = 0.18, which was not considered to indicate significant heteroscedacity. In addition, the MSE from this second ANOVA was about one-half that of the first ANOVA (48.1 vs. 93.7). The author considered it reasonable to proceed using the results from the second ANOVA (Table 5-18).

The results of the ANOVA show that all three of the main factors have a highly significant effect on the response variable, gold recovery. There are also two highly significant 2-way interactions between size and shape, and size and concentration ratio (CR). Figures 5-12 (a-f) show the main and interaction effects graphically. Because of the size x shape and size x CR interactions no multiple comparisons of the differences between size factor level means are presented; the graphical presentation of Figures 5-12 a-f convey the complex relationships well. Multiple comparisons for shape factor levels and CR factor levels have been done for each level of the factor "gold size" (Table 5-19 to 5-28).

The multiple comparisons between shape and concentration ratio factor levels and Figures 5-12 a-f lead to the following summary of conclusion concerning Phase 4 data.

1) There is a highly significant effect of gold size on its recovery by the CWC. Furthermore this gold size effect is extremely dependent upon the levels of concentration ratio and gold shape. One of the most surprising discoveries of this study was the poor gold recovery of 20 x 50 mesh gold at high concentration ratios. The author believes this

Table 5-14

Feed pressure factor levels comparisons (S cone)

	$P_{(4)}$=98.01%	$P_{(6)}$=97.14%	$P_{(8)}$=96.91%	
$P_{(8)}$	1.10%*	0.23% n.s		s^2 = 0.10 T = 2.15 E = 0.68%
$P_{(6)}$	0.87%*			
P(4)				

Summary: $P_{(4)}$ $\underline{P_{(6)}\ P_{(8)}}$

Conclusion: A feed pressure of 4 psig gives significantly better gold recovery than either 6 psig or 8 psig. Recall that lower feed pressure is accompanied by a lower concentration ratio. There is no significant difference between 6 psig and 8 psig feed pressures.

Table 5-15

Test Sequence Assignment

Fine	Rep 1 Even	Rep 2 Even	Rep 2 Odd	Rep 1 Odd	Coarse
80 x 100 x .05	6	8	5	11	20 x 30 x .05
150 x 200 x .05	12	2	9	13	20 x 30 x .3
150 x 200 x .3	8	10	3	5	20 x 30 x .6
150 x 200 x .6	4	4	13	1	40 x 50 x .05
270 x 400 x .05	14	6	1	15	40 x 50 x .3
270 x 400 x .3	10	14	15	7	40 x 50 x .6
370 x 400 x .6	2	12	7	9	80 x 100 x .3
			11	3	80 x 100 x .6

poor recovery is due to the top size scalping action of the CWC when operated at high concentration ratios.

2) The influence of gold shape increased as the size of the gold decreased, reaching a point of maximum effect at 140 x 200 mesh gold.

3) The influence of concentration ratio decreased as the gold size decreased, showing its greatest impact on coarse gold recovery.

Phase 5

The purpose of Phase 5 was to investigate the influence of 3 factors; (1) topsize of the feed, (2) presence or absence of heavy minerals in the feed, and (3) percentage of -400 mesh slimes in the feed, on gold recovery by the CWC. The importance of the first two factors was suggested by the literature review, while study of the third factor could be of

Table 5-16
CWC gold recovery (%) data as a function of gold size,
gold shape and concentration ratio

	COREY SHAPE FACTOR RANGE								
	0.5 x 0.15			0.3 x 0.4			0.6 x 0.8		
	CONCENTRATION RATIO								
GOLD SIZE	10	20	93	10	20	93	10	20	93
20x30	(31) 72.9	(33) 32.6	(32) 6.3	(37) 76.0	(38) 60.8	(39) 19.0	(13) 84.7	(14) 14.7	(15) 2.0
	(58) 87.2	(60) 46.9	(59) 9.0	(72) 64.3	(71) 29.3	(70) 9.0	(54) 95.0	(52) 79.5	(53) 4.5
40x50	(1) 91.0	(2) 84.5	(3) 61.8	(43) 94.9	(45) 89.2	(44) 78.5	(20) 97.0	(21) 91.8	(19) 74.6
	(84) 91.1	(83) 85.5	(82) 64.5	(48) 98.0	(47) 93.6	(46) 77.2	(88) 95.0	(90) 81.2	(89) 50.0
80x100	(17) 82.0	(16) 68.8	(18) 50.7	(27) 92.5	(26) 93.1	(25) 89.3	(8) 92.4	(7) 98.0	(9) 77.5
	(68) 83.3	(69) 69.9	(67) 53.3	(66) 95.4	(65) 88.7	(64) 89.8	(77) 99.0	(78) 95.6	(76) 90.0
140x200	(35) 65.0	(36) 42.2	(34) 54.4	(24) 82.5	(22) 80.7	(23) 84.5	(12) 94.0	(10) 87.9	(11) 90.0
	(50) 52.6	(49) 33.8	(51) 41.5	(73) 73.6	(74) 72.8	(75) 64.0	(55) 93.5	(57) 92.1	(56) 85.7
270x400	(42) 48.5	(40) 37.1	(41) 35.0	(29) 51.3	(28) 42.0	(30) 42.4	(5) 62.2	(6) 55.5	(4) 51.0
	(61) 43.8	(62) 45.0	(63) 38.7	(86) 61.4	(85) 54.2	(87) 45.4	(80) 72.2	(81) 57.4	(79) 55.6

Parenthetic integers indicate test number.

Table 5-17

3-way ANOVA of phase 4 data for factors; gold size, gold shape, and concentration ratio.

Response Variable = Gold Recovery (%)

Source of Variation	df	MS	F_{Test}	F*	Comment
MAIN EFFECTS					
A. Gold Size	4	6241.3	66.6	3.83	$p < 0.001$
B. Gold Shape	2	2665.8	28.4	5.18	$p < 0.001$
C. Concentration Ratio	2	5296.1	56.5	5.18	$p < 0.001$
2-WAY INTERACTIONS					
A x B	8	467.4	5.0	3.00	$p < 0.01$
A x C	8	1075.7	11.5	3.00	$p < 0.001$
B x C	4	120.0	1.3	3.83	n.s
3-WAY INTERACTIONS					
A x B x C	16	50.2	0.5	2.52	n.s
TREATMENTS	44	1239.0			
ERROR	45	93.7	(MSE)		
TOTAL	89	659.9			

Bonferroni B = 7, $\alpha = 0.1$, $(1 - \frac{\alpha}{B}) = 0.986$ $F(.986,\ 2, 45) = 5.18$ $F(.986,\ 4, 45) = 3.83$

$F(.986,\ 8, 45) = 3.00$ $F(.986,\ 16, 46) = 2.52$

Table 5-18

3-Way ANOVA of phase 4 data for factors; gold size, gold shape, and concentration ratio after deletion of variant treatment

Response Variable = Gold Recovery (%)

Source of Variation	df	MS	F_{Test}	F*	Comment
MAIN EFFECTS					
A. Gold Size	4	6052.4	125.7	3.85	$p < 0.001$
B. Gold Shape	2	2678.6	55.6	5.20	$p < 0.001$
C. Concentration Ratio	2	5300.1	110.1	5.20	$p < 0.001$
2-WAY INTERACTIONS					
A x B	8	460.6	9.6	3.03	$p < 0.001$
A x C	8	1075.8	22.3	3.03	$p < 0.001$
B x C	4	120.3	2.5	3.85	n.s
3-WAY INTERACTIONS					
A x B x C	15	53.4	1.1	2.55	n.s
TREATMENTS	43	1249.8			
ERROR	44	48.1	(MSE)		
TOTAL	87				

Bonferroni B = 7, $\alpha = 0.1$, $(1 - \frac{\alpha}{B}) = 0.986$ $F(.986,\ 2, 44) = 5.20$ $F(.986,\ 4, 44) = 3.85$

$F(.986,\ 8, 44) = 3.03$ $F(.986,\ 15, 44) = 2.55$

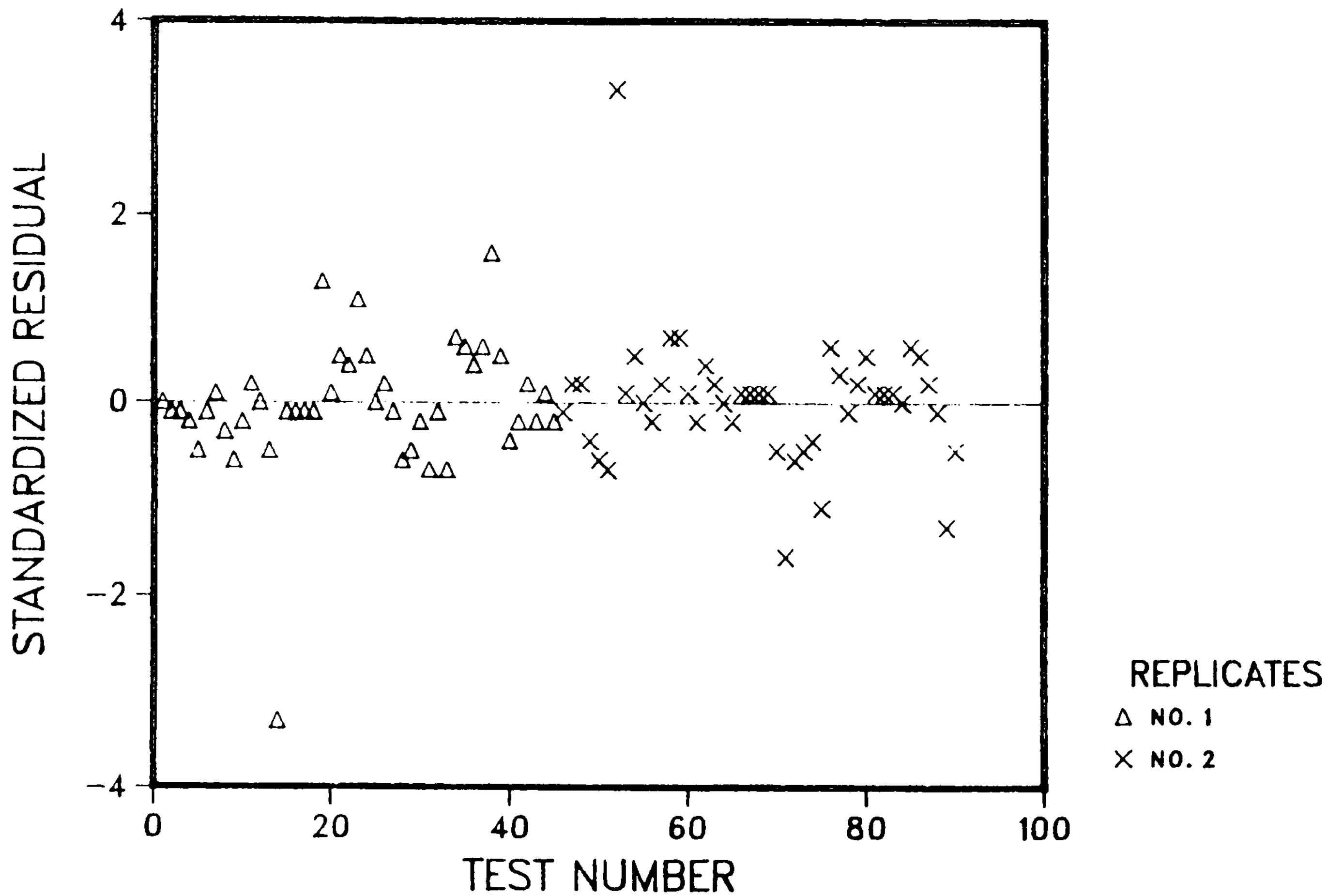

Figure 5-11. Standardized residuals versus test number for phase four data.

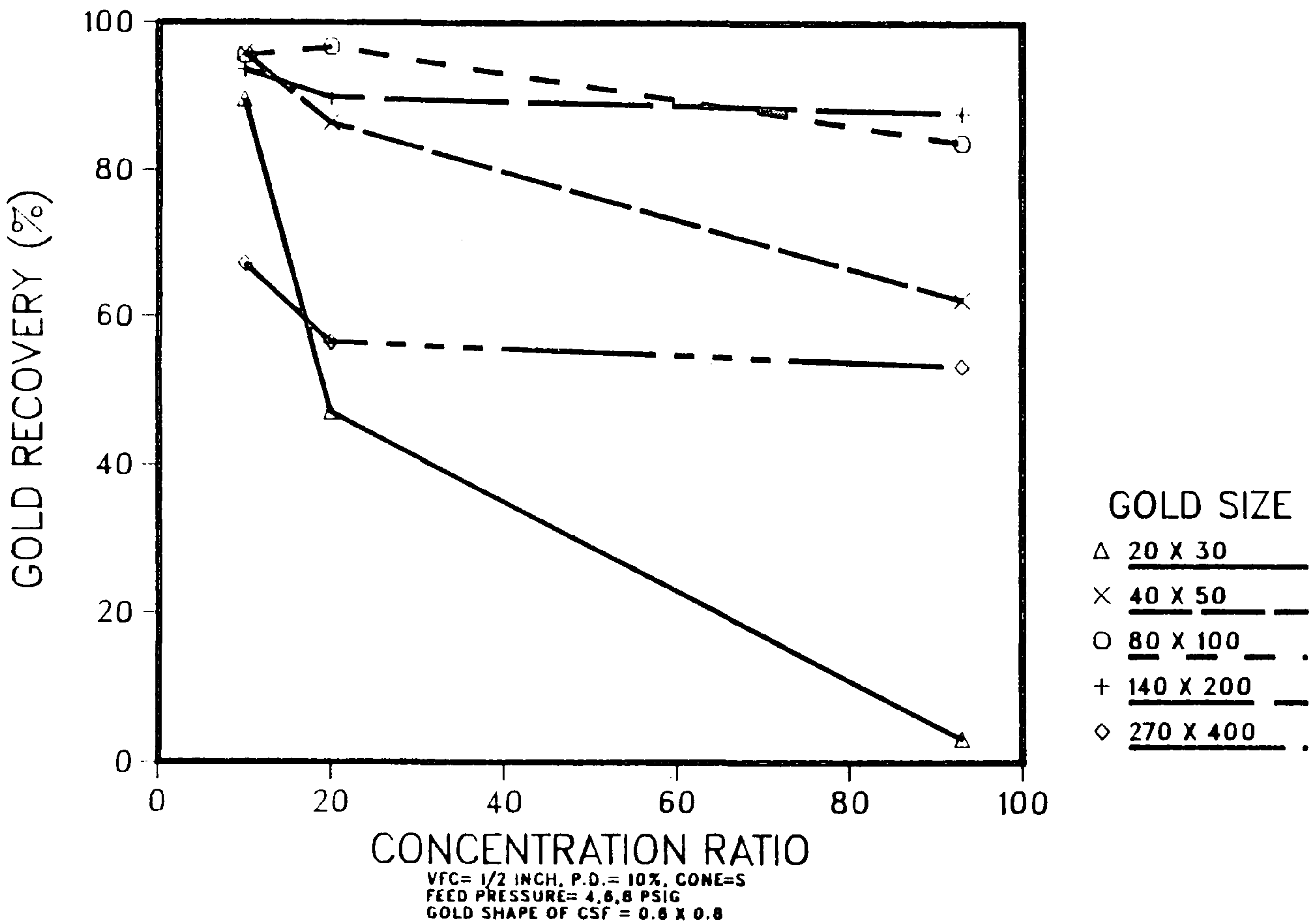

Figure 5-12a. Gold recovery versus gold size and CWC concentration ratio for a gold particle shape of CSF = 0.6 x 0.8.

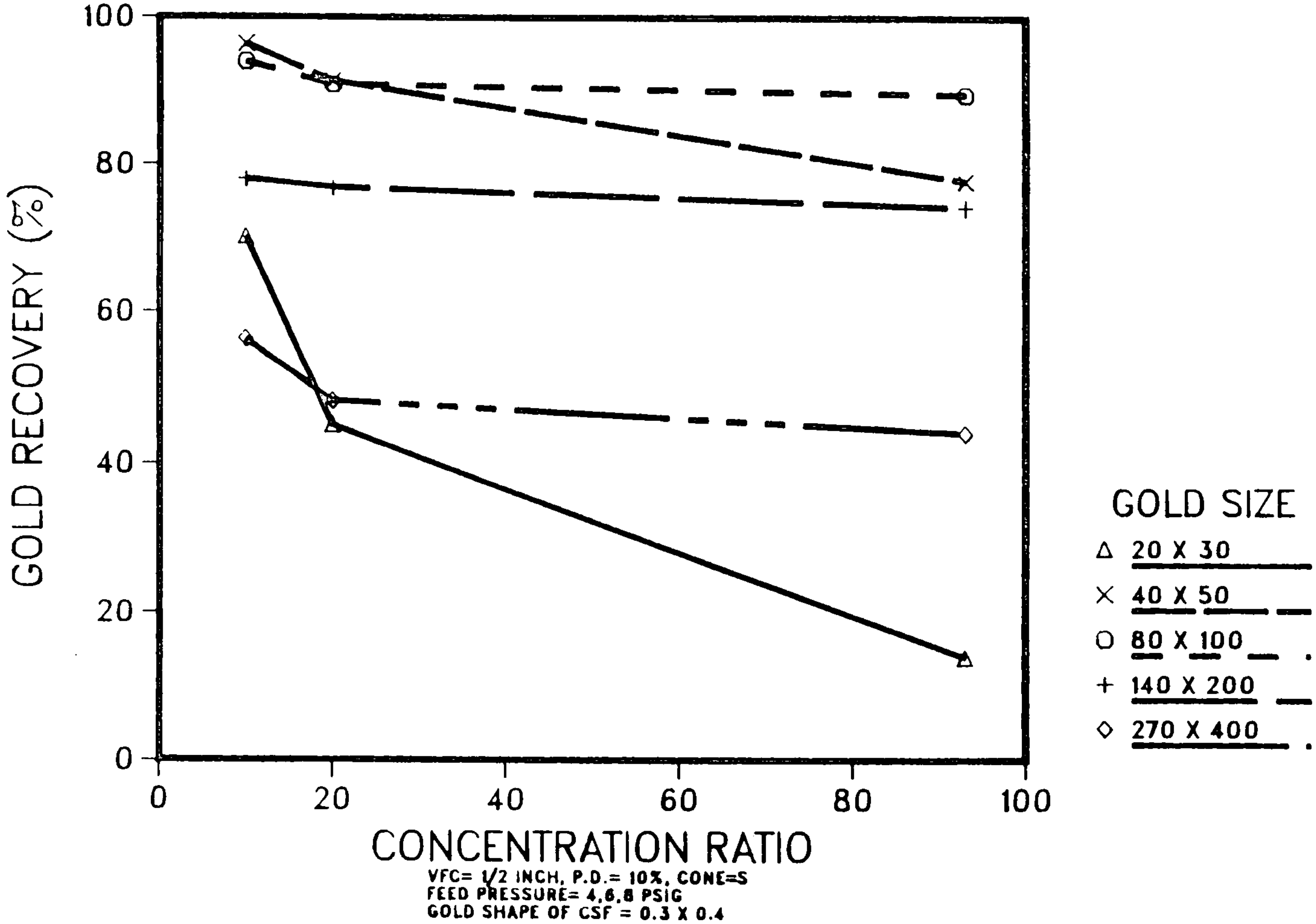

Figure 5-12b. Gold recovery versus gold size and CWC concentration ratio for a gold particle shape of CSF = 0.3 x 0.4.

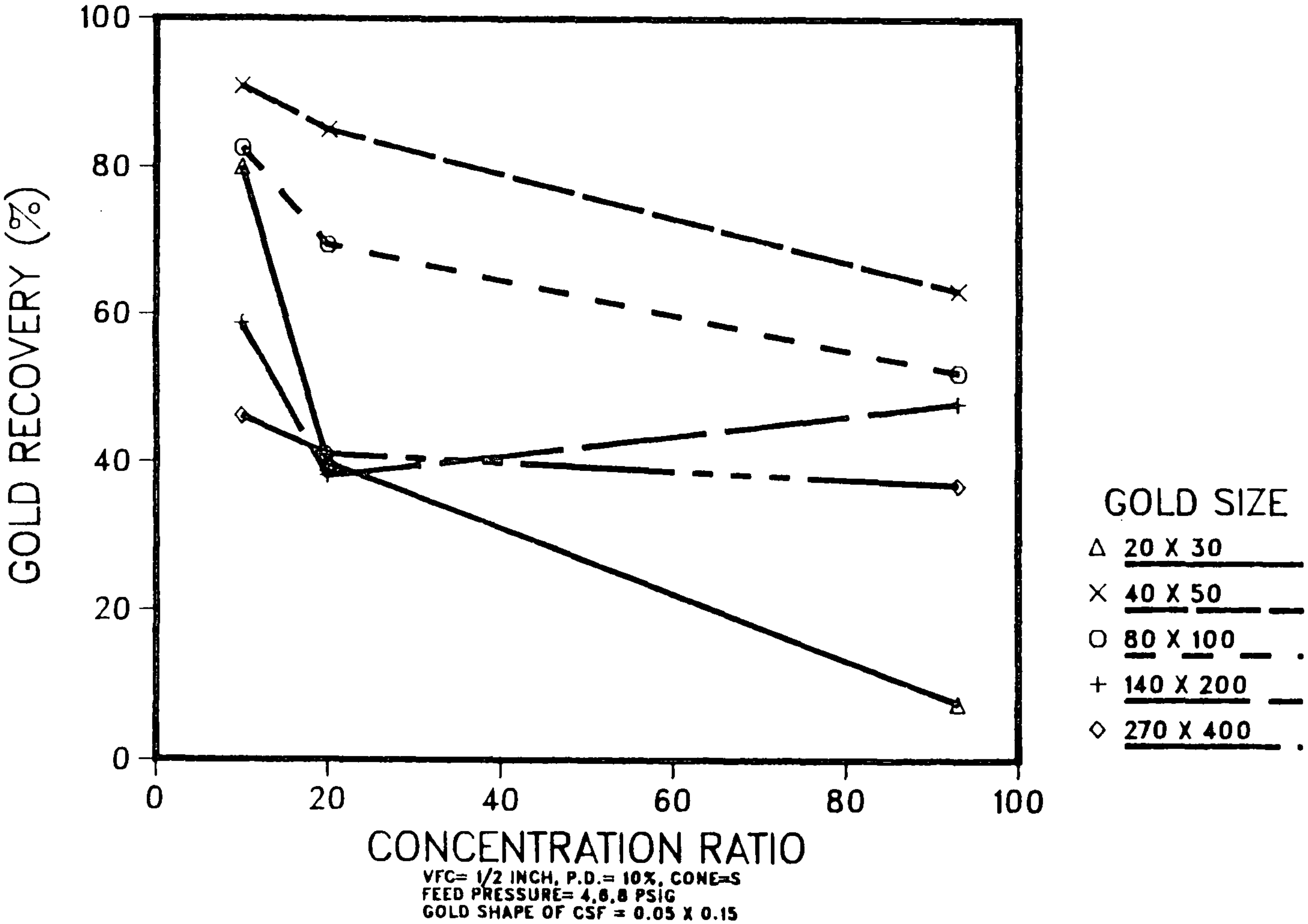

Figure 5-12c. Gold recovery versus gold size and CWC concentration ratio for a gold particle shape of CSF = 0.05 x 0.15.

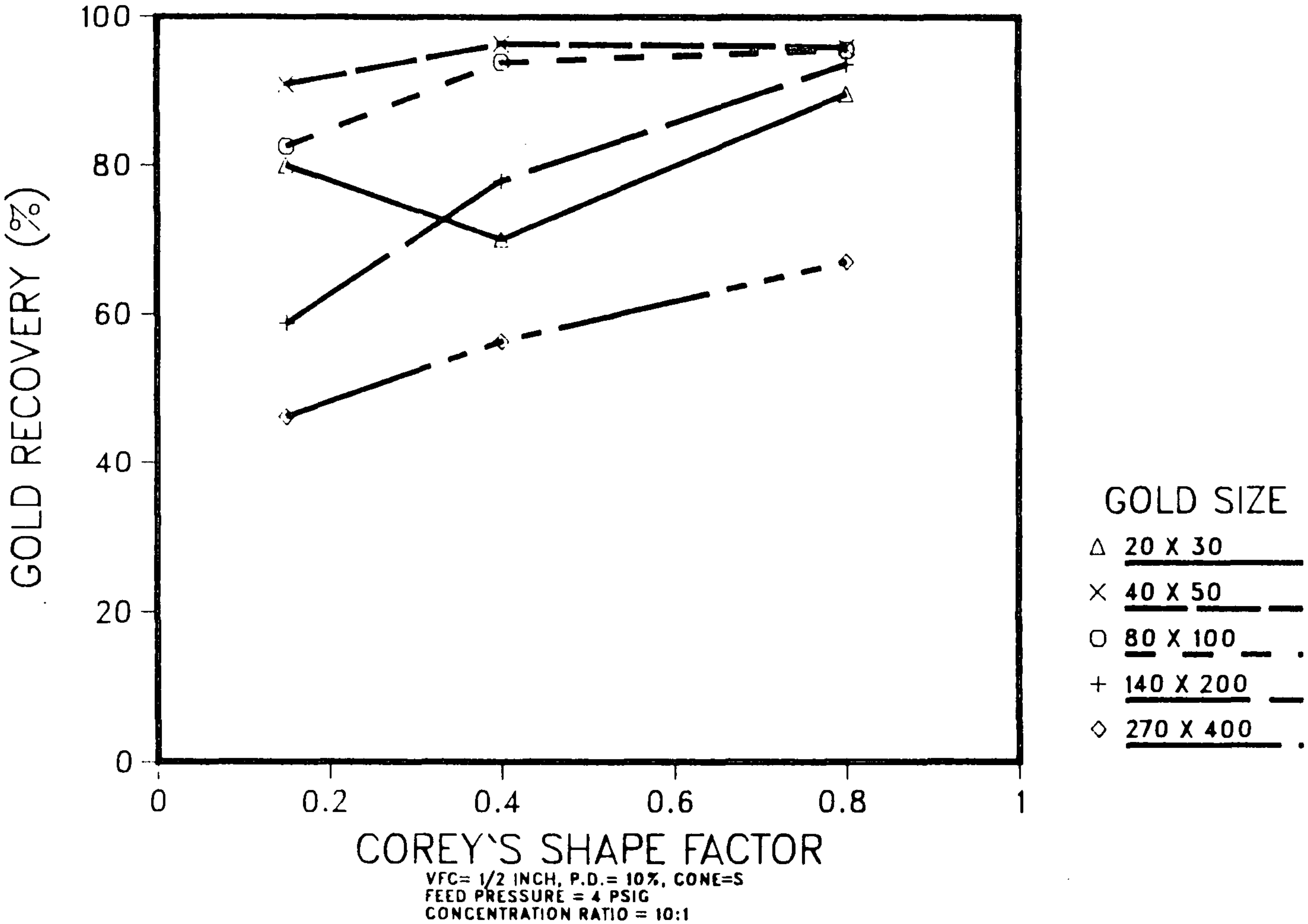

Figure 5-12d. Gold recovery versus gold size and gold shape for a CWC concentration ratio of 10:1.

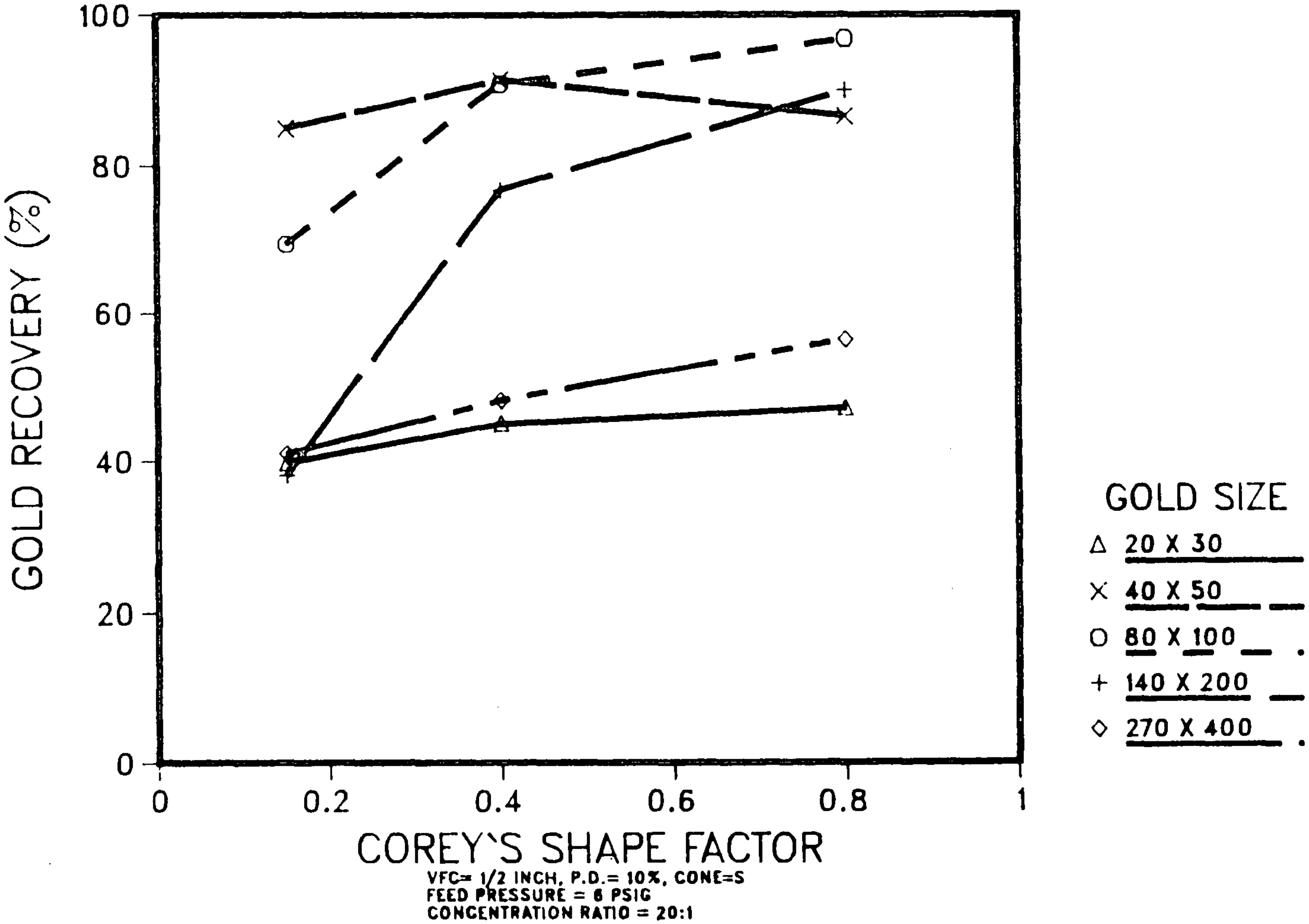

Figure 5-12e. Gold recovery versus gold size and gold shape for a CWC concentration ratio of 20:1.

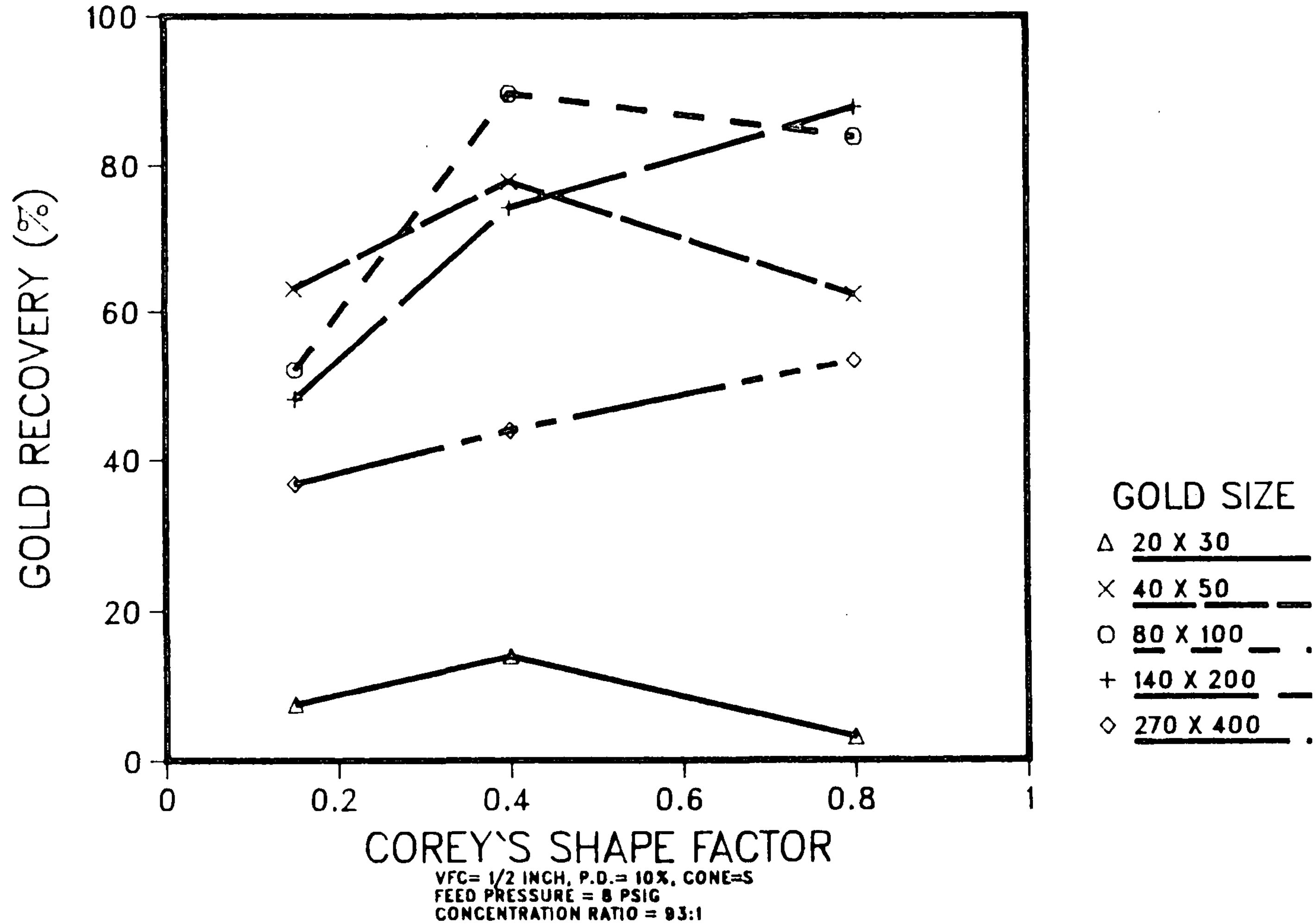

Figure 5-12f. Gold recovery versus gold size and gold shape for a CWC concentration ratio of 93:1.

Table 5-19

Gold shape factor levels comparisons (20 x 30 mesh gold)

	P(0.6) 46.55%	P(0.3) 43.07%	P(.05) 42.48%	
P(.05)	4.07% n.s	0.59% n.s		$s^2 = 16.0$
				T = 2.35
P(0.3)	3.48% n.s			E = 9.4%
P(0.6)				

Summary: P(0.6) P(0.3) P(0.05)

Conclusion: For the 20 x 30 mesh gold size factor level, gold shape has no significant effect on gold recovery.

Table 5-20

Concentration ratio factor levels comparisons (20 x 30 mesh gold)

	$P_{(10)}$ 88.02%	$P_{(20)}$ 42.40%	$P_{(93)}$ 8.30%	
$P_{(93)}$	71.7%*	34.1*		$s^2 = 16.0$
				T = 2.35 **
$P_{(20)}$	37.6%*			E = 9.4%
$P_{(10)}$				

Summary: $P_{(10)}$ $P_{(20)}$ $P_{(93)}$

Conclusion: For the 20 x 30 mesh gold size factor level, concentration ratio, as regulated by feed pressure, has a significant effect on gold recovery. Gold recovery increases with decreasing concentration ratio.

** These values of s^2, T, and E remain constant across all size levels and are omitted from other multiple comparison arrays.

Table 5-21

Gold shape factor levels comparisons (40 x 50 mesh gold)

	$P_{(0.3)}$ = 88.57%	$P_{(0.6)}$ = 81.60%	$P_{(.05)}$ = 79.73%
$P_{(.05)}$	8.84% n.s	1.87% n.s	
$P_{(0.6)}$	6.67% n.s		
$P_{(0.3)}$			

Summary: $P_{(.3)}$ $P_{(.6)}$ $P_{(.05)}$

Conclusion: For the 40 x 50 mesh gold size factor level, gold shape has no significant effect on gold recovery.

Table 5-22

Concentration ratio factor levels comparisons (40 x 50 mesh gold)

	P(10) = 94.50%	P(20) = 87.63%	P(93) = 67.77%
P(93)	26.73%*	19.86%*	
P(20)	6.87% n.s		
P(10)			

Summary: $\underline{P_{(10)}\ P_{(20)}}\ P_{(93)}$

Conclusion: For the 40 x 50 mesh gold size factor level, concentration ratio, as regulated by feed pressure, has a significant effect upon gold recovery. Gold recovery is significantly improved by reducing the pressure from 8 psig (93:1) to 6 psig (20:1) or 4 psig (10:1). There is no significant difference in gold recovery between concentration ratios of 20:1 and 10:1.

Table 5-23

Gold shape factor levels comparisons (80 x 100 mesh gold)

	$P_{(0.6)}$ = 92.08%	$P_{(0.3)}$ = 91.47%	$P_{(.05)}$ = 68.0%
$P_{(.05)}$	24.08%*	24.47%*	
$P_{(0.3)}$	0.61% n.s		
$P_{(0.6)}$			

Summary: $\underline{P(0.6)\ P(0.3)}$ P(.05)

Conclusion: For the 80 x 100 mesh gold size factor level the gold recovery for CSF (0.3 x 0.4) gold and CSF (0.6 x 0.8) gold is significantly better than that for CSF (0.05 x 0.15) gold. There is no significant difference in gold recovery between CSF (0.6 x 0.8) gold and CSF (0.3 x 0.4) gold.

Table 5-24

Concentration ratio factor levels comparisons (80 x 100 mesh gold)

	$P_{(10)}$ = 90.77%	$P_{(20)}$ = 85.68%	$P_{(93)}$ = 75.10%
$P_{(93)}$	15.67%*	10.58%*	
$P_{(20)}$	5.09% n.s		
$P_{(10)}$			

Summary: $\underline{P_{(10)}\ P_{(20)}}\ P_{(93)}$

Conclusion: For the 80 x 100 mesh gold size factor level, there is a significant increase in gold recovery when the concentration ratio is reduced from 93:1 to 20:1 or 10:1. There is no significant difference between gold recoveries attained at 20:1 and 10:1 concentration ratios.

Table 5-25

Gold shape factor levels comparison (140 x 200 mesh gold)

	$P_{(0.6)}$ = 90-53%	$P_{(0.3)}$ = 76.35%	$P_{(.05)}$ = 48.28%
$P_{(.05)}$	42.25%*	28.07%*	
$P_{(0.3)}$	14.18%*		
$P_{(0.6)}$			

Summary: $P_{(.6)}$ $P_{(.3)}$ $P_{(.5)}$

Conclusion: For the 140 x 200 mesh gold size factor level, gold recovery significantly increases as gold flatness decreases.

Table 5-26

Concentration ratio factor levels comparisons
(140 x 200 mesh gold)

	$P_{(10)}$ = 76.87%	$P_{(93)}$ = 70.02%	$P_{(20)}$ = 68.28%
$P_{(20)}$	8.59% n.s	1.74% n.s	
$P_{(93)}$	6.85% n.s		
$P_{(10)}$			

Summary: $\underline{P_{(10)}\ P_{(93)}\ P_{(20)}}$

Conclusion: Concentration ratio has no significant effect on 140 x 200 mesh gold recovery.

Table 5-27

Gold shape factor levels comparison (270 x 400 mesh gold)

	$P_{(0.6)}$ = 59.00%	$P_{(0.3)}$ = 49.45%	$P_{(.05)}$ = 41.35%
$P_{(.05)}$	17.65*	8.10% n.s	
$P_{(0.3)}$	9.55%*		
$P_{(0.6)}$			

Summary: $P_{(0.6)}$ $\underline{P_{(0.3)}\ P_{(.05)}}$

Conclusion: For the 270 x 400 mesh gold size factor level, gold recovery for CSF (0.6 x 0.8) gold is significantly better than for CSF (0.05 x 0.15) gold. Gold recovery for CSF (0.6 x 0.8) gold is also superior to CSF (0.3 x 0.4) gold. There is no significant difference in gold recovery between gold of CSF (0.3 x 0.4) and CSF (0.05 x 0.15).

Table 5-28

Concentration ratio factor levels comparisons (270 x 400 mesh gold)

	$P_{(10)}$ = 56.57%	$P_{(20)}$ = 48.55%	$P_{(93)}$ = 44.68%
$P_{(93)}$	11.89%*	3.87% n.s	
$P_{(20)}$	8.02% n.s		
$P_{(10)}$			

Summary: $P_{(10)}$ $P_{(20)}$ $P_{(93)}$

Conclusion: For the 270 x 400 mesh gold size factor level, gold recovery is significantly better at a 10:1 concentration ratio than at 93:1. Between other factor levels of concentration ratio there is no significant difference.

Table 5-29

CWC gold recovery (%) data as a function of feed top size, presence or absence of heavy minerals, and -400 mesh slimes content.

	Low Slimes		High Slimes	
Top Size of Feed	W/ Heavy Minerals	W/O Heavy Minerals	W/ Heavy Minerals	W/O Heavy Minerals
- 4 mesh	(11) 82.1	(5) 79.0	(12) 84.8	(6) 78.8
	(17) 84.5	(19) 82.9	(18) 86.8	(20) 84.5
-12 mesh	(9) 87.7	(7) 84.5	(10) 83.8	(8) 86.2
	(21) 84.4	(23) 86.4	(22) 90.9	(24) 86.6
-30 mesh	(3) 94.8	(1) 91.3	(4) 91.8	(2) 92.8
	(13) 97.0	(15) 97.0	(14) 93.6	(16) 97.0

Parenthetic integers indicate test number.

importance for CWC application in high recycle operations.

100 pounds of the CWC feed sample was processed through a 4 inch x 6 inch Denver mineral jig in order to remove a large percentage of its heavy minerals. The jig tails were collected and screened into 4 x 12, 12 x 30 and -30 mesh fractions. These were then dried and stored in separate containers. The top size of the CWC feed solid was to be varied over three levels; -4 mesh, -12 mesh, and -30 mesh. The pulp density level of each test (prior to additional -400 mesh material addition) was 10%. For top sizes above 30 mesh, the weights of the dried fractions were blended to yield a product containing size fraction weight percents equal to the original feed material, had it been scalped at the desired top size.

In order to increase the percentage of -400 mesh slimes in the feed, a 50 pound sack of potter's clay was purchased. Taking into account the volume of the sump-cyclone system (112 liters), the CWC feed material gave the system a -400

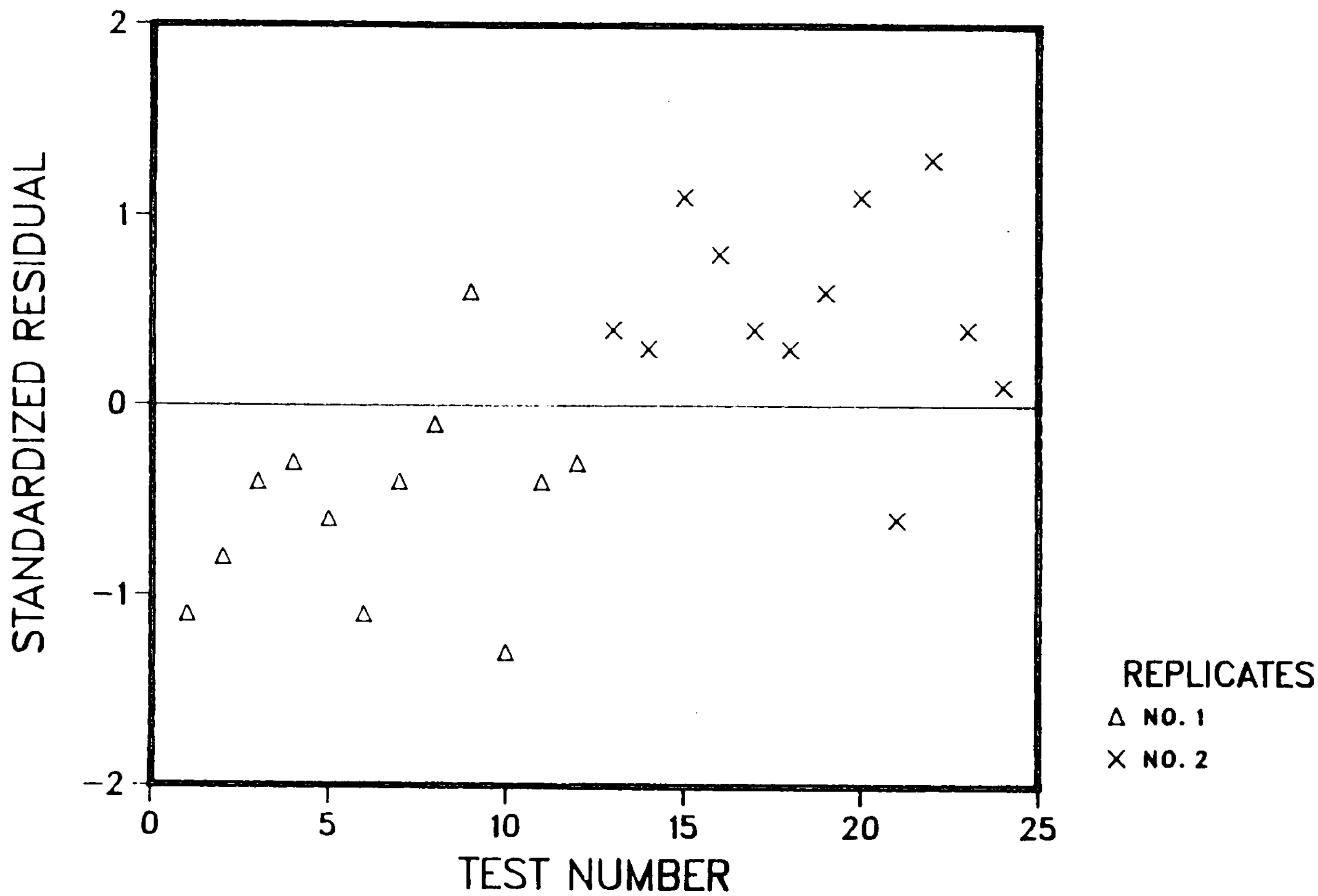

Figure 5-13. Standardized residuals versus test number for phase five data.

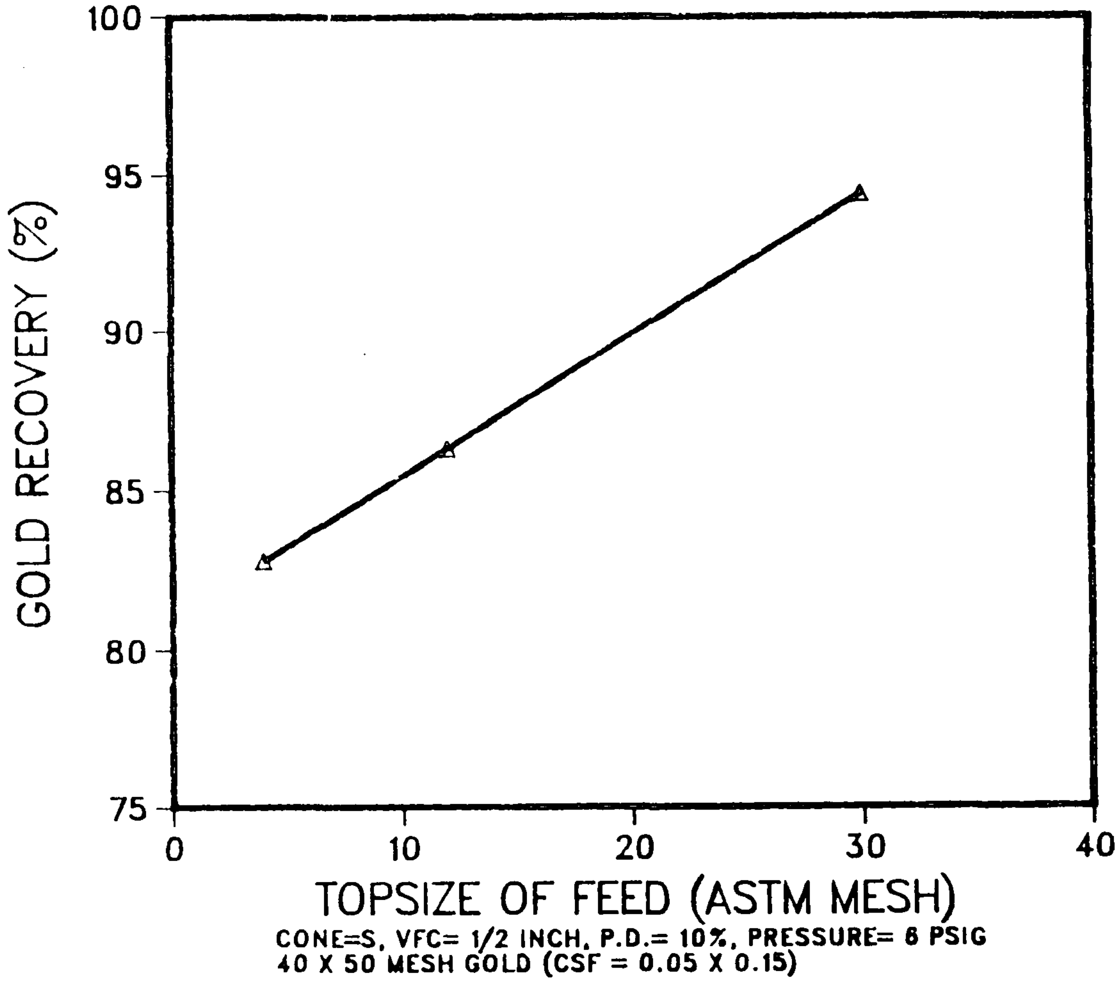

Figure 5-14. 40 x 50 mesh gold (CSF = 0.05 x 0.15) recovery versus CWC feed top-size.

Table 5-30

3 Way ANOVA of phase 5 data for factors; feed top-size, presence or absence of heavy minerals, and -400 mesh slimes content.

Response Variable = Gold Recovery (%)

Source of Variation	df	MS	F_{Test}	F*	Comment
MAIN EFFECTS					
A. Top Size	2	283.7	39.0	6.4	p < 0.001
B. Heavy Minerals	1	10.4	1.4	8.6	n.s.
C. Slimes	1	1.8	0.2	8.6	n.s.
2-WAY INTERACTIONS					
A x B	2	7.0	1.0	6.4	n.s
A x C	2	4.9	0.7	6.4	n.s
B x C	1	0.9	0.1	8.6	n.s
3-WAY INTERACTIONS					
A x B x C	2	3.9	0.5	6.4	n.s
TREATMENT	11	55.6			
ERROR	12	7.3	(MSE)		
TOTAL	23				

Bonferroni B = 7, $\alpha = 0.1$ $(1 - \frac{\alpha}{B}) = 0.986$

F(0.986, 1, 12) = 8.59
F(0.986, 2, 12) = 6.44

Table 5-31

Feed top size factor level comparisons

	$P_{(-30)}$ 94.41%	$P_{(-12)}$ 86.31%	$P_{(-4)}$ 82.80%	
$P_{(-4)}$	11.61%*	3.51%*		$s^2 = 1.82$ T = 2.26
$P_{(-12)}$	8.10%*			E = 3.04%
$P_{(-30)}$				

Summary: $P_{(-30)}$ $P_{(-12)}$ $P_{(-4)}$

Conclusion: At the CWC settings used and for 40 x 50 mesh gold (CSF = 0.15 x 0.05) the top size of the feed has a significant influence on gold recovery. Gold recovery is increased by decreasing the top size of the feed.

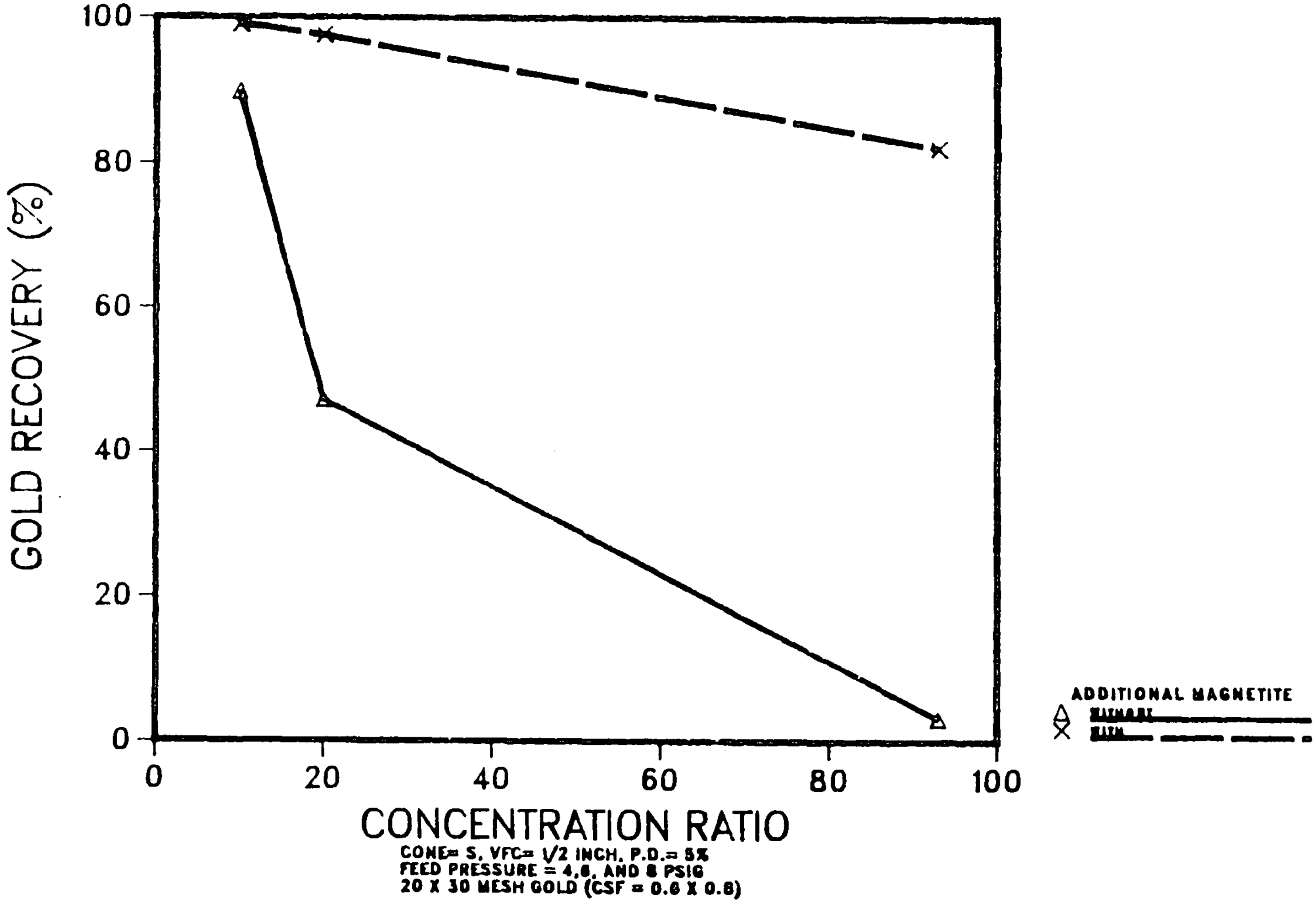

Figure 5-15a. Effect of additional magnetite (105 grams, -6 mesh) on CWC recovery of 20 x 30 mesh gold. (CSF = 0.6 x 0.8)

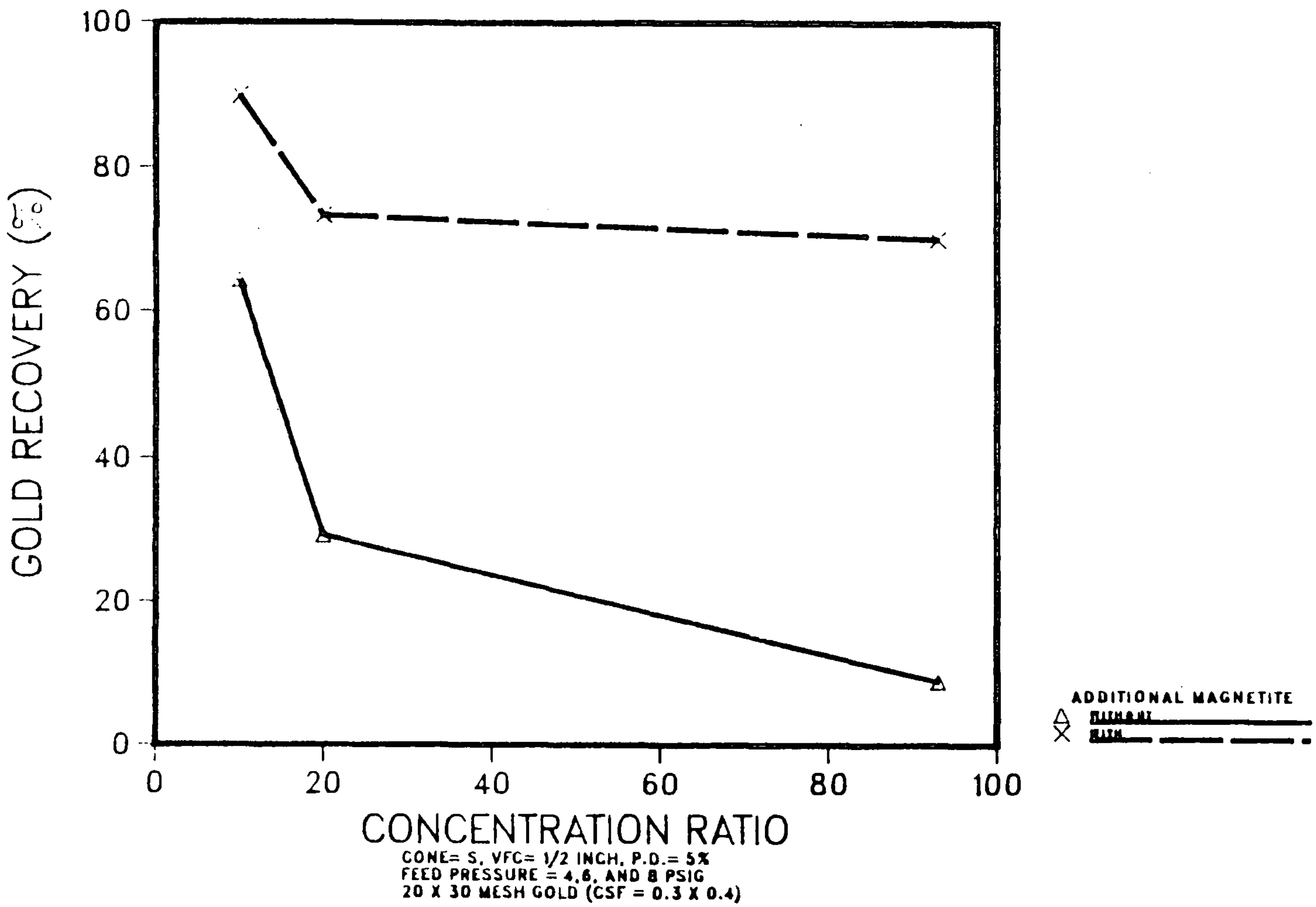

Figure 5-15b. Effect of additional magnetite (105 grams, -6 mesh) on CWC recovery of 20 x 30 mesh gold. (CSF = 0.3 x 0.4)

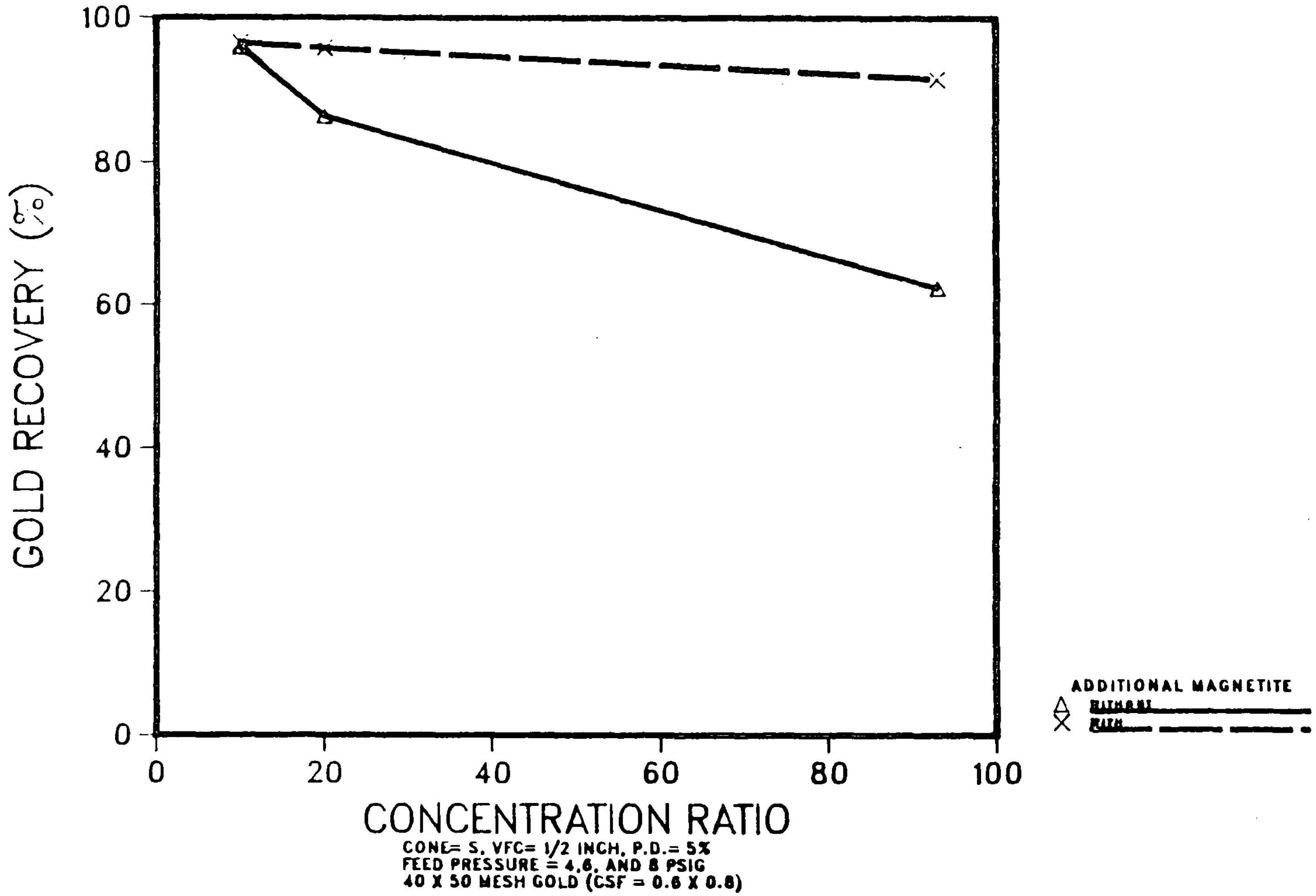

Figure 5-15c. Effect of additional magnetite (105 grams, -6 mesh) on CWC recovery of 40 x 50 mesh gold. (CSF = 0.6 x 0.8)

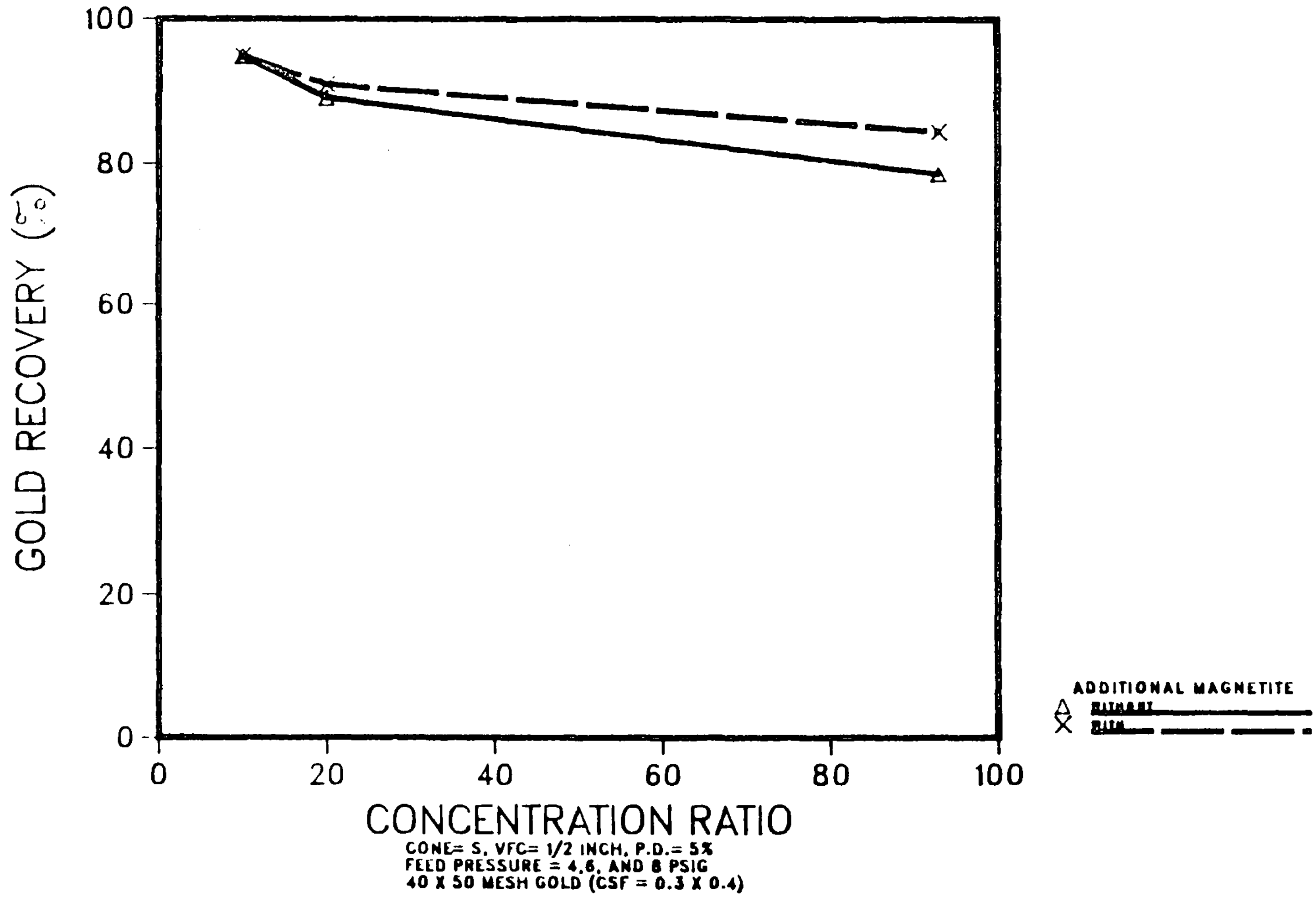

Figure 5-15d. Effect of additional magnetite (105 grams, -6 mesh) on CWC recovery of 40 x 50 mesh gold. (CSF = 0.3 x 0.4)

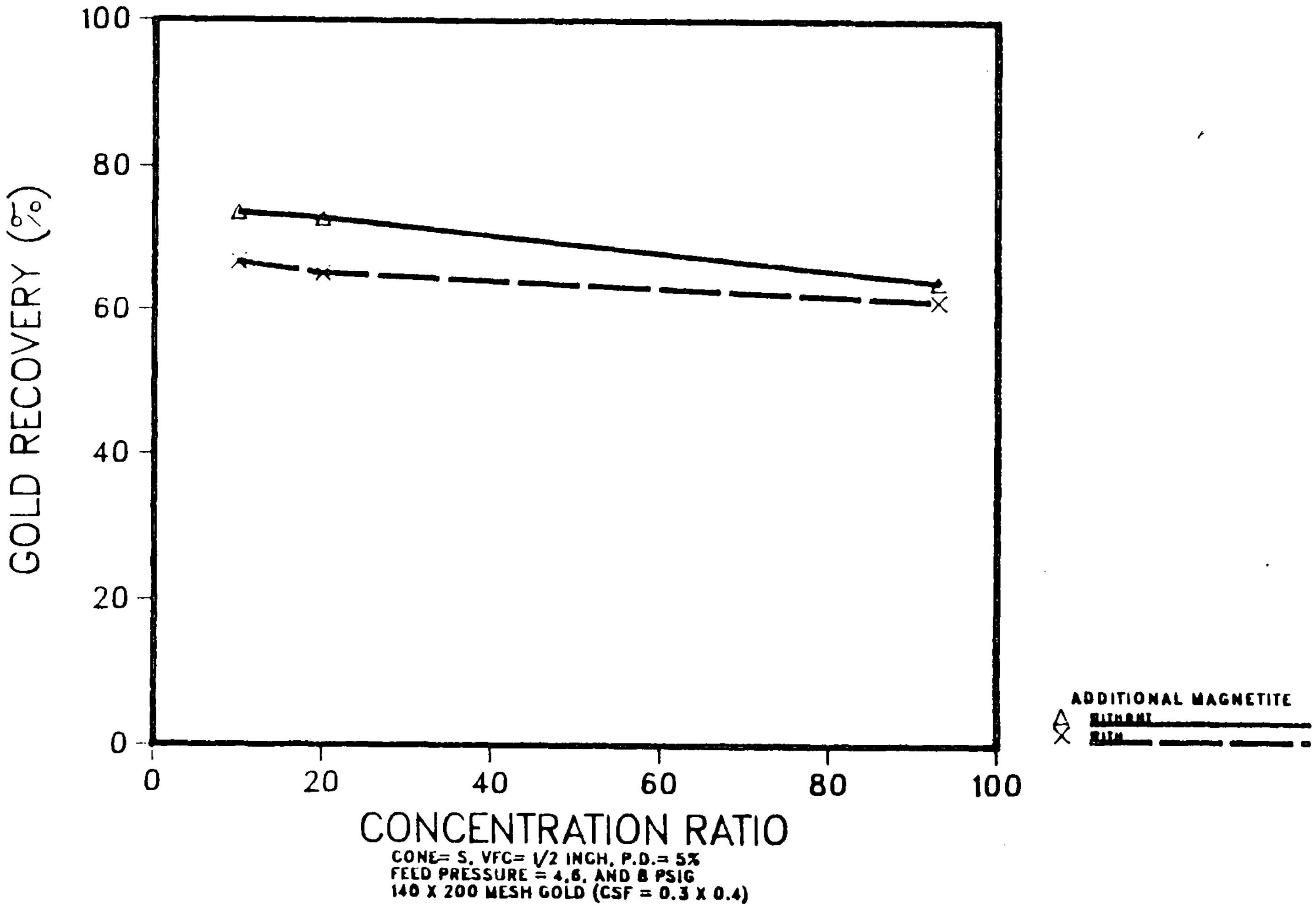

Figure 5-15e. Effect of additional magnetite (105 grams, -6 mesh) on CWC recovery of 140 x 200 mesh gold. (CSF = 0.3 x 0.4)

Table 5-32

Gold recovery (%) of size-shape fractions as affected by the addition of coarse magnetite to the CWC System

GOLD SIZE X GOLD SHAPE	FEED PRESSURE (PSIG)/CR	REPLICATION NO. 1 WITHOUT ADDITIONAL MAGNETITE	REPLICATION NO. 1 WITH ADDITIONAL MAGNETITE	REPLICATION NO. 2 WITHOUT ADDITIONAL MAGNETITE	REPLICATION NO. 2 WITH ADDITIONAL MAGNETITE
	4/10	84.7	+99	95.0	+99
20 x 30	6/20	14.7	96.0	79.5	+99
(0.6 x 0.8)	8/93	2.0	75.6	4.5	88.9
	4/10	76.0	-	64.3	90.0
20 x 30	6/20	60.8	-	29.3	73.3
(0.3 x 0.4)	8/93	19.0	-	9.0	70.0
40 x 50	4/10	97.0	98.0	95.0	95.0
(0.6 x 0.8)	6/20	91.8	97.0	81.2	94.6
	8/93	74.6	77.2	50.0	86.0
40 x 50	4/10	94.9	94.9	98.0	-
(0.3 x 0.4)	6/20	89.2	91.0	93.6	-
	8/93	78.5	84.5	77.2	-
140 x 200	4/10	82.5	-	73.6	66.8
(0.3 x 0.4)	6/20	80.7	-	72.8	65.2
	8/93	84.5	-	64.0	61.3

mesh suspended solids concentration of between 3,850 mg/liter and 7,150 mg/liter depending upon the topsize of the feed charge at 10% pulp density. In all cases, an additional 1,125 grams of potters' clay were added to the CWC closed circuit system during treatments including "excess slimes". This quantity of clay increased the system's pulp density by approximately 1% and increased its -400 mesh suspended solids by 10,000 mg/liter, to levels between 13,850 mg/liter and 17,150 mg/liter. Suspended solids concentrations on the order of 10,000 mg/liter can be expected in the process water of well maintained and operated total recycle placer operations (Shannon and Wilson, Inc., 1985).

The randomization of the test sequence was complete with respect to feed top size and the presence or absence of heavy minerals. However, once the system was charged with its appropriate feed, the "low slimes" treatment was always run first, followed by the addition of the excess -400 mesh clay, and completion of the "high slimes" treatment.

Where a treatment required the presence of heavy minerals, 100 grams of magnetite was added to the system. This magnetite was of the same topsize as the CWC feed solids and ranged through 65 mesh. This 12 treatment test series was run using 40 x 50 mesh gold with a CSF range of 0.05 x 0.15, and with CWC settings,; Cone Type S, VFC = 1/2 inch, P.D.=10%, and Feed pressure = 6 psig (CR = 20:1).

Table 5-29 presents the phase 5 data; table 5-30 shows the ANOVA results for the same. A plot of the standardized residuals, Figure 5-13, confirms independence of treatment observations. Bartlett's F test for homogeneity of variance yields p = 0.87. The ANOVA shows that only the factor "top size of the feed" has a significant effect upon gold recovery. There are no significant interaction terms. Figure 5-14 graphically displays the feed top size effect. A multiple comparison of the factor level means of top size is given in Table 5-31.

The results of Phase 5 were surprising since they were unexpected. The reader will recall that several sources referenced in Chapter 2 stated that a certain amount of coarse, heavy minerals are required for efficient CWC

Table 5-33

Phase 7 vs. phase 4 gold recovery data

GOLD SIZE SHAPE	PSIG/ CR	Recovery (%) Rep.1,	Rep.2	+ Coarse Magnetite to Rep. 2	Phase 4 Data PSIG/ CR	Recovery (%) Rep.1,	Rep.2
	4/5	99,	+99	–	4/10	76.0,	64.3
20 x 30	8/10	99,	+99	–	6/20	60.8,	29.3
(0.3x0.4)					8/93	19.0,	9.0
	4/5	+99,	+99	–	4/10	84.7,	95.0
20 x 30	8/10	+99,	+99	–	6/20	14.7,	79.5
(0.6x0.8)					8/93	2.0,	4.5
	4/5	+99,	+99	–	4/10	94.9,	98.0
40 x 50	8/10	+99,	+99	–	6/20	89.2,	93.6
(0.3x0.4)					8/93	78.5,	77.2
					4/10	97.0,	95.0
40 x 50	4/5	+99,	+99	–	6/20	91.8,	81.2
(0.6x0.8)	8/10	96,	99	–	8/93	74.6,	50.0
80 x 100	4/5	89.7,	91.0	95.0	4/10	82.0,	83.3
(0.05x0.15)	8/10	91.5,	88.0	90.5	6/20	68.8,	69.9
					8/93	50.7,	53.3
140 x 200	4/5	85.6,	87.0	90.0	4/10	82.5,	73.6
(0.3x0.4)	8/10	82.5,	86.0	85.1	6/20	80.7,	72.8
					8/93	84.5,	64.0

Phase 7 CWC Settings (VFC = 1", S-Cone, 5% P.D.)
Phase 4 CWC Settings (VFC = 1/2", S-Cone, 5% P.D.)

operation. The data from Phase 5 tends to cast some doubt upon these statements, at least under certain conditions of CWC operation. Not only does the ANOVA show that heavy minerals have no significant effect on gold recovery, it also shows that coarse material in the feed actually lowers CWC efficiency.

Phase 6

Phase 6 and Phase 7 were not included in the experimental design, rather their inclusion was suggested by the results of phases 4 and 5. No statistical analysis of the data is presented since it was deemed that their scope was too narrow for significant conclusions. They are presented here in a descriptive fashion; their inclusion intended to offer support for, or challenge of the earlier conclusions of the previous phases.

Phase 6 was conducted after it was noticed that 20 x 30 mesh gold of CSFs (0.6 x 0.8) and (0.3 x 0.4) appeared to have a longer residence time within the CWC body than did the finer size fractions. Throughout the course of the study, the residence time of gold particles within the CWC had been checked by allowing only a single particle of activated gold to cycle through the closed circuit system. The gamma survey meter was held close to the CWC feed inlet. When the particle was detected by the survey meter a stop watch was started, and stopped when the particle was detected as a pulse on the chart recorder. Thus CWC residence time was actually slightly shorter than the observed time. In most cases (40 x 400 mesh gold) the residence time was barely measurable with the stop watch used, being on the order of 1 second or less. This is close to the calculated residence time for water within the CWC.

For 20 x 30 mesh gold however, the residence time was on the order of 5-10 seconds and at times up to 30 seconds or more. This fact coupled with the extremely poor recovery by the CWC of 20 x 30 mesh gold at high concentration ratios suggested that recovery of this coarse gold might be significantly improved if enough coarse heavy minerals were added to the system to "flush" the gold through the CWC. It was felt that the coarse heavy minerals might also act as a shield for the coarse gold, protecting it from the powerful scour current across Section I of the compound cone.

Therefore, during the later stages of Phase 4, after a test series with coarse gold had been completed through the three pressure levels, 100 grams of -6 mesh magnetite was added to the system in addition to the 60 grams of 12 x 70 mesh magnetite already present. The gold recovery of the CWC was again checked at each of the three pressure levels. Table 5-32 presents the data from Phase 6. Figures 5-15 (a-e) show plots of the gold recoveries for the system with and without additional coarse magnetite. Note too that one series of tests using 140 x 200 mesh (CSF 0.3 x 0.4) gold was also studied in this manner.

These results suggest a definite improvement for larger sizes of gold with higher Corey shape factors. The effect of adding additional coarse magnetite seems to be less pronounced as the gold size decreases and the gold becomes more flattened. At 140 x 200 mesh the coarse magnetite may even lower gold recovery.

Note that for 40 x 50 mesh (CSF 0.3 x 0.4) gold, the coarse magnetite influence is questionable. Recall the results from Phase 5, which showed that heavy minerals did not significantly affect recovery; that coarser feed topsizes lowered the recovery of 40 x 50 mesh (CSF 0.05 x 0.15) gold. Therefore, at 40 x 50 mesh (CSF 0.05 x 0.15) the negative influence of the coarser material may outweigh the benefits, if any, of the heavy minerals. This author suggests that had CWC feed top size been lowered below 30 mesh, to approach 40 mesh, in Phase 5 testing, the benefits of top size reduction may have reversed itself and a decrease in gold recovery been observed. If such had been the case, Phase 6 data suggests that the addition of magnetite (-30 mesh) might then act to improve gold recovery.

Though this data comes from only a few tests, it does lend support to Phase 5 conclusions. At the same time, it shows that for certain gold size-shape combinations, "coarse" heavy minerals may improve CWC gold recovery, "coarse" being relative to the size and shape of the gold in question.

Phase 7

The poor gold recoveries of coarse, chunky gold from Phase 4 also inspired the tests of Phase 7. Here it was desired to investigate the recovery of gold, coarse gold in particular, at a lower concentration ratio. The CWC was operated at 4 and 8 psig with a VFC of 1 inch, a type S cone, and at 5% pulp density. This produced concentration ratios of approximately 5:1 at 4 psig and 10:1 at 8 psig. Tests for various sizes and shapes of gold were run in duplicate and in two cases, the effect of adding additional coarse magnetite was again studied. Table 5-33 shows the data from these tests along with some data from Phase 4 tests for comparison.

For 20 x 30 mesh and 40 x 50 mesh gold, recovery appears to be increased by the CWC operational parameters of Phase 7. It seems reasonable that reducing the concentration ratio to 5:1 would increase gold recovery, but there also appears to be an advantage in the 10:1 CR used in Phase 7 to that of the 10:1 CR used in Phase 4. These differed only by the CWC parameters adjusted to achieve them, indicating that gold recovery as a function of CWC concentration ratio may not be independent of how the concentration ratio is achieved. This data also suggests an alternative to the addition of coarse heavy minerals in order to improve coarse gold recovery.

As the size of the gold decreases, the advantage of the lower concentration ratio seems to diminish as does the differential in gold recoveries between the Phase 7 and Phase 4 10:1 concentration ratios. The addition of coarse magnetite (100 g) to the second replicate of tests using 80 x 100 mesh and 140 x 200 mesh gold yields only a slight increase in recovery; so slight, that it is very likely insignificant based on the brevity of the data.

SUMMARY

The conclusions to be drawn from each phase of this study have already been stated throughout the text of Chapter 5. The reader is referred to this chapter for detailed conclusions but a brief recapitulation of the findings of this project are given below. These conclusions are valid only over the range of the factors studied.

1) The concentration ratio of the CWC is affected by cone type, VFC, feed pressure and pulp density. Their influence from greatest to least is; cone > VFC ≥ feed pressure > pulp density, for the material studied.

2) The top size of the CWC underflow solid is determined by CWC operational parameters and may be significantly less than the top size of the CWC feed solids.

3) CWC cone type, VFC, and feed pressure all significantly influence the recovery of 80 x 100 mesh gold (CSF = 0.3 x 0.4). Feed pulp density does not affect gold recovery.

4) Gold recovery is significantly affected by gold size, gold shape, and concentration ratio. These effects are complex, there being significant interaction between size and concentration ratio and between size and shape.

5) The recovery of 40 x 50 mesh gold (CSF 0.05 x 0.15) is unaffected by the presence or absence of heavy minerals in the feed. A -400 mesh slimes content of approximately 17,000 mg/liter also shows no effect on recovery. However, the feed top size significantly influences gold recovery, with higher recoveries being associated with a smaller feed top-size.

6) The presence of coarse heavy mineral in the feed solids (5% by weight) appears to increase recovery of coarse gold. This influence diminishes with decreasing gold size and CSF.

7) The recovery of coarse gold is improved at lower concentration ratios (wider VFCs, lower feed pressures). Again, finer gold seems less affected by concentration ratio and/or the CWC parameters varied in order to achieve a given concentration ratio.

With respect to previous CWC research efforts cited in Chapter 2 some comments must be made. The work by Lopatin et al. (1977) agrees well with the findings of this project despite the differences in cyclone diameter and cone design. Not only does the nature of the factor effects they studied compare well, but in general gold recoveries for -200 mesh gold ranged from 20% to 50%. This project has shown a range of gold recoveries for 270 x 400 mesh gold of 37% to 67%.

Concerning the work of Soviet researchers Man'kov (1976) only one factor in common existed; heavy minerals. Man'kov experienced 10-15% better recovery of -100 mesh gold when heavy minerals were added to the cyclone feed. This author's recent work showed no significant heavy minerals effect at 40 x 50 mesh (CSF 0.05 x 0.15) gold. Though coarse heavy minerals did improve coarse gold recovery their impact was slight at finer gold sizes. The work of the South African team (Bath, et al., 1973) cites gold recovery trends with size for -60 mesh gold that agrees well with those experienced during the phases of this study. The reader should compare Tables 2-8 and 2-9 with Table 5-17. Their work with 4 inch CWC concentration ratios did not include sufficient data in the range of this project to afford comparison.

Radiotracer techniques used in the course of this study have shown that gold particles ranging in size from 40 mesh to 400 mesh have a residence time within the CWC of approximately 1 second. This casts considerable doubt on the three stage CWC separation mechanism proposed by Dr. Visman, when applied to free gold recovery. This short residence time agrees closely with that calculated considering the control volume of the cyclone and the flow rates involved. This coupled to the data of phase 2 describing the underflow's top size variation with CWC operational parameters suggests to this author that gold recovery by the CWC is a function of particle size, particle density and the scouring currents within the cyclone. "Bed density" is considered important only as a protective, thin layer, which shields the coarser gold particles from the entraining currents and facilitates their movement through the CWC.

Similarly short, gold particle, residence times dispute the contention that gold of all sizes tends to accumulate in the compound cone during CWC operation. Hence, CWC bed material collected after batch tests should not include a disproportionate amount of the batch sample's gold values.

In conclusion, the CWC should be considered in applications of fine, placer gold recovery not as a "miracle" concentrator but as an efficient fine gold, recovery unit with limitations imposed by desired concentration ratios and gold size and shape. The CWC could find considerable application as a preconcentrator ahead of more costly processing equipment and perhaps, at the same time, function as a sizing (scalping) device and/or a thickener. The data contained in this thesis should serve as a useful source from which data for preliminary design calculations for CWC applications may be drawn.

Though it is anticipated that the data and conclusions from this study will be of both practical and scientific importance, it is this author's belief that the radiotracer technique developed for this project is the thesis' principal contribution. This technique may be extended to evaluate a host of other gravity concentrators with respect to gold recovery. No doubt it will also find application to study recovery of other minerals and to investigate other physical parameters of mineral grains. The technique is simple, accurate, and time effective, as testified to by the quantity and quality of the data in this thesis. It enjoys its greatest utility when a large number of tests are run in order to evaluate the recovery of a concentrator as a function of several factors, i.e. a factorial design.

REFERENCES

1. Aluru, R., 1983, Application of Hydrocyclones for the Beneficiation of Scheelite Ores, University of Alaska, Fairbanks, Master's Thesis, 108 p.

2. Bath, M. D., Duncan, A. J., and Rudolf, E. R., 1973, Some Factors Influencing Gold Recovery by Gravity

Concentration, Journal of the South African Institute of Mining and Metallurgy, p. 363-383.

3. Bradley, D., and Pulling, D. J., 1959, Flow Patterns in the Hydraulic Cyclone and Their Interpretation in Terms of Performance, Transactions of the Institute of Chemical Engineers, vol. 37, p. 87-104.

4. Cook, D. J., 1954, Gold Recovery in a Sluice Box, University of Alaska, Fairbanks, Professional Degree Engineer of Mines Thesis, 93 p.

5. _______, and Rao, P. D., 1973, Distribution, Analysis, and Recovery of Fine Gold from Alluvial Deposits, University of Alaska, Fairbanks, MIRL Report No. 32, 102 p.

6. _______, _______,1979, Influence of Particle Shape and Size on Recovery of Gold, Conference on Alaskan Placer Mining, University of Alaska, Fairbanks, MIRL Report No. 43, p. 1-19.

7. Corey, A. T., 1949, Influence of Shape on the Fall Velocity of Sand Grains, Colorado A and M College (now Colorado State University), Fort Collins, unpublished Master's Thesis, 102 p.

8. Cyclone Engineering Sales Ltd., 1978, Compound Water Cyclones, Edmonton, Alberta, Canada, 16 p.

9. _______, 1979, Compound Water Cyclone Manual No. 4-l, Edmonton, Alberta, Canada, 24 p.

10. Dreissen, H. H., and Fontein, F. J., 1963, Applications of Hydrocyclones and Sieve Bends in Wet Treatment of Coal Minerals and Mineral Products, Transactions of the Society of Mining Engineers of AIME, March, vol. 226, p. 101-107.

11. Fano, U., 1953, Gamma Ray Attenuation, Nucleonics, August and September.

12. Gardner, R. P., and Ely, R. L., 1967, Radioisotope Measurement Applications in Engineering, Reinhold Co., New York.

13. _______, 1975, Evaluation of a Radioisotope Tracer Method for Determination of Simulation Parameters in Open Circuit Continuous Ball Mills, Transactions of the Society of Mining Engineers of AIME, vol. 258, no. 4, p. 46-54.

14. Gaudin, A. M., and De Bruyn, P. L., 1949, Radioactive Tracers in Mineral Engineering Problems and Particularly in Flotation, Canadian Mining and Metallurgical Bulletin, p. 331-337.

15. _______, Spedden, H. R., and Kaufman, D. F., 1951, Progency in Comminution, Transactions of the Society of Mining Engineers of AIME, vol. 190, p. 969-970.

16. Guest, R., 1980, A Survey of the Literature on Gravity Separation, South African National Institute of Metallurgy, Report No. 2082, Randburg, South Africa.

17. Heath, R. L., 1964, Scintillation Spectrometry: Gamma Ray Spectrum Catalogue, Phillips Petroleum Co., U.S. Atomic Energy Commission Contract, 2nd Edition, vol. 2.

18. Heywood, H., 1933, Calculation of the Specific Surface of a Powder, Institute of Mechanical Engineering Proceedings, vol. 125, p. 383-459.

19. Hukki, R. T., 1944, Principles of Comminution - Size and Surface Distribution, Massachusetts Institute of Technology, Doctoral Thesis.

20. Johnson, R., 1976, Elementary Statistics, Duxbury Press, North Scituate, Massachusetts, 550 p.

21. Jull, N. A., 1972, Parameters for Cyclone Selection, Canadian Mining Journal, vol. 93, no. 6, p. 37-43.

22. Kelly, E. G., and Spottiswood, D. J., 1982, Introduction to Mineral Dressing, Wiley-Interscience Publication, John Wiley and Sons, New York.

23. Kelsall, D. F., 1952, A Study of the Motion of Solid Particles in a Hydraulic Cyclone, Transactions of the Institute of Chemical Engineers, vol. 30, p. 285-337.

24. Kohl, J., Zentner, R. D., and Lukens, H. R., 1961, Radioisotope Applications Engineering, D. Co. Inc., Princeton, New Jersey, 562 p.

25. Lopatin, A. G., Nikolin, A. l., Artem'ev, l. V., Kurochkin, S. M., and Kuroshev, S. P., 1977, Industrial Use of Short-Cone Wet Cyclones to Extract Free Gold, Tsvetnye Metally, no. 7, p. 74-77.

26. Man'kov, V. M., and Sannikova, N. P., 1976, Improving the Efficiency of Auriferous Sand Concentration in Short Cone Wet Cyclones, Tsvetnye Metally, vol. 4, p. 95-96.

27. Mayer, F. W., 1964, Fundamentals of a Potential Theory of the Jigging Process, VII International Mineral Processing Congress.

28. Meadley, C. K., 1972, Basic Theory of Hydrocyclone Mechanics, Journal de Macanique, vol. II, no. 3, p. 393-401.

29. Mildren, J., no date, Resume of High Capacity Gravity Separation Equipment for Placer Gold Recovery, Reichert Aggregates, Sacramento, California, 54 p.

30. Neter, J., and Wasserman, W., 1974, Applied Linear Statistical Models, Richard P. Irwin Inc., 842 p.

31. Nio, T. H., 1984, Some Aspects of Gold Recovery with IHC Jigs, Alaska Miners Association Ninth Annual Convention, Anchorage, 24 p.

32. Poling, G. W., and Wang, W., 1983, Methods for Recovering Fine Placer Gold, Canadian Mining and Metallurgical Bulletin, December, p. 47-56.

33. Rao, P. D., Wolff, E. N., and Maneval, D. R., 1982, Application of Hydrocyclones for Recovery of Fine Gold from Placer Material, University of Alaska, Fairbanks, MIRL Report No. 55, 26 p.

34. ________, Maneval, D. R., Walsh, D. E., 1983, Application of Compound Water Cyclones for Fine Gold Recovery, Alaska Miners Association Eighth Annual Convention, Anchorage, 18 p.

35. ________, ________, ________, and Aluru, R., 1985, Beneficiation of Gold and Scheelite Using a Compound Water Cyclone, XV International Mineral Processing Congress, Cannes, France, 13 p.

36. Saks, S. Ye., 1975, Principles of Hydronamic Equivalence of Clastic Particles, International Geology Review, vol. 18, no. 5, p. 541-544.

37. Shannon and Wilson, Inc., 1985, Placer Mining Wastewater Treatment Technology Project Phase 2 Report, State of Alaska Department of Environmental Conservation, Fairbanks.

38. Shilo, N. A., and Shumilov, Yu. U., 1970, New Experimental Data on Settling of Gold Particles in Water, Doklady Akademii, Nauk, SSSR, vol. 195, no. 1, p. 193-196.

39. Shumilov, Yu. U., and Shumovskiy, A. G., 1975, Experimental Data on the Hydraulic Size of Some Placer Minerals in the Northeast USSR, Doklady Akademii, Nauk, SSSR, vol. 225, no. 5, p. 1174-1176.

40. Spinks, J. W. T., 1956, Use of Radioactive Tracers in Research and Instrumentation in the Mineral Industry, Canadian Mining and Metallurgical Bulletin, May, p. 368-371.

41. Streeter, V. L., and Wylie, B. E., 1975, Fluid Mechanics, McGraw-Hill, New York, 752 p.

42. Svarovsky, L., 1984, Hydrocyclones, Technomic Publishing Co., Lancaster, Pennsylvania, 198 p.

43. Urlich, C., November, 1983, Report on Preliminary Evaluation of Mine Equipment and Process Technology Proposed for Precious Metal Recovery Sombrio Point Placer Property, Reimchem Urlich Geological Engineering, Vancouver, British Columbia, Canada.

44. ________, December, 1983, Report On Bulk Sample Concentration Testing, Particle Mineralogy Analysis, and Gold Recovery Chemistry Studies, Sombrio Point Placer Property, Reimchen Urlich Geological Engineering, Vancouver, British Columbia, Canada.

45. ________, 1984, Recovery of Fine Gold by Knelson Hydrostatic Cone and Compound Water Cyclone Technologies, Fourth Annual RMS-ROSS Seminar on Placer Gold Mining, Vancouver, British Columbia, Canada.

46. ________, 1985, Compound Water Cyclones: Recovery of Micron Size Precious Metals from an Ancient Beach Deposit at Sombrio Point Vancouver Island, Fifth Annual RMS-ROSS Seminar on Placer Gold Mining, Vancouver, British Columbia, Canada.

47. Tourtelot, H. A., 1968, Hydraulic Equivalence of Grains of Quartz and Heavier Minerals and Implications for the Study of Placers, Geological Survey Professional Paper 594-F, U.S. Government Printing Office, Washington, D. C., 13 p.

48. Visman, J., 1962, The Cleaning of Highly Friable Coals by Water Cyclones, Transactions Fourth International Coal Preparation Congress, Paper C2, Harrogate.

49. ________, 1963, The Compound Water Cyclone: A New Cleaner for Fine Coal and Slurry, Canadian Department of Mines and Technical Surveys, Fuels, and Mining Practice Division, Internal Reports 63/173-Prep., Ottawa.

50. ________, 1966, Bulk Processing of Fine Materials by Compound Water Cyclones, Canadian Mining and Metallurgical Bulletin, March, p. 333-346.

51. ________, 1967, Two Stage Beneficiation of Washery Effluents with Compound Water Cyclones, Department of Mines and Technical Surveys, Edmonton, Alberta, Canada, 13 p.

52. ________, and Andersen, N. E., 1975, Application of Compound Water Cyclones for the Processing of Placer Sand from the Burwash Creek, Yukon Territory, Canada, Department of Energy, Mines, and Resources, Edmonton, Alberta, Canada, 20 p.

53. Walsh, D. E., 1984, Determination of Gold Loss from Fish Creek Sluicing Operation, Report to Northwest Exploration Co. by MIRL, University of Alaska, Fairbanks, 30 p.

54. Wasp, E. J., Kennedy, J. P., and Gandhi, R. L., 1977, Solid Liquid Flow Slurry Pipeline Transportation, Trans. Tech. Publications, 224 p.

55. Wells, J. H., 1969, Placer Examination, Technical Bulletin No. 4, U.S. Department of the Interior, Bureau of Land Management, U.S. Government Printing Office, Washington, D. C., 155 p.

56. Weyher, L. H. E., and Lovell, H. L., 1969, Hydrocyclone Washing of Fine Coal, Transactions of the Society of Mining Engineers of AIME, vol. 244, no. 2, p. 191-203.

57. Wills, B. A., 1979, Mineral Processing Technology, William Clowes (Beccles) Limited, London, 418 p.

58. Zamyatin, 0. V., and Konyukova, A. T., 1970, Extracting Various Sizes of Gold from Sand on a Concentrating Table, Soviet Journal of Nonferrous Metals, vol. 43(2).